Universidad de Córdoba
Facultad de Medicina Veterinaria y Zootecnia
Doctorado en Microbiología y Salud Tropical

Tesis Doctoral

Evaluación del Potencial Antifúngico del Isoespintanol Extraído de *Oxandra xylopioides* Diels (Annonaceae), Contra Aislamientos Intrahospitalarios de *Candida tropicalis*

Orfa Inés Contreras Martínez

Director
Dr. Gílmar Santafé Patiño

Montería, Colombia
2023

Universidad de Córdoba
Facultad de Medicina Veterinaria y Zootecnia
Doctorado en Microbiología y Salud Tropical

Tesis Doctoral

Evaluación del Potencial Antifúngico del Isoespintanol Extraído de *Oxandra xylopioides* Diels (Annonaceae), Contra Aislamientos Intrahospitalarios de *Candida tropicalis*

Orfa Inés Contreras Martínez

Director
Dr. Gílmar Santafé Patiño

Jurados Evaluadores:

Dr. Alex Sáez Vega
Dra. Nerlis Pajáro Castro
Dr. Edwin Pérez Hernández

Montería, Colombia
2023

DEDICATORIA

A mi sol, mi esposo, Alberto Angulo Ortíz, a quien agradezco profundamente su apoyo y acompañamiento incondicional en cada etapa de este proceso y en mi vida personal.

A mis estrellas, Carito, Tefy y Luci, de quienes recibí su comprensión y apoyo constante.

AGRADECIMIENTOS

A Dios por hacerme sentir su presencia siempre en cada instante de mi vida.

Al programa de becas del Ministerio de Ciencia, Tecnología e Innovación de Colombia, por el otorgamiento de la beca doctoral.

A la Universidad de Córdoba por la oportunidad de formación, con el otorgamiento de la comisión de estudio doctoral.

Al Programa de doctorado en Microbiología y Salud Tropical de la Universidad de Córdoba, bajo la coordinación del doctor Salim Mattar, por mi formación doctoral.

A la Clínica Salud Social IPS S.A.S. Sincelejo, Sucre, Colombia. Bajo la coordinación de la Dra. Eimi Brango Tarra por la donación de los aislados clínicos utilizados en este estudio.

Al doctor Gilmar Santafé Patiño mi director, por sus valiosos aportes y apoyarme incondicionalmente en el desarrollo de esta tesis.

Al profesor Alberto Angulo Ortíz, por su apoyo constante en el desarrollo de esta investigación.

A los coordinadores de laboratorios de investigación que gentilmente prestaron sus espacios y equipos en pro de este estudio:

Laboratorio de Productos Naturales, Universidad de Córdoba.
Laboratorio de Biomédica y Biología Molecular, Universidad del Sinú.
Laboratorio de Toxicología, Universidad de Córdoba.
Laboratorio de Investigación en Virología, Universidad del Norte.
Laboratorio de Investigaciones Microbiológicas y Biomédicas de Córdoba, Universidad de Córdoba.
Laboratorio de Biotecnología, Universidad de Córdoba.
Laboratorio de Cultivo celular, Universidad Federal de São Carlos, Brasil
Laboratorio de Aguas, Universidad de Córdoba.

La realización de esta tesis doctoral contó con la colaboración de muchas personas que me brindaron su apoyo a nivel laboral y/o personal por lo que quiero agradecerles de corazón:

A las doctoras: María Fernanda Yasnot y María Camila Velasco

A los biólogos, Leidy Mendoza, Jesús Sierra, Rosalía Seña, Ana Marcela Peñata, Daniela Sierra, Ricardo Berrio, Marcio de Avila y Yasmith Villegas.

Al químico, Luis Guillermo Cuadrado Durango.

A mis padres por su comprensión, amor y apoyo incondicional.

TABLA DE CONTENIDO

RESUMEN 3

ABSTRACT 5

CAPITULO 1. INTRODUCCIÓN 7

1.1. Problema y Justificación 7

1.2. OBJETIVOS 10

1.2.1. Objetivo general 10

1.2.2. Objetivos específicos 10

CAPITULO 2. MARCO TEÓRICO 11

2.1. Bases teóricas 11

2.1.1. Infecciones Asociadas a la Atención en Salud (IAAS) 11

2.1.2. Infecciones por Candida spp. 12

2.1.3. *Candida tropicalis* 13

2.1.4. Factores de virulencia en *Candida tropicalis* 13

2.1.5. Mecanismos de resistencia 14

2.1.6. La familia Annonaceae 15

2.1.7. El género Oxandra 16

2.1.8. *Oxandra xylopioides* Diels 16

2.1.9. Metabolitos secundarios 16

2.1.10. Isoespintanol 17

2.2. Antecedentes 19

CAPITULO 3. METODOLOGÍA 21

3.1. Aislamiento, Purificación, e Identificación del Isoespintanol 21

3.2. Ensayos de citotoxicidad del isoespintanol 21

3.2.1. Cultivo celular 22

3.2.2. Ensayo de MTT 22

3.2.3. Ensayo de viabilidad con CV 22

3.3. Sensibilidad de bacterias y levaduras del género Candida frente al isoespintanol. 23

3.3.1. Sensibilidad de bacterias frente al ISO 24

3.3.2. Sensibilidad de levaduras del género Candida frente al ISO 25

3.4. Filogenómica de *Candida tropicalis* 26

3.4.1. Extracción de ADN genómico 26

3.4.2. Secuenciación genómica de *C. tropicalis* WGS (Whole genome shotgun) 27

3.5. Ensayos de sensibilidad antifúngica de *C. tropicalis* 27

3.5.1. Ensayo de reducción de MTT 27

3.5.2. Curva de inhibición del crecimiento fúngico 28

3.6. Exploración de mecanismos de acción antifúngico del isoespintanol contra *C. tropicalis* mediante su acción sobre diferentes dianas 28

3.6.1. Efecto del ISO sobre la membrana celular fúngica 28

3.6.1.1. Ensayos con citometría de flujo empleando Ioduro de propidio (IP) 28
3.6.1.2. Pérdida de material intracelular a través de la membrana celular 29
3.6.1.3. Medida de pH extracelular 29
3.6.1.4. Ensayos LIVE/DEAD 30
3.6.1.5. Tinción con azul de Evans 30
3.6.1.6. Determinación del contenido de ergosterol 30
3.6.2. Efecto del ISO sobre la morfología e integridad de las células 31
3.6.3. Efecto del ISO sobre la producción de especies reactivas de oxígeno intracelular (EROi) 32
3.6.4. Efecto del ISO sobre el potencial de membrana mitocondrial (ΔΨm) 32
3.6.5. Efecto del ISO sobre biopelículas fúngicas 33
3.6.6. Efecto del ISO sobre la integridad de la pared celular 34
3.7. Efecto del ISO sobre el transcriptoma de *C. tropicalis* 35
3.7.1. Secuenciación de ARN y datos de recuentos de lectura. 35
3.7.2. Análisis bioinformático 35
CAPITULO 4. RESULTADOS Y DISCUSIÓN 37
CAPITULO 5. CONCLUSIONES 38
Referencias 39
Anexos 50

RESUMEN

Actualmente, la incidencia de Infecciones Asociadas a la Atención en Salud (IAAS) representa un grave problema por el aumento, no solo de los índices de morbilidad y mortalidad, sino también los costos en los servicios de salud a nivel global. Un factor importante en el aumento de la mortalidad de las IAAS es la creciente prevalencia de microorganismos multirresistentes, que pueden hacer que los fármacos sean ineficaces en el tratamiento de muchas enfermedades infecciosas comunes. Los hongos son uno de los principales agentes etiológicos de estas infecciones; infectan a un gran número de personas cada año aumentando las tasas de morbi-mortalidad especialmente en personas inmunocomprometidas. El número cada vez mayor de pacientes con riesgo de micosis invasivas tiene un manejo complejo, pues la intolerancia a los antifúngicos, las interacciones farmacológicas, los espectros de acción, la toxicidad limitante de la dosis, así como la expresión de mecanismos de resistencia a los antifúngicos actualmente disponibles, plantean un grave problema para su tratamiento.

El aumento creciente de infecciones por *Candida* spp. no albicans, sumado a la farmacoresistencia expresada y la alta mortalidad, especialmente en pacientes inmunocomprometidos, han hecho de las candidemias un gran desafío. Recientemente se ha reportado la eficacia de compuestos de origen vegetal con potencial antifúngico como una alternativa a ser empleada. Por esto, el objetivo de esta investigación fue evaluar el potencial antimicrobiano del isoespintanol (ISO), tomando como modelo la levadura patógena *Candida tropicalis*, estimar su capacidad para inhibir biopelículas y hacer una exploración a los mecanismos de acción antifúngica de este compuesto.

El ISO se obtuvo a partir del extracto bencínico de las hojas de *Oxandra xylopioides*, mediante hidrodestilación y cristalizaciones sucesivas, verificando su pureza por cromatografía de gases acoplada a espectrometría de masas (CG-EM). Los ensayos de microdilución, revelaron inhibición del crecimiento fúngico, mostrando valores de concentración mínima inhibitoria (CMI) entre 326.6 y 500 µg/mL. La capacidad de ISO para inhibir la formación de biopelículas fue, hasta de un 89.35%, y los ensayos de erradicación de biopelículas maduras, mostraron porcentajes de erradicación entre el 20.3 y 25.8%, después de 1 h de exposición, siendo en todos los

casos superiores al efecto causado por la anfotericina B (AFB). La citometría de flujo mostró cambios en la permeabilidad de la membrana plasmática, ocasionando la pérdida del material intracelular y el equilibrio osmótico; la microscopía electrónica de transmisión (MET), ratificó el daño en la integridad de la membrana plasmática. Además, el ISO indujo la producción de especies reactivas de oxígeno intracelular (EROi). Los experimentos con rodamina 123 (Rh123) y blanco de calcoflúor (CFW), analizados por citometría de flujo, mostraron la capacidad de ISO para causar disfunción mitocondrial y afectar la integridad de la pared celular respectivamente.

En cuanto al efecto del ISO, sobre el transcriptoma de *C. tropicalis*, el análisis de expresión génica diferencial permitió una visión integral de los cambios fisiológicos, estructurales y metabólicos de *C. tropicalis* que ocurren en presencia de ISO. Se encontraron 186 genes expresados diferencialmente (GED). En particular, ~ 85% de los GED están experimentando inducción en su expresión. Interesantemente, 159 genes inducidos están relacionados principalmente con la biosíntesis de ergosterol, el plegamiento de proteínas, la respuesta al daño del ADN, el daño de la pared celular, la alteración de la actividad mitocondrial y la respuesta celular a las sustancias orgánicas. Se identificaron 27 genes reprimidos relacionados con la traducción citoplasmática, el punto de control de daños en el ADN, proteínas de membrana y procesos biológicos que implican: transmetilación, transulfuración y transpropilaminación.

En general, esta investigación resalta que la actividad antifúngica de ISO es un proceso complejo que involucra múltiples objetivos de acción. En conjunto, estos resultados establecieron una descripción completa de posibles dianas moleculares en *C. tropicalis* que podrían explorarse en terapias antifúngicas y destacan posibles enfoques terapéuticos para vencer las infecciones generadas por estas levaduras patógenas. Además, se aporta conocimiento nuevo sobre el potencial antimicrobiano del monoterpeno ISO, generando una base para estudios futuros y fortaleciendo una línea de investigación que contribuye en la búsqueda de compuestos bioactivos de fuentes naturales con potencial antimicrobiano en la flora cordobesa.

ABSTRACT

Currently, the incidence of Healthcare Associated Infections (HAI) represents a serious problem due to the increase, not only in morbidity and mortality rates, but also in the costs of health services globally. An important factor in the increased mortality of HAIs is the increasing prevalence of multidrug-resistant microorganisms, which can render drugs ineffective in the treatment of many common infectious diseases. Fungi are one of the main etiological agents of these infections; They infect a large number of people each year, increasing morbidity and mortality rates, especially in immunocompromised people. The increasing number of patients at risk of invasive mycoses has complex management, since intolerance to antifungals, drug interactions, spectrums of action, dose-limiting toxicity, as well as the expression of resistance mechanisms to antifungals. Currently available antifungals pose a serious problem for their treatment.

The increasing increase in infections by *Candida* spp. non-albicans, further to the expressed drug resistance and high mortality, especially in immunocompromised patients, have made candidemias a great challenge. Recently, the effectiveness of compounds of plant origin with antifungal potential has been reported as an alternative to be used. Therefore, the objective of this research was to evaluate the antimicrobial potential of Isoespintanol (ISO), taking the pathogenic yeast *Candida tropicalis* as a model, estimate its capacity to inhibit biofilms and explore the mechanisms of antifungal action of this compound.

The ISO was obtained from the benzine extract of the leaves of *Oxandra xylopioides*, through hydrodistillation and successive crystallizations, verifying its purity by gas chromatography coupled to mass spectrometry (GC-MS). Microdilution assays revealed inhibition of fungal growth, showing minimum inhibitory concentration (MIC) values between 326.6 and 500 μg/mL. The capacity of ISO to inhibit the formation of biofilms was up to 89.35%, and the eradication tests of mature biofilms showed eradication percentages between 20.3 and 25.8%, after 1 h of exposure, being in all cases superior to the effect caused by amphotericin B (AFB). Flow cytometry showed changes in the permeability of the plasma membrane, causing the loss of intracellular material and osmotic balance; Transmission electron microscopy (TEM) confirmed the damage to the integrity of the plasma membrane. Furthermore, ISO

induced the production of intracellular reactive oxygen species (ROSi). Experiments with rhodamine 123 (Rh123) and calcofluor white (CFW), analyzed by flow cytometry, showed the ability of ISO to cause mitochondrial dysfunction and affect cell wall integrity respectively.

Regarding the effect of ISO on the transcriptome of *C. tropicalis*, the differential gene expression analysis allowed a comprehensive view of the physiological, structural and metabolic changes of *C. tropicalis* that occur in the presence of ISO. 186 differentially expressed genes (DEG) were found. In particular, ~85% of DEGs are undergoing induction in their expression. Interestingly, 159 induced genes are mainly related to ergosterol biosynthesis, protein folding, DNA damage response, cell wall damage, alteration of mitochondrial activity, and cellular response to organic substances. 27 repressed genes were identified related to cytoplasmic translation, the DNA damage checkpoint, membrane proteins and biological processes involving: transmethylation, transsulfuration and transpropylamination.

Overall, this research highlights that the antifungal activity of ISO is a complex process involving multiple targets of action. Together, these results established a comprehensive overview of potential molecular targets in *C. tropicalis* that could be explored in antifungal therapies and highlight potential therapeutic approaches to overcome infections generated by these pathogenic yeasts. In addition, new knowledge is provided about the antimicrobial potential of the ISO monoterpene, generating a basis for future studies and strengthening a line of research that contributes to the search for bioactive compounds from natural sources with antimicrobial potential in the flora of Córdoba.

CAPITULO 1. INTRODUCCIÓN

1.1. Problema y Justificación

Las enfermedades infecciosas ocasionadas principalmente por patógenos resistentes a los antimicrobianos se han convertido en la actualidad en una amenaza para la salud y el desarrollo mundial. Entre estos patógenos se incluyen principalmente las cepas bacterianas MDR (multirresistentes) llamadas ESKAPE (*Enterococcus faecium*, *Staphylococcus aureus*, *Klebsiella pneumoniae*, *Acinetobacter baumannii*, *Pseudomonas aeruginosa* y especies de *Enterobacter*), las cuales son responsables de los principales casos de infecciones adquiridas en hospitales (IAAS) a nivel mundial y han sido incluidos en la lista de 12 bacterias de la Organización Mundial de la Salud (OMS), contra las cuales el desarrollo de nuevos antibióticos es vital. No sólo provocan estancias hospitalarias prolongadas, sino también mayores costos médicos y una mayor mortalidad (1). Si bien, las bacterias Gram negativas principalmente, y las bacterias Gram positivas multiresistentes son la causa primordial de las IAAS, los hongos especialmente del género *Candida* generan un gran desafío en la práctica médica.

Las infecciones fúngicas constituyen una continua y grave amenaza para la salud humana especialmente en personas inmunocomprometidas, donde la incidencia de candidiasis sistémica ha aumentado sustancialmente en los últimos años (2–6). Hoy día, estas infecciones han captado significativa atención en la ciencia médica y farmacéutica, debido al aumento rápido de su incidencia, con altas tasas de morbilidad y mortalidad especialmente en pacientes hospitalizados. Actualmente, más de mil millones de personas se ven afectadas por estas infecciones (7) y más de 1.5 millones de muertes son producidas al año (8). Estudios recientes estiman que las infecciones causadas por hongos, que incluyen especialmente a *Candida* spp., son de difícil tratamiento y la mortalidad asociada sigue siendo muy alta, incluso cuando existen tratamientos antifúngicos disponibles (9). Más del 90% de personas infectadas con VIH desarrollan enfermedades debilitantes por especies del género *Candida*, siendo estos, los patógenos más comunes aislados de pacientes en cuidados intensivos. A nivel regional, estudios en la ciudad de Montería – Córdoba, han reportado una prevalencia del 47.8 % de candidiasis, destacándose como la micosis

con mayor incidencia y prevalencia en esta población en el periodo de 2011-2015 (10). La candidemia es una de las micosis oportunistas más frecuentes en todo el mundo, *C. albicans* es considerada la levadura patógena más prevalente y de mayor importancia clínica (7). Sin embargo, se ha observado un importante cambio epidemiológico en las últimas décadas; especies como *C. glabrata*, *C. tropicalis*, *C. krusei*. *C. parapsilosis*, *C. auris*, se han empezado a aislar con frecuencia en candidemias graves alrededor del mundo (11). *Los Centros para el Control y la Prevención de Enfermedades* predicen, además, que estas infecciones plantean una amenaza que empeorará y puede volverse urgente (12).

Candida tropicalis, ha emergido como una de las *Candida* spp., no albicans más importantes, debido a su alta incidencia en candidiasis sistémica y a una mayor resistencia a los antifúngicos de uso común (13). Esta levadura ha sido considerada ampliamente, la segunda especie del género *Candida* más virulenta, solo precedida por *C. albicans* (14); es un hongo oportunista capaz de propagarse a órganos vitales (15). *Candida tropicalis*, es reconocida como una fuerte productora de biopelículas, superando a *C. albicans* en la mayoría de los estudios; asimismo, produce una amplia gama de otros factores de virulencia, que incluyen: la adhesión (a células epiteliales, células endoteliales, otras superficies del huésped y dispositivos médicos), la secreción de enzimas líticas, y la llamada morfogénesis expresada por esta levadura; *C. tropicalis* puede ser el segundo o tercer agente etiológico de candidemia más importante, específicamente en países de América Latina y Asia (14). En Colombia, la candidemia es una causa frecuente de infección en el torrente sanguíneo, en especial en Unidades de Cuidado Intensivo (UCI); representa el 88% de infecciones fúngicas en pacientes hospitalizados con una mortalidad entre el 36% y 78%; su incidencia es mayor a la reportada en países desarrollados e incluso en otros países de Latinoamérica (16). Se ha documentado que *C. tropicalis* se asocia con una mayor mortalidad en comparación con *C. albicans* y otras especies de *Candida* no albicans, mostrando al parecer, un mayor potencial de diseminación en individuos neutropénicos; esta levadura, se asocia a malignidad, especialmente pacientes que requieren cateterismo prolongado, reciben antibióticos de amplio espectro o padecen cáncer (17).

En este contexto, la búsqueda y desarrollo de nuevos compuestos con potencial antimicrobiano, que sean eficaces y seguros, así, como el desarrollo de nuevas

estrategias de tratamiento con una mejor tolerancia del huésped es apremiante hoy día (18). Desde la antigüedad, los productos naturales han hecho una importante contribución a la farmacoterapia especialmente en enfermedades infecciosas y cáncer; se estima que entre el 65 y el 80 % de la población mundial en los países en desarrollo depende esencialmente de plantas para la atención primaria de salud debido a la falta de acceso a medicina. Además, entre el 25 y el 30 % de todos los medicamentos disponibles como terapia se derivan de productos naturales, lo que mueve alrededor de 20000 millones de dólares anuales en el mercado farmacéutico mundial (19,20). En este escenario, las plantas juegan un rol primordial como fuente de metabolitos especializados con propiedades medicinales reconocidas (21,22). Debido a su amplia diversidad química, estos metabolitos pueden ser usados directamente como compuestos bioactivos, como prototipos de drogas o ser usados como herramientas farmacológicas para diferentes blancos (23). Además, la eficacia potencial y los efectos secundarios mínimos o nulos son las ventajas clave de los productos de origen vegetal, lo que los convierte en opciones adecuadas para tratamientos médicos (1).

Basado en lo anterior, un metabolito que ha resultado de gran interés, es el isoespintanol [ISO] (2-isopropil-3,6-dimetoxi-5-metilfenol), un monoterpeno extraído de *Oxandra xylopioides* (Annonaceae), al cual se le ha reportado su efecto antioxidante (24), antiinflamatorio (25), antiespasmódico (26), vasodilatador (27), crioprotector en semen canino (28), así, como su actividad insecticida (29) y antifúngica contra fitopatógenos (30). Además, el efecto del ISO en el corazón durante perfusión isquémica también ha sido reportado, indicando su efecto cardioprotector (31). Sin embargo, a pesar de estas múltiples acciones biológicas, el potencial antimicrobiano del ISO contra patógenos humanos no había sido reportado. De este modo, nosotros hipotetizamos que el ISO podría tener actividad antimicrobiana contra patógenos humanos, especialmente contra levaduras del género *Candida*.

La presente investigación tuvo como propósito evaluar el potencial antimicrobiano del ISO, tomando como modelo la levadura patógena *C. tropicalis*, estimar su capacidad para inhibir biopelículas y hacer una exploración a los mecanismos de acción antifúngica de este compuesto, para así, dar respuesta a las preguntas de investigación: ¿Cuál es el efecto del ISO contra bacterias y levaduras del género

Candida? ¿Cuál es el mecanismo de acción antifúngica del ISO? Nuestros resultados aportan conocimiento nuevo sobre el potencial antimicrobiano del ISO generando una base para estudios futuros y de esta forma contribuir en la búsqueda de compuestos bioactivos de fuentes naturales con potencial antimicrobiano en la flora cordobesa.

1.2. OBJETIVOS

1.2.1. Objetivo general

Evaluar el potencial antifúngico del isoespintanol extraído de *Oxandra xylopioides* contra aislamientos clínicos de *Candida tropicalis*.

1.2.2. Objetivos específicos

- Obtener isoespintanol presente en *Oxandra xylopioides* recolectada en el departamento de Córdoba.
- Evaluar la citotoxicidad del isoespintanol sobre células VERO a través de los métodos de MTT y cristal violeta.
- Realizar un estudio exploratorio de sensibilidad de bacterias y levaduras del género *Candida* frente al isoespintanol.
- Identificar a nivel molecular la especie *C. tropicalis* a través de un estudio taxonómico basado en genoma completo, usando librerías Truseq Nano DNA y la plataforma Illumina NovaSeq.
- Determinar el potencial antifúngico del isoespintanol contra *C. tropicalis* calculando el porcentaje de inhibición del crecimiento, empleando el método de microdilución.
- Explorar el mecanismo de acción antifúngica del isoespintanol contra *C. tropicalis*, mediante su acción sobre diferentes dianas.
- Analizar el efecto del isoespintanol sobre el transcriptoma de *C. tropicalis*, mediante el análisis de la expresión diferencial de genes.

CAPITULO 2. MARCO TEÓRICO

2.1. Bases teóricas

2.1.1. Infecciones Asociadas a la Atención en Salud (IAAS)

Las Infecciones Asociadas a la Atención en Salud (IAAS), son aquellas que surgen en cualquier entorno de hospitalización o ambulatorio y aparezcan 48 horas después de la hospitalización, o dentro de los 30 días posteriores a la recepción de la atención médica, o hasta 90 días después de haber sido sometidos a ciertos procedimientos quirúrgicos (32). La incidencia de estas infecciones, las ha convertido en un problema desafiante en la práctica médica, sus altas tasas de mortalidad y los costos financieros en los hospitales, representan un grave problema para los sistemas de salud a nivel mundial (33). En la actualidad, los médicos se enfrentan a patógenos que tienen un cuadro de determinantes de resistencia que restringen severamente las opciones terapéuticas; la plasticidad genética de los microbios les permite adaptarse a los factores estresantes a través de mutaciones, la adquisición o el intercambio de material genético y la modulación de la expresión genética que conduce a la resistencia a prácticamente cualquier antimicrobiano utilizado en la práctica clínica (34); la diseminación e incremento excesivo en los últimos años de cepas con altos niveles de resistencia a fármacos y el aumento de infecciones causadas por cepas New Delhi, empeoran esta situación (33–36).

En los Estados Unidos las IAAS, son un factor importante en la morbilidad de los pacientes, constituyen la sexta causa principal de muerte, superando las muertes por SIDA, cáncer y accidentes de tránsito (32). Las bacterias Gram negativas multirresistentes representan el motor principal de estas infecciones; en la última década se ha observado un aumento de la incidencia de IAAS inducidas por Gram negativos, bacterias resistentes a múltiples fármacos incluidas las Enterobacteriaceae y bacterias Gram negativas no fermentadoras (*Pseudomonas aeruginosa* y *Acinetobacter baumannii*). Algunas de estas bacterias son naturalmente resistentes a ciertas familias de antibióticos y otras, cuando se someten a antibioticoterapia prolongada, eventualmente desarrollan resistencia contra fármacos a los que eran sensibles anteriormente y pueden transmitir esta resistencia a su descendencia; la aparición de multirresistencia en estas bacterias es un

problema terapéutico crucial para los pacientes y empeora el pronóstico de su enfermedad (37). En los últimos años, la *Infectious Diseases Society of America* ha destacado una facción de bacterias resistentes a los antibióticos (*Enterococcus faecium*, *Staphylococcus aureus*, *Klebsiella pneumoniae*, *Acinetobacter baumannii*, *Pseudomonas aeruginosa* y Enterobacter spp.) – acrónimo denominados "los patógenos ESKAPE", capaces de "escapar" de la acción biocida de los antibióticos, representando nuevos paradigmas en patogénesis, transmisión y resistencia (38). Los hongos igualmente son causa importante de IAAS destacándose especialmente las infecciones causadas por especies del género *Candida*, las cuales en los últimos años han aumentado su incidencia, acrecentando las tasas de morbilidad y mortalidad debido a la resistencia a antifúngicos expresada por estas levaduras patógenas (3,5,39–43); las personas inmunodeprimidas, con antibioticoterapia prolongada o que están bajo tratamiento médico invasivo son las más vulnerables a las infecciones por este tipo de patógenos.

2.1.2. Infecciones por Candida spp.

Los hongos son causa importante de infecciones oportunistas. Infectan a un sinnúmero de personas cada año elevando los índices de morbilidad y mortalidad, especialmente en personas inmunocomprometidas; en los últimos años, estas infecciones han captado significativa atención en la ciencia médica y farmacéutica, debido al aumento rápido de su incidencia. Actualmente, más de mil millones de personas se ven afectadas por infecciones fúngicas (7) y más de 1.5 millones de muertes son producidas al año (8). Estudios recientes estiman que las infecciones causadas por hongos, que incluyen especialmente a *Candida* spp., son de difícil tratamiento y la mortalidad asociada sigue siendo muy alta, incluso cuando existen tratamientos antifúngicos disponibles (9). Las *Candida* spp., están asociadas con altas tasas de resistencia antifúngica y una mayor capacidad para formar biopelículas, que hacen el tratamiento de estas infecciones difícil; según los Institutos Nacionales de Salud de EE.UU., las biopelículas microbianas representan el 65% de las infecciones nosocomiales y más del 80% de las crónicas (39). Más del 90% de personas infectadas con VIH desarrollan enfermedades debilitantes por especies del género *Candida*, siendo estos, los patógenos más comunes aislados de pacientes en cuidados intensivos.

La candidemia es una de las micosis oportunistas más frecuentes en todo el mundo, *C. albicans* es considerada la levadura patógena más prevalente y de mayor importancia clínica (7). Sin embargo, se ha observado un importante cambio epidemiológico en las últimas décadas; especies como *C. glabrata* (5,44), *C. tropicalis* (6,45,46), *C. krusei* (41), *C. parapsilosis* (42,47), *C. auris* (48–50), entre otras, se han empezado a aislar con frecuencia en candidemias graves alrededor del mundo (11). El creciente número de pacientes con riesgo de micosis invasivas tiene un manejo complejo, pues, las interacciones farmacológicas, la intolerancia de los antifúngicos actualmente disponibles y la resistencia innata o adquirida plantean un problema para su tratamiento, el cual está restringido a cinco clases establecidas de medicamentos antimicóticos; el *Centers for Disease Control and Prevention* (CDC) predice además, que estas infecciones plantean una amenaza que empeorará y puede volverse urgente (12).

2.1.3. Candida tropicalis

Candida tropicalis se encuentra entre las especies de *Candida* más importantes en términos de epidemiología, virulencia y resistencia. A nivel mundial, la incidencia de la candidemia causada por *C. tropicalis* oscila entre el 3% y el 66%, con una alta incidencia en las regiones tropicales y subtropicales del mundo (51); se considera altamente invasiva con la capacidad de inducir un daño tisular significativo (52). *Candida tropicalis* es una especie clínicamente relevante, se asocia con una mayor mortalidad en comparación con *C. albicans* y otras especies de *Candida* no albicans, mostrando al parecer, un mayor potencial de diseminación en individuos neutropénicos; esta levadura, se asocia a malignidad, especialmente en pacientes que requieren cateterismo prolongado, reciben antibióticos de amplio espectro o padecen cáncer (17).

2.1.4. Factores de virulencia en Candida tropicalis

Varios mecanismos de patogenicidad se han asociado con *C. tropicalis*, estos incluyen: la capacidad de adhesión a superficies abióticas, células y tejidos humanos; se conoce que estas levaduras tienen varias adhesinas (proteínas especiales de la pared celular), que les permiten la adhesión a sustratos específicos. Varios estudios

demostraron la capacidad de *C. tropicalis* de adherirse y, en consecuencia, formar biopelículas en sustratos clínicamente relevantes como dispositivos médicos, y en diferentes situaciones ambientales, tanto *in vitro* como *in vivo*. La formación de hifas y la producción de enzimas que le ayudan a penetrar en los tejidos más profundos, además de la capacidad y diseminación son fundamentales en el establecimiento de la infección (14,17). Además, *C. tropicalis* es bien conocida por la capacidad de formar fuertes biopelículas, que varían según el origen de la infección (46,53); estas biopelículas asocian a estos patógenos con una alta mortalidad, posiblemente por la baja permeabilidad de la matriz a los fármacos antifúngicos convencionales (54).

2.1.5. Mecanismos de resistencia

Las cepas de *Candida* resistentes a los medicamentos plantean una amenaza para los pacientes infectados y tiene impactos clínicos importantes a nivel global. Los mecanismos implicados en la resistencia de *C. tropicalis* son diversos y pueden implicar, entre otros factores, disminución de afinidad por la molécula diana, un aumento o disminución en la cantidad de moléculas diana, y la extrusión del fármaco desde el interior de la célula a través de bombas de expulsión. Comúnmente, estos procesos involucran mutaciones o deleciones en genes específicos y alteraciones en la expresión génica, como la sobreexpresión (43,55). De esta forma, la creciente resistencia antifúngica a los azoles observada en estas levaduras patógenas, esta principalmente asociada con la sobreexpresión de ERG11, ERG11 y/o mutaciones en ERG3 (genes involucrados en la biosíntesis de ergosterol) y actividad de la bomba de expulsión. Aparte de esto, la resistencia de *C. tropicalis* a equinocandinas, anfotericina B, y flucitosina también se ha informado (56). En los últimos años la resistencia a los antifúngicos de *C. tropicalis* se ha incrementado gradualmente, se ha reportado que la resistencia a los azoles es principalmente debida a mutación o sobreexpresión no solo del gen que codifica la ergosterol sintasa (ERG11) si no también el gen que codifica el factor de transcripción de la familia de zinc UPC2 (6,57). En Colombia, se han observado diferentes tasas de resistencia a los antimicóticos. Las variaciones en la resistencia al fluconazol se deben fundamentalmente al tipo de técnica utilizada y a los pacientes observados. Las tasas de resistencia también varían según la especie identificada, ya que *C. krusei* es intrínsecamente resistente al fluconazol y *C. glabrata* tiene sensibilidad disminuida

frente a este. Sin embargo, se han identificado aislamientos con mutaciones de resistencia en nuestro medio (16). Consecuentemente, el interés por los productos naturales como fuentes de fármacos ha aumentado sustancialmente, particularmente para abordar la resistencia antimicrobiana (58). Algunos compuestos bioactivos derivados de plantas tienen la capacidad de revertir la resistencia a los antibióticos y mejorar la acción sinérgica con los agentes antibióticos actuales. Por lo tanto, el avance de los agentes farmacológicos basados en bioactivos puede ser un método auspicioso para el tratamiento de infecciones resistentes a los antibióticos (59).

2.1.6. La familia Annonaceae

La familia Annonaceae es una de las angiospermas más antiguas, considerada en los bosques tropicales como una de las familias de plantas más diversas; ha sido empleada por mucho tiempo en medicinas tradicionales para curar diversas afecciones patológicas, como mordedura de serpientes, analgésico, diarrea, disentería, dolor de artritis y neuralgia etc. Especies de esta familia tienen gran relevancia por su amplia gama de actividad antiinflamatoria, estudios *in vitro* e *in vivo* que incluyen compuestos aislados, así como extractos crudos rudimentarios han mostrado una potente actividad en todo tipo de inflamación. El análisis fitoquímico de esta familia ha informado la presencia de alcaloides, flavonoides, triterpenos, diterpenos, glucósidos de diterpenflavonas, esteroles, lignanos y acetogeninas. Numerosos estudios han resaltado las actividades farmacológicas pleotrópicas de los extractos crudos y compuestos aislados de especies de esta familia (60). La base de datos del Global Biodiversity Information Facility (GBIF) enumera 162 géneros y 3049 especies de la familia Annonaceae, distribuidas principalmente en la región tropical y subtropical de América Central y del Sur, África, Asia y Australia (61). Se han reportado para Colombia alrededor de 240 especies pertenecientes a 30 géneros (62), no obstante, el número de especies en Colombia aumentará, pues se siguen describiendo nuevos taxones.

2.1.7. El género Oxandra

Dentro del género se reconocen 27 especies, la mayoría se encuentran en la zona tropical de América del Sur, mientras que unos pocos se encuentran en México y América Central y dos en las Indias Occidentales (Antillas Mayores y Menores). Las especies de *Oxandra* son principalmente árboles, los más grandes de hasta 50 m de alto. Más de la mitad son árboles pequeños, de menos de 20 m de altura, pero sólo unas pocas especies pueden seguir siendo arbustos de menos de 3 m de altura, por ejemplo *O. rheophytica* y *O. surinamensis*. Algunas de las especies más altas son *O. sphaerocarpa*, *O. venezuelana* y *O. xylopioides*, donde todos pueden alcanzar una altura de 40 m o más. Los árboles de *Oxandra* son bastante esbeltos, sólo en siete especies el tronco puede superar los 50 cm de diametro, como, *O. espintana*, *O. martiana*, *O. polyantha*, *O. saxicola*, *O. sphaerocarpa*, *O. venezuelana* y *O. xylopioides* (63).

2.1.8. Oxandra xylopioides Diels

De *O. xylopioides* hasta la fecha son pocos los metabolitos aislados (24,64), sin embargo, se han encontrado en grandes cantidades. Los nombres vernaculares para esta especie incluyen: carguero, yaya, entre otros; *O. xylopioides* es una especie muy recolectada, fácilmente reconocible por sus hojas estrechas (parecidas a ciertas especies de *Xylopia*), que son totalmente verruculosas (verrugas que cubren completamente la superficie de la hoja) y basalmente proporcionado con dos proyecciones en forma de dientes. Además, la nervadura de la hoja es apenas visible (63).

2.1.9. Metabolitos secundarios

El metabolismo secundario de la planta se define como la ruta y los productos del metabolismo de moléculas pequeñas que no son esenciales para la supervivencia del organismo. En la naturaleza, una variedad de vías del metabolismo secundario, generan una variedad de compuestos defensivos de las plantas llamados metabolitos secundarios (MS). Los MS son las moléculas prescindibles para el metabolismo y el crecimiento de las plantas, sin embargo, la amplia variedad de productos secundarios son componentes clave para que las plantas interactúen con el medio ambiente en la adaptación a condiciones de estrés biótico y abiótico. Los

MS de las plantas no solo son una variedad útil de productos naturales, sino también una parte importante del sistema de defensa de las plantas contra los ataques de patógenos y el estrés ambiental. Con notables actividades biológicas, los MS de plantas se utilizan cada vez más como ingredientes de medicamentos y aditivos alimentarios con fines terapéuticos, aromáticos y culinarios (65). Para la especie *O. xylopioides* son pocos los metabolitos secundarios aislados, estos incluyen alcaloides de tipo azafluorenos (64) y terpenos como el isoespintanol y berenjenol (25).

2.1.10. Isoespintanol

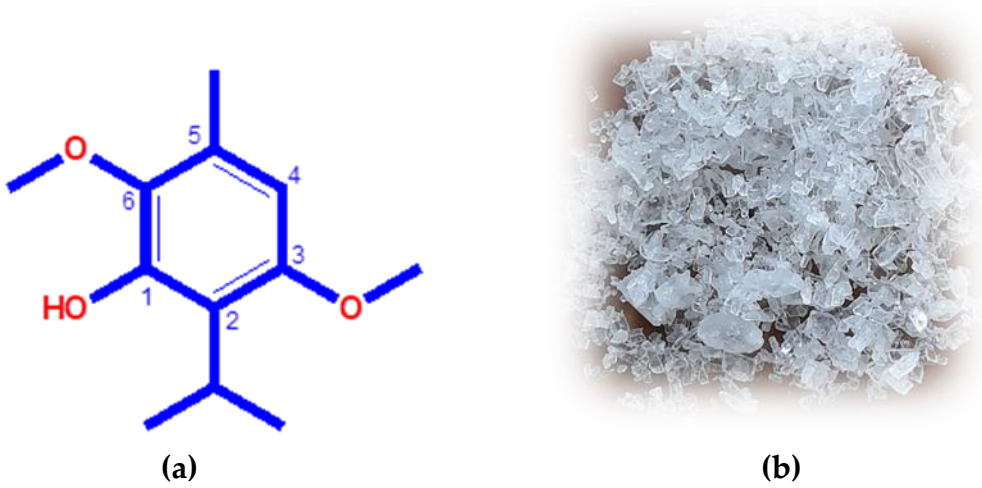

(a) **(b)**

Figura 1. (a) Estructura química del Isoespintanol, un monoterpeno aromático. (b) Cristales de Isoespintanol obtenidos por lavado con n-hexano.

El ISO (2-isopropil-3,6-dimetoxi-5-metilfenol), es un monoterpeno aromático, sólido, incoloro y cristalino de peso molecular 210 g/mol, obtenido por primera vez de las partes aéreas de *Eupatorium saltense* (66) cuya síntesis igualmente ha sido reportada (67). También, ha sido extraído de las hojas de *O. xylopioides* Diels (Annonaceae). El ISO es bien conocido por su actividad antioxidante (24,68–70), la cual ha sido probada en diferentes medios, mostrando que el ISO reacciona lentamente cuando atrapa radicales libres, por lo tanto su efecto protector es tardío permitiendo un posible uso en la conservación de alimentos con alto contenido de grasas o sistemas alimenticios emulsificados. Por otra parte, su actividad antioxidante en semen equino sometido a criopreservación también ha sido reportada (70).

La actividad antiinflamatoria (25) y antiespasmódica (26) del ISO de igual forma han sido documentadas; estudios con ratas, demuestran que el ISO es un muy buen antiespasmódico intestinal, urinario y uterino, con mayor potencia que las otras drogas utilizadas en la terapéutica. Además, el ISO ha mostrado efecto vasodilatador (27), a través de vías dependientes de NO sugiriendo que la inhibición de la entrada de calcio podría ser el mecanismo implicado. Asimismo, el ISO ha sido reportado como crioprotector en semen canino (28), reduciendo cambios nocivos en los espermatozoides y estrés oxidativo en el semen descongelado.

La actividad insecticida del ISO contra el gusano cogollero *Spodoptera frugiperda*, que ataca cultivos de maíz, soya, algodón, arroz, pastos, caña de azúcar, fríjol y tabaco también ha sido investigada (28), indicando que los mayores porcentajes de mortalidad de larvas de *S. frugiperda* se lograron con las dosis más altas ensayadas (900 y 2700 ppm) del ISO. Otros estudios, han revelado la actividad antifúngica contra hongos fitopatógenos del género *Coletotricum* (*Colletotrichum gloeosporioides* y *Colletotrichum acutatum*), mostrando un porcentaje de inhibición fúngico del 44.6 % a una concentración de 100 ppm; indicando este estudio, que el empleo del ISO podría ser beneficioso en la industria agrícola para el tratamiento de enfermedades por hongos, ocasionadas por especies de este género (30).

Por otra parte, el efecto del ISO en el corazón durante perfusión isquémica también ha sido reportado, indicando su efecto cardioprotector; en un modelo de isquemia global redujo la muerte celular, la disfunción contráctil y el deterioro de la irrigación (31). Estudios de citotoxicidad han mostrado que el ISO a concentraciones entre 3-1620 μM muestran efecto protector sobre el daño del ADN de los linfocitos humanos inducida por H_2O_2 y no muestran efectos citotóxicos o genotóxicos a concentraciones entre 3-80 μM, lo que sugiere que bajas concentraciones pueden usarse como antioxidante sin esperar efectos negativos en la salud (71). Asimismo, experimentos (ISO 100 μM) con macrófagos RAW 264.7 murinos, no mostraron ningún efecto sobre la viabilidad celular, indicando su posible uso como un aditivo alimentario seguro (72).

2.2. Antecedentes

En la última década muchas investigaciones han reportado las propiedades anti-Candida de productos naturales aislados de diferentes fuentes, que incluyen principalmente las plantas; la mayoría de estos compuestos son alcaloides, policétidos, terpenoides, fenoles, macrólidos y péptidos. Entre ellos, los terpenoides son el grupo más abundante, a los cuales se ha reportado su acción contra *Candida* spp., incluida *C. tropicalis* (73). Sin embargo, del monoterpeno ISO, aparte de nuestros hallazgos (74–76), no existen reportes sobre su potencial contra levaduras patógenas de humanos.

Iraji y colaboradores (77), mostraron el potencial antifúngico de varios monoterpenos, incluidos carvona, limoneno, pineno, mentona, mentol, alcanfor, tujona, citronelol y piperitona contra aislados clínicos de *Candida* spp., incluida *C. tropicalis*. Así mismo, Gallucci y colaboradores (78), reportan esta actividad del eugenol y de los monoterpenos timol y carvacrol contra estos patógenos.

Xiong y colaboradores (79), mediante parámetros transcriptómicos, reportaron actividad antifúngica del monoterpeno D-limoneno, indicando que inhibe a *C. tropicalis* por interrupción del metabolismo celular. Así mismo, Yu y colaboradores (80), indicaron otros mecanismos de acción de este monoterpeno contra *C. tropicalis*.

Kowalczyk y colaboradores (81), han reportado además actividad antibiopelículas del monoterpeno timol contra especies de *Candida* indicando el mecanismo de acción de este compuesto. Dias de Castro (82); Marchese (83) y Jafri (84) indicaron, también, la interacción sinérgica del timol y antifúngicos convencionales contra las biopelículas de patógenos que incluyen a *C. tropicales*.

Oliveira Lima y colaboradores (85), reportaron actividad antifúngica del monoterpeno carvacrol contra *C. albicans* indicando el mecanismo de acción. Además, su actividad contra biopelículas de *C. tropicalis* también fue reportada al encapsularse este monoterpeno con nanopartículas de quitosano (86).

Chatrath y colaboradores (87), mostraron actividad antifúngica y antibiopelículas del monoterpeno citral contra *C. tropicalis*.

Silva y colaboradores (88), revelaron actividad antifungica de los monoterpenos (R)-(+)-β-citronelol y (S)-(−)-β-citronelol contra *C. tropicalis* y *C. albicans.* Por su parte, Kim y colaboradores (89), evidenciaron la actividad inhibitoria y antibiopelículas de hinokitiol, contra *Candida* spp., incluida *C. tropicalis*.

Lemos y colaboradores (90) documentaron otros compuestos como la escopoletina, una cumarina antifúngica, con eficacia contra *C. tropicalis* resistente a múltiples fármacos, y propiedades que afectan tanto las formas planctónicas como las de biopelículas de este patógeno. Kumar y colaboradores (91) reportaron la excavarina A, otra cumarina, también con actividad antifúngica contra este patógeno.

CAPITULO 3. METODOLOGÍA

Objetivo 1. *Obtener isoespintanol presente en Oxandra xylopioides recolectada en el departamento de Córdoba.*

3.1. Aislamiento, Purificación, e Identificación del Isoespintanol

El ISO fue obtenido a partir de hojas de *O. xylopioides*, recolectadas de un espécimen ubicado en el municipio de Montería, departamento de Córdoba, con las coordenadas 08°48'17'' latitud norte y 75°42'07'' longitud oeste. Un ejemplar de herbario se encuentra depositado en el Jardín Botánico Joaquín Antonio Uribe de la ciudad de Medellín, Colombia, con el número de colección JAUM 037849. El aislamiento y purificación se realizó a partir del extracto bencínico de las hojas por hidrodestilación del mismo con una mezcla diclorometano/agua 1:5, seguida de extracción con diclorometano, cristalizaciones sucesivas con *n*-hexano y monitoreo por cromatografía en capa delgada siguiendo la metodología descrita por (92), con algunas modificaciones. La identificación se realizó mediante cromatografía de gases acoplada a espectrometría de masas (CG-EM), por comparación de su tiempo de retención y patrón de fragmentación de masas, con los de una muestra auténtica de ISO purificada e identificada en nuestro laboratorio.

Objetivo 2. *Evaluar la citotoxicidad del isoespintanol sobre células VERO a través de los métodos de MTT y cristal violeta.*

3.2. Ensayos de citotoxicidad del isoespintanol

Los ensayos de citotoxicidad se realizaron utilizando las células epiteliales inmortalizadas del riñón de mono verde africano [*Cercopithecus aethiops*] (VERO) a través de los métodos de cristal violeta (CV) y Bromuro de 3-(4,5-dimetiltiazol-2-il) -2,5-difeniltetrazolio) [MTT].

3.2.1. Cultivo celular

Las células fueron cultivadas en el medio RPMI 1640 suplementado con 10% de suero fetal bovino (SFB) y 1% de penicilina/estreptomicina, y fueron mantenidas en una atmósfera humidificada con 5% de CO_2 a 37°C. Se realizaron recambios de medio cada 2-3 días para su mantenimiento. Se hicieron subcultivos dos veces por semana hasta que alcanzaron aproximadamente el 80% de confluencia para la realización de los ensayos. Las células VERO son una de las líneas celulares de mamíferos, que por su homología con las células humanas y su fácil cultivo son empleadas comúnmente como un modelo útil para evaluar *in vitro*, la actividad citotóxica de productos naturales (19,93).

3.2.2. Ensayo de MTT

El ensayo de MTT se basa en la capacidad que tienen las enzimas deshidrogenasas de células metabólicamente viables para reducir los anillos de tetrazolio y formar cristales de formazán; en consecuencia, el número de células viables es directamente proporcional al nivel de formazán producido (94–96). Para ello, las células VERO se sembraron en microplacas de 96 pozos (Nest®) a una densidad de $4x10^4$ células/cm^2, lo que permitió su adhesión y proliferación durante 24 h. Pasado este tiempo, las células se incubaron con medio RPMI 1640 que contenía diferentes concentraciones del ISO (9.76 a 2500 μg/mL) durante 24 horas. Luego de la incubación se retiraron los tratamientos, y se añadieron 100 μL de MTT a cada pozo en una concentración de 0.125 mg/mL, la placa se incubó a 5% de CO_2 a 37 °C durante 4 h. Posteriormente, se descartó el MTT y los cristales de formazán depositados en el fondo de cada pozo se disolvieron en 100 μL de dimetilsulfóxido (DMSO). La absorbancia se determinó a una densidad óptica (DO) de 570 nm usando un lector de microplacas Epoch 2 (Biotek). Como control negativo se emplearon células sin tratamientos. Los valores de absorbancia fueron normalizados considerando como 100% la absorbancia obtenida de cultivos no tratados.

3.2.3. Ensayo de viabilidad con CV

El ensayo de viabilidad con CV se basa en la tinción del ADN y proteínas de las células disponibles en los pozos de cultivo y la intensidad del color es proporcional

al número de células viables (97). Las células VERO se sembraron en microplacas de 96 pozos a una densidad de $4x10^4$ células/cm^2, permitiendo su adhesión y proliferación por 24 h. Pasado este tiempo, las células se incubaron con medio RPMI 1640 que contenía ISO (a concentraciones previamente descritas), durante 24 horas. Al final de los tratamientos, se retiró el medio y las células se lavaron con PBS, posteriormente se fijaron depositando en cada pozo 100 µL de solución de paraformaldehído al 4% por 30 min a temperatura ambiente. Se descartó el paraformaldehído y se adicionó en cada pozo 100 µL de solución de CV al 0.5% en metanol al 6% por 30 min a temperatura ambiente. Se descartó el CV y se enjuagó cuidadosamente cada pozo con agua destilada hasta extraer el colorante remanente. Se dejó secar la placa al aire durante 24 h. Para extraer el CV enlazado al ADN se usaron 200 µL/pozo de metanol (Merck), la placa se incubó por 20 min a temperatura ambiente sobre un agitador orbital con una frecuencia de 20 oscilaciones por minuto. Finalmente, la absorbancia se determinó como se indicó anteriormente. Los resultados para ambos ensayos se expresaron mediante curvas de dosis respuesta, empleando 16 concentraciones del ISO (9.76 a 2500 µg/mL). Los valores CI_{50} (concentración inhibitoria del 50% de la población celular) se calcularon a partir del ajuste ($R2> 0.95$) de la curva de pendiente de Hill de los datos experimentales usando un análisis de regresión no lineal en el Software GraphPad Prism versión 8.0.

Objetivo 3. *Realizar un estudio exploratorio de sensibilidad de bacterias y levaduras del género Candida frente al isoespintanol.*

3.3. Sensibilidad de bacterias y levaduras del género Candida frente al isoespintanol.

Teniendo en cuenta la ausencia de estudios sobre el potencial antimicrobiano del ISO contra patógenos humanos, inicialmente, se realizó un screening exploratorio evaluando 106 aislamientos clínicos que incluían: 90 aislamientos bacterianos y 16 aislamientos clínicos de levaduras pertenecientes al género *Candida*.

La bacterias en este estudio incluyeron: *Escherichia coli* [38]; *Pseudomonas aeruginosa* [12]; *Klebsiella pneumoniae* [13]; *Acinetobacter baumannii* [3]; *Proteus mirabilis* [7]; *Staphylococcus epidermidis* [3]; *Staphylococcus aureus* [5]; *Enterococcus faecium* [1];

Enterococcus faecalis [1]; *Stenotrophomonas maltophilia* [2]; *Citrobacter koseri* [2]; *Serratia marcescens* [1]; *Aeromonas hydrophila punctata* [1]; *Providencia rettgeri* [1], todas las bacterias fueron identificados por sistemas estándar: Vitek® 2 Compact. Biomerieux SA. (AST-P577, AST-N272, AST-GN93, AST-N271, AST- P612). Los medios: caldo Brain Heart Infusion (BHI), Tryptic Soy Broth (TSB), Tryptic Soy Agar (TSA), Mueller-Hinton broth (MHB), Mueller-Hinton agar (MHA) y Blood Agar (BA), fueron empleados para el mantenimiento de los cultivos hasta la realización de los experimentos. Las *Candida* spp., incluyeron: *C. albicans* [7]; *C. tropicalis* [7]; *C. glabrata* [1]; *C. auris* [1], todas las levaduras fueron identificados por sistemas estándar: Vitek 2 Compact. Biomerieux SA., YST vitek 2 Card y AST-YS08 Vitek 2 Card (Ref 420739). El medio, Sabouraud Dextrose Agar (SDA) fue utilizado para el mantenimiento de los cultivos hasta la realización de los ensayos. Los microorganismos fueron aislados de muestras de secreciones de tejidos, aspirado traqueal, hemocultivos, lavado bronco alveolar, secreción bronquial, secreciones de herida quirúrgica, urocultivos, esputo y abscesos de pacientes hospitalizados en la clínica Salud Social S.A.S de la ciudad de Sincelejo, Sucre, Colombia, previo consentimiento informado del Comité de Ética y Científico de la institución donadora de los patógenos para la investigación.

3.3.1. Sensibilidad de bacterias frente al ISO

La concentración mínima inhibitoria (CMI) del ISO contra los aislamientos clínicos, se definió como la concentración más baja a la cual el 90% (CMI_{90}) del crecimiento bacteriano fue inhibido, comparados con el control (células no tratadas). La CMI_{50} fue definida como la concentración más baja a la cual el 50% del crecimiento bacteriano fue inhibido. La CMI fue determinada realizando los ensayos de microdilución en caldo, empleando cajas de microtitulación de 96 pozos (Nunclon Delta, Thermo Fisher Scientific, Waltham, MA, USA), como se describe en el *Clinical Laboratory Standards Institute* (CLSI) método (M07-A9) (98), con modificaciones menores. Se realizaron diluciones seriadas en MHB, para obtener concentraciones finales de 19.53, 39.10, 78.12, 156.2, 312.5, 625, y 1000 μg/mL del ISO en cada pozo de reacción. Una solución stock de ISO a 20000 μg/mL in DMSO fue preparada para la realización de los experimentos, además, soluciones stock de los ATBs empleados como controles también fueron preparadas (98). Los ensayos se desarrollaron a un volumen final de 200 μL por pozo de la siguiente manera: 100 μL del inoculo

bacteriano a una concentración de 10^8 UFC/mL empleando un lector de microplacas Synergy LX (Biotek), a 600nm y 100 μL del ISO ajustado para alcanzar en un sistema de reacción final las concentraciones previamente descritas. Pozos con inóculos bacterianos sin ISO y con ATBs (ciprofloxacina [CIP], amikacina [AMK], ampicilina/sulbactam [SAM], gentamicina [GEN], meropenem [MEM], vancomicina [VAN], tetraciclina [TCY], trimetoprim/sulfametoxazol [SXT]), fueron empleados como controles de crecimiento y controles positivos respectivamente. Pozos con medios de cultivo sin inóculo y sin ISO fueron empleados como controles negativos. Para cada experimento, los controles fueron hechos con las diferentes concentraciones del ISO en medio de cultivo sin inóculo. Las cajas fueron incubadas a 37°C por 24 horas. Los experimentos fueron realizados por triplicado. La inhibición del crecimiento bacteriano por el ISO fue determinada por cambio en la densidad óptica (DO) a 600nm, desde el inicio de la incubación hasta el momento final (24 horas). Finalmente, el porcentaje de inhibición del crecimiento bacteriano fue calculado (99) usando la siguiente ecuación:

$$\%\text{Inhibición} = (1 - (DOt24 - DOt0/DOgc24 - DOgc0)) \times 100$$

donde, DOt24: densidad óptica de los pozos 24 h post-inoculación; DOt0: densidad óptica de los pozos a 0 h post-inoculación; DOgc24: densidad óptica del control de crecimiento a 24 h post-inoculación; DOgc0: densidad óptica del control de crecimiento a 0 h post-inoculación.

3.3.2. Sensibilidad de levaduras del género Candida frente al ISO

La concentración mínima inhibitoria (CMI) del ISO frente a los aislamientos clínicos de *Candida* spp., se definió como la concentración más baja a la cual el 90% (CMI_{90}) del crecimiento fúngico fue inhibido, comparados con el control. La CMI_{50} fue definida como la concentración más baja a la cual el 50% del crecimiento fúngico fue inhibido. La CMI fue determinada realizando los ensayos de microdilución en caldo, empleando cajas de microtitulación de 96 pozos (Nunclon Delta, Thermo Fisher Scientific, Waltham, MA, USA), como se describe en el *Clinical Laboratory Standards Institute* (CLSI) método (M27-A3) (100) y el *European Committee for Antimicrobial Susceptibility Testing* (EUCAST) (101), con modificaciones menores. Se realizaron diluciones seriadas en caldo RPMI 1640 (pH 7.0) bufereado con 0.165 M de ácido 3-

N-morpholinopropanosulfonico (MOPS) para obtener concentraciones finales de 15.62 a 500 μg/mL del ISO en cada pozo de reacción. Los ensayos se desarrollaron a un volumen final de 200 μL por pozo de la siguiente manera: 100 μL del inóculo fúngico a una concentración de $1x10^5$ UFC/mL leído a 530nm en un espectrofotómetro Spectroquant® Prove 300 y 100 μL del ISO ajustado para alcanzar en un sistema de reacción final las concentraciones descritas anteriormente. Los aislamientos de las levaduras sin ISO y con fluconazol (FLZ) fueron empleados como controles. Las cajas fueron incubadas a 37°C por 24 horas. Los experimentos fueron realizados por triplicado. La inhibición del crecimiento fúngico por el ISO, fue determinada por cambio en la DO empleando un lector de microplacas Synergy LX (Biotek) a 590nm, desde el inicio de la incubación hasta el momento final (24 horas) y el porcentaje de reducción del crecimiento fue calculado (99). El valor de la DO_{590} de las células no tratadas se les asigno el 100% de crecimiento. Posteriormente, la concentración mínima fungicida (CMF) fue determinada tomando 10 μL de cada pozo e inoculándola sobre SDA. Las cajas fueron selladas e incubadas a 37°C por 24/48 horas revisando para detectar crecimiento microbiano. La CMF se consideró la concentración más baja capaz de inhibir el 99% de las levaduras (11). Los experimentos fueron realizados por triplicado.

Objetivo 4. *Identificar a nivel molecular la especie C. tropicalis a través de un estudio taxonómico basado en genoma completo, usando librerías Truseq Nano DNA y la plataforma Illumina NovaSeq.*

3.4. Filogenómica de *Candida tropicalis*

3.4.1. Extracción de ADN genómico

Las colonias de *C. tropicalis* en SDA fueron utilizadas para la extracción de ADN genómico (ADNg) empleando el Qiagen DNeasy PowerLyzer PowerSoil kit., siguiendo las indicaciones del fabricante. El ADNg extraído fue cuantificado por absorción de luz a 260 nm usando el NanoDrop™ 2000-Thermo Scientific™ y congelado a -20°C para los experimentos posteriores de secuenciación genómica.

3.4.2. Secuenciación genómica de C. tropicalis WGS (Whole genome shotgun)

El secuenciamiento del ADNg extraído de *C. tropicalis*, se llevó a cabo usando librerías Truseq Nano DNA [350] y la plataforma Illumina NovaSeq, mediante la cual se generaron *reads* pareados de 150 bases. Posteriormente se realizó el ensamblaje del genoma de *C. tropicalis* empleando el programa SPADES. Para los análisis filogenéticos, se usaron genes conservados de copia única. Posteriormente se alinearon y se concatenaron esos genes con MAFFT, se usó el software iqTREE para seleccionar los modelos de sustitución y generar el árbol (Maximum Likelihood), que fue visualizado con FIGTREE.

Objetivo 5. *Determinar el potencial antifúngico del isoespintanol contra C. tropicalis calculando el porcentaje de inhibición del crecimiento, empleando el método de microdilución.*

3.5. Ensayos de sensibilidad antifúngica de *C. tropicalis*

Las CMIs fueron establecidas realizando los ensayos de microdilución en caldo, empleando cajas de microtitulación de 96 pozos (Nunclon Delta, Thermo Fisher Scientific, Waltham, MA, USA), como se describe en el *Clinical Laboratory Standards Institute* (CLSI) método (M27-A3) (100) y el *European Committee for Antimicrobial Susceptibility Testing* (EUCAST) (101). La CMI_{50} y la CMF (concentración más baja capaz de inhibir el 99% de las levaduras) también fueron determinadas. Todos los experimentos fueron realizados por triplicado.

3.5.1. Ensayo de reducción de MTT

Para evaluar la viabilidad celular de *C. tropicalis* en presencia del ISO, se realizó el ensayo colorimétrico de reducción del MTT (3-(4,5-dimetiltiazol-2-il)-2,5-difenil-2H-tetrazolio) según lo descrito por Maldonado (102). El MTT se disolvió en PBS a 5 mg/mL y se filtró. El inóculo fúngico a una concentración celular de $1x10^6$ UFC/mL fue inoculado en cajas de 96 pozos a concentraciones del ISO determinadas, las cajas fueron incubadas por 24 h a 37°C. Las células con medio fueron empleadas como control. Luego 50µL de la solución de MTT fue adicionado a las células en evaluación a una concentración de 500 µg/mL. Las cajas fueron incubadas en

oscuridad durante 4 h a 37°C. Las células viables con actividad metabólica convierten al MTT (de color amarillo) en formazán, el cual se solubilizó con DMSO presentando un color violeta, luego se realizaron mediciones a una longitud de onda de 550 nm en un lector de microplacas Synergy LX (Biotek).

3.5.2. Curva de inhibición del crecimiento fúngico

La curva de inhibición del crecimiento de *C. tropicalis* por el ISO se realizó siguiendo la metodología propuesta por Zhang (103). Los aislamientos de *C. tropicalis* fueron cultivados en medio (SDB) por 24 h a 35°C. El inoculo fúngico fue estandarizado hasta alcanzar una concentración celular de $1x10^6$ UFC/mL en tubos de vidrio, luego el ISO fue adicionado (la CMI para cada aislamiento), los tubos fueron incubados a 35 °C por 48h. Posteriormente, se tomó 1mL de cada tubo a los tiempos: 0, 2, 4, 8, 12, 24, 36 y 48h y se leyeron a 600nm en un lector de microplacas Synergy LX (Biotek). Tubos con el inoculo fúngico y FLZ se emplearon como controles.

Objetivo 6. *Explorar el mecanismo de acción antifúngica del isoespintanol contra C. tropicalis, mediante su acción sobre diferentes dianas.*

3.6. Exploración de mecanismos de acción antifúngico del isoespintanol contra *C. tropicalis* mediante su acción sobre diferentes dianas

3.6.1. Efecto del ISO sobre la membrana celular fúngica

Teniendo en cuenta que los cambios en la permeabilidad de la membrana celular han sido objetivos para muchos agentes antifúngicos, se llevaron a cabo los siguientes experimentos para evaluar el daño de la membrana causado por el ISO:

3.6.1.1. Ensayos con citometría de flujo empleando Ioduro de propidio (IP)

Para evaluar el efecto del ISO sobre la integridad de la membrana celular de las levaduras, se procedió acorde con la metodología propuesta por Zhao (104). Las células fúngicas ($1x10^6$ UFC/mL), fueron suspendidas en medio RPMI 1640 y tratadas con la CMI de ISO para cada aislamiento e incubadas por 12 h a 30°C. Células sin ISO y células tratadas con FLZ (100 μg/mL) se emplearon como controles.

Posteriormente, las células se incubaron con 1.49 μM de ioduro de propidio (IP) en agua a 30 °C por 50 min. Luego, las células fueron colectadas por centrifugación (5000g, 10 min, 4 °C), resuspendidas en PBS y finalmente analizadas por citometría de flujo, usando el citómetro de flujo BD FACS CANTO II y analizadas con el BD FACS DIVA software. La excitación y emisión para IP es de 488 nm y 630 nm respectivamente. El IP es un agente intercalante fluorescente, que se une a los ácidos nucleicos, es excluido de células vivas y solo puede entrar en células que tienen membranas permeables, cuando cambia la permeabilidad de la membrana celular, se une al ácido nucleico y muestran fluorescencia roja (104,105). Todos los experimentos fueron realizados por triplicado.

3.6.1.2. Pérdida de material intracelular a través de la membrana celular

La pérdida de material intracelular fue evaluada acorde con la metodología propuesta por Tao (106) con algunas modificaciones. Las levaduras crecidas en SDB fueron centrifugadas a 3000g durante 20 min, lavadas tres veces y resuspendidas en 20 mL de PBS (pH 7.0). Luego, la suspensión celular fue tratada con ISO (CMI para cada aislamiento) e incubadas a 37 °C por 0, 30, 60 y 120 min. Subsecuentemente, 2 mL de las muestras fueron colectadas y centrifugadas a 3000g por 20 min. Luego, para determinar la concentración de los constituyentes liberados, 2 mL de sobrenadante fueron usados para medir la absorbancia a 260/280 nm con el espectrofotómetro UV/Vis Spectroquant® Prove 300. Como controles se utilizaron muestras sin ISO y muestras con FLZ.

3.6.1.3. Medida de pH extracelular

Los cambios en el pH extracelular fueron medidos para evaluar la pérdida de iones a través de la membrana celular, conforme a lo descrito por Tao (106). 100 μL de la suspensión de levaduras ($1x10^5$ UFC/mL) fueron adicionados a 20 mL de SDB e incubados a 37 °C por 48 h. Luego, las muestras fueron centrifugadas a 3000g por 20 min; el pellet fue colectado, resuspendido, lavado tres veces con agua bidestilada y resuspendido nuevamente en 20 mL de agua bidestilada estéril. Después de la adición de ISO (CMI de cada aislamiento), el pH extracelular de *C. tropicalis* fue determinado a 0, 30, 60 y 120 min, usando un pHmetro Schott® Instruments Handylab pH 11. Las muestras sin ISO y muestras con FLZ se emplearon como controles.

3.6.1.4. Ensayos LIVE/DEAD

Se realizaron ensayos de LIVE/DEAD siguiendo la metodología propuesta por Zhang (103). Una suspensión de *C. tropicalis* ($1x10^6$ UFC/mL), fue puesta sobre portaobjetos estériles e incubada por 24 h. Luego, las células fueron lavadas tres veces con PBS. Posteriormente, la CMI del ISO para cada levadura y FLZ, fueron adicionados a los grupos experimentales y el inoculo fúngico en caldo RPMI 1640 fue usado como control. Los portaobjetos preparados se incubaron a 35°C por 24 h y luego fueron lavados tres veces con PBS. Conjuntamente, la naranja de acridina (NA) (5µL, 100 mg/L) y el bromuro de etidio (BE) (5µL, 100 mg/L) fueron mezclados en oscuridad y adicionados a los portaobjetos en condiciones de oscuridad por 30 seg. Seguidamente, las muestras fueron observadas en un microscopio de fluorescencia Olympus BX43 y fotografiadas con cámara DP72. La NA puede penetrar la membrana celular intacta, incrustar el ADN nuclear y hacer que emita una fluorescencia verde brillante. Sin embargo, BE solo puede penetrar la membrana celular dañada, incrustar ADN nuclear y emitir una fluorescencia de color rojo anaranjado.

3.6.1.5. Tinción con azul de Evans

El daño a las membranas celulares también se evidenció usando la tinción de azul de Evans (Sigma-Aldrich) acorde con la metodología propuesta por Chaves-Lopez (107) con algunas modificaciones. Antes de los ensayos, el azul de Evans se preparó al 1% en PBS. 100 µL de la suspensión fúngica en SDB fueron incubados en cubreobjetos (22mm x 22mm) por triplicado a 37 °C por 24 horas. Posteriormente, las muestras se trataron con ISO (CMI) por una hora, y luego, 1 mL de azul de Evans fue adicionado a las muestras por 5 minutos. Células no tratadas fueron usadas como control. Las muestras fueron observadas bajo el microscopio, Olympus CX31. El azul de Evans es un colorante no permeable a células con membranas intactas, tiñe selectivamente células muertas (108).

3.6.1.6. Determinación del contenido de ergosterol

El contenido de ergosterol total de los aislamientos de *C. tropicalis* tratados con ISO, fue determinado siguiendo el protocolo descrito por Zhang (103), con modificaciones. Las células fueron tratadas con ISO (CMI de cada aislamiento), a 35

°C durante 3 h. Luego, se centrifugaron y lavaron con PBS. Un peso húmedo de 0.5 g de células mezcladas con PBS fueron saponificadas por adición de 4 mL de una solución recién preparada al 30% (peso/volumen) de KOH metanólico y 8 mL de etanol absoluto a 80 °C por 1 hora. La mezcla fue extraída con éter de petróleo y lavada con solución saturada de NaCl. Las muestras fueron concentradas al vacío a 60 °C, el residuo disuelto en 0.5 mL de metanol y filtrada a través de una micromembrana de 0.45 μm. Luego, determinamos la concentración de ergosterol en muestras con y sin ISO comparando las áreas de los picos de las muestras con una curva estándar generada a partir de ergosterol (95% Sigma-Aldrich) a concentraciones de 1, 10, 50, 100, 250, 500, 750 y 1000 mg/L. Los contenidos de ergosterol se analizaron utilizando un UHPLC Ultimate 3000 (Thermo Scientific, USA), con detector de arreglo de diodos DAD, Se utilizó una columna C18 Hypersil Gold (150 mm × 4,6 mm, 5 μm) a 30 °C. El volumen de inyección fue de 30 μL y una fase móvil de metanol/agua (97/3, 100% grado HPLC), con un caudal de 0.6 mL/min. Todas las inyecciones fueron hechas por triplicado. La longitud de onda de detección fue 205 nm. La relación de inhibición de ergosterol = (1 - contenido de ergosterol de las células tratadas/contenido de ergosterol de las células no tratadas) × 100%.

3.6.2. Efecto del ISO sobre la morfología e integridad de las células

La morfología de *C. tropicalis* después del tratamiento con ISO fue analizada a través de microscopía electrónica de transmisión (MET). La concentración de *C. tropicalis* fue ajustada a $1x10^6$ UFC/mL; la suspensión fue mezclada con ISO e incubada a 37 °C por 24 h. Subsecuentemente, las células fueron colectadas y fijadas en glutaraldehído al 2.5% en buffer fosfato pH 7.2 a 4 °C; se centrifugaron a 13000 rpm por 3 min y el botón en el fondo del vial se posfijó en tetróxido de osmio al 1% en agua, por 2 h a 4 °C. Luego se realizó pre-imbibición con acetato de uranilo al 3% por 1 h a temperatura ambiente, luego las células se deshidrataron en gradiente de etanol (50% por 10 min, 70% por 10 min, 90% por 10 min, 100% por 10 min), acetona-etanol (1:1) por 15 min y embebidas en resina epóxica SPURR. Las muestras fueron cortadas en un ultramicrótomo Leica EM UC7, a 130 nm de grosor y contrastadas con acetato de uranilo al 6% y citrato de plomo, finalmente fueron observadas en un

microscopio electrónico de transmisión JEOL 1400 plus. Las fotografías fueron obtenidas con una cámara CCD Gatan Orius.

3.6.3. Efecto del ISO sobre la producción de especies reactivas de oxígeno intracelular (EROi)

Para detectar la formación de oxidantes intracelulares, se empleó la sonda fluorescente 2',7'-diclorofluoresceina diacetato (DCFH-DA), siguiendo el protocolo descrito por da Silva (109). Las células fúngicas ($1x10^6$ UFC/mL) fueron incubadas en PDB con la CMI del ISO para cada aislamiento por 24 h a 35°C. Una suspensión celular bajo las mismas condiciones sin ISO fue usada como control negativo y una suspensión celular tratadas con peróxido de hidrógeno (H_2O_2) como inductor de EROi, fue usado como control positivo. Luego las células fueron incubadas con 20 μM de DCFH-DA (Sigma-Aldrich, St. Louis, MO, USA) por 30 min en oscuridad a 35°C. A continuación, las células fueron colectadas, lavadas, resuspendidas en PBS y analizadas por citometría de flujo. La excitación y emisión para DCFH-DA es de 485 y 535nm respectivamente. Después de la absorción celular DCFH-DA es desacetilado por esterasas celulares a diclorofluorescina (DCFH) un compuesto no fluorescente, que luego es oxidado en 2′-7′diclorofluoresceína (DCF) un compuesto altamente fluorescente, como resultado de un gran estrés oxidativo intracelular causado por EROi, distintas del H_2O_2. La intensidad de la fluorescencia de DCF es proporcional a la cantidad de ERO formada intracelularmente (110).

3.6.4. Efecto del ISO sobre el potencial de membrana mitocondrial (ΔΨm)

Para evaluar el efecto del ISO sobre el ΔΨm, las levaduras fueron teñidas con Rodamina 123 (Rh123) acorde con lo descrito por Chang (111), con modificaciones menores. Las células fúngicas ($3×10^8$ UFC/mL) se trataron con la CMI del ISO durante 1 h, luego, fueron colectadas por centrifugación y resuspendidas con 25 μM de Rh123 en 50 mM de citrato de sodio, enseguida se incubaron a 30 °C durante 10 min. Posteriormente las células se lavaron tres veces con PBS y se analizaron por citometría de flujo. Se usaron células sin tratamiento como controles negativos, mientras que células tratadas con H_2O_2 15 mM durante 1 h se usaron como controles positivos. La excitación y longitud de onda para Rh 123 es de 488 y 525nm

respectivamente. La Rh123, es un fluorocromo catiónico lipofílico, permeable (112), que se acumula selectivamente en las mitocondrias de células activas; esta interacción específica depende del alto potencial transmembrana mantenido por las mitocondrias funcionales, por lo tanto, la disipación del $\Delta\Psi m$ por ionóforos o inhibidores del transporte de electrones, elimina la asociación mitocondrial selectiva de estos compuestos (113). Consecuentemente, la activación mitocondrial induce la extinción de la fluorescencia Rh123 y la tasa de disminución de la fluorescencia es proporcional al $\Delta\Psi m$ (114,115).

3.6.5. Efecto del ISO sobre biopelículas fúngicas

Los aislamientos de *C. tropicalis*, fueron evaluados para cuantificar la reducción de biopelículas maduras en presencia del ISO siguiendo la metodología reportada por Donadu (11). Para la formación de las biopelículas, en cajas de 96 pozos, 200 μL de las células fueron cultivadas en cada pozo, con caldo yeast peptone dextrose (YPD) e incubadas a 37 °C por 48 h. Luego el caldo fue removido de las microplacas y 200 μL de la CMI del ISO para cada aislamiento en caldo YPD, fueron adicionados e incubados a 37 °C por 1 h. Luego, las células flotantes fueron removidas y la biopelícula en el fondo de los pozos se lavó tres veces con agua desionizada. Se realizaron seis réplicas de cada muestra. Los cultivos sin ISO se usaron como control negativo y células tratadas con AFB (4 μg/mL) se emplearon como control positivo. Las reducciones de las biopelículas fueron cuantificadas por tinción de los pozos con 0.1% de cristal violeta (Sigma-Aldrich, Italy) durante 20 min. Las muestras fueron lavadas con agua desionizada hasta remover el exceso de colorante. Finalmente, las muestras fueron remojadas en 250 μL de ácido acético glacial al 30%. El efecto del ISO sobre la formación de biopelículas también fue evaluado. Para esto, la CMI del ISO fue adicionada al tiempo de la inoculación con *C. tropicalis*. Los valores de absorbancia fueron medidos a 590nm (DO_{590}), usando un lector de microplacas Synergy LX (Biotek). La producción de biopelículas fue agrupada en las siguientes categorías: $DO_{590} < 0.1$: no productores (NP), DO_{590} 0.1-1.0: productores débiles (PD), DO_{590} 1.1- 3.0: productoras moderadas (PM) y $DO_{590} > 3.0$: productoras fuertes (PF). La reducción de biopelículas fue calculada usando la siguiente ecuación:

% de reducción de biopelícula: AbsCO-AbsISO/AbsCO x100

Donde, AbsCO: absorbancia de la muestra control y AbsISO: absorbancia de la muestra tratada con ISO.

3.6.6. Efecto del ISO sobre la integridad de la pared celular

El daño a la integridad de la pared fúngica por ISO se evaluó midiendo el contenido de quitina de la pared celular mediante la tinción con calcofluor blanco [CFW], siguiendo el protocolo descrito por Costa de Oliveira (116) con modificaciones menores. El CFW es un tinte fluorescente soluble en agua que exhibe selectividad; se une a las paredes celulares de los hongos (específico para quitina) (117) y emite fluorescencia azul/verde cuando se ilumina con luz ultravioleta (118). Las levaduras fueron cultivadas en caldo YPD ($1x10^6$ células/mL) a 35 °C, tratadas con la CMI del ISO durante 2 h y teñidas con CFW [2.5 g/mL] durante 15 min en la oscuridad. Posteriormente, las células se lavaron y resuspendieron en PBS y finalmente se analizaron en un citómetro de flujo BD FACS CANTO II (canal azul pacífico: 405–450/50 nm; 20000 eventos por ensayo) utilizando la versión 6.1.3 del software BD FACS DIVA. Todos los experimentos fueron realizados por triplicado.

Se definió un índice de tinción (SI) (116), cuyo valor estaba directamente relacionado con la cantidad de quitina y tenía en cuenta los diferentes niveles de auto fluorescencia. Se analizó la intensidad media de fluorescencia (IMF) emitida por levaduras teñidas (población positiva) y no teñidas (población negativa), y en cada experimento, el SI se calculó utilizando la siguiente ecuación:

SI: (IMFpp - IMFpn)/2 × DEpn

donde IMFpp: intensidad media de fluorescencia de la población positiva; IMFpn: intensidad media de fluorescencia de la población negativa; y DEpn: desviación estándar de la población negativa.

Objetivo 7. *Analizar el efecto del isoespintanol sobre el transcriptoma de C. tropicalis, mediante el estudio de la expresión diferencial de genes.*

3.7. Efecto del ISO sobre el transcriptoma de *C. tropicalis*

3.7.1. Secuenciación de ARN y datos de recuentos de lectura.

Se procesó ARN total a partir de muestras de levaduras tratadas durante 4 horas con la CMI del ISO, y levaduras sin tratamiento usadas como controles. El procedimiento para la extracción del ARN se realizó utilizando el reactivo TRIzol, de acuerdo con las instrucciones estándar del fabricante (TRIzol TM Reagent, Invitrogen; protocolo de extracción de ARN total). El ARN total obtenido se cuantificó mediante el método colorimétrico ribogreen (Invitrogen) y su integridad (RIN) se evaluó mediante electroforesis capilar en un bioanalizador Agilent 2100 (Agilent Technologies, Santa Clara, CA, EE. UU.). Se empleó una puntuación RIN > 7.0 como valor de corte. Luego, el ARN se empleó para construir la biblioteca RNA-Seq para la secuenciación en la plataforma Illumina Novaseq de 150 pb de extremo pareado (Illumina-Transcriptome, TruSeq mRNA/Illumina). Los recuentos de ARN se obtuvieron con Bowtie 2 empleando los archivos Ensemble GTF correspondientes al genoma de referencia *Candida_tropicalis* REF GCA000006335v3.

3.7.2. Análisis bioinformático

3.7.2.1. *Análisis de expresión genética diferencial.*

Se utilizaron recuentos de lectura para identificar genes expresados diferencialmente (GED). El análisis diferencial de expresión génica se realizó utilizando el paquete EdgeR en el entorno RStudio. El conjunto de datos se analizó para determinar la direccionalidad del cambio en la expresión en la etapa A (muestras de control/*C. tropicalis* no tratadas) en comparación con la etapa B (*C. tropicalis* tratada con el ISO). Se consideraron valores Log2FC > 1 y FDR < 0.05 para determinar los GED. Los genes que tuvieron valores de p significativos con un cambio log2 veces positivo representaron una expresión aumentada (UP). Aquellos con un cambio log2 negativo se consideran con expresión disminuida (DN),

mientras que la expresión génica con valores de p superiores a 0.05 no representa ningún cambio entre etapas (NC).

3.7.2.2. *Análisis de enriquecimiento funcional para GEDs*

Se evaluó el análisis de enriquecimiento funcional para los 186 GEDs en el conjunto de datos de *C. tropicalis* utilizando el análisis de enriquecimiento de conjunto de genes (GSEA). El análisis de enriquecimiento incluye todos los términos de Gene Ontology (GO). Los términos GO se filtraron si sus valores estaban por encima de 0.05. Los valores de p resultantes se ajustaron para pruebas de hipótesis múltiples utilizando el enfoque de Benjamini y Hochberg (119). Para el análisis del enriquecimiento funcional de los términos GO en los conjuntos de genes UP y DN, el universo de fondo fue el número total de GEDs. Se utilizó la herramienta ShinyGO 0.77 (120) que utiliza el genoma de *C. tropicalis* basado en STRING-db para el análisis y visualización de datos (//bioinformatics.sdstate.edu/go, consultado el 10 de mayo de 2023).

3.7.2.3. *Predicción computacional de GEDs*

Para la anotación funcional del transcriptoma, se obtuvo una lista de pares de genes ortólogos entre *C. tropicalis* y *C. albicans* de la base de datos Ensembl utilizando el paquete BioMart que emplea scripts R. Los 186 GEDs se filtraron para seleccionar aquellos enriquecidos en funciones biológicas de mitocondrias, membranas, pared celular, lípidos y metabolismo. Para la visualización de datos, los genes seleccionados se trazaron utilizando el entorno RStudio.

CAPITULO 4. RESULTADOS Y DISCUSIÓN

Los resultados y discusión correspondiente a los objetivos de esta investigación se encuentran reflejados en los siguientes artículos publicados, anexos a este documento.

Objetivos 1, 4, 5 y 6 en Anexo 1:

"Mechanism of Antifungal Action of Monoterpene Isoespintanol against Clinical Isolates of *Candida tropicalis*"

Objetivo 2 en Anexo 2:

"Isoespintanol Antifungal Activity Involves Mitochondrial Dysfunction, Inhibition of Biofilm Formation, and Damage to CellWall Integrity in *Candida tropicalis*"

Objetivo 3 en Anexos 3 y 4:

"Antibacterial Screening of Isoespintanol, an Aromatic Monoterpene Isolated from *Oxandra xylopioides* Diels"

"Antifungal potential of isoespintanol extracted from *Oxandra xylopioides* diels (Annonaceae) against intrahospital isolations of *Candida* SPP"

Objetivo 7 en Anexo 5:

"Transcriptional Reprogramming of *Candida tropicalis* in Response to Isoespintanol Treatment"

CAPITULO 5. CONCLUSIONES

Esta investigación demostró el potencial antifúngico del isoespintanol extraído de *Oxandra xylopioides* contra aislamientos clínicos de *Candida tropicalis*, evidenciando sus mecanismos de acción sobre diferentes dianas celulares.

El potencial antifúngico del ISO es un proceso complejo que involucra múltiples objetivos moleculares que incluyen: factores de transcripción, ADN, proteínas, membrana celular, pared celular, potencial de membrana mitocondrial e inducción de especies reactivas de oxígeno intracelular.

Además, demostramos el amplio espectro de acción del ISO, evidenciando su potencial antimicrobiano no solo contra levaduras del género *Candida* sino también contra bacterias Gram negativas y bacterias Gram positivas.

Se evidenció el potencial antibiopelículas del ISO, este monoterpeno, no solo inhibe la formación de biopelículas, sino que, además, tiene efecto contra las biopelículas maduras, demostrando un mayor potencial en comparación con AFB.

Estos resultados, representan una descripción de los posibles objetivos moleculares clínicos en *C. tropicalis* que podrían explorarse en el futuro para tratar esta levadura patógena en la rutina clínica.

Referencias

1. Bhatia P, Sharma A, George AJ, Anvitha D, Kumar P, Dwivedi VP, et al. Antibacterial activity of medicinal plants against ESKAPE: An update. Heliyon. 2021;7(2):e06310.

2. Morais A, Araujo H, Arias L, Ramírez W, Porangaba G, Penha S, et al. Nanocarriers of Miconazole or Fluconazole: Effects on Three-Species Candida Biofilms and Cytotoxic Effects *In Vitro*. J. Fungi. 2021;7(7):500.

3. Boonsilp S, Homkaew A, Phumisantiphong U, Nutalai D, Wongsuk T. Species distribution, antifungal susceptibility, and molecular epidemiology of candida species causing Candidemia in a tertiary care hospital in Bangkok, Thailand. J. Fungi. 2021;7(7).

4. Steinmann J, Schrauzer T, Kirchhoff L, Meis JF, Rath PM. Two *Candida auris* cases in Germany with no recent contact to foreign healthcare—epidemiological and microbiological investigations. J. Fungi. 2021;7(5):1–6.

5. Hassan Y, Chew SY. *Candida glabrata*: Pathogenicity and Resistance Mechanisms for Adaptation and Survival. J. Fungi. 2021;7.

6. Chen P, Chuang Y, Wu U, Sun H, Wang J, Sheng W, et al. Mechanisms of Azole Resistance and Trailing in *Candida tropicalis* Bloodstream Isolates. J. Fungi. 2021;7 (8).

7. Kakar A, Holzknecht J, Dubrac S, Gelmi ML, Romanelli A. New Perspectives in the Antimicrobial Activity of the Amphibian Temporin B : Peptide Analogs Are Effective Inhibitors of *Candida albicans* Growth. J. Fungi. 2021;7 (6).

8. Bongomin F, Gago S, Oladele R, Denning D. Global and multi-national prevalence of fungal diseases-estimate precision. J. Fungi. 2017;3:1–29.

9. Janbon G, Quintin J, Lanternier F, D´Enfert. Studying fungal pathogens of humans and fungal infections : fungal diversity and diversity of approaches. Genes Immun. 2019; Available from: http://dx.doi.org/10.1038/s41435-019-0071-2

10. Galvis-acosta D, Aycardi-morinelly MP, Contreras-martínez OI, Lorduy-Rodríguez AJ. Prevalencia de infecciones fúngicas en centros hospitalarios de Montería, Córdoba, Colombia. Rev Cubana Hig Epidemiol. 2020;57:413.

11. Donadu MG, Peralta-ruiz Y, Usai D, Maggio F, Molina-hernandez JB, Rizzo D, et al. Colombian Essential Oil of *Ruta graveolens* against Nosocomial

Antifungal Resistant Candida Strains. J. Fungi. 2021;7:383.

12. Scorneaux B, Angulo D, Borroto-esoda K, Ghannoum M, Peel M, Wring S. SCY-078 Is Fungicidal against Candida Species in Time-Kill Studies. Antimicrob Agents Chemother. 2017;61(3):1–10.

13. El-kholy MA, Helaly GF, El Ghazzawi EF, El-sawaf G, Shawky SM. Virulence factors and antifungal susceptibility profile of *C. tropicalis* isolated from various clinical specimens in Alexandria, Egypt. J. Fungi. 2021;7(5):351.

14. Zuza-Alves DL, Sila-Rocha WP, Chaves G. An update on *Candida tropicalis* based on basic and clinical approaches. Front Microbiol. 2017;8.

15. Munhoz-Alves N, Nishiyama Mimura LA, Viero RM, Bagagli E, Schatzmann J, Sartori A, et al. *Candida tropicalis* systemic infection redirects leukocyte infiltration to the kidneys attenuating Encephalomyelitis. J. Fungi. 2021;7:757.

16. Cortés JA, Ruiz JF, Melgarejo-Moreno LN, Lemos E V. Candidemia in Colombia. Biomedica. 2020;40(1):195–207.

17. Silva S, Negri M, Henriques M, Oliveira R, Williams DW, Azeredo J. *Candida glabrata*, *Candida parapsilosis* and *Candida tropicalis*: Biology, epidemiology, pathogenicity and antifungal resistance. FEMS Microbiol Rev. 2012;36(2):288–305.

18. Gintjee TJ, Donnelley MA, Thompson III GR. Aspiring Antifungals : Review of Current Antifungal Pipeline Developments. J. Fungi. 2020;6(28).

19. Araldi RP, dos Santos MO, Barbon FF, Manjerona BA, Meirelles BR, de Oliva Neto P, et al. Analysis of antioxidant, cytotoxic and mutagenic potential of *Agave sisalana* Perrine extracts using Vero cells, human lymphocytes and mice polychromatic erythrocytes. Biomed Pharmacother. 2018;98:873–85.

20. Mekonnen Bayisa Y, Aga Bullo T. Optimization and characterization of oil extracted from *Croton macrostachyus* seed for antimicrobial activity using experimental analysis of variance. Heliyon. 2021;7.

21. Aylate A, Agize M, Ekero D, Kiros A, Ayledo G, Gendiche K. *In-vitro* and *In-vivo* antibacterial activities of *Croton macrostachyus* methanol extract against *E. coli* and *S. aureus*. Adv Anim Vet Sci. 2017;5:107–14.

22. Naman CB, Benatrehina PA, Kinghorn AD. Pharmaceuticals, Plant Drugs. Second Edi. Vol. 2, Encyclopedia of Applied Plant Sciences. Elsevier; 2016. 93–99 p.

23. Avato P. Editorial to the special issue –"Natural products and drug

discovery". Molecules. 2020;25:1128.

24. Rojano B, Saez J, Schinella G, Quijano J, Vélez E, Gil A, et al. Experimental and theoretical determination of the antioxidant properties of isoespintanol (2-isopropyl-3,6-dimethoxy-5-methylphenol). J. Mol Struct. 2008;877:1–6.

25. Rojano B, Pérez E, Figadère B, Martin MT, Recio MC, Giner R, et al. Constituents of *Oxandra* cf. *xylopioides* with anti-inflammatory activity. J. Nat Prod. 2007;70(5):835–8.

26. Gavilánez Buñay TC, Colareda GA, Ragone MI, Bonilla M, Rojano BA, Schinella GR, et al. Intestinal, urinary and uterine antispasmodic effects of isoespintanol, metabolite from *Oxandra xylopioides* leaves. Phytomedicine. 2018 Dec 1;51:20–8.

27. Rinaldi GJ, Rojano B, Schinella G, Mosca SM. Participation of NO in the vasodilatory action of isoespintanol. Vitae. 2019;26:78–83.

28. Usuga A, Tejera I, Gómez J, Restrepo O, Rojano B, Restrepo G. Cryoprotective effects of ergothioneine and isoespintanol on canine semen. Animals. 2021;11:2757.

29. Rojano BA, Montoya S, Yépez F, Saez J. Evaluación de isoespintanol aislado de *Oxandra* cf. *xylopioides* (Annonaceae) sobre *Spodoptera frugiperda* J.E. Smith (Lepidoptera: Noctuidae). Rev. Fac. Nal. Agr. 2007,Vol. 60.

30. Arango N, Vanegas N, Saez J, García C, Rojano B. Actividad antifúngica del isoespintanol sobre hongos del género *Colletotricum*. Sci Tech. 2007;33:279–80.

31. González Arbeláez L, Ciocci Pardo A, Fantinelli JC, Rojano B, Schinella G, Mosca SM. Isoespintanol, a monoterpene isolated from *Oxandra* cf *xylopioides*, ameliorates the myocardial ischemia-reperfusion injury by AKT/PKCε/eNOS-dependent pathways. Naunyn-Schmiedeberg's Arch Pharmacol. 2020;393 (4):629–38.

32. Liu JY, Dickter JK. Nosocomial Infections: A History of Hospital-Acquired Infections. Gastrointest Endosc Clin N Am. 2020;30(4):637–52.

33. Lemiech-Mirowska E, Kiersnowska Z, Michalkiewicz M, Depta A, Marczak M. Nosocomial infections as one of the most important problems of the healthcare system. Ann Agric Environ Med. 2021;28:361–6.

34. Khan A, Miller WR, Arias CA. Mechanisms of antimicrobial resistance among hospital-associated pathogens. Expert Rev Anti Infect Ther. 2018;16:269–87.

35. Contreras-Omaña R, Escorcia-Saucedo AE, Velarde-Ruiz Velasco JA.

Prevalencia e impacto de resistencias a antimicrobianos en infecciones gastrointestinales: una revisión. Rev Gastroenterol Mex. 2021;86:265–75.

36. Resurrección-Delgado C, Montenegro-Idrogo J, Chiappe-Gonzalez A, Vargas-Gonzalez R, Cucho-Espinoza C, Mamani-Condori D, et al. *Klebsiella pneumoniae* Nueva Delhi metalo-betalactamasa en el hospital nacional Dos de mayo. Lima, Perú. Rev Peru Med Exp Salud Publica. 2017;34:261–7.

37. Ghodhbane H, Elaidi S, Sabatier J-M, Achour S, Benhmida J, Regaya I. Bacteriocins Active Against Multi-Resistant Gram Negative Bacteria Implicated in Nosocomial Infections. Infect Disord Drug Targets. 2015;15:2–12.

38. Pendleton JN, Gorman SP, Gilmore BF. Clinical relevance of the ESKAPE pathogens. Expert Rev Anti Infect Ther. 2013;11(3):297–308.

39. Černáková L, Light C, Salehi B, Rogel-Castillo C, Victoriano M, Martorell M, et al. Novel Therapies for Biofilm-Based Candida spp. Infections. Adv Exp Med Biol. 2019;1214:93–123.

40. Chowdhary A, Tarai B, Singh A, Sharma A. Multidrug-resistant *Candida auris* infections in critically ill coronavirus disease patients, India, april-july 2020. Emerg Infect Dis. 2020;26:2694–6.

41. Jamiu AT, Albertyn J, Sebolai OM, Pohl CH. Update on *Candida krusei*, a potential multidrug-resistant pathogen. Med Mycol. 2020;59(1):1–17.

42. Öncü B, Belet N, Emecen AN, Birinci A. Health care-associated invasive Candida infections in children. Med Mycol. 2019;57(8):929–36.

43. Whaley S, Berkow E, Rybak J, Nishimoto A, Barker K, Rogers D. Azole antifungal resistance in *Candida albicans* and emerging non-albicans candida species. Front Microbiol. 2017;7:1–12.

44. Rasheed M, Battu A, Kaur R. Host–pathogen interaction in *Candida glabrata* infection: current knowledge and implications for antifungal therapy. Expert Rev Anti Infect Ther. 2020;00(00):1093–103.

45. Wang D, An N, Yang Y, Yang X, Fan Y, Feng J. *Candida tropicalis* distribution and drug resistance is correlated with ERG11 and UPC2 expression. 2021;1–9.

46. Da Silva MA, Baronetti JL, Páez PL, Paraje MG. Oxidative Imbalance in *Candida tropicalis* Biofilms and Its Relation With Persister Cells. Front Microbiol. 2021;11(February):1–14.

47. Tóth R, Nosek J, Mora-Montes HM, Gabaldon T, Bliss JM, Nosanchuk JD, et

al. *Candida parapsilosis*: From genes to the bedside. Clin Microbiol Rev. 2019;32(2).

48. Carvajal SK, Alvarado M, Rodriguez YM, Parra-Giraldo CM, Var C, Morales-l SE, et al. Pathogenicity Assessment of Colombian Strains of *Candida auris* in the *Galleria mellonella* Invertebrate Model. J. Fungi. 2021;7:1–10.

49. Jeffery-Smith A, Taori SK, Schelenz S, Jeffery K, Johnson EM, Borman A, et al. *Candida auris*: A review of the literature. Clin Microbiol Rev. 2018;31(1).

50. Colombo AL, Júnior JNDA, Guinea J. Emerging multidrug-resistant Candida species. Curr Opin Infect Dis. 2017;30(6):528–38.

51. De Souza CM, dos Santos MM, Furlaneto-Maia L, Furlaneto MC. Adhesion and biofilm formation by the opportunistic pathogen *Candida tropicalis*: What do we know?. Can J. Microbiol. 2023;69(6):207–18.

52. Silva S, Hooper SJ, Henriques M, Oliveira R, Azeredo J, Williams DW. The role of secreted aspartyl proteinases in *Candida tropicalis* invasion and damage of oral mucosa. Clin Microbiol Infect. 2011;17(2):264–72.

53. Guembe M, Cruces R, Peláez T, Mu P, Bouza E. Assessment of biofilm production in Candida isolates according to species and origin of infection. Enferm Infecc Microbiol Clin. 2017;35 (1):37–40.

54. Tascini C, Sozio E, Corte L, Sbrana F. The role of biofilm forming on mortality in patients with candidemia : a study derived from real world data. Infect Dis (Auckl). 2017;50 (3)(0):1–6.

55. Grosset M, Desnos-Ollivier M, Godet C, Kauffmann-Lacroix C, Cazenave-Roblot F. Recurrent episodes of candidemia due to *Candida glabrata, Candida tropicalis* and *Candida albicans* with acquired echinocandin resistance. Med Mycol Case Repots. 2016;14:20–3.

56. De Oliveira JS, Pereira VS, Castelo-Branco D de SCM, Cordeiro R de A, Sidrim JJC, Brilhante RSN, et al. The yeast, the antifungal, and the wardrobe: A journey into antifungal resistance mechanisms of *Candida tropicalis*. Can J. Microbiol. 2020;66(6):377–88.

57. Wang D, Na A, Yang Y, Yang X, Fan Yy, Feng J. *Candida tropicalis* distribution and drug resistance is correlated with ERG11 and UPC2 expression. Antimicrob Resist Infect Control. 2021;10.

58. Atanasov A, Zotchev S, Dirsch V, Taskforce TINPS, Supuran C. Natural products in drug discovery: advances and opportunities. Nat Rev.

2021;20:200–16.

59. Mickymaray S. Efficacy and mechanism of traditional medicinal plants and bioactive compounds against clinically important pathogens. Antibiotics. 2019;8:257.

60. Attiq A, Jalil J, Husain K. Annonaceae: Breaking the Wall of Inflammation. Front Pharmacol. 2017;8:1–24.

61. Hernández Fuentes LM, González EM, Magaña M de LG, Esparza LMA, González YN, Villagrán Z, et al. Current situation and perspectives of fruit Annonaceae in mexico: Biological and agronomic importance and bioactive properties. Plants. 2022;11(1):1–22.

62. Murillo J. Las Annonaceae de Colombia. Biota Colomb. 2001;2(1):49–58.

63. Junikka L, Maas PJM, Maas-van de Kamer H, Westra LYT. Revision of Oxandra (Annonaceae). Blumea J Plant Taxon Plant Geogr. 2016;61(3):215–66.

64. Zhang J, El-Shabrawy A, El-Shanawany M, Schiff P, Slatkin D. New azafluorene alkaloids from *Oxandra xylopioides*. J. Nat Prod. 1987;50:800–6.

65. Yang L, Wen K-S, Ruan X, Zhao Y-X, Wei F, Wang Q. Response of plant secondary metabolites to environmental factors. Molecules. 2018;23:762.

66. Morales I, De La Fuente J, Sosa V. Componentes de *Eupatorium saltense*. An Asoc Quim Argent. 1991;79(3):141–4.

67. Hocquemiller R, Cortes D, Arango GJ, Myint SH, Cave A. Isolement et synthese de L´Espintanol, nouveau monoterpene antiparasitaire. J Nat Prod. 1991;54:445–52.

68. Rojano B, Gaviria CA, Sáez J. Determinación de la actividad antioxidante en un modelo de peroxidación lipídica de mantequilla inhibida por el isoespintanol. Vitae. 15:212–8.

69. Restrepo G, Rojano B. Efecto del isoespintanol y el timol en la actividad antioxidante de semen equino diluido con fines de congelación. Rev Med Vet. 2017;35:149–58.

70. Restrepo G, Rojano B. Actividad antioxidante del isoespintanol y el timol en el semen equino criopreservado. Rev Inv Vet Perú. 2018;29:205–16.

71. Marquez-Fernandez M, Munoz-Lasso D, Bautista Lopez J, Zapata K, Puertas Mejia M, Lopez-Alarcon C, et al. Effect of isoespintanol isolated from *Oxandra* cf. *xylopioides* against DNA damage of human lymphocytes. Pak J Pharm Sci.

2018;31:1777–82.

72. Zapata K, Arias J, Cortés F, Alarcon C, Durango D, Rojano B. Oxidative stabilization of palm olein with isoespintanol (2-isopropyl-3,6-dimethoxy-5-methylphenol) isolated from *Oxandra* cf *xylopioides*. J. Med Plants Res. 2017;11:218–25.

73. Sun F-J, Li M, Gu L, Wang M, Yang M. Recent progress on anti-Candida natural products. Chin J. Nat Med. 2021;19(8):561–79.

74. Contreras Martínez OI, Angulo Ortíz AA, Santafé Patiño G. Antifungal potential of isoespintanol extracted from *Oxandra xylopioides* diels (Annonaceae) against intrahospital isolations of Candida spp. Heliyon. 2022;8(10).

75. Contreras Martínez OI, Angulo Ortíz AA, Santafé Patiño G. Mechanism of Antifungal Action of Monoterpene Isoespintanol against Clinical Isolates of *Candida tropicalis*. Molecules. 2022;27:5808.

76. Contreras Martínez OI, Angulo Ortíz AA, Santafé Patiño G, Peñata-Taborda A, Berrio Soto R. Isoespintanol Antifungal Activity Involves Mitochondrial Dysfunction, Inhibition of Biofilm Formation, and Damage to Cell Wall Integrity in *Candida tropicalis*. Int J. Mol Sci. 2023;24(12):10187.

77. Iraji A, Yazdanpanah S, Alizadeh F, Mirzamohammadi S, Ghasemi Y, Pakshir K, et al. Screening the antifungal activities of monoterpenes and their isomers against Candida species. J Appl Microbiol. 2020;129(6):1541–51.

78. Gallucci MN, Carezzano ME, Oliva MM, Demo MS, Pizzolitto RP, Zunino MP, et al. *In vitro* activity of natural phenolic compounds against fluconazole-resistant Candida species: A quantitative structure-activity relationship analysis. J. Appl Microbiol. 2014;116(4):795–804.

79. Xiong H, Zhou X, Xiang W, Huang M, Lin Z, Tang J, et al. Integrated transcriptome reveals that D -limonene inhibits *Candida tropicalis* by disrupting metabolism. LWT- Food Sci Technol. 2023;176:114535.

80. Yu H, Lin Z, Xiang W, Huang M, Tang J, Lu Y, et al. Antifungal activity and mechanism of D -limonene against foodborne opportunistic pathogen *Candida tropicalis*. LWT-Food Sci Technol. 2022;159:113144.

81. Kowalczyk A, Przychodna M, Sopata S, Bodalska A, Fecka I. Thymol and thyme essential oil-new insights into selected therapeutic applications. Molecules. 2020;25:4125.

82. Dias de Castro R, Souza PA de, Dornelas Bezerra L, Silva Ferreira G, Melo de Brito Costa E, Leite Cavalcanti A. Antifungal activity and mode of action of thymol and its synergism with nystatin against Candida species involved with infections in the oral cavity: an *in vitro* study. BMC Complement Altern Med. 2015;15 (1).

83. Marchese A, Orhan IE, Daglia M, Barbieri R, Di Lorenzo A, Nabavi SF, et al. Antibacterial and antifungal activities of thymol: A brief review of the literature. Food Chem. 2016;210:402–14.

84. Jafri H, Ahmad I. *Thymus vulgaris* essential oil and thymol inhibit biofilms and interact synergistically with antifungal drugs against drug resistant strains of *Candida albicans* and *Candida tropicalis*. J. Mycol Med. 2020;30(1):100911.

85. Oliveira Lima I, de Oliveira Pereira F, Araújo de Oliveira W, de Oliveira Lima E, Albuquerque Menezes E. Antifungal activity and mode of action of carvacrol against *Candida albicans* strains. J. Essent Oil Res. 2013;25 (2):37–41.

86. Vitali A, Stringaro A, Colone M, Muntiu A, Angiolella L. Antifungal carvacrol loaded chitosan nanoparticles. Antibiotics. 2022;11(1).

87. Chatrath A, Kumar M, Prasad R. Comparative proteomics and variations in extracellular matrix of *Candida tropicalis* biofilm in response to citral. Protoplasma. 2022;259(2):263–75.

88. Silva D, Diniz-neto H, Silva-neta M, Silva S, Andrade-j F, Leite M, et al. (R)-(+)-B-Citronellol and (S)-(-)-B-Citronellol in Combination with Amphotericin B against Candida Spp. Int J Mol Sci. 2020;21:1785.

89. Kim DJ, Lee MW, Choi JS, Lee SG, Park JY, Kim SW. Inhibitory activity of hinokitiol against biofilm formation in fluconazole-resistant Candida species. PLoS One. 2017;12(2):1–11.

90. Lemos ASO, Florêncio JR, Pinto NCC, Campos LM, Silva TP, Grazul RM, et al. Antifungal Activity of the Natural Coumarin Scopoletin Against Planktonic Cells and Biofilms From a Multidrug-Resistant *Candida tropicalis* Strain. Front Microbiol. 2020;11(July):1–11.

91. Kumar R, Saha A, Saha D. A new antifungal coumarin from *Clausena excavata*. Fitoterapia. 2012;83(1):230–3.

92. Ramírez RD, Páez MS, Angulo AA. Obtención de isoespintanol por hidrodestilación y cristalización a partir del extracto bencínico de *Oxandra xylopioides*. Inf Tecnol. 2015;26(6):13–8.

93. Hussein HA, Maulidiani M, Abdullah MA. Microalgal metabolites as anti-cancer/anti-oxidant agents reduce cytotoxicity of elevated silver nanoparticle levels against non-cancerous vero cells. Heliyon. 2020;6(10):e05263.

94. Motlhatlego K, Ali M, Leonard C, Eloff J, McGaw L. Inhibitory effect of Newtonia extracts and myricetin-3-o-rhamnoside (myricitrin) on bacterial biofilm formation. BMC Complement Med Ther. 2020;20:358.

95. Negrette-Guzmán M, Huerta-Yepez S, Vega MI, León-Contreras JC, Hernández-Pando R, Medina-Campos ON, et al. Sulforaphane induces differential modulation of mitochondrial biogenesis and dynamics in normal cells and tumor cells. Food Chem Toxicol. 2017;100:90–102.

96. Mosmann T. Rapid Colorimetric Assay for Cellular Growth and Survival: Application to Proliferation and Cytotoxicity Assays. J Immunol. 1983;65:55–63.

97. Feoktistova M, Geserick P, Leverkus M. Crystal violet assay for determining viability of cultured cells. Cold Spring Harb Protoc. 2016;2016(4):343–6.

98. Clinical and Laboratory Standards Institute. Methods for Dilution Antimicrobial Susceptibility Tests for Bacteria That Grow Aerobically ; Approved Standard — Ninth Edition. Vol. 32. 2012.

99. Quave CL, Plano LRW, Pantuso T, Bennett BC. Effects of extracts from Italian medicinal plants on planktonic growth, biofilm formation and adherence of methicillin-resistant *Staphylococcus aureus*. J. Ethnopharmacol. 2008;118(3):418–28.

100. Cantón E, Martín E, Espinel-Ingroff A. Métodos estandarizados por el CLSI para el estudio de la sensibilidad a los antifúngicos (documentos M27-A3, M38-A y M44-A). Rev Iberoam Micol. 2007;

101. Rodriguez-tudela JL. Method for Determination of Minimal Inhibitory Concentration (MIC) by Broth Dilution of Fermentative Yeasts. Clin Microbiol Infect. 2003;(August).

102. Maldonado J, Casaña R, Martínez I, San Martín E. La espectroscopia UV-Vis en la evaluación de la viabilidad de células de cáncer de mama. Latin-American J Phys Educ. 2018;12(2):1–7.

103. Zhang X, Zhang T, Guo S, Zhang Y, Sheng R, Sun R, et al. In vitro antifungal activity and mechanism of Ag3PW12O40 composites against Candida species. Molecules. 2020;25:6012.

104. Zhao F, Dong HH, Wang YH, Wang TY, Yan ZH, Yan F, et al. Synthesis and synergistic antifungal effects of monoketone derivatives of curcumin against fluconazole-resistant Candida spp. Medchemcomm. 2017;8(5):1093–102.

105. Vermes I, Haanen C, Reutelingsperger C. Flow cytometry of apoptotic cell death. J Immunol Methods. 2000;243(1–2):167–90.

106. Tao N, Ouyang Q, Jia L. Citral inhibits mycelial growth of *Penicillium italicum* by a membrane damage mechanism. Food Control. 2014;41:116–21.

107. Chaves-lopez C, Nguyen HN, Oliveira RC, Nadres ET, Paparella A, Rodrigues DF. A morphological, enzymatic and metabolic approach to elucidate apoptotic-like cell death in fungi exposed to h- and α-molybdenum trioxide nanoparticles. Nanoscale. 2018;10:20702–16.

108. Song J, Kanazawa I, Sun K, Murata T, Yokoyama K. Color coding the cell death status of plant suspension cells. Biotechniques. 1999;26(6):1060–2.

109. Da Silva CR, Campos R de S, Neto JB de A, Sampaio LS, do Nascimento F, do AV Sa LG, et al. Antifungal activity of B-lapachone against azole-resistant Candida spp. and its aspects upon biofilm formation. Future Microbiol. 2020;15:1543–54.

110. Neto JBA, Da Silva CR, Neta MAS, Campos RS, Siebra JT, Silva RAC, et al. Antifungal activity of naphthoquinoidal compounds *in vitro* against fluconazole-resistant strains of different Candida species: A special emphasis on mechanisms of action on *Candida tropicalis*. PLoS One. 2014;9(5):1–10.

111. Chang CK, Kao MC, Lan CY. Antimicrobial activity of the peptide lfcinb15 against *Candida albicans*. J. Fungi. 2021;7(7).

112. Marika GJ, Saez GT, O'Connor J-E. A fast kinetic method for assessing mitochondrial membrane potential in isolated hepatocytes with rhodamine 123 and flow cytometry. Cytometry. 1994;15(4):335–42.

113. Johnson LV V., Walsh MLL, Bockus BJ, Chen LB. Monitoring of relative mitochondrial membrane potential in living cells by fluorescence microscopy. J Cell Biol. 1981;88(3):526–35.

114. Baracca A, Sgarbi G, Solaini G, Lenaz G. Rhodamine 123 as a probe of mitochondrial membrane potential: Evaluation of proton flux through F0 during ATP synthesis. Biochim Biophys Acta - Bioenerg. 2003;1606(1–3):137–46.

115. Zorova LD, Popkov VA, Plotnikov EY, Silachev DN, Pevzner IB, Jankauskas

SS, et al. Mitochondrial membrane potential. Anal Biochem. 2018;552:50–9.

116. Costa de Oliveira S, Silva A, Miranda I, Salvador A, Azevedo M, Munro C, et al. Determination of chitin content in fungal cell wall: an alternative flow cytometric method. Cytom part A. 2013;83A:324–8.

117. Hoch HC, Galvani CD, Szarowski DH, Turner JN. Two new fluorescent dyes applicable for visualization of fungal cell walls. Mycologia. 2005;97(3):580–8.

118. Monheit JG, Brown G, Kott MM, Schmidt WA, Moore DG. Calcofluor white detection of fungi in cytopathology. Am J Clin Pathol. 1986;85(2):222–5.

119. Benjamini Y, Hochberg Y. Controlling the False Discovery Rate: A Practical and Powerful Approach to Multiple Testing. J R Stat Soc Ser B. 1995;57(1):289–300.

120. Ge SX, Jung D, Yao R. ShinyGO: A graphical gene-set enrichment tool for animals and plants. Bioinformatics. 2020;36(8):2628–9.

Anexos

Anexo 1

"Mechanism of Antifungal Action of Monoterpene Isoespintanol against Clinical Isolates of *Candida tropicalis*"

molecules

MDPI

Article

Mechanism of Antifungal Action of Monoterpene Isoespintanol against Clinical Isolates of *Candida tropicalis*

Orfa Inés Contreras Martínez [1,*], Alberto Angulo Ortíz [2] and Gilmar Santafé Patiño [2]

[1] Biology Department, Faculty of Basic Sciences, University of Córdoba, Montería 230002, Colombia
[2] Chemistry Department, Faculty of Basic Sciences, University of Córdoba, Montería 230002, Colombia
* Correspondence: oicontreras@correo.unicordoba.edu.co

Abstract: The growing increase in infections by *Candida* spp., non-albicans, coupled with expressed drug resistance and high mortality, especially in immunocompromised patients, have made candidemia a great challenge. The efficacy of compounds of plant origin with antifungal potential has recently been reported as an alternative to be used. Our objective was to evaluate the mechanism of the antifungal action of isoespintanol (ISO) against clinical isolates of *Candida tropicalis*. Microdilution assays revealed fungal growth inhibition, showing minimum inhibitory concentration (MIC) values between 326.6 and 500 µg/mL. The eradication of mature biofilms by ISO was between 20.3 and 25.8% after 1 h of exposure, being in all cases higher than the effect caused by amphotericin B (AFB), with values between 7.2 and 12.4%. Flow cytometry showed changes in the permeability of the plasma membrane, causing loss of intracellular material and osmotic balance; transmission electron microscopy (TEM) confirmed the damage to the integrity of the plasma membrane. Furthermore, ISO induced the production of intracellular reactive oxygen species (iROS). This indicates that the antifungal action of ISO is associated with damage to membrane integrity and the induction of iROS production, causing cell death.

Keywords: isoespintanol; antifungal; *Oxandra xylopioides*; *Candida tropicalis*

Citation: Contreras Martínez, O.I.; Angulo Ortíz, A.; Santafé Patiño, G. Mechanism of Antifungal Action of Monoterpene Isoespintanol against Clinical Isolates of *Candida tropicalis*. *Molecules* **2022**, *27*, 5808. https://doi.org/10.3390/molecules27185808

Academic Editor: Luisella Verotta

Received: 17 August 2022
Accepted: 2 September 2022
Published: 8 September 2022

1. Introduction

Fungal infections constitute a continuing and serious threat to human health, especially in immunocompromised people, where the incidence of systemic candidiasis has increased substantially in recent years [1–5]. *Candida tropicalis* has emerged as one of the most important *Candida* spp., non-albicans, due to its high incidence in systemic candidiasis and its greater resistance to commonly used antifungals [6]. This yeast has been widely considered to be the second most virulent candida species, preceded only by *C. albicans* [7]; it is an opportunistic fungus that affects immunocompromised people and is capable of spreading to vital organs [8]. *Candida tropicalis* is recognized as a strong producer of biofilms, surpassing *C. albicans* in most studies; likewise, it produces a wide range of other virulence factors, including adhesion to epithelial cells, endothelial cells and other host surfaces as well as medical devices; secretion of lytic enzymes; and the so-called morphogenesis expressed by this yeast. *C. tropicalis* is a clinically relevant species and may be the second or third most important etiologic agent of candidemia, specifically in Latin American and Asian countries [7]. In Colombia, candidemia is a frequent cause of infection in the bloodstream, especially in Intensive Care Units (ICU); it represents 88% of fungal infections in hospitalized patients, with a mortality between 36% and 78%, and its incidence in Colombia is higher than that reported in developed countries and even in other Latin American countries [9]. It has been documented that *C. tropicalis* is associated with higher mortality compared to *C. albicans* and other non-albicans candida species, apparently showing a greater potential for dissemination in neutropenic individuals. This yeast is associated with malignancy, especially in patients who require prolonged catheterization, receive broad-spectrum antibiotics, or have cancer [10].

In this context, the search and development of new compounds with antifungal potential that are tolerable, effective and safe is urgent today. Various studies have reported the role of plants as a source of secondary metabolites with recognized medicinal properties [11], which can be used directly as bioactive compounds, as drug prototypes and/or as pharmacological tools for different targets [12]. Isoespintanol (ISO) (2-isopropyl-3,6-dimethoxy-5-methylphenol) is a monoterpene obtained for the first time from the aerial parts of *Eupatorium saltense* (Asteraceae) [13], and its synthesis was also reported [14]. Also, it has been extracted from *Oxandra xylopioides* (Annonaceae), whose antioxidant [15], anti-inflammatory [16], antispasmodic [17], vasodilator [18] and cryoprotectant in canine semen [19] effects have been reported, as well as its insecticide [20] and antifungal activity against *Colletotrichum* [21]. However, its antifungal potential against human pathogens has not been reported, so we hypothesize that ISO could have an effect against human pathogenic fungi such as *Candida* spp. The purpose of this research was to evaluate the antifungal activity of ISO, estimate its ability to eradicate mature biofilms and explore the mechanisms of action against clinical isolates of *C. tropicalis*, contributing to the search for new compounds of natural origin that can serve as adjuvants in the treatment of pathogenic yeasts resistant to antifungals.

2. Results

2.1. Obtaining and Identifying Isoespintanol

The ISO (1.2 g) was purified as a crystalline amorphous solid, with a purity greater than 99%, verified by GC-MS. Its structural identification by ^{1}H-NMR, ^{13}C-NMR, DEPT, COSY ^{1}H-^{1}H, HMQC and HMBC led unequivocally to propose the structure of 2,5-dimethoxy-3-hydroxy-*p*-cymene, isoespintanol, Figure 1. The EI-MS: $[M]^{+}$ m/z 210 (49%) and fragments m/z 195 (100%), 180, 165, 150, 135 and 91. ^{1}H-NMR ($CDCl_3$): δ 6.22 s, 1H (H6), δ 5.85 s, 1H (HO-3), δ 3.77 s, 3H (H12), δ 3.76 s, 3H (H11), δ 3.52 hep, J = 7.1 Hz, 1H (H8), δ 2.29 s, 3H (H7), δ 1.33 d, J = 7.1 Hz, 6H (H9-H10). ^{13}C-NMR ($CDCl_3$): δ 154.3 (C5), δ 147.4 (C3), δ 139.7 (C2), δ 126.8 (C1), δ 120.4 (C4), δ 104.4 (C6), δ 24.6 (C8), δ 60.8 (C11), δ 55.7 (C12), δ 20.6 (C9, C10), δ 15.8 (C7).

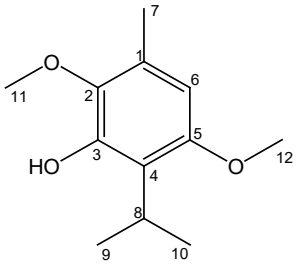

Figure 1. Structure of Isoespintanol.

2.2. Phylogenomics of Candida tropicalis

Genome-wide based taxonomic study of the *C. tropicalis* clinical isolate confirmed the identification of this yeast. The results of the gDNA extraction, quantification and purity measurement (260/280) by spectrophotometry, as well as the general statistics of the NGS sequencing, the general statistics of the *C. tropicalis* genome assembly and the phylogenetic study, are shown in the Supplementary Materials.

2.3. Antifungal Susceptibility Testing

ISO showed antifungal activity against all clinical isolates of *C. tropicalis* studied; we observed a reduction in the growth percentage of yeasts treated with ISO, compared to untreated isolates used as control. Figure 2 shows the similar tendency among the isolates to increase the percentage of growth reduction as the ISO concentration increases. All isolates showed FLZ MIC (MIC_{90}) values $\geq$ 128 μg/mL. Table 1 shows the values of MIC (MIC_{90}),

MIC_{50} and MFC of the ISO; we observed ISO MIC values between 326.6 and 500 µg/mL and this effect on *C. tropicalis* was shown to be dependent on the ISO concentration.

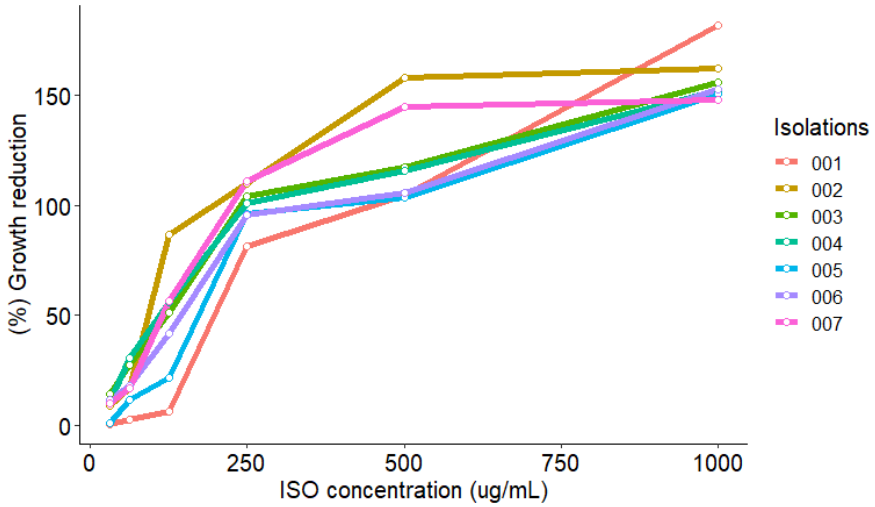

Figure 2. Growth reduction of *C. tropicalis* isolates exposed to ISO (MIC of each isolate). A strong and positive linear relationship between the ISO concentration and the yeast growth reduction percentage is observed, i.e., as the ISO concentration increases, the yeast growth reduction percentage also increases, which coincides with the Pearson correlation coefficient ($0.83 < r < 0.96$) in all isolates. In addition, the hypothesis test on the correlation coefficient yields a p-value < 0.05, which indicates that, with 95% confidence, there is a significant linear relationship.

Table 1. Minimum inhibitory concentration (MIC) and minimum fungicidal concentration (MFC) values (µg/mL) of ISO and FLZ against *C. tropicalis*.

C. tropicalis	ISO			FLZ
	MIC_{90}	**MIC_{50}**	**MFC**	**MIC_{90}**
CLI 001	470	261.2	500	875.1
CLI 002	326.6	59.38	350	751
CLI 003	413.3	124.4	400	875.1
CLI 004	420.8	121.5	450	751
CLI 005	500	234.6	500	256
CLI 006	463.9	179.8	450	128
CLI 007	391.6	107	400	751

We observed that after 48 h the values were between 350, 400, 450 and 500 µg/mL; as evidenced, the efficacy of ISO was different between strains of the same species. There was no visible growth of the yeasts in the presence of FLZ (MIC µg/mL) in SDA medium.

2.4. MTT Reduction Assay

The effect of ISO on the viability of *C. tropicalis* isolates was tested using the MTT reduction colorimetric method. As shown in Table 2, after treatment with different ISO concentrations, the viability of *C. tropicalis* cells had a significant reduction with increasing ISO concentration, compared to the control group (100% viability). We observed that at 125 µg/mL, the viability percentage was reduced by 56.3, 59.2, 57.4 and 67.0% for isolates 002, 003, 004 and 007, respectively, while at 250 µg/mL the viability percentage was reduced by 50, 48 and 51.7% for isolates 001, 005 and 006, respectively.

Table 2. Viability percentages with MTT.

	Isolations						
ISO (µg/mL)	**001**	**002**	**003**	**004**	**005**	**006**	**007**
31.25	109.1	101.8	102.0	101.3	111.7	107.7	100.6
62.5	108.6	65.9	101.7	100.6	107.1	100.8	74.0
125	101.3	56.3	59.2	57.4	104.6	100.1	67.0
250	50.0	8.7	14.2	10.2	48.0	51.7	0.0
500	0.9	1.8	0.3	0.0	1.3	0.9	0.0
1000	1.1	0.0	0.8	0.6	0.0	0.2	0.0
MIC_{50}	236.8	103.1	141.8	136.4	230.9	235.2	113.7

As shown in Figure 3, the viability of all isolates decreases by 50% at concentrations below 250 µg/mL.

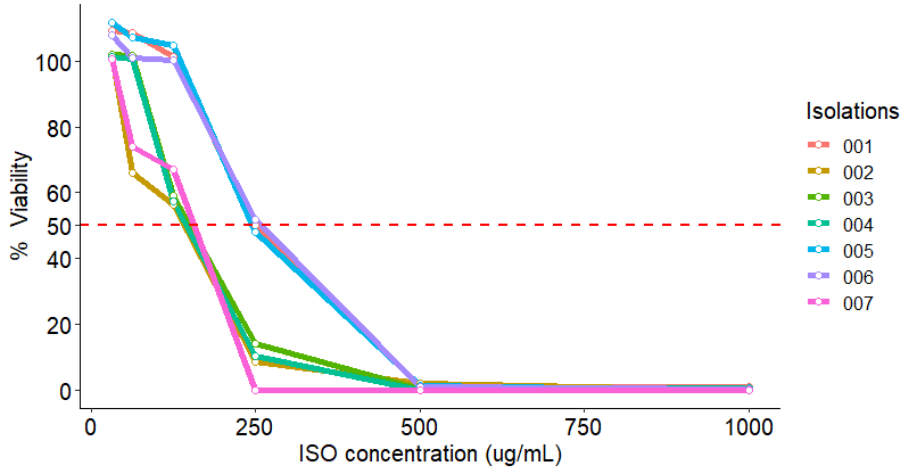

Figure 3. MIC_{50} of viability percentage of *C. tropicalis* isolates exposed to ISO (MIC for each isolate).

2.5. Growth Inhibition Curve

The growth inhibition effect of ISO on *C. tropicalis* is shown in Figure 4. As observed in the two isolates of *C. tropicalis*, the number of yeasts began to proliferate rapidly at 6 h in the control group (cells untreated), unlike the yeasts treated with ISO where a significant delay in their growth was observed, beginning to proliferate after 12 and 24 h. After 24 h, the curve increased rapidly in these groups (this behavior was similar in all the isolates studied). The cells treated with FLZ (MIC µg/mL) showed in some cases a behavior similar to that of the cells treated with ISO, but in others the behavior was similar to the control group; no reduction in inhibition was observed with extension of time.

2.6. LIVE/DEAD Assay

Isolates of *C. tropicalis* treated with ISO and FLZ and without treatment were observed under fluorescence microscopy. AO diffuses across intact cytoplasmic membranes in living cells [22] where it interacts with DNA by emitting a bright green fluorescence [23]. In contrast, EB penetrates only cells with damaged membranes and cell walls in dead cells [24], intercalates with DNA, and emits a red-orange fluorescence. As seen in Figure 5, untreated cells with entirely green fluorescence grew well after 24 h (a), while dead cells with red fluorescence were massively observed in the group treated with ISO (b). The group treated with FLZ showed a lower proportion of dead cells (c).

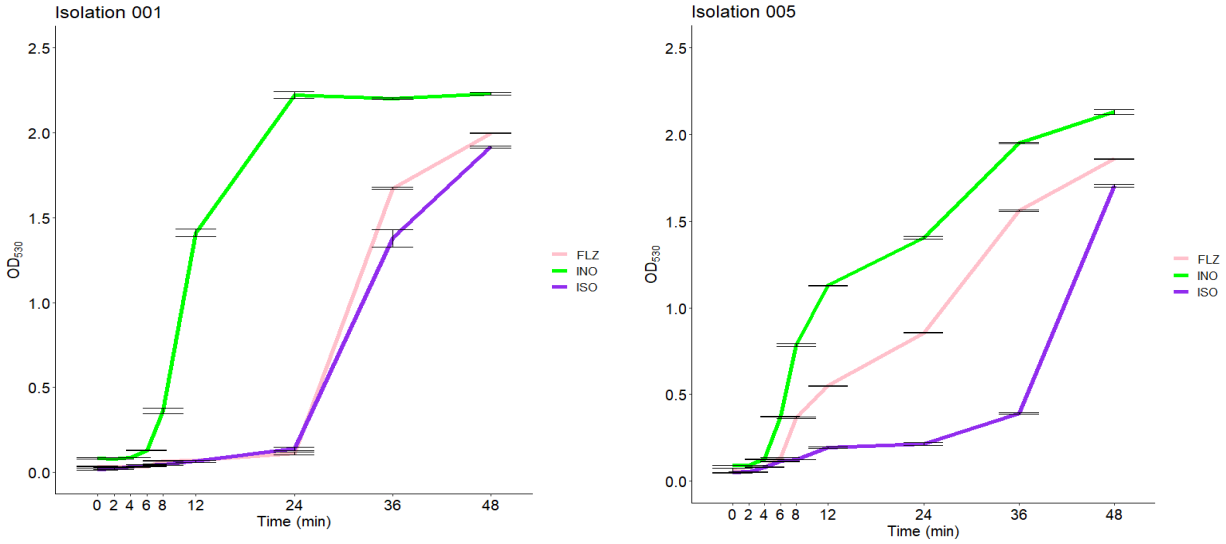

Figure 4. Inhibitory effect of ISO on *C. tropicalis* (001 and 005), at different times. The delay in the growth of *C. tropicalis* treated with ISO is observed, unlike the untreated cells (INO). The behavior of the cells treated with FLZ (MIC µg/mL) is also observed.

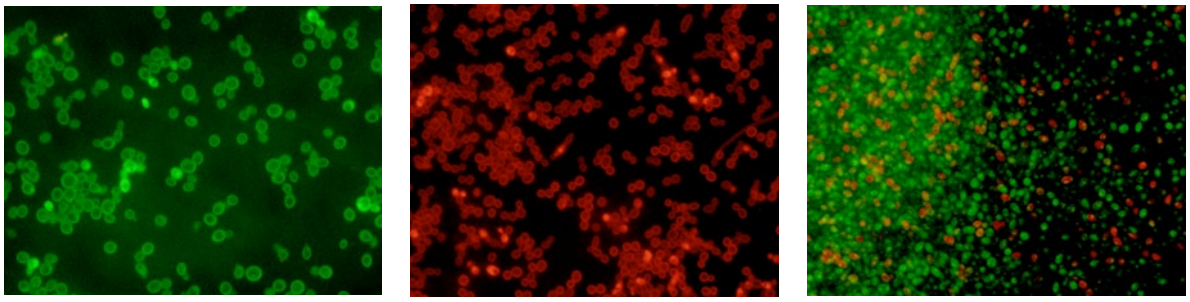

(**a**) (**b**) (**c**)

Figure 5. Fluorescence microscopy of *C. tropicalis* without treatment (**a**), treated with ISO (**b**) and treated with FLZ (**c**) after 24 h. Live cells with intact membranes appear green, while dead cells with damaged membranes appear red.

2.7. Biofilm Reduction

All *C. tropicalis* isolates produced strong biofilms on polystyrene microplates as shown in Figure 6a. When the MIC of ISO was added to the biofilms formed from each isolate, a biofilm biomass eradication percentage between 20.3 and 25.8% was obtained after 1 h of exposure to ISO, while the percentage of biomass eradication of biofilms in cells treated with AFB was lower (7.2 and 12.4%).

2.8. Effect of ISO on Cell Membrane Integrity

Our results evidence the loss of membrane integrity, as shown in Figure 7, noticing a rare and insignificant PI fluorescence in untreated cells, but a considerable increase in PI fluorescence observed when the cells were treated with ISO in each isolate of *C. tropicalis* (Figure 7b). Evidencing differences in the intensity of fluorescence between the different isolates, the PI permeated percentage of cells treated with ISO for 12 h was between 1 and 39.1%, in all cases much higher than that of untreated cells (0.0–0.2); this indicates damage to the permeability of the membranes induced by ISO. In addition, this effect is different in each isolation. Cells treated with FLZ (Figure 7c) showed a significant decrease in fluorescence intensity compared to the fluorescence emitted by cells treated with ISO, with the percentage of fluorescence intensity of this group (0.1–0.5) being closest to that of the control (untreated cells).

2.9. Leakage of Nucleic Acids and Proteins through the Fungal Membrane

The action of ISO on the integrity of the membranes of *C. tropicalis* was also evaluated by release assays of intracellular constituents that absorb at 260/280 nm, such as nucleic acids and proteins. These assays were performed at 0, 30, 60 and 120 min after treatment with ISO MIC for each isolate. As seen in Figure 8, the OD_{260}/OD_{280} values in the groups treated with ISO are significantly higher from time zero with a tendency to increase over time, compared to the groups treated with FLZ, in which a minimal and almost constant release of intracellular material was observed in all isolates of *C. tropicalis*. These results confirm fungal cell membrane damage caused by ISO.

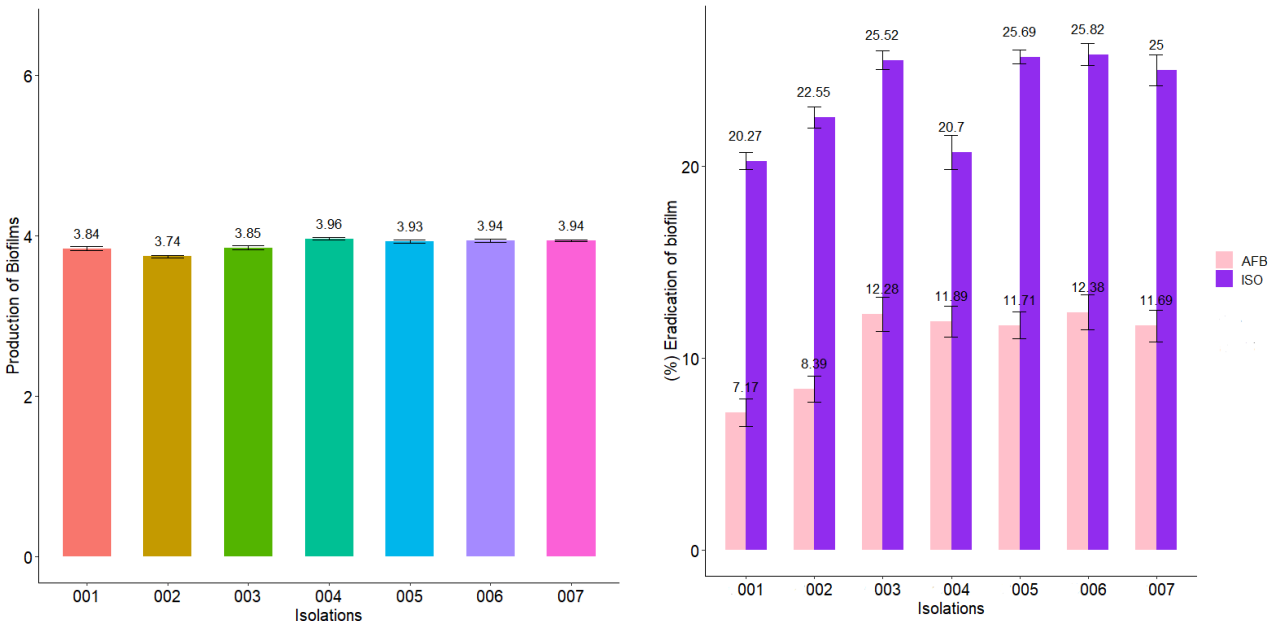

Figure 6. Action of ISO and AFB on *C. tropicalis* biofilms. (**a**) Biofilm formation at 37 °C for 48 h, where $OD_{590} > 3$ indicates strong biomass production in biofilms. (**b**) Percentage reduction of biofilms after 1 h of treatment with ISO MIC for each isolate and AFB (50 µg/mL). The results of the ANOVA showing a value of $p < 0.05$ and the Tukey test with a confidence level of 95% indicate that there is a significant difference between the effect of ISO and the effect of AFB on the reduction of biofilms.

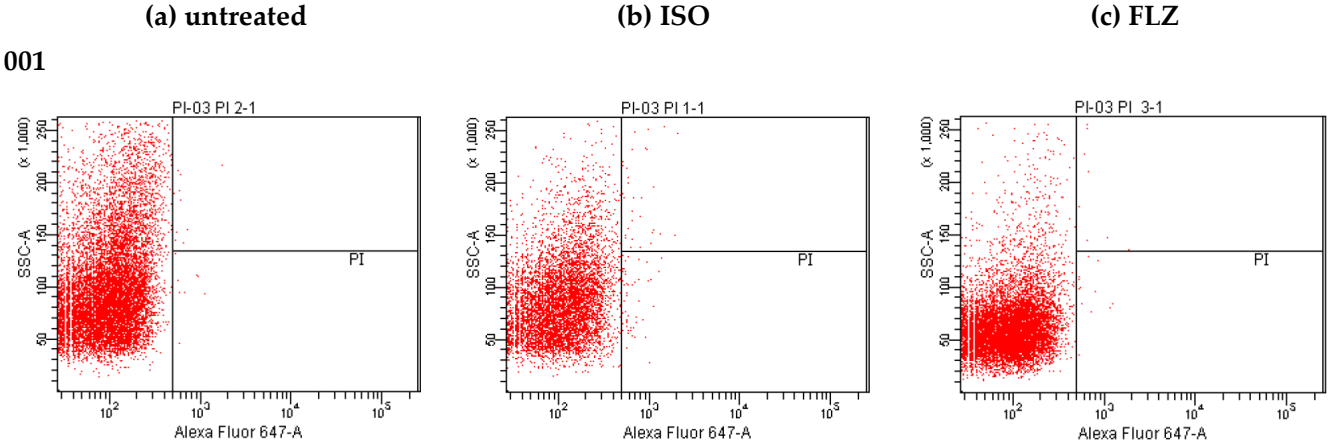

Figure 7. *Cont.*

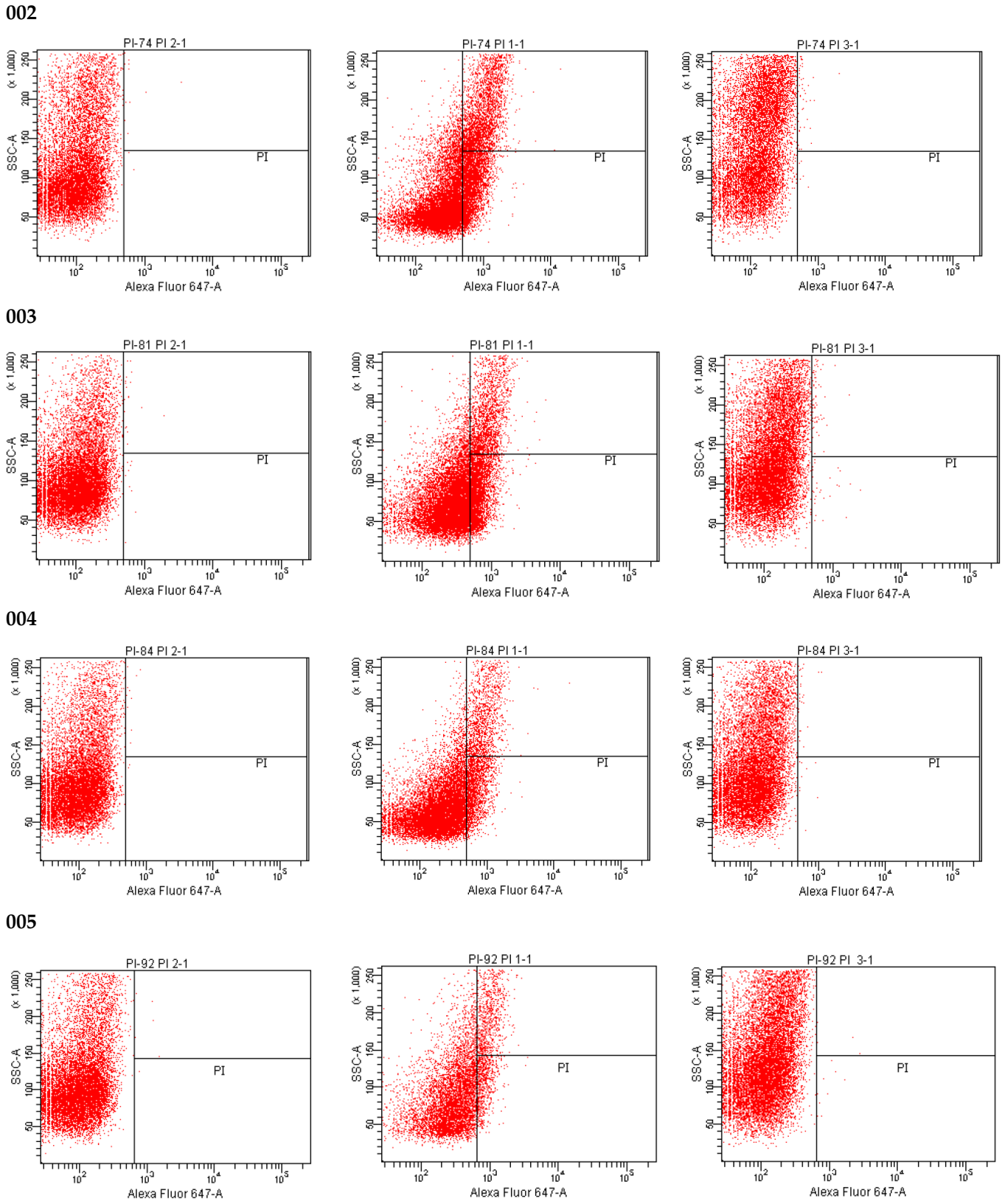

Figure 7. *Cont.*

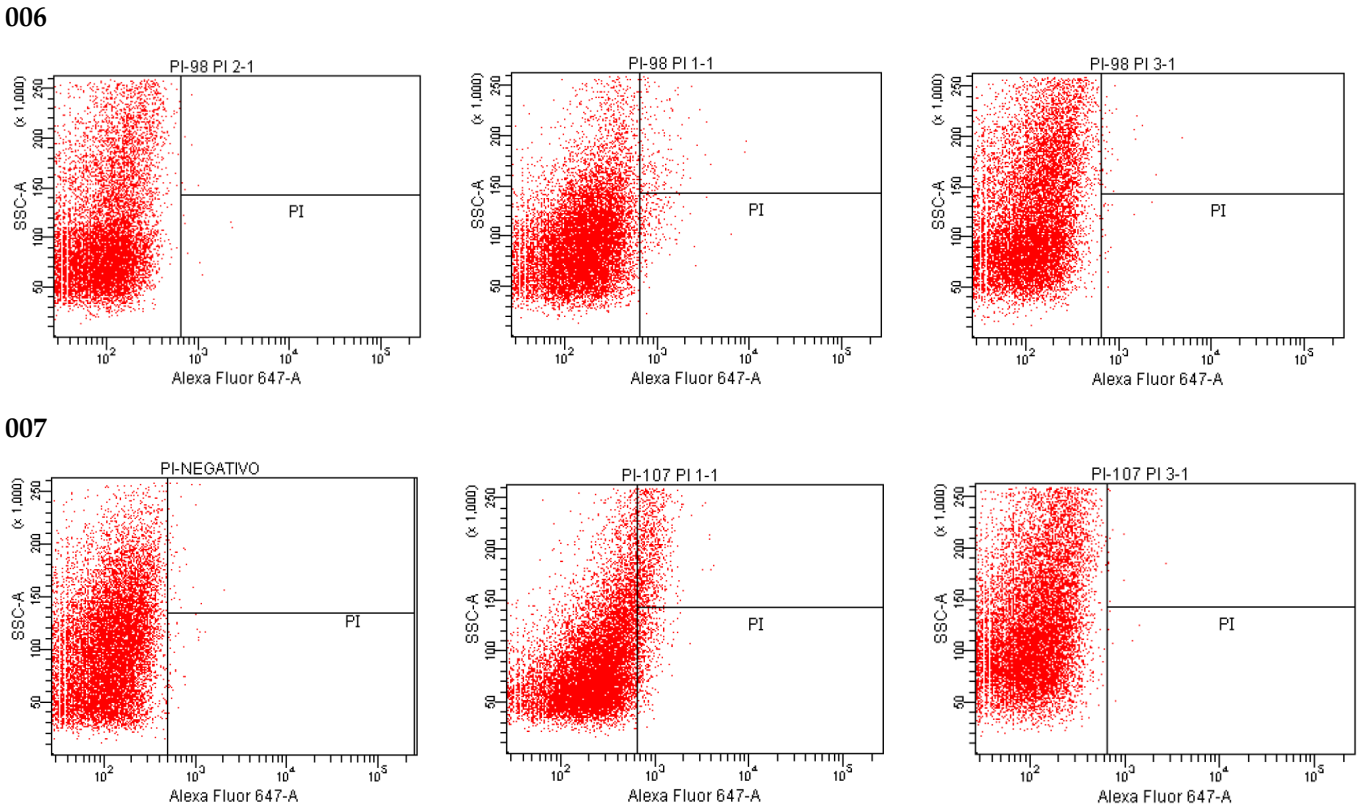

Figure 7. Changes in membrane permeability of clinical isolates of *C. tropicalis* treated with ISO: PI staining for detection of membrane permeability disruption in *C. tropicalis*. (**a**) untreated cells, (**b**) cells treated with ISO, and (**c**) cells treated with FLZ (MIC μg/mL).

2.10. Measurement of Extracellular pH

Extracellular pH measurements of *C. tropicalis* treated with ISO and FLZ and of untreated cells are shown in Figure 9. As observed in the four isolates shown, the cells treated with ISO showed an early significant increase in extracellular pH, compared with untreated cells (INO) in which the pH was observed to decrease. Cells treated with FLZ (MIC μg/mL) showed higher extracellular pH values compared to untreated cells, but in all cases these values were significantly lower compared to those of cells treated with ISO; these results confirm fungal cell membrane damage caused by ISO.

2.11. Transmission Electron Microscopy (TEM)

TEM was used to directly observe the effect of ISO on the morphology, intracellular changes and integrity of *C. tropicalis*. As shown in Figure 10a, in the untreated cells used as control, normal and intact cell morphology is observed, no damage to cell wall and membrane integrity is seen, there is no apparent disruption or release of intracellular content, and a homogeneous electronic density is observed at the level of the cytoplasm. However, after treatment with ISO (Figure 10c), the cells exhibited evident damage: irregular and deformed morphology, the cell membrane with holes and desquamation appearing partially dissolved, with loss of intracellular material and showing a heterogeneous electronic density with intense vacuolization and retraction at the level of the cytoplasm. In the cells treated with FLZ, some remained normal with intact cell walls and the damage at the membrane and cytoplasmic level was significantly less evident than that observed in cells treated with ISO.

2.12. Effect of Isoespintanol on the Production of Intracellular Reactive Oxygen Species (iROS)

Our results show that ISO treatment significantly increased the iROS load (represented by relative fluorescence intensity) in all *C. tropicalis* isolates compared to untreated cells

(Figure 11) and to those treated with H_2O_2 (iROS-inducing control). The fluorescence intensity of DCFH-DA was different among the *C. tropicalis* isolates. Figure 12 shows differences in the fluorescence emitted by DCFH-DA from untreated, ISO-treated and H_2O_2-treated cells, evidencing an increase in iROS production in ISO-treated cells compared to the other two groups. The oxidative stress generated by the overproduction of iROS induced by ISO could damage intracellular components of these yeasts and induce cell death.

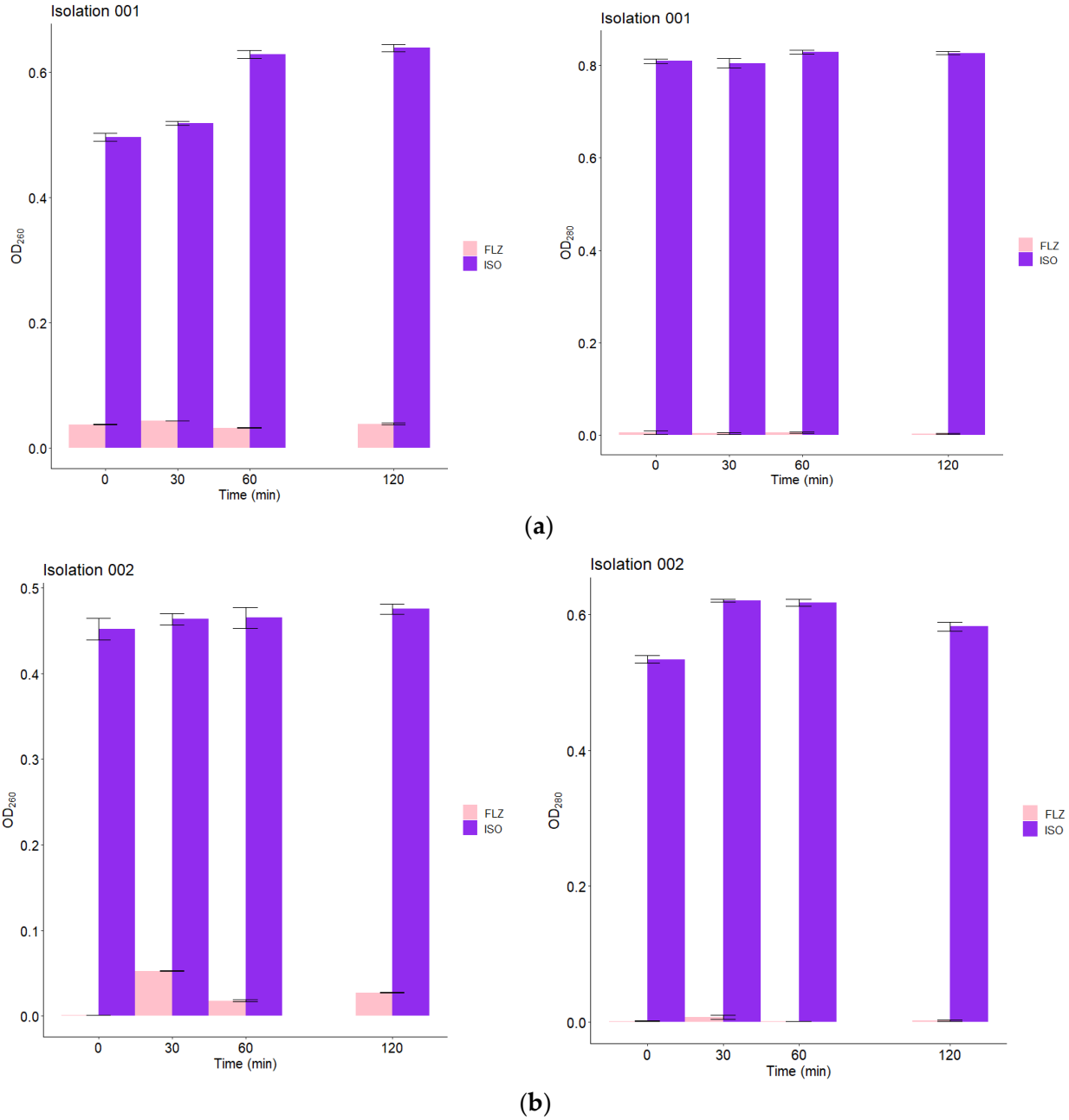

Figure 8. Release of intracellular content at 260/280 nm versus time of *C. tropicalis* treated with ISO (MIC µg/mL) and FLZ (MIC µg/mL). The figure shows the OD260/OD280 values of isolate 001 (**a**) and isolate 002 (**b**) treated with ISO and FLZ at different times. Results are expressed as the absorbance of the sample (treated with ISO) minus the absorbance of the control (samples without ISO). The results of the ANOVA and the Tukey test with a confidence level of 95% show statistically significant differences between the effect of ISO and the effect of FLZ on the leakage of intracellular material from all *C. tropicalis* isolates in this study.

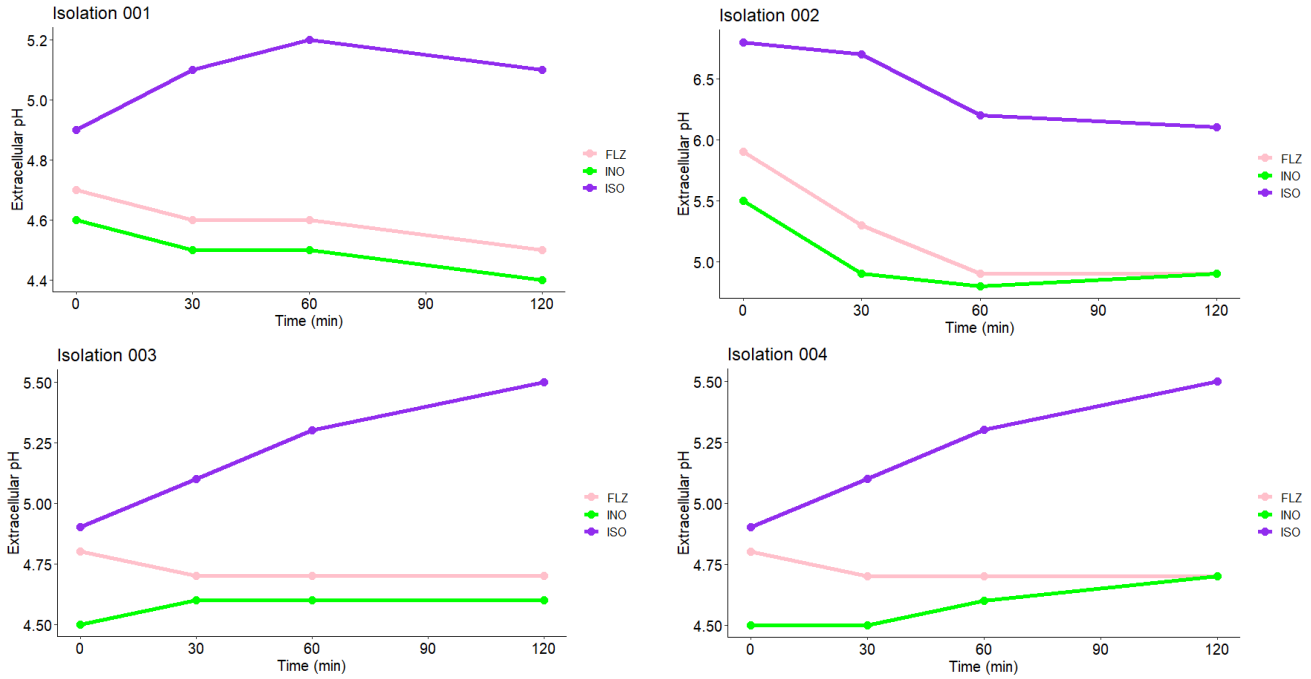

Figure 9. Measurement of extracellular pH of *C. tropicalis* treated with ISO, FLZ and untreated cells (INO). According to the results obtained by the Kruskal-Wallis test with a value of $p = 0.05$, there are significant differences between the treatments on the extracellular pH output of the yeasts.

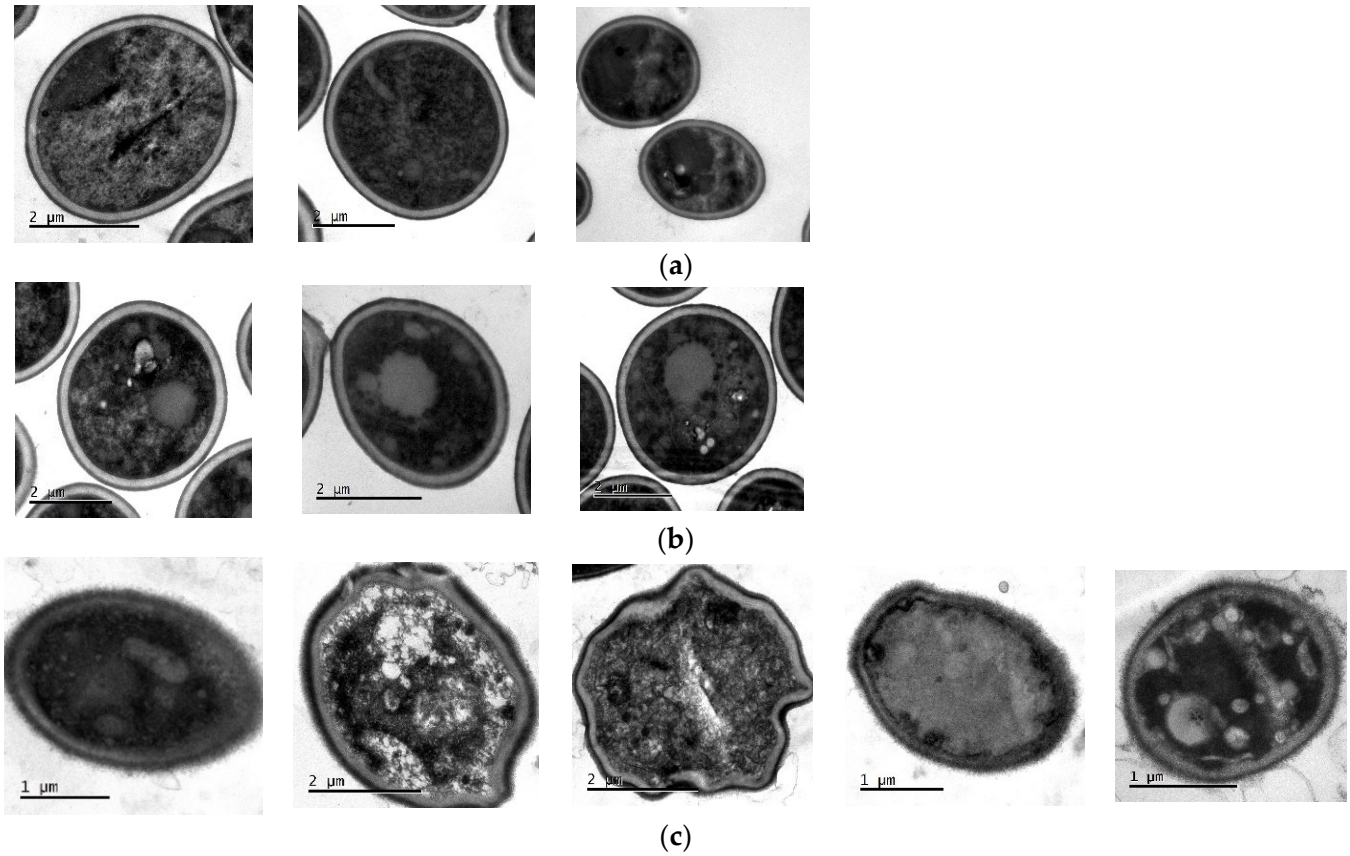

Figure 10. TEM of *C. tropicalis* untreated (**a**), treated with FLZ (**b**) and treated with ISO (**c**). The evident change in the morphology of the cells treated with ISO, as well as the damage to the integrity of the fungal cell membrane, is observed.

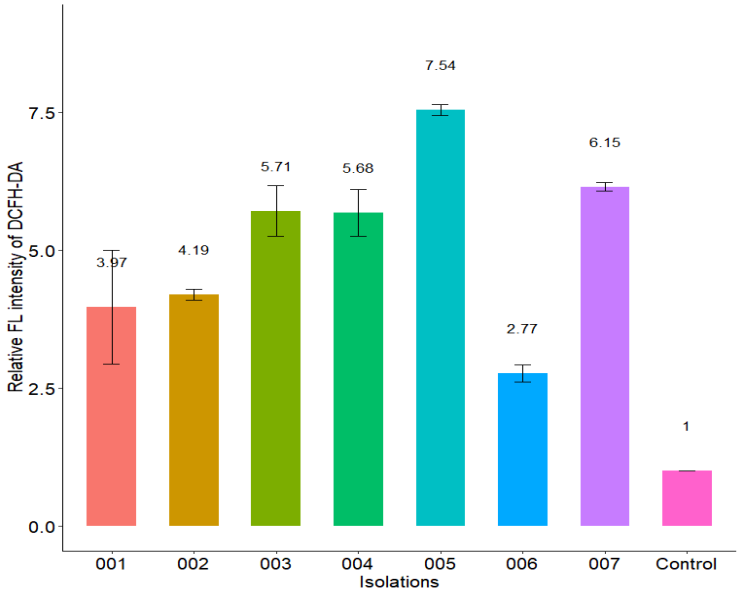

Figure 11. Effect of ISO treatment on iROS production in *C. tropicalis*. The relative fluorescence intensity of the isolates treated with the ISO MIC for each one was compared with that of the control group (untreated cells).

(a) untreated **(b) H_2O_2** **(c) ISO**

001

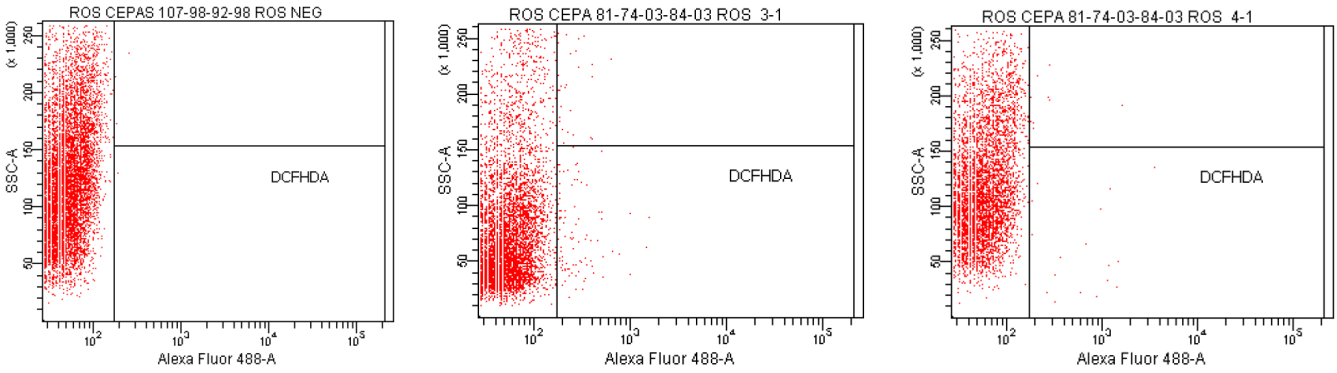

002

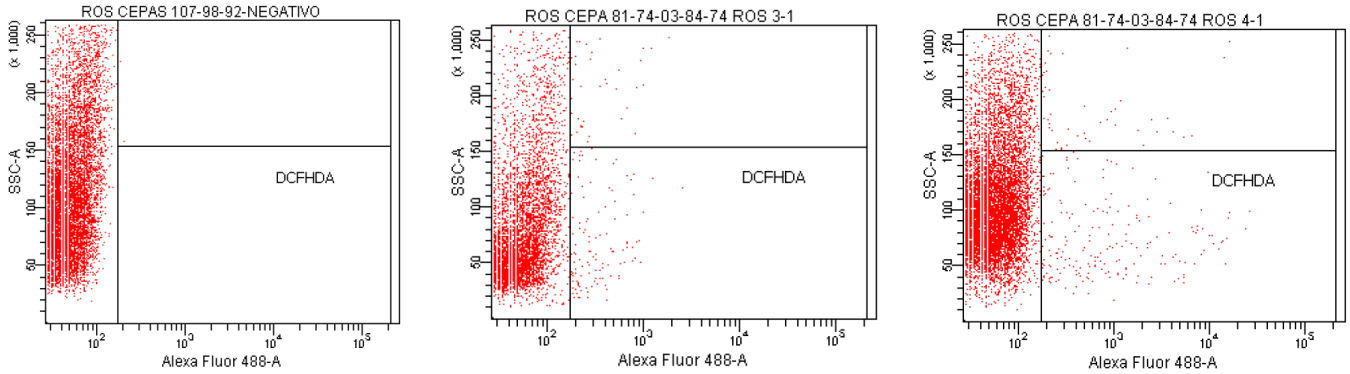

Figure 12. *Cont.*

003

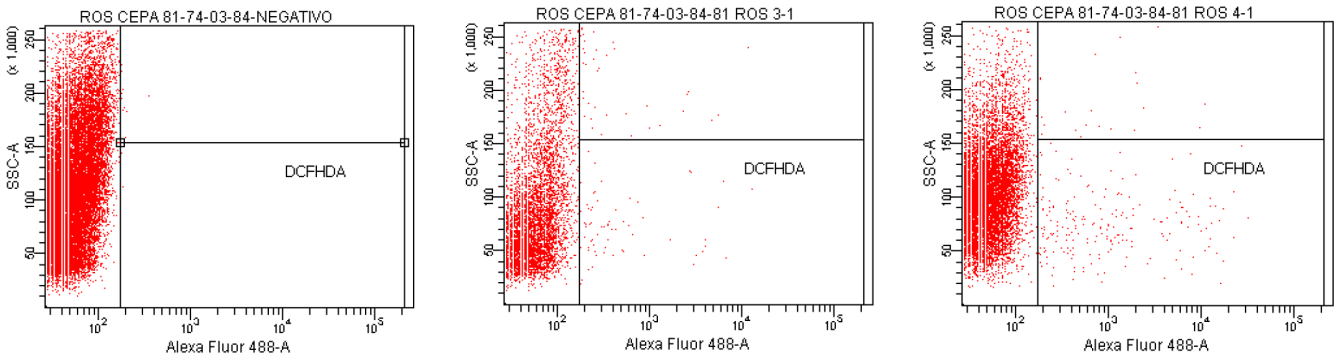

004

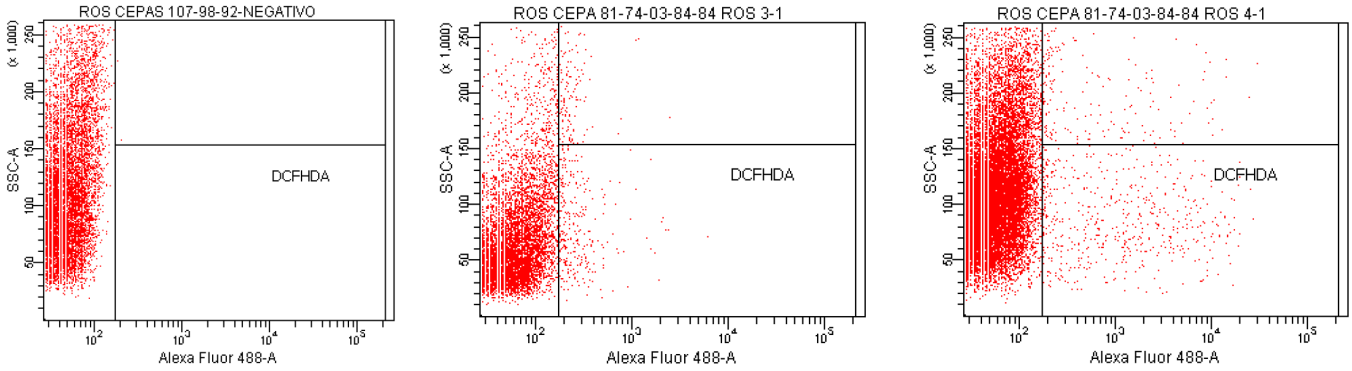

005

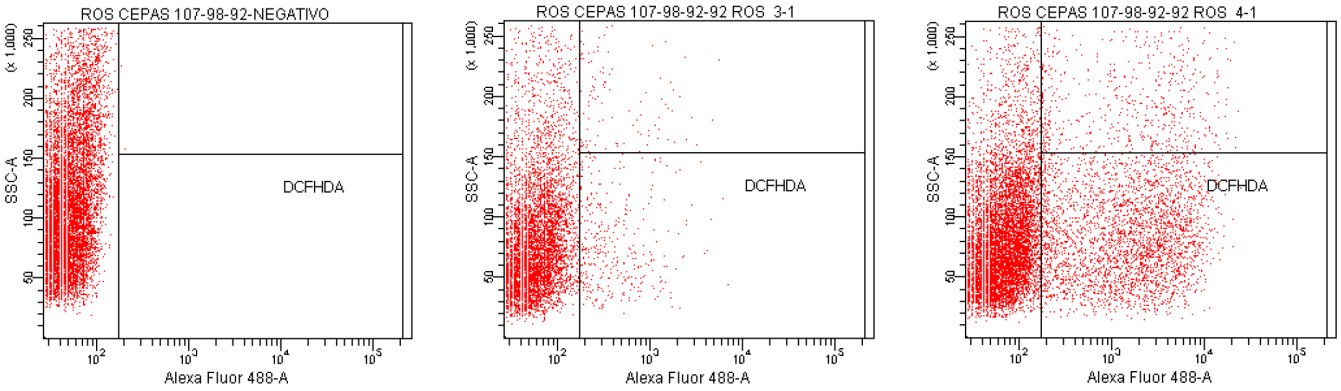

006

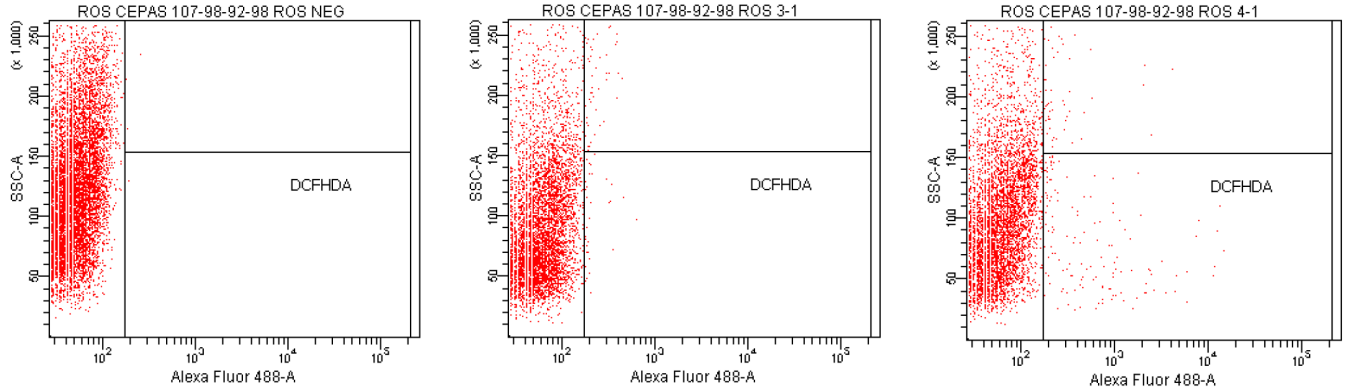

Figure 12. *Cont.*

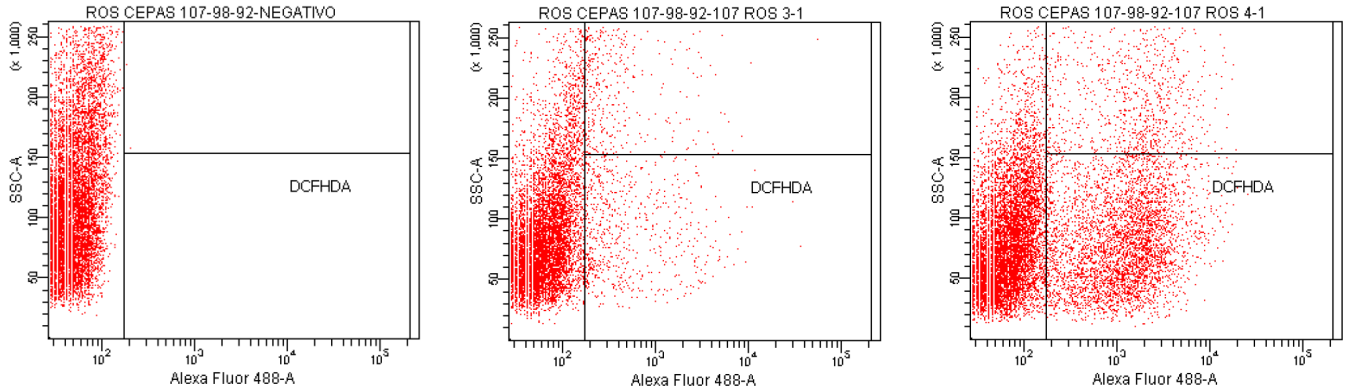

Figure 12. DCFH-DA fluorescence emitted by *C. tropicalis* yeasts untreated (**a**), treated with H_2O_2 (**b**) and treated with ISO (**c**).

3. Discussion

Currently, the growing increase in candidemia caused by *Candida* spp., non-albicans, the resistance to conventional drugs used for its control, as well as the limitation of available antifungals, have made these infections a challenging problem in medical practice, stimulating the search for new molecules with antifungal properties. In this context, chemical compounds of natural origin become an excellent alternative.

In this research, we demonstrated that ISO, a monoterpene extracted from *O. xylopioides* leaves, has antifungal activity against clinical isolates of *C. tropicalis*, which were shown to be resistant to FLZ. The effects of ISO on various *C. tropicalis* cells were different, despite their being yeasts of the same species, and these results are consistent with those reported by [25] who found differences in the efficiency of the essential oil of *Ruta graveolens* against *Candida* spp., not only for different species but even among members of the same species. Previous studies have reported the antifungal activity of terpenes isolated from plants, indicating the influence of their chemical structure on their antimicrobial action; for example, the lipophilicity of monoterpenes has been shown to allow interaction with the fungal cell wall, facilitating their penetration of the cell membrane [26]. The antifungal activity of monoterpenes such as carvacrol [27], thymol [28,29], citral [30] and linalool [31], as well as compounds with chemical structures similar to ISO such as cinnamaldehyde [32] and eugenol, highlight its antifungal potential associated with damage to the integrity of the fungal plasma membrane and related to its lipophilic nature, a factor that increases fluidity and the permeability of the cell membrane of microorganisms; these compounds interfere with ion transport, causing an osmotic imbalance in the membrane and rendering its associated proteins ineffective, leading to inhibition of microbial growth and cell lysis [33]. This is consistent with our results. We report damage to the integrity of the fungal membrane of *C. tropicalis* caused by exposure to ISO, which is probably associated with the lipophilic nature of its structure. In addition, we do not rule out a possible interaction with ergosterol of the fungal membrane, taking into account the studies reported with thymol [34], a monoterpene very similar to ISO, indicating that the damage to the fungal membrane is associated with the interaction with yeast ergosterol. Results obtained by flow cytometry with PI (a fluorescent dye which can only enter cells that have permeable membranes, where it binds to nucleic acid and fluoresces red) [35], revealed changes in permeability of the fungal membrane caused by ISO. It is known that damage to the plasma membrane can cause the collapse of the electrochemical potential, due to the formation of pores [28], where the loss of osmotic balance and the entry of ions and liquids, as well as the loss of the cytoplasmic content of cells such as soluble proteins, carbohydrates and ribonucleic acids, make the cell unable to self-regulate, resulting in cell death [36]. This is consistent with our results, which show a significant and early release of intracellular material (at 260/280 nm) in yeasts treated with ISO, with a tendency to increase over

time compared to untreated cells; in addition, the evident loss of intracellular protons (demonstrated by increased extracellular pH) confirmed the compromise of permeability in the plasmatic membrane of these ISO-treated pathogens.

In addition, the damage to the membrane integrity of *C. tropicalis* by ISO was also evidenced by TEM, which showed damage to the morphology and envelope of yeasts treated with ISO; these relevant morphological abnormalities are of great importance since they can impede the growth, viability and virulence of these yeasts, as suggested by studies with eugenol and *Trichophyton rubrum* [33]. The morphological changes could be associated with the inhibitory effect shown by ISO on mature biofilms of *C. tropicalis*, taking into account what was reported by [37], who indicates the inhibitory effect on the development of *C. tropicalis* biofilms due to morphological changes caused by the drug. On the other hand, fluorescence microscopy with AO/EB confirmed the damage to the cell membrane, which has been reported as a target point for the antimicrobial action of terpenes, which, due to their lipophilic nature, can interact with it causing its expansion, increased fluidity and permeability, with consequent damage to its structure and function [38], which is consistent with the results reported in this study.

On the other hand, the results found show that ISO stimulates the production of iROS in *C. tropicalis*; similar results were reported in previous studies with thymol [29]. The regulated synthesis of ROS by specific fungal NADPH oxidases plays a key role in fungal cell differentiation and development. In low concentration, they are an important intracellular messenger in many molecular events and play a key role in host defense [39], but in large quantities, it is well known that oxygen radicals can rapidly lead to the disintegration of biological membranes, resulting in cell death. iROS accumulation causes oxidative damage to mitochondrial proteins that appear to be disproportionately affected under oxidative stress, inducing mitochondrial membrane potential collapse [36], which in turn leads to increased iROS generation [40]. Likewise, it has been reported that the accumulation of iROS is necessary and sufficient to induce apoptosis in yeast, its presence being one of the first changes involved in this type of cell death [41]. High levels of iROS can cause oxidative stress in yeast due to the formation of oxidized cellular macromolecules, including lipids, proteins and nucleic acids, thus triggering the onset of apoptosis [42] and loss of viability [43]. Our results show that treatment with ISO significantly increased the load of cells with high levels of iROS production in all clinical isolates of *C. tropicalis*, showing different fluorescence intensities of DCFH-DA depending on the strain studied, compared to untreated strains where no fluorescence was observed; in addition, the fluorescence emitted in the cells treated with ISO was much higher in contrast to the fluorescence emitted in the cells treated with H_2O_2 (ROS-inducing control) in all cases. Some studies have reported the antioxidant capacity of ISO in oily matrices, as well as its free radicals scavenging capacity [44] and its participation in the oxidative stabilization of palm olein [45]; however, our studies with pathogenic yeasts differ from these results, showing the ability of ISO to induce the production of iROS in isolates of *C. tropicalis*. This leads us to think that the oxidative stress generated by the overproduction of iROS induced by ISO could damage intracellular components of these yeasts and induce cell death, and this could be another mechanism of antifungal action of ISO against *C. tropicalis*.

Candida tropicalis is well known for its ability to form strong biofilms, which vary depending on the origin of the infection [46]; these biofilms associate these pathogens with high mortality, possibly due to the low permeability of the matrix to conventional antifungal drugs [47]. The *C. tropicalis* isolates in this study were strong biofilm producers, consistent with studies reported by [37], who reported strains of *C. tropicalis* with strong, fast-growing biofilms as a result of their high metabolic activity. Comparing the efficacy of ISO with AFB, we highlight the role of ISO in the eradication of mature biofilms during 1 h of treatment (between 20.3 and 25.8%), and in all cases it was greater than with AFB (between 7.2 and 12.4%); this is consistent with the studies reported by [37] indicating the ability of liposomal AFB to inhibit further biofilm growth, but its ineffectiveness in eradicating mature biofilms, even at high doses. It is important to highlight that natural compounds

obtained from plants can potentially be used to combat multiresistant and biofilm-forming strains of *Candida* spp., thus becoming a promising alternative to antifungal drugs [48]. In addition, the cytotoxicity of ISO on human peripheral blood lymphocytes [49] and murine macrophages (RAW 264.7) [45] has been reported, indicating that this compound does not have genotoxic or cytotoxic effects on these cells at the concentrations tested. Our results add new and important information about the antifungal potential of ISO monoterpene, showing more than one target of action on *C. tropicalis* cells; in addition, we provide information that serves as a basis for future research in the exploration of other possible targets of antifungal action of this monoterpene that could serve as adjuvants for the therapy of infections by these pathogenic yeasts.

4. Materials and Methods

4.1. Reagents

RPMI 1640, phosphate buffered saline (PBS), and yeast peptone dextrose broth (YPD) were obtained from (Thermo Fisher Scientific, Waltham, MA, USA); 3-N-morpholinopropanesulfonic acid (MOPS) was obtained from (Merck); propidium iodide (PI), 2′,7′-dichlorofluorescin diacetate (DCFH-DA), potato dextrose broth (PDB), sabouraud dextrose agar (SDA), sabouraud dextrose broth (SDB), amphotericin B (AFB), acridine orange (OA), ethidium bromide (EB), and crystal violet used in this study were obtained from Sigma-Aldrich, United States; glacial acetic acid was obtained from Carlo Erba Reagents, Italy; and Fluconazole (FLZ) was obtained from Pfizer.

4.2. Obtaining and Identification of Isoespintanol

ISO was isolated from leaves of *O. xylopioides*, collected in October 2019 from a specimen located in the Municipality of Monteria, Department of Córdoba, with coordinates 08°48′17″ north latitude and 75°42′07″ west longitude. An herbarium specimen is deposited in the Joaquin Antonio Uribe Botanical Garden of Medellin, Colombia, with the collection number JAUM 037849. The ISO was obtained by hydrodistillation and crystallization, from 5 g of petroleum benzyne extract of the leaves of *O. xylopioides*, following the methodology described in a previous work [50], with some modifications that included successive crystallizations with n-hexane that led to obtaining 1.2 g of the pure compound. The purity was verified using a gas chromatograph coupled to a Thermo Scientific model Trace 1310 mass spectrometer, with an AB-5MS column, (30 m × 0.25 mm i.d. × 0.25 µm). The temperature gradient system started at 80 °C for 10 min up to 200 °C at 10 °C/min. The temperature was increased to 240 °C at 4 °C/min and finally it was brought up to 290 °C for 10 min at 10 °C/min. The injection was splitless type, with an injection volume of 1 µL. The mass spectrum was obtained in electron impact ionization mode at 70 eV. The structure of the ISO was determined using ^{1}H-NMR, ^{13}C-NMR, DEPT, COSY ^{1}H-^{1}H, HMQC and HMBC spectra, performed on a 400 MHz Bruker Advance DRX spectrometer, in deuterated chloroform ($CDCl_3$).

4.3. Strains

Seven clinical isolates of *C. tropicalis* (001 to 007) were used in this study. The isolates were cultured from blood culture and tracheal aspirate samples from hospitalized patients at the Salud Social S.A.S. from the city of Sincelejo, Colombia. All microorganisms were identified by standard methods: Vitek 2 Compact, Biomerieux SA, YST Vitek 2 Card and AST-YS08 Vitek 2 Card (Ref 420739). SDA medium and BBL CHROMagar Candida medium were used to maintain the cultures until the tests were carried out. The identification of one of the *C. tropicalis* isolates was confirmed through a genome-wide taxonomic study.

4.4. Phylogenomics of Candida tropicalis

4.4.1. Extraction of Genomic DNA from *Candida tropicalis*

Colonies of *C. tropicalis* in SDA were used for genomic DNA (gDNA) extraction using the Qiagen DNeasy PowerLyzer PowerSoil kit, following the manufacturer's in-

structions. The extracted gDNA was quantified by light absorption at 260 nm using the NanoDrop™ 2000-Thermo Scientific™ and frozen at −20 °C for subsequent genomic sequencing experiments.

4.4.2. WGS (Whole Genome Shotgun) Genomic Sequencing of *Candida tropicalis* on the Illumina Novaseq Platform

The sequencing of the gDNA extracted from *C. tropicalis* was carried out using Truseq Nano DNA libraries (350) and the Illumina NovaSeq platform, through which 150-base paired reads were generated. Subsequently, the assembly of the *C. tropicalis* genome was carried out using the SPADES program. For phylogenetic analyses, conserved single-copy genes were used. Afterwards, these genes were aligned and concatenated with MAFFT; the iqTREE software was used to select the substitution models and generate the tree (Maximum Likelihood), which was visualized with FIGTREE.

4.5. Antifungal Susceptibility Testing

The minimum inhibitory concentration (MIC) of ISO against clinical isolates of *C. tropicalis* was defined as the lowest concentration at which 90% (MIC_{90}) of fungal growth was inhibited, compared to the control. MIC was established by performing broth microdilution assays, using 96-well microtiter plates (Nunclon Delta, Thermo Fisher Scientific, Waltham, MA, USA), as described in *Clinical Laboratory Standards Institute* (CLSI) method (M27-A3) [51] and *The European Committee for Antimicrobial Susceptibility Testing* (EUCAST) [52], with minor modifications. Serial dilutions were made in RPMI 1640 broth (pH 7.0) buffered with 0.165 M MOPS, to obtain final concentrations of 31.25 to 1000 μg/mL of ISO in each reaction well. Stock solutions of ISO at 20,000 μg/mL in DMSO and FLZ at 1500 μg/mL in 10% DMSO in distilled water were prepared. Assays were performed with a final volume of 200 μL per well as follows: 100 μL of fungal inoculum at a concentration of 10^6 CFU/mL and 100 μL of ISO adjusted to achieve the concentrations described above in a final reaction system. Isolates of *C. tropicalis* without ISO and with FLZ were used as growth controls and positive controls, respectively; wells with culture medium without inoculum and without ISO were used as negative controls. For each test, controls were made with the different concentrations of ISO in culture medium without inoculum. The plates were incubated at 37 °C for 24 h. Inhibition of fungal growth by ISO was determined by change in optical density using a SYNERGY LX microplate reader (Biotek), at 530 nm, from the start of incubation to the end time (24 h), and the reduction percentage of growth was calculated [53] using the following equation:

$$\%\text{Reduction} = (1 - (OD_{t24} - OD_{t0}/OD_{gc24} - OD_{gc0})) \times 100$$

where, OD_{t24}: optical density of the test well at 24 h post-inoculation; OD_{t0}: optical density of the test well at 0 h post-inoculation; OD_{gc24}: optical density of the growth control well at 24 h post-inoculation; OD_{gc0}: optical density of the growth control well at 0 h post-inoculation.

Subsequently, the minimum fungicidal concentration (MFC) was determined by taking 10 μL from each well and inoculating it onto SDA. The plates were sealed and incubated at 37 °C for 24/48 h. MFC was considered the lowest concentration capable of inhibiting 99% of yeasts [25]. All experiments were performed in triplicate.

4.6. MTT-Reduction Assay

To evaluate the cell viability of *C. tropicalis* in the presence of ISO, the colorimetric assay for the reduction of MTT (3-(4,5-dimethylthiazol-2-yl)-2,5-diphenyl-2H-tetrazolium) was performed as described by [54]. MTT was dissolved in PBS at 2.5 mg/mL and filtered. The fungal inoculum at a cell concentration of 10^6 CFU/mL was inoculated into 96-well plates at the previously described ISO concentrations, and the plates were incubated for 24 h at 37 °C. Cells with medium were used as control. Then 50 μL of the MTT solution was added to the cells under evaluation at a concentration of 500 μg/mL. The plates were

incubated in the dark for 4 h at 37 °C. The tests were performed in triplicate. Viable cells with metabolic activity convert MTT (yellow color) to formazan, which was solubilized with dimethyl sulfoxide (DMSO) showing a purple color; for this, 50 µL of supernatant is removed from each well and 50 µL of DMSO is added, which was read at a wavelength of 550 nm in a SYNERGY LX microplate reader (Biotek) after shaking in the equipment.

4.7. Growth Inhibition Curves

The growth inhibition curve of *C. tropicalis* by ISO was performed following the methodology proposed by [23], with minor modifications. Isolates of *C. tropicalis* were cultured in SDB medium for 24 h at 37 °C. The fungal inoculum was standardized until reaching a cell concentration of 10^6 CFU/mL in glass tubes, then the ISO was added (the MIC for each isolate) and the tubes were incubated at 37 °C for 48 h. Subsequently, 1 mL was taken from each tube at times 0, 2, 4, 8, 12, 24, 36 and 48 h and read at 530 nm in a SYNERGY LX microplate reader (Biotek). Tubes with the fungal inoculum and FLZ were used as controls. All assays were performed in triplicate.

4.8. LIVE/DEAD Assays

The LIVE/DEAD assays were developed following the methodology proposed by [23], with some modifications. A suspension of *C. tropicalis* (10^6 CFU/mL) was placed on sterile slides and incubated for 24 h. The cells were then washed three times with PBS. Subsequently, the ISO MIC for each yeast and FLZ were added to the experimental groups and the fungal inoculum in RPMI 1640 broth was used as a control. Prepared slides were incubated at 37 °C for 24 h and then washed three times with PBS. Together, AO (5 µL, 100 mg/L) and EB (5 µL, 100 mg/L) were mixed under dark conditions and added to slides under dark conditions for 30 s. Next, the samples were observed in an Olympus BX43 fluorescence microscope and photographed with a DP72 camera.

4.9. Quantitative Assessment of Biofilm Formation

Isolates of *C. tropicalis* were evaluated to quantify the reduction of biofilms in the presence of ISO following the methodology reported by [25], with some modifications. For biofilm formation, yeast colonies in SDA with 24 h of incubation were used to standardize the inoculum until reaching a concentration of 10^6 cells/mL. Then, in 96-well plates, 200 µL of the fungal inoculum was cultured in each well in YPD broth and incubated at 37 °C for 48 h. Then the broth was removed from the microplates and 200 µL of the ISO MIC for each isolation in YPD broth was added and incubated at 37 °C for 1 h. Then, the floating cells were removed and the biofilm at the bottom of the wells was washed with deionized water three times. Six replicates of each sample were made. Cultures without ISO were taken as control and AFB was used as positive control. Biofilm reductions were quantified by staining wells with 0.1% crystal violet for 20 min. The samples were washed with deionized water until the excess dye was removed. Finally, the samples were soaked in 250 µL of 30% glacial acetic acid. Absorbance values were measured at 590 nm (OD_{590}) using a SYNERGY LX microplate reader (Biotek). Biofilm production was grouped into the following categories: OD_{590} < 0.1: non-producers (NP), OD_{590} 0.1–1.0: weak producers (WP), OD_{590} 1.1–3.0: moderate producers (MP) and OD_{590} > 3.0: strong producers (SP). Biofilm reduction was calculated using the following equation:

$$\% \text{ Biofilm reduction: AbsCO} - \text{AbsISO/AbsCO} \times 100$$

where, AbsCO: absorbance of the control and AbsISO: absorbance of the sample treated with ISO.

4.10. Effect of Isoespintanol on Cell Membrane Integrity

To evaluate the effect of ISO on cell membrane integrity, the methodology proposed by [35] was used, with minor modifications. The fungal cells (10^6 CFU/mL) were suspended in RPMI 1640 medium and treated with ISO MIC for each isolation and incubated

for 12 h at 30 °C. Cells without ISO and cells treated with FLZ (100 µg/mL) were used as controls. Subsequently, the cells were incubated with 1.49 µM PI in water at 30 °C for 50 min. Then, the cells were collected by centrifugation (3000× *g* 10 min, 4 °C), resuspended in PBS and finally analyzed by flow cytometry (20,000 events analyzed per assay), using the BD FACS CANTO II flow cytometer and analyzed with the BD FACS DIVA software. The excitation and emission for PI were 488 nm and 630 nm, respectively. All experiments were performed in triplicate.

4.11. Leakage of Nucleic Acids and Proteins through the Fungal Membrane

The release of intracellular material was measured according to the methodology proposed by [30], with some modifications. Yeasts grown in SDB were centrifuged at 3000× *g* for 20 min, washed three times and resuspended in 20 mL of PBS (pH 7.0). Then, the cell suspension was treated with ISO (MIC for each isolation) and incubated at 37 °C for 0, 30, 60 and 120 min. Subsequently, 2 mL of the samples were collected and centrifuged at 3000× *g* for 20 min. Then, to determine the concentration of the released constituents, 2 mL of supernatant was used to measure the absorbance at 260/280 nm with the Spectroquant® Prove 300 UV/Vis spectrophotometer. Samples without ISO and samples with FLZ were used as controls. All assays were performed in triplicate.

4.12. Measurement of Extracellular pH

The measurement of extracellular pH of *C. tropicalis* after treatment with ISO was determined according to [30], with some modifications. 100 µL of the yeast suspension (10^5 CFU/mL) was added to 20 mL of SDB and incubated at 37 °C for 48 h. Then, the samples were centrifuged at 3000× *g* for 20 min; the pellet was collected, resuspended, and washed three times with bidistilled water and resuspended again in 20 mL of sterile bidistilled water. After the addition of ISO (MIC of each isolate), the extracellular pH of *C. tropicalis* was determined at 0, 30, 60 and 120 min, using a Schott® Instruments Handylab pH 11 pHmeter. Samples without ISO and samples with FLZ were used as controls.

4.13. Transmission Electron Microscopy (TEM)

The morphology of *C. tropicalis* after ISO treatment was analyzed by TEM. The concentration of *C. tropicalis* was adjusted to 10^6 CFU/mL; the suspension was mixed with ISO (200 µg/mL) and incubated at 37 °C for 24 h. Subsequently, the cells were collected and fixed in 2.5% glutaraldehyde in phosphate buffer pH 7.2 at 4 °C; they were centrifuged at 13,000 rpm for 3 min and the button at the bottom of the vial was postfixed in 1% osmium tetroxide in water for 2 h at 4 °C. Then, pre-imbibition with 3% uranyl acetate was performed for 1 h at room temperature, after which the cells were dehydrated in an ethanol gradient (50% for 10 min, 70% for 10 min, 90% for 10 min, 100% for 10 min), acetone-ethanol (1:1) for 15 min and embedded in SPURR epoxy resin. The samples were cut in a Leica EM UC7 ultramicrotome, at 130 nm thickness, and contrasted with 6% uranyl acetate and lead citrate, and then finally observed in a JEOL 1400 plus transmission electron microscope. The photographs were obtained with a Gatan Orius CCD camera.

4.14. Effect of Isoespintanol on the Production of Intracellular Reactive Oxygen Species (ROS)

The detection of intracellular ROS (iROS) was carried out according to the protocol described by [55], with minor modifications. Fungal cells (10^6 CFU/mL) were incubated in PDB with the MIC of the ISO for each isolate for 24 h at 35 °C. A cell suspension under the same conditions without ISO was used as a negative control. The cells were then incubated with 20 µM of DCFH-DA for 30 min in the dark at 35 °C. Afterwards, the cells were collected, washed, resuspended in PBS and analyzed by flow cytometry. The excitation and emission for DCFH-DA were at 485 and 535 nm. H_2O_2 was used as iROS-inducing positive control [56].

4.15. Data Analysis

The results were analyzed using the statistical software R version 4.1.1 and the Excel program. Initially, the Shapiro Wilk test was used to find out the distribution of the data. Subsequently, the Pearson correlation coefficient was used to measure the degree of linear correlation between ISO concentration and percentage reduction of fungal growth. To compare the effects of ISO and AFB on the reduction of biofilms, the Tukey test was used; this test was also used to compare the effects of ISO and FLZ on the leakage of intracellular material through the membrane (260/280 nm). The Kruskal–Wallis test was used to compare the effects of the treatments on the extracellular pH of *C. tropicalis*.

5. Conclusions

In this study, we investigated the antifungal effect of ISO against clinical isolates of *C. tropicalis*, as well as its role in biofilm disruption. In addition, we explored the mechanisms of action presented by this monoterpene. Our study shows antifungal action of ISO against these pathogenic yeasts, this effect being associated with damage to the plasma membrane and the induction of iROS production, in addition to its action against fungal biofilms, showing that ISO has more than one cellular target in its antifungal potential.

Supplementary Materials: The following supporting information can be downloaded at: https://www.mdpi.com/article/10.3390/molecules27185808/s1. Table S1. Extraction of genomic DNA of *Candida tropicalis*. Table S2. *Candida tropicalis* NGS sequencing results. Table S3. Statistical results of the assembly of *Candida tropicalis.* Table S4. % Growth reduction of *Candida tropicalis* isolates exposed to ISO (MIC of each isolate). Table S5. Viability percentages with MTT. Figure S1. Dot plots created in R, showing the mean depth (DEPTH) and the length of the scaffold (LENGTH) for the *C. tropicalis* isolate analyzed. Figure S2. Phylogenetic tree (Maximum Likelihood) based on single-copy conserved genes of *C. tropicalis* strains. CLI107 corresponds to the isolate under study. Figure S3. Chromatograms of the purification of Isoespintanol. Figure S4. EI-MS spectra of Isoespintanol.

Author Contributions: Conceptualization, O.I.C.M.; methodology, O.I.C.M. and A.A.O.; formal analysis, O.I.C.M. and A.A.O.; investigation, O.I.C.M.; resources, A.A.O. and G.S.P.; writing—original draft preparation, O.I.C.M. and A.A.O.; writing—review and editing, O.I.C.M., A.A.O. and G.S.P.; visualization, O.I.C.M.; supervision, O.I.C.M., A.A.O. and G.S.P.; funding acquisition, A.A.O. and G.S.P. All authors have read and agreed to the published version of the manuscript.

Funding: This research was funded with resources from the FCB-02-19 project of the University of Córdoba, Montería, Colombia.

Institutional Review Board Statement: Not applicable.

Informed Consent Statement: Not applicable.

Data Availability Statement: The data presented in this study are available in the article and the supporting information.

Acknowledgments: Thanks are due to the Social Health Clinic IPS S.A.S., Sincelejo, Colombia, under the coordination of Eimi Brango Tarra and Yuly Paulin Ortíz, for donating the clinical isolates used in this study and to Marcio Andrés De Avila for his kind support with the flow cytometry measurements. O.C.M. thanks the scholarship program of the Ministry of Science, Technology and Innovation of Colombia for the granting of the doctoral scholarship.

Conflicts of Interest: The authors declare no conflict of interest.

Sample Availability: The ISO is available from the authors.

References

1. Morais, A.; Araujo, H.; Arias, L.; Ramírez, W.; Porangaba, G.; Penha, S.; Pelim, J.; Monteiro, D. Nanocarriers of miconazole or fluconazole: Effects on three-species *Candida* biofilms and cytotoxic effects in vitro. *J. Fungi* **2021**, *7*, 500. [CrossRef]
2. Boonsilp, S.; Homkaew, A.; Phumisantiphong, U.; Nutalai, D.; Wongsuk, T. Species distribution, antifungal susceptibility, and molecular epidemiology of *Candida* species causing candidemia in a tertiary care hospital in Bangkok, Thailand. *J. Fungi* **2021**, *7*, 577. [CrossRef] [PubMed]

3. Steinmann, J.; Schrauzer, T.; Kirchhoff, L.; Meis, J.; Rath, P. Two *Candida auris* cases in Germany with no recent contact to foreign healthcare—Epidemiological and microbiological investigations. *J. Fungi* **2021**, *7*, 380. [CrossRef]
4. Hassan, Y.; Chew, S.; Lung, L. *Candida glabrata*: Pathogenicity and resistance mechanisms for adaptation and survival. *J. Fungi* **2021**, *7*, 667. [CrossRef]
5. Chen, P.; Chuang, Y.; Wu, U.; Sun, H.; Wang, J.; Sheng, W.; Chen, Y.; Chang, S. Mechanisms of azole resistance and trailing in *Candida tropicalis* bloodstream isolates. *J. Fungi* **2021**, *7*, 612. [CrossRef]
6. El-kholy, M.; Helaly, G.; El Ghazzawi, E.; El-Sawaf, G.; Shawky, S. Virulence factors and antifungal susceptibility profile of *C. tropicalis* isolated from various clinical specimens in Alexandria, Egypt. *J. Fungi* **2021**, *7*, 351. [CrossRef]
7. Zuza, D.; Sila, W.; Chaves, G. An update on *Candida tropicalis* based on basic and clinical approaches. *Front. Microbiol.* **2017**, *8*, 1927. [CrossRef]
8. Munhoz, N.; Nishiyama, L.; Viero, R.; Bagagli, E.; Schatzmann, P.; Sartori, A.; Fraga, T. *Candida tropicalis* systemic infection redirects leukocyte infiltration to the kidneys attenuating encephalomyelitis. *J. Fungi* **2021**, *7*, 757. [CrossRef]
9. Cortés, J.; Ruiz, J.; Melgarejo, L.; Lemos, E. Candidemia in Colombia. *Biomedica* **2020**, *40*, 195–207. [CrossRef]
10. Silva, S.; Negri, M.; Henriques, M.; Oliveira, R.; Williams, D.; Azeredo, J. *Candida glabrata*, *Candida parapsilosis* and *Candida tropicalis*: Biology, epidemiology, pathogenicity and antifungal resistance. *FEMS Microbiol. Rev.* **2012**, *36*, 288–305. [CrossRef] [PubMed]
11. Aylate, A.; Agize, M.; Ekero, D.; Kiros, A.; Ayledo, G.; Gendiche, K. In-vitro and in-vivo antibacterial activities of *Croton macrostachyus* methanol extract against *E. coli* and *S. aureus*. *Adv. Anim. Vet. Sci.* **2017**, *5*, 107–114. [CrossRef]
12. Avato, P. Editorial to the special issue—"Natural Products and Drug Discovery". *Molecules* **2020**, *25*, 1128. [CrossRef]
13. Morales, I.; De La Fuente, J.; Sosa, V. Componentes de *Eupatorium saltense*. *An. Asoc. Quim. Argent.* **1991**, *79*, 141–144.
14. Hocquemiller, R.; Cortes, D.; Arango, G.J.; Myint, S.H.; Cave, A. Isolement et synthese de l'espintanol, nouveau monoterpene antiparasitaire. *J. Nat. Prod.* **1991**, *54*, 445–452. [CrossRef]
15. Rojano, B.; Saez, J.; Schinella, G.; Quijano, J.; Vélez, E.; Gil, A.; Notario, R. Experimental and theoretical determination of the antioxidant properties of isoespintanol (2-isopropyl-3,6-dimethoxy-5-methylphenol). *J. Mol. Struct.* **2008**, *877*, 1–6. [CrossRef]
16. Rojano, B.; Pérez, E.; Figadère, B.; Martin, M.; Recio, M.; Giner, R.; Ríos, J.; Schinella, G.; Sáez, J. Constituents of *Oxandra* Cf. xylopioides with anti-inflammatory activity. *J. Nat. Prod.* **2007**, *70*, 835–838. [CrossRef]
17. Gavilánez, T.; Colareda, G.; Ragone, M.; Bonilla, M.; Rojano, B.; Schinella, G.; Consolini, A. Intestinal, urinary and uterine antispasmodic effects of isoespintanol, metabolite from *Oxandra xylopioides* Leaves. *Phytomedicine* **2018**, *51*, 20–28. [CrossRef] [PubMed]
18. Rinaldi, G.; Rojano, B.; Schinella, G.; Mosca, S. Participation of NO in the vasodilatory action of isoespintanol. *Vitae* **2019**, *26*, 78–83. [CrossRef]
19. Usuga, A.; Tejera, I.; Gómez, J.; Restrepo, O.; Rojano, B.; Restrepo, G. Cryoprotective effects of ergothioneine and isoespintanol on canine semen. *Animals* **2021**, *11*, 2757. [CrossRef]
20. Rojano, B.; Montoya, S.; Yépez, F.; Saez, J. Evaluación de isoespintanol aislado de *Oxandra* cf. *xylopioides* (Annonaceae) sobre *Spodoptera frugiperda* J.E. Smith (Lepidoptera: Noctuidae). *Rev. Fac. Nac. Agron. Medellín* **2007**, *60*, 3691–3702.
21. Arango, N.; Vanegas, N.; Saez, J.; García, C.; Rojano, B. Actividad antifungica del isoespintanol sobre hongos del género *Colletotricum*. *Sci. Tech.* **2007**, *33*, 279–280. [CrossRef]
22. Byvaltsev, V.; Bardonova, L.; Onaka, N.; Polkin, R.; Ochkal, S.; Shepelev, V.; Aliyev, M.; Potapov, A. Acridine orange: A review of novel applications for surgical cancer imaging and therapy. *Front. Oncol.* **2019**, *9*, 925. [CrossRef] [PubMed]
23. Zhang, X.; Zhang, T.; Guo, S.; Zhang, Y.; Sheng, R.; Sun, R.; Chen, L.; Lv, R.; Qi, Y. In vitro antifungal activity and mechanism of $Ag_3PW_{12}O_{40}$ composites against *Candida* species. *Molecules* **2020**, *25*, 6012. [CrossRef] [PubMed]
24. Wu, G.; Chen, S.; Levin, R. Application of ethidium bromide monoazide for quantification of viable and dead cells of *Salmonella enterica* by real-time loop-mediated isothermal amplification. *J. Microbiol. Methods* **2015**, *117*, 41–48. [CrossRef]
25. Donadu, M.; Peralta, Y.; Usai, D.; Maggio, F.; Molina, J.; Rizzo, D.; Bussu, F.; Rubino, S.; Zanetti, S.; Paparella, A.; et al. Colombian essential oil of *Ruta graveolens* against nosocomial antifungal resistant *Candida* strains. *J. Fungi* **2021**, *7*, 383. [CrossRef]
26. Iraji, A.; Yazdanpanah, S.; Alizadeh, F.; Mirzamohammadi, S.; Ghasemi, Y.; Pakshir, K.; Yang, Y.; Zomorodian, K. Screening the antifungal activities of monoterpenes and their isomers against *Candida* species. *J. Appl. Microbiol.* **2020**, *129*, 1541–1551. [CrossRef]
27. Oliveira, I.; De Oliveira, F.; Araújo, W.; De Oliveira, E.; Albuquerque, E.; Cunha, F.; Formiga, M. Antifungal activity and mode of action of carvacrol against *Candida albicans* strains. *J. Essent. Oil Res.* **2013**, *25*, 138. [CrossRef]
28. De Castro, R.; Pereira, T.; Dornelas, L.; Silva, G.; Melo, E.; Leite, A. Antifungal activity and mode of action of thymol and its synergism with nystatin against *Candida* species involved with infections in the oral cavity: An in vitro study. *BMC Complement. Altern. Med.* **2015**, *15*, 417. [CrossRef]
29. Kowalczyk, A.; Przychodna, M.; Sopata, S.; Bodalska, A.; Fecka, I. Thymol and thyme essential oil-new insights into selected therapeutic applications. *Molecules* **2020**, *25*, 4125. [CrossRef]
30. Tao, N.; Ouyang, Q.; Jia, L. Citral inhibits mycelial growth of *Penicillium italicum* by a membrane damage mechanism. *Food Control* **2014**, *41*, 116–121. [CrossRef]
31. De Oliveira, M.; Araújo, A.; Souza, K.; Cardoso, G.; de Oliveira, E.; de Oliveira, F. Investigation of the antifungal potential of linalool against clinical isolates of fluconazole resistant *Trichophyton rubrum*. *J. Mycol. Med.* **2017**, *27*, 195–202. [CrossRef]

32. Wei, J.; Bi, Y.; Xue, H.; Wang, Y.; Zong, Y.; Prusky, D. Antifungal activity of cinnamaldehyde against *Fusarium sambucinum* involves inhibition of ergosterol biosynthesis. *J. Appl. Microbiol.* **2020**, *129*, 256–265. [CrossRef]
33. De Oliveira, F.; Moura, J.; De Oliveira, E. Investigation on mechanism of antifungal activity of eugenol against *Trichophyton rubrum*. *Med. Mycol.* **2013**, *51*, 507–513. [CrossRef]
34. De Castro, A.; De Oliveira, R.; De Oliveira, E.; De Oliveira, W.; De Oliveira, I. Antifungal activity study of the monoterpene thymol against *Cryptococcus neoformans*. *Nat. Prod. Res.* **2018**, *34*, 2630–2633. [CrossRef]
35. Zhao, F.; Dong, H.; Wang, Y.; Wang, T.; Yan, Z.; Yan, F.; Zhang, D.; Cao, Y.; Jin, Y. Synthesis and synergistic antifungal effects of monoketone derivatives of curcumin against fluconazole-resistant *Candida* spp. *Med. Chem. Commun.* **2017**, *8*, 1093–1102. [CrossRef]
36. Qin, G.; Liu, J.; Cao, B.; Li, B.; Tian, S. Hydrogen peroxide acts on sensitive mitochondrial proteins to induce death of a fungal pathogen revealed by proteomic analysis. *PLoS ONE* **2011**, *6*, e21945. [CrossRef]
37. Kawai, A.; Yamagishi, Y.; Mikamo, H. Time-lapse tracking of *Candida tropicalis* biofilm formation and the antifungal efficacy of liposomal amphotericin B. *Jpn. J. Infect. Dis.* **2017**, *70*, 559–564. [CrossRef]
38. Trombetta, D.; Castelli, F.; Sarpietro, M.; Venuti, V.; Cristani, M.; Daniele, C.; Saija, A.; Mazzanti, G.; Bisignano, G. Mechanisms of antibacterial action of three monoterpenes. *Antimicrob. Agents Chemother.* **2005**, *49*, 2474. [CrossRef]
39. Scott, B.; Eaton, C. Role of reactive oxygen species in fungal cellular differentiations. *Curr. Opin. Microbiol.* **2008**, *11*, 488–493. [CrossRef]
40. Zorov, D.; Juhaszova, M.; Sollott, S. Mitochondrial ROS-induced ROS release: An update and review. *Biochim. Biophys. Acta* **2006**, *1757*, 509–517. [CrossRef]
41. Choi, H.; Lee, D. Lycopene induces apoptosis in *Candida albicans* through reactive oxygen species production and mitochondrial dysfunction. *Biochimie* **2015**, *115*, 108–115. [CrossRef] [PubMed]
42. Da Silva, M.; Baronetti, J.; Páez, P.; Paraje, M. Oxidative imbalance in *Candida tropicalis* biofilms and its relation with persister cells. *Front. Microbiol.* **2021**, *11*, 598834. [CrossRef]
43. Zhang, Z.; Qin, G.; Li, B.; Tian, S. Effect of cinnamic acid for controlling gray mold on table grape and its possible mechanisms of action. *Curr. Microbiol.* **2015**, *71*, 396–402. [CrossRef] [PubMed]
44. Rojano, B.; Gaviria, C.; Sáez, J. Determinación de la actividad antioxidante en un modelo de peroxidación lipídica de mantequilla inhibida por el isoespintanol. *Vitae* **2008**, *15*, 212–218.
45. Zapata, K.; Arias, J.; Cortés, F.; Alarcon, C.; Durango, D.; Rojano, B. Oxidative stabilization of palm olein with isoespintanol (2-isopropyl-3,6-dimethoxy-5-methylphenol) isolated from *Oxandra* cf *xylopioides*. *J. Med. Plants Res.* **2017**, *11*, 218–225. [CrossRef]
46. Guembe, M.; Cruces, R.; Peláez, T.; Muñoz, P.; Bouza, E. Assessment of biofilm production in *Candida* isolates according to species and origin of infection. *Enferm. Infecc. Microbiol. Clin.* **2017**, *35*, 37–40. [CrossRef]
47. Tascini, C.; Sozio, E.; Corte, L.; Sbrana, F.; Scarparo, C.; Ripoli, A.; Bertolino, G.; Merelli, M.; Tagliaferri, E.; Corcione, A.; et al. The role of biofilm forming on mortality in patients with candidemia: A study derived from real world data. *Infect. Dis.* **2017**, *50*, 214–219. [CrossRef] [PubMed]
48. Karpiński, T.; Ożarowski, M.; Seremak, A.; Wolski, H.; Adamczak, A. Plant preparations and compounds with activities against biofilms formed by *Candida* spp. *J. Fungi* **2021**, *7*, 360. [CrossRef]
49. Marquez, M.; Munoz, D.; Bautista, J.; Zapata, K.; Puertas, M.; Lopez, C.; Rojano, B. Effect of isoespintanol isolated from *Oxandra* cf. xylopioides against DNA damage of human lymphocytes. *Pak. J. Pharm. Sci.* **2018**, *31*, 1777–1782.
50. Ramírez, R.; Páez, M.; Angulo, A. Obtención de isoespintanol por hidrodestilación y cristalización a partir del extracto bencínico de *Oxandra xylopioides*. *Inf. Tecnol.* **2015**, *26*, 13–18. [CrossRef]
51. Clinical and Laboratory Standards Institute. *Reference Method for Broth Dilution Antifungal Susceptibility Testing of Yeasts; Approved Standard*, 3rd ed.; CLSI document M27-A3; Clinical and Laboratory Standards Institute: Wayne, PA, USA, 2008.
52. Rodriguez, J.; Barchiesi, F.; Bille, J.; Chryssanthou, E.; Cuenca, M.; Denning, D.; Donnelly, J.; Dupont, B.; Fegeler, W.; Moore, C.; et al. Method for determination of minimal inhibitory concentration (MIC) by broth dilution of fermentative yeasts. *Clin. Microbiol. Infect.* **2003**, *9*, i–viii. [CrossRef]
53. Quave, C.; Plano, L.; Pantuso, T.; Bennett, B. Effects of extracts from italian medicinal plants on planktonic growth, biofilm formation and adherence of methicillin-resistant *Staphylococcus aureus*. *J. Ethnopharmacol.* **2008**, *118*, 418–428. [CrossRef]
54. Maldonado, J.; Casaña, R.; Martínez, I.; San Martín, E. La espectroscopia UV-Vis en la evaluación de la viabilidad de células de cáncer de mama. *Lat. Am. J. Phys. Educ.* **2018**, *12*, 1–7.
55. Da Silva, C.; Campos, R.; Neto, J.; Sampaio, L.; do Nascimento, F.; do AV Sa, L.; Candido, T.; Magalhaes, H.; da Cruz, E.; da Silva, E.; et al. Antifungal activity of β-lapachone against azole-resistant *Candida* spp. and its aspects upon biofilm formation. *Future Microbiol.* **2020**, *15*, 1543–1554. [CrossRef]
56. Kakar, A.; Holzknecht, J.; Dubrac, S.; Gelmi, M.; Romanelli, A.; Marx, F. New perspectives in the antimicrobial activity of the amphibian temporin B: Peptide analogs are effective inhibitors of *Candida albicans* growth. *J. Fungi* **2021**, *7*, 457. [CrossRef]

Anexo 2

"Isoespintanol Antifungal Activity Involves Mitochondrial Dysfunction, Inhibition of Biofilm Formation, and Damage to Cell Wall Integrity in *Candida tropicalis*"

International Journal of
Molecular Sciences

MDPI

Article

Isoespintanol Antifungal Activity Involves Mitochondrial Dysfunction, Inhibition of Biofilm Formation, and Damage to Cell Wall Integrity in *Candida tropicalis*

Orfa Inés Contreras Martínez [1,*], Alberto Angulo Ortíz [2], Gilmar Santafé Patiño [2], Ana Peñata-Taborda [3] and Ricardo Berrio Soto [1]

[1] Biology Department, Faculty of Basic Sciences, Universidad de Córdoba, Montería 230002, Colombia
[2] Chemistry Department, Faculty of Basic Sciences, Universidad de Córdoba, Montería 230002, Colombia; aaangulo@correo.unicordoba.edu.co (A.A.O.); gsantafe@correo.unicordoba.edu.co (G.S.P.)
[3] Biomedical and Molecular Biology Research Group, Universidad del Sinú E.B.Z., Montería 230001, Colombia
* Correspondence: oicontreras@correo.unicordoba.edu.co

Abstract: The growing increase in infections caused by *C. tropicalis*, associated with its drug resistance and consequent high mortality, especially in immunosuppressed people, today generates a serious global public health problem. In the search for new potential drug candidates that can be used as treatments or adjuvants in the control of infections by these pathogenic yeasts, the objective of this research was to evaluate the action of isoespintanol (ISO) against the formation of fungal biofilms, the mitochondrial membrane potential (ΔΨm), and its effect on the integrity of the cell wall. We report the ability of ISO to inhibit the formation of biofilms by up to 89.35%, in all cases higher than the values expressed by amphotericin B (AFB). Flow cytometric experiments using rhodamine 123 (Rh123) showed the ability of ISO to cause mitochondrial dysfunction in these cells. Likewise, experiments using calcofluor white (CFW) and analyzed by flow cytometry showed the ability of ISO to affect the integrity of the cell wall by stimulating chitin synthesis; these changes in the integrity of the wall were also observed through transmission electron microscopy (TEM). These mechanisms are involved in the antifungal action of this monoterpene.

Keywords: antifungal mechanism; isoespintanol; *Candida tropicalis*; antibiofilm activity

Citation: Contreras Martínez, O.I.; Angulo Ortíz, A.; Santafé Patiño, G.; Peñata-Taborda, A.; Berrio Soto, R. Isoespintanol Antifungal Activity Involves Mitochondrial Dysfunction, Inhibition of Biofilm Formation, and Damage to Cell Wall Integrity in *Candida tropicalis*. *Int. J. Mol. Sci.* **2023**, *24*, 10187. https://doi.org/10.3390/ijms241210187

Academic Editor: Pavel Zelenikhin

Received: 17 May 2023
Revised: 7 June 2023
Accepted: 7 June 2023
Published: 15 June 2023

1. Introduction

Candida tropicalis is one of the most important non-albicans candida (NAC) species, due to its high incidence of systemic candidiasis and greater resistance to commonly used antifungals [1]. This yeast has been considered the second-most virulent *Candida* species, only preceded by *C. albicans*. It expresses a wide range of virulence factors, including adhesion to buccal epithelium and endothelial cells, the secretion of lytic enzymes, hyphal budding, and the phenomenon called phenotypic switching, which allows them to rapidly adapt in response to environmental challenges. This yeast has been recognized as a strong producer of biofilms, surpassing *C. albicans* in most studies [2]. *Candida tropicalis* is an opportunistic pathogen that affects immunosuppressed individuals and is capable of spreading to vital organs [3]. It has been reported that this yeast is associated with higher mortality compared to *C. albicans* and other NAC species, showing a greater potential for dissemination in neutropenic individuals; it is associated with malignancy, cancer patients, patients with long-term catheter use, and broad-spectrum antibiotic therapy [4]. In Colombia, candidemia is a frequent cause of infection in the bloodstream, especially in intensive care units (ICU), representing 88% of fungal infections in hospitalized patients, with a mortality rate between 36% and 78%. The incidence in Colombia is superior to that reported in developed countries and even in other Latin American countries [5].

In this context, the search for compounds with antifungal potential against these pathogens is urgent. Natural products feature prominently in the discovery and development of many drugs used today with recognized medicinal properties; especially, plants have played a major role as a source of specialized metabolites with curative effects, which can be used directly as bioactive compounds, as drug prototypes, and/or as pharmacological tools for different targets [6].

Isoespintanol (ISO) (2-isopropyl-3,6-dimethoxy-5-methylphenol) has been recognized as a natural bioactive compound. It is a monoterpene that was first obtained from *Eupatorium saltense* (Asteraceae) [7], whose synthesis has been reported [8], and also from *Oxandra xylopioides* (Annonaceae) [9]. The biological potential of this compound as a natural antioxidant [10], anti-inflammatory [9], antispasmodic [11], vasodilator [12], cardioprotective [13], and cryoprotectant in canine semen [14], as well as its insecticidal activity [15] and antifungal activity against phytopathogens of the genus *Colletotrichum* [16], has been documented. We have also reported its potential against human pathogens, specifically intra-hospital bacteria [17] and yeasts of the genus *Candida*, reporting its action against the cell membrane, its ability to induce intracellular reactive oxygen species, and its ability to eradicate mature biofilms as responsible for its antifungal activity [18,19]. Continuing with the study of this compound, we hypothesize that ISO may have other targets of action against *C. tropicalis*. The purpose of this research was to evaluate other target sites of action of ISO by investigating its action against the mitochondrial membrane potential ($\Delta\Psi m$), its ability to prevent the formation of fungal biofilms, and its effect on the integrity of the cell wall, thus contributing to the knowledge of the mechanisms of action of this monoterpene, which could serve as adjuvants in the treatment and control of these pathogenic yeasts with resistance to conventional antifungals.

2. Results

2.1. Obtaining and Identification of Isoespintanol

ISO was obtained as a crystalline amorphous solid from the petroleum benzine extract of *O. xylopioides* leaves, and its structural identification was performed by GC-MS, ^{1}H-NMR, ^{13}C-NMR, DEPT, COSY ^{1}H-^{1}H, HMQC, and HMBC. Information related to obtaining and identifying the ISO was reported in our previous study [19].

2.2. Antifungal Susceptibility Testing

Table 1 shows the minimum inhibitory concentration (MIC_{90} and MIC_{50}) and minimum fungicidal concentration (MFC) values of the ISO against the clinical isolates of *C. tropicalis* evaluated in this study and in previous work [19].

Table 1. Minimum inhibitory concentration (MIC) and minimum fungicidal concentration (MFC) [μg/mL] of ISO against *C. tropicalis*.

Candida tropicalis	ISO		
	MIC_{90}	**MIC_{50}**	**MFC**
CLI 001	470	261.2	500
CLI 002	326.6	59.38	350
CLI 003	413.3	124.4	400
CLI 004	420.8	121.5	450
CLI 005	500	234.6	500
CLI 006	463.9	179.8	450
CLI 007	391.6	107	400

2.3. Effect of ISO on the Formation of Biofilms

ISO inhibited the formation of biofilms in all *C. tropicalis* isolates evaluated, as shown in Figure 1a. Biofilm formation was significantly less in ISO-treated cells compared to untreated cells used as a negative control and AFB-treated cells. As observed in Figure 1b, ISO showed higher percentages of inhibition of biofilm formation compared to AFB. Table 2 presents the percentages of inhibition of biofilm formation for each isolate of *C. tropicalis*.

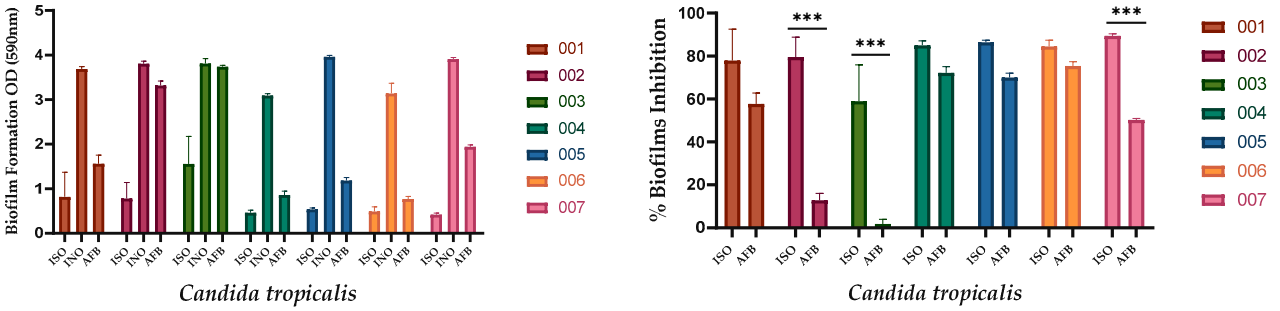

(**a**) (**b**)

Figure 1. Action of ISO and AFB on the formation of biofilms. (**a**) Biofilm formation at 37 °C for 48 h. Where, ISO: cells treated with ISO; INO: untreated cells (negative control); AFB: cells treated with AFB (4 µg/mL). (**b**) Percentage reduction in biofilm formation after treatment with ISO and AFB. The ANOVA results showed a value of *** $p < 0.001$, and the Tukey test with a confidence level of 95% indicates that there are significant differences between the effect of ISO and the effect of AFB (for isolates 002, 003, and 007); while for the rest of the isolates (001, 004, 005, and 006) there are no significant differences.

Table 2. Percentages of inhibition of the formation of fungal biofilms of ISO vs. AFB in *C. tropicalis*.

Candida tropicalis	ISO	AFB
001	77.80	57.70
002	79.48	12.86
003	59.18	1.87
004	85.09	72.23
005	86.46	70.09
006	84.38	75.45
007	89.35	50.30

2.4. Effect of ISO on Mitochondrial Membrane Potential (ΔΨm)

Our results show that the mitochondrial function of *C. tropicalis* was significantly affected after ISO exposure. In Figure 2, the ΔΨm loss of ISO-treated cells compared to untreated cells and H_2O_2-treated cells is observed. Rhodamine 123 (Rh123) accumulates in the highly negatively charged interior of mitochondria, and its fluorescence intensity reflects the ΔΨm across the inner mitochondrial membrane. A loss of ΔΨm results in leakage of Rh123 from mitochondria, with a consequent decrease in fluorescence.

As shown in flow cytometric analysis (Figure 3), fluorescence intensity was significantly decreased in ISO-treated cells, suggesting that ISO caused mitochondrial depolarization of *C. tropicalis*, causing mitochondrial dysfunction and consequent death.

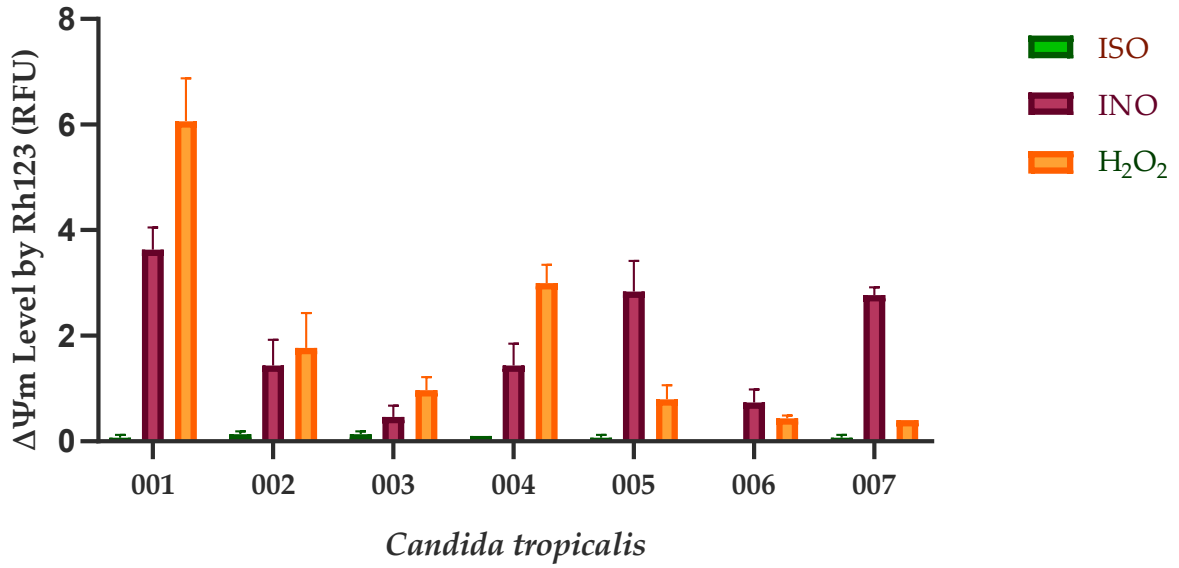

Figure 2. Mitochondrial depolarization of *C. tropicalis* caused by ISO. Depolarization of the mitochondrial membrane was detected by Rh123 staining, and the fluorescence intensity of the cells was analyzed using a flow cytometer. RFU, relative fluorescent units. INO corresponds to the negative control group (cells without treatment). H_2O_2 (15 mM) was used as a positive control for disruption of the mitochondrial membrane potential (ΔΨm). The results are expressed as the mean ± standard deviation of three independent experiments; Dunn's test shows us that there are statistically significant differences between the ISO-INO and ISO-H_2O_2 treatments ($p < 0.005$); however, these differences do not exist between the INO-H_2O_2 treatments ($p > 0.005$).

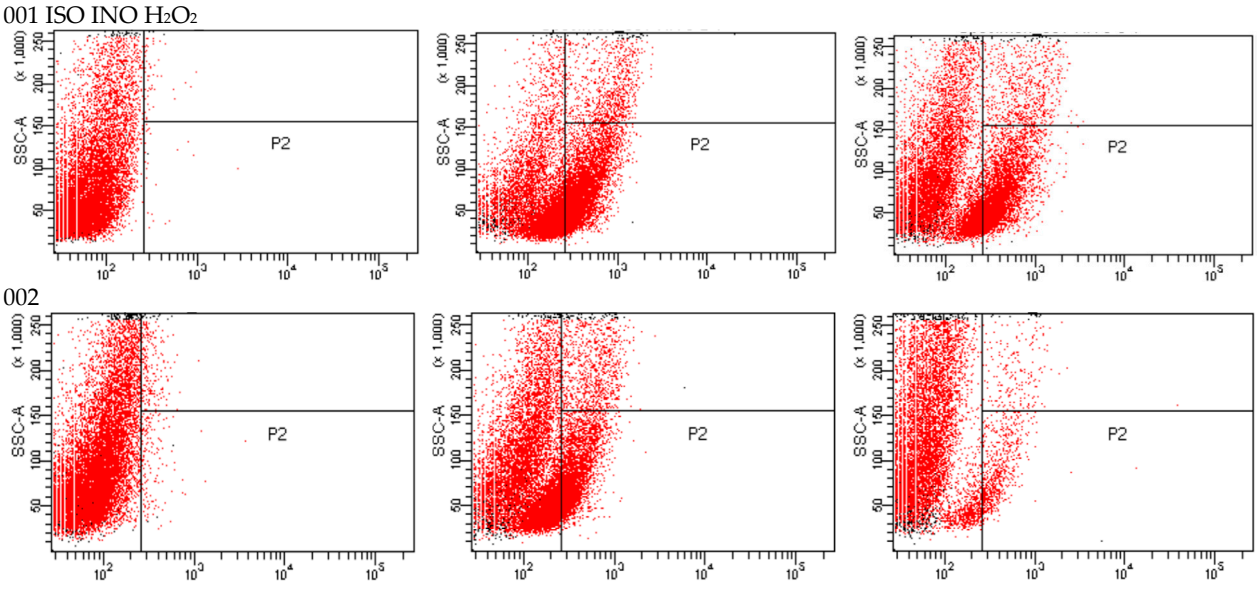

Figure 3. *Cont.*

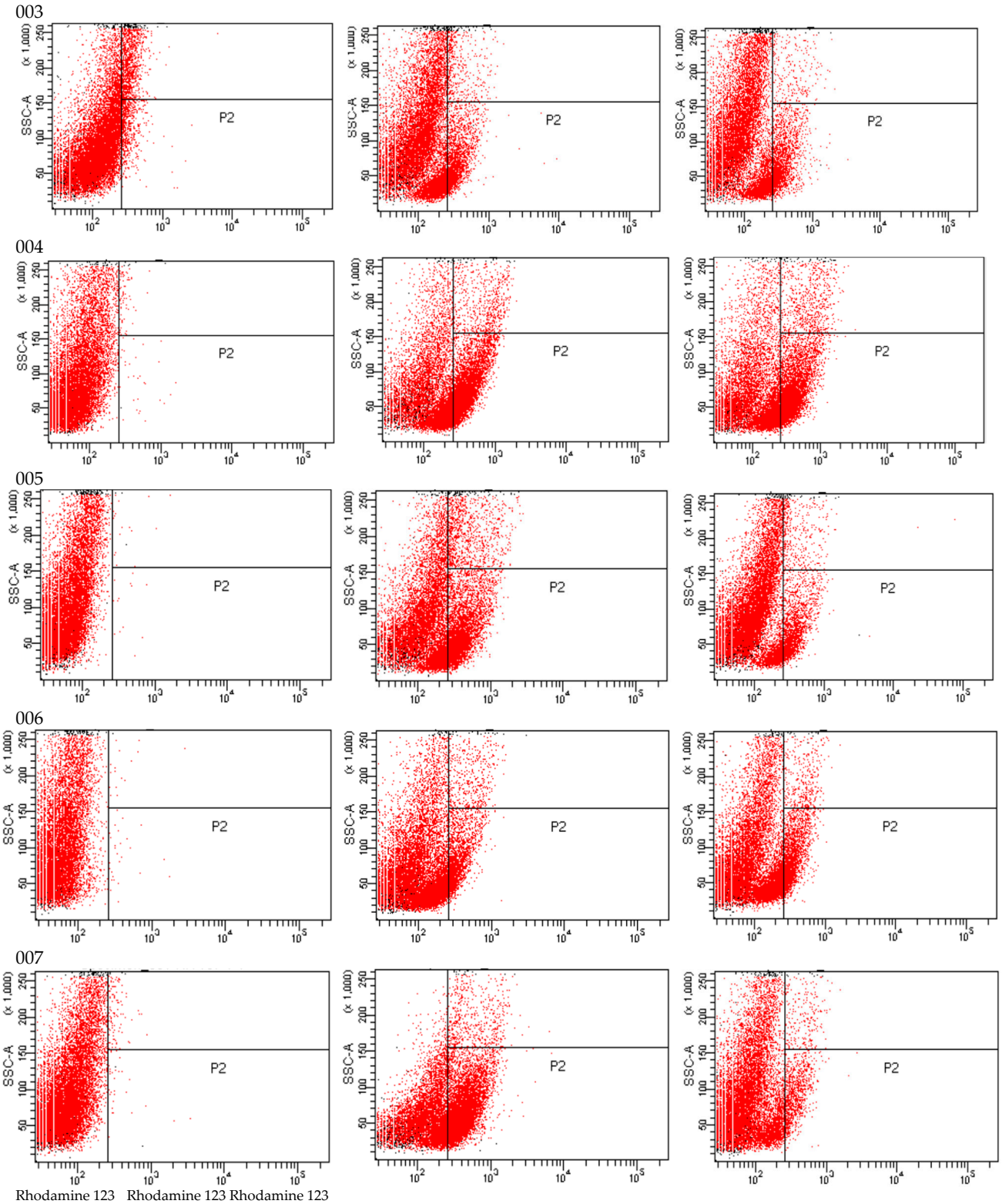

Figure 3. Rh123 fluorescence emitted by ISO-treated, INO-treated, and H_2O_2-treated *C. tropicalis* yeasts.

2.5. Effect of ISO on Cell Wall Integrity

All ISO-treated *C. tropicalis* isolates showed higher chitin content than untreated control cells, as revealed by staining index (SI) values. However, cells treated with caspofungin (CASP) showed the highest chitin concentration compared to the other two experimental groups. Figure 4 represents the SI values calculated for the three experimental groups.

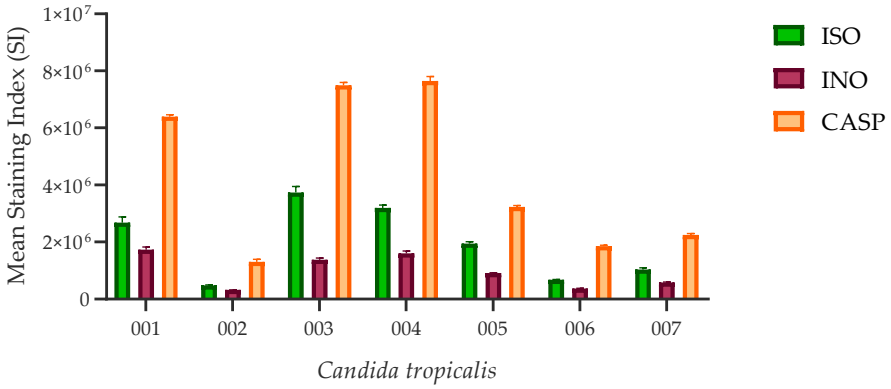

Figure 4. Chitin content in the cell wall of *C. tropicalis*. ISO-treated cells have higher SI values (indicating higher chitin content revealed by CFW staining) compared to untreated (INO) cells; however, these values are lower compared to CASP-treated cells, although there are no statistically significant differences between the ISO vs. INO and ISO vs. CASP treatments ($p > 0.005$).

Figure 5 shows the fluorescence emitted by cells treated with ISO, cells without treatment (INO), and cells treated with CASP after staining with 2.5 µg/mL calcofluor white (CFW). Histograms show higher CFW fluorescence in ISO-treated cells (i.e., higher chitin content) compared to untreated cells and the highest CFW fluorescence was revealed in CASP-treated cells.

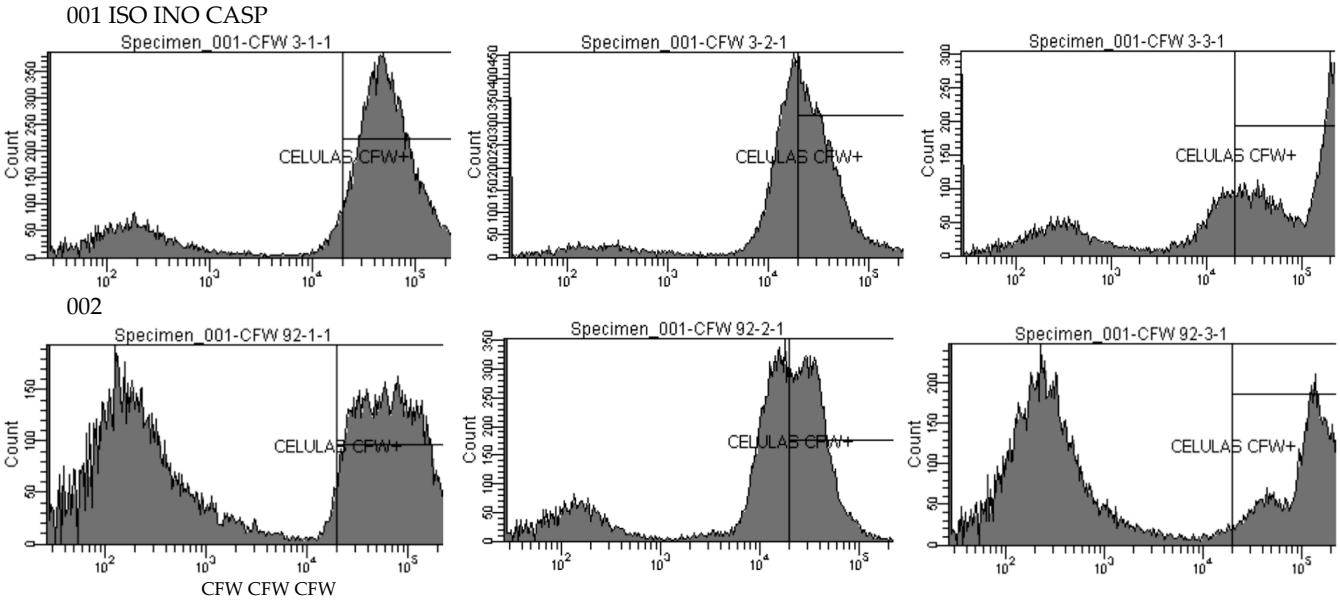

Figure 5. Histograms of the fluorescence emitted by isolates 001 and 002. ISO (cells treated with ISO); INO (untreated cells) and CASP (CASP-treated cells), after staining with 2.5 µg/mL CFW.

Transmission Electron Microscopy (TEM)

TEM showed damage to the cell wall integrity and morphology of ISO-treated *C. tropicalis* isolates compared to untreated control cells. As shown in Figure 6a,b, untreated cells show intact cell morphology with intact cell walls. However, after ISO treatment, as observed in Figure 6c–e, the cells revealed damage to the integrity of their envelope, with partially dissolved cell walls.

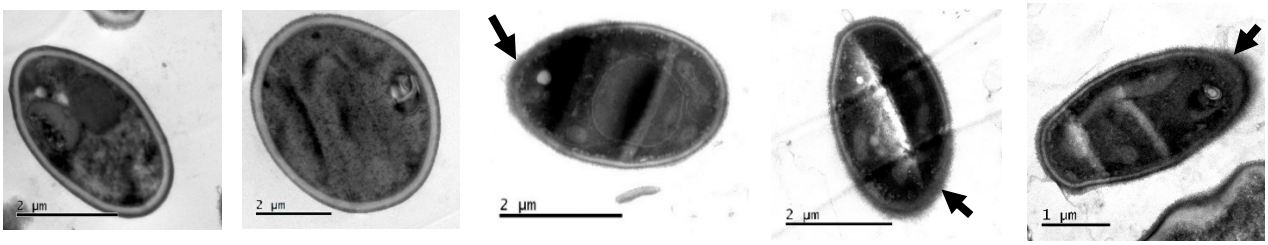

(**a**) (**b**) (**c**) (**d**) (**e**)

Figure 6. TEM of *C. tropicalis* untreated (**a**,**b**) and treated with ISO (**c**–**e**). Changes (indicated with the arrows) are evident in the morphology of the cells treated with ISO, as well as damage to the integrity of the cell wall.

2.6. Isoespintanol Cytotoxicity Assays

Cytotoxicity assays showed different profiles in the cytotoxicity methods tested, revealing statistically significant differences ($p < 0.05$) between cells treated with ISO and untreated cells used as negative controls. As shown in Figure 7a,b, cytotoxicity was dose dependent. The higher the ISO concentration, the lower the percentage of cell viability observed. The inhibitory concentration 50 (IC_{50}) obtained by the crystal violet (CV) assay was 48.64 µg/mL, significantly lower ($p < 0.0001$) than that found by the 3-(4,5-dimethylthiazol-2-yl)-2,5-diphenyl tetrazolium bromide (MTT) (77.34 µg/mL).

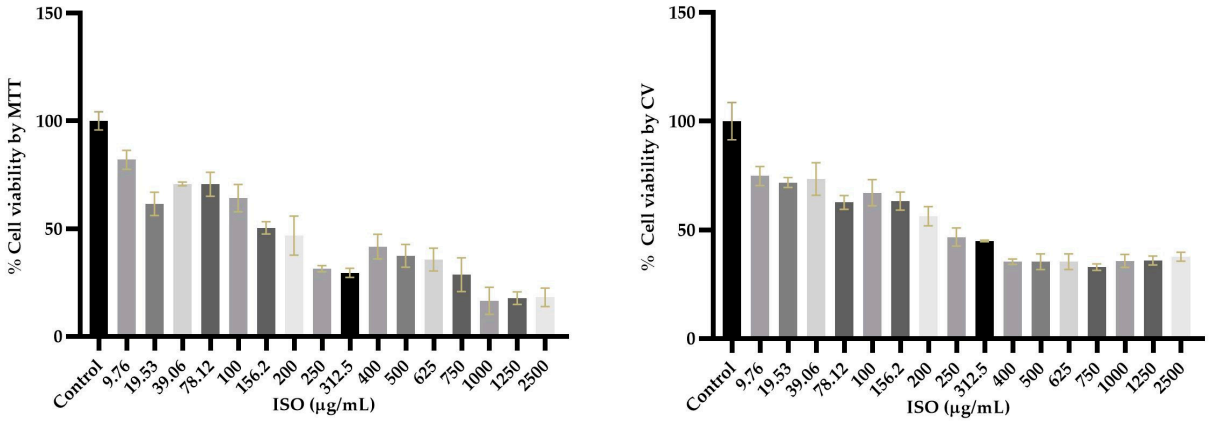

(**a**) (**b**)

Figure 7. Percentage of viability of VERO cells exposed to ISO (9.76–2500 µg/mL) using the MTT (**a**) and CV (**b**) methods. With both methods, a 50% reduction in viability is observed from 250 µg/mL. Results are expressed as mean ± standard error of the mean. The percentages are expressed in relation to the control, and significant differences are evident between the cells treated with ISO ($p < 0.05$).

Figure 8 shows the dose–response curves of the viability profile of VERO cells treated with ISO, using the MTT and CV assays. IC_{50} values were calculated from the fit ($R^2 > 0.95$) of the Hill slope curve using nonlinear regression analysis in GraphPad Prism Software version 8.0.

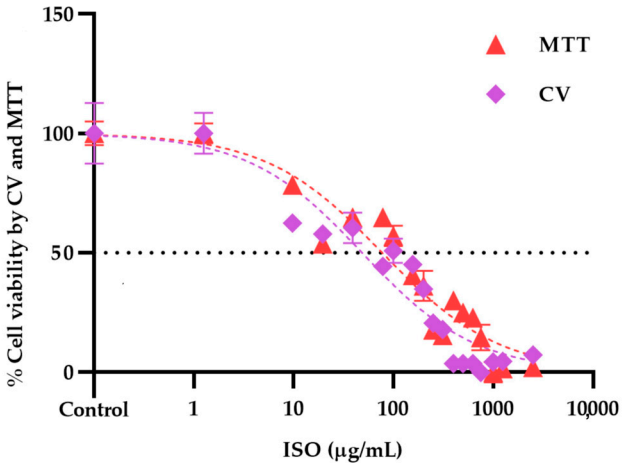

Figure 8. Dose–response curves of the effect of ISO (9.76–2500 µg/mL) on the viability of VERO cells through the CV and MTT assays at 24 h; the calculated IC_{50} was 48.64 and 77.34 µg/mL, respectively. Results are expressed as mean ± standard error of the mean.

3. Discussion

The increase in *C. tropicalis* infections in recent years and the resistance to commonly used antifungals expressed by these yeasts, especially in immunocompromised patients, have made these candidemias a great challenge, not only due to the increase in rates of morbidity and mortality but also due to the financial costs at a global level. Therefore, the search for new effective and safe compounds with antifungal potential is urgent today.

In this research, we demonstrated that the ISO monoterpene extracted from *O. xylopioides* inhibits the formation of fungal biofilms. Consistent with our previous work, where we reported its ability to inhibit mature biofilms in *C. tropicalis* [19], with inhibition percentages between 20.3% and 25.8% higher than the percentages shown with AFB (7.2% and 12.4%). Moreover, the effect of ISO on the mature biofilms of other *Candida* species has been reported, even in those isolates where AFB did not show an effect [18]. Our results show percentages of inhibition in the formation of biofilms by ISO greater than 50% (between 59.18% and 89.35), higher than those shown by AFB. This information is of great value considering that *C. tropicalis* is a pathogen well known for the formation of strong biofilms as a result of its high metabolic activity [20]. These biofilms represent one of the main virulence factors of these yeasts and vary depending on the origin of the infection [21]. They have been associated with the high mortality caused by these pathogens, probably due to the low permeability of the matrix to commonly used antifungals [22]. Comparing the efficacy of ISO against AFB, we highlight the role of ISO with percentages higher than 80% in the inhibition of biofilm formation, higher than those shown by AFB. Studies reported by [20] have documented the ability of liposomal AFB to inhibit the growth of biofilms but its ineffectiveness in eradicating mature biofilms, even at high doses. These results allow us to suggest that ISO could be a promising alternative to combat multiresistant pathogenic yeasts that form biofilms [23].

On the other hand, taking into account that many antifungal agents of vegetable origin can inhibit the function of the fungal mitochondrial electron transport chain, leading to the reduction of ΔΨm [24], which is an important indicator of mitochondrial function [25–27], we investigated the possible effect of ISO against *C. tropicalis* mitochondria. In this work, we use Rh123, a permeable lipophilic cationic fluorochrome [28], which selectively accumulates in the mitochondria of active cells. This specific interaction depends on the high transmembrane potential maintained by functional mitochondria; therefore, the dissipation of ΔΨm by ionophores or electron transport inhibitors eliminates the selective mitochondrial association of these compounds [29]. Consequently, mitochondrial activation induces quenching of Rh123 fluorescence, and the rate of fluorescence decay is proportional to ΔΨm [30,31]. The loss of ΔΨm is considered the earliest event in the apoptotic cascade,

where the mitochondrial permeability transition pore (MPTP) opens and leads to the collapse of ΔΨm and irreversibly initiates cell apoptosis [32–34]. Therefore, mitochondrial depolarization is an indicator of mitochondrial-mediated apoptosis. We reported the loss in ΔΨm in yeasts treated with ISO as being significantly higher compared to the control group (untreated cells) and cells treated with H_2O_2. These results allow us to infer that ISO causes cell apoptosis mediated by mitochondria in *C. tropicalis*, this being another mechanism responsible for the antifungal activity of this monoterpene.

We also evaluated the effect of ISO on the integrity of the cell wall through the measurement of chitin content based on CFW staining and analysis by flow cytometry. Chitin is one of the main structural components in fungal cell walls. Together with β-1,3-glucan, they play a fundamental role in maintaining the integrity of the cell wall, giving it structural rigidity during growth and morphogenesis [35,36]. All ISO-treated isolates showed higher chitin content (revealed by higher CFW fluorescence intensity) compared to untreated strains. These results are consistent with studies reported by other researchers [37–40], who postulate that perturbation of cell wall synthesis in some yeasts, either by mutations in synthesis-related genes or by adding compounds that interfere with normal cell wall assembly, triggers a compensatory response to ensure the integrity of the cell wall; this response includes increased levels of chitin in the cell wall, suggesting that cell wall stress in fungi can generally lead to activation of the chitin biosynthetic pathway. This allows us to suggest that ISO could be acting on the integrity of the cell wall of these yeasts and inducing the compensatory synthesis of chitin. Reported studies [39] show the ability of these yeasts to grow in the presence of CASP, an antifungal that acts on the synthesis of β-1,3-glucan. The action of CASP on these yeasts causes them to activate a compensatory pathway, inducing the synthesis of chitin. This is consistent with our results, which reveal a higher chitin content in CASP-treated cells compared to untreated and ISO-treated cells.

Finally, we evaluated the cytotoxic effect of ISO on VERO cells through the MTT and CV methods. The results showed significant differences between the cytotoxicity methods used. The IC_{50} obtained by the CV assay was significantly lower (48.64 μg/mL) than that found by the MTT assay (77.34 μg/mL). This observation can be explained by the nature of each test; the MTT assay is mainly based on the enzymatic conversion of MTT in mitochondria, so it could be influenced by inhibitors of mitochondrial components [41]. Therefore, a cytotoxicity assay based on mitochondrial respiratory activity would give early signs of toxicity after exposure to mitochondrial toxicants; ISO affects mitochondrial function, which could influence the cytotoxicity results of this method. Furthermore, the MTT assay can be significantly influenced by compounds that modify cell metabolism and reaction conditions [42]. Since various investigations have linked mitochondrial metabolism to the progression of cancer and other pathologies [43], ISO could be used in a tumor cell model to evaluate its effect on them. Furthermore, in tumor cells, there are higher levels of reactive oxygen species than in their non-tumor cells of origin, and, therefore, they must employ various metabolic strategies to prevent oxidative stress [44]. Taking into account the effect of ISO on the induction of intracellular reactive oxygen species [19], this could help in its action against these cells. On the other hand, with the CV method, cells that undergo cell death lose their adherence and are subsequently lost from the cell population, which reduces the amount of CV staining in the wells. Therefore, the amount of dye absorbed depends on the total DNA and/or protein content in the culture, thus allowing estimation of the number of viable cells in the wells [45]. It has been previously reported that different cytotoxicity assays may give different results depending on the test agent used and the cytotoxicity assay employed [46]. For this reason, it is important to consider what effect is expected, that is, the mechanism of action of the agent evaluated.

Our results are consistent with other studies that show that ISO at low concentrations does not have toxic effects. ISO cytotoxicity assays on human peripheral blood lymphocytes have indicated that at 3.0 μM, 8.0 μM, and 80 μM, it has no genotoxic or cytotoxic effects on these cells, and at concentrations between 3 and 1620 μM, it shows a protective effect

on damage to the DNA from lymphocytes induced by H_2O_2, suggesting that at low concentrations it can be used without expecting negative effects on human health [47]. Likewise, the cytotoxic effect of ISO against murine macrophages (RAW 264.7) has been investigated, revealing that ISO at 100 μM does not have significant cytotoxic effects against these cells, considering the possible use of ISO as a food additive [48]. The findings on the biological potential of ISO could serve as a starting point to understand the mechanisms of action at low doses. Previous research has established that mitochondria are a fundamental element of apoptotic signaling [44], so the cell death mechanisms observed in this study support the effects on the indicated targets.

Likewise, the cytotoxicity results could have implications in the search for new therapeutic alternatives and the reduction of the adverse effects of fungal diseases. This evidence gives rise to exploring the individual or combined effects of ISO and its mechanisms of action on cell proliferation and its association with mitochondrial metabolic pathways. The integration of these approaches in future research is required to contribute to the understanding of its antifungal activity and the potential use of this compound in the clinical setting.

4. Materials and Methods

4.1. Reagents

RPMI 1640, phosphate-buffered saline (PBS), and yeast peptone dextrose broth (YPD) were obtained from Thermo Fisher Scientific, Waltham, MA, USA; 3-N-morpholinopropanesulfonic acid (MOPS) was obtained from Merck; potato dextrose broth (PDB), sabouraud dextrose agar (SDA), sabouraud dextrose broth (SDB), amphotericin B (AFB), rhodamine 123 (Rh123), calcofluor white (CFW), caspofungin (CASP), and crystal violet (CV) used in this study were obtained from Sigma-Aldrich, USA; glacial acetic acid was obtained from Carlo Erba Reagents, Italy.

4.2. Strains

Seven clinical isolates of *C. tropicalis* (001 to 007) were used in this study. The isolates were cultured from blood cultures and tracheal aspirate samples from hospitalized patients at the Salud Social S.A.S. from the city of Sincelejo, Colombia. All microorganisms were identified by standard methods: Vitek 2 Compact, Biomerieux SA, YST Vitek 2 Card, and AST-YS08 Vitek 2 Card (Ref 420739). SDA medium and BBL CHROMagar Candida medium were used to maintain the cultures until the tests were carried out. The identification of one of the *C. tropicalis* isolates was confirmed through a genome-wide taxonomic study (information reported in previous work) [19].

4.3. Antifungal Susceptibility Testing

The ISO minimal inhibitory concentration (MIC) against *C. tropicalis* was defined as the lowest concentration at which 90% (MIC_{90}) of fungal growth was inhibited, compared to the negative control (untreated cells). MICs were established following the protocols described in the Clinical Laboratory Standards Institute (CLSI) method (M27-A3) [49] and The European Committee for Antimicrobial Susceptibility Testing (EUCAST) [50]. The MIC_{90}, MIC_{50} (lowest concentration at which 50% of fungal growth was inhibited), and MFC (minimum fungicidal concentration) of ISO against *C. tropicalis* were previously reported [19].

4.4. Effect of ISO on the Formation of Biofilms

The effect of ISO on biofilm formation was evaluated following the protocol described in previous works [19]. In the present study, the ISO MIC was added at the time of inoculation with *C. tropicalis*. The yeast colonies in SDA were used to standardize the inoculum until it reached a concentration of 10^6 cells/mL. Then, in 96-well boxes, 200 μL of the inoculum in YPD broth with the ISO MIC for each isolate was cultured in each reaction well and incubated at 37 °C for 48 h. Subsequently, the broth was removed from the

microplates, and the biofilms in the wells were washed three times with deionized water. Three replicates of each sample were made. Cultures without ISO were used as a negative control, and AFB (4 μg/mL) was used as a positive control. The percentage reduction in biofilm formation was quantified by staining the wells with 0.1% crystal violet for 20 min. The wells were washed with deionized water until excess dye was removed. Finally, the samples were treated with 250 μL of glacial acetic acid, and the absorbance values were measured at 590 nm (OD_{590}) using a SYNERGY LX (Biotek, Wichita, KS, USA) plate reader. Biofilm production was grouped into the following categories: OD_{590} < 0.1: non-producers (NP), OD_{590} 0.1–1.0: weak producers (WP), OD_{590} 1.1–3.0: moderate producers (MP), and OD_{590} > 3.0: strong producers (SP). Biofilm reduction was calculated using the following equation:

$$\% \text{ reduction in biofilm formation: } AbsCO - AbsISO/AbsCO \times 100$$

where AbsCO: absorbance of the control and AbsISO: absorbance of the sample treated with ISO.

4.5. Effect of ISO on Mitochondrial Membrane Potential (ΔΨm)

To evaluate the effect of ISO on ΔΨm, yeasts were stained with Rhodamine 123 (Rh123) as described by Chang [25] with minor modifications. Fungal cells (3×10^8 UFC/mL) were treated with the ISO MIC for 1 h, harvested by centrifugation, resuspended with 25 μM Rh123 (in 50 mM sodium citrate), and incubated at 30 °C for 10 min. After staining, cells were washed three times with PBS, and the fluorescence intensity was measured using the BD FACS CANTO II flow cytometer and analyzed with the BD FACS DIVA software version 6.1.3. (Ext: 488 nm/Emi:525 nm). Cells without ISO treatment were used as negative controls, whereas cells treated with 15 mM hydrogen peroxide (H_2O_2) for 1 h were used as positive controls.

Rh123 is a permeable lipophilic cationic fluorochrome [28], and it selectively accumulates in the mitochondria of active cells. This specific interaction depends on the high transmembrane potential maintained by functional mitochondria; therefore, the dissipation of the mitochondrial transmembrane potential by ionophores or electron transport inhibitors eliminates the selective mitochondrial association of these compounds [29]. Consequently, mitochondrial activation induces quenching of Rh123 fluorescence, and the rate of fluorescence decay is proportional to ΔΨm [30,31].

4.6. Effect of ISO on Cell Wall Integrity

Damage to the integrity of the fungal wall by ISO was evaluated by measuring the chitin content of the cell wall using CFW staining, following the protocol described in [39] with minor modifications. CFW is a water-soluble fluorescent dye that exhibits selective binding to fungal cell walls (specific for chitin) [51] and fluoresces blue/green when illuminated with UV light [52]. Yeasts grown in YPD broth (1×10^6 cells/mL) at 35 °C were treated with ISO MIC for 2 h and stained with CFW [2.5 μg/mL] for 15 min in the dark. Subsequently, cells were washed and resuspended in PBS and finally analyzed on a BD FACS CANTO II flow cytometer (pacific blue channel: 405–450/50 nm; 20,000 events per assay) using the BD FACS DIVA software version 6.1.3. All experiments were performed in triplicate. A staining index (SI) was defined [39], whose value was directly related to the amount of chitin and took into account the different levels of autofluorescence. The mean fluorescence intensity (MFI) emitted from stained (positive population) and unstained (negative population) yeasts was analyzed, and in each experiment, the SI was calculated using the following equation:

$$SI: (MFIpp - MFIpn)/2 \times SDpn$$

where MFIpp: mean fluorescence intensity of the positive population; MFIpn: mean fluorescence intensity of the negative population; and SDpn: standard deviation of the negative population.

Transmission Electron Microscopy (TEM)

The damage to the integrity of the cell wall as well as the general morphology of *C. tropicalis* after treatment with ISO was also analyzed through TEM, following the protocol described in previous studies [19]. The concentration of *C. tropicalis* was adjusted to 10^6 CFU/mL; the suspension was mixed with ISO (200 µg/mL) and incubated at 37 °C for 24 h. Subsequently, the cells were collected and fixed in 2.5% glutaraldehyde in phosphate buffer pH 7.2 at 4 °C; they were centrifuged at 13,000 rpm for 3 min, and the button at the bottom of the vial was postfixed in 1% osmium tetroxide in water for 2 h at 4 °C. Then, pre-imbibition with 3% uranyl acetate was performed for 1 h at room temperature, after which the cells were dehydrated in an ethanol gradient (50% for 10 min, 70% for 10 min, 90% for 10 min, 100% for 10 min), acetone:ethanol (1:1) for 15 min, and embedded in SPURR epoxy resin. The samples were cut in a Leica EM UC7 ultramicrotome at 130 nm thickness, contrasted with 6% uranyl acetate and lead citrate, and then finally observed in a JEOL 1400 plus transmission electron microscope (JEOL Ltd., Tokyo, Japan). The photographs were obtained with a Gatan Orius CCD camera (Gatan Inc., Pleasanton, CA, USA).

4.7. Isoespintanol Cytotoxicity Assays

The cytotoxicity assays were carried out using immortalized epithelial cells from the African green monkey kidney (*Cercopithecus aethiops*) (VERO), which, due to their homology with human cells and their easy culture, are commonly used as a useful model to evaluate in vitro the cytotoxic activity of natural products [53,54]. These assays were performed using the crystal violet (CV) and 3-(4,5-dimethylthiazol-2-yl)-2,5-diphenyltetrazolium bromide) (MTT) methods.

4.7.1. Cell Culture

Cells were grown in RPMI 1640 medium supplemented with 10% fetal bovine serum (FBS) and 1% penicillin/streptomycin and maintained in a humidified atmosphere with 5% CO_2 at 37 °C. Medium changes were made every 2–3 days for maintenance. Subcultures were made twice a week until they reached approximately 80% confluence for assays.

4.7.2. MTT Assay

The MTT assay is based on the ability of dehydrogenase enzymes from metabolically viable cells to reduce tetrazolium rings and form formazan crystals; consequently, the number of viable cells is directly proportional to the level of formazan produced [55–57]. VERO cells were seeded in 96-well microplates (Nest®) at a density of 4×10^4 cells/cm^2, which allowed their adhesion and proliferation for 24 h. After this time, the cells were incubated with RPMI 1640 medium containing different concentrations of ISO (9.76 to 2500 µg/mL) for 24 h. After incubation, the treatments were removed, and 100 µL of MTT was added to each well at a concentration of 0.125 mg/mL. The plate was incubated at 5% CO_2 at 37 °C for 4 h. Subsequently, the MTT was discarded, and the formazan crystals deposited at the bottom of each well were dissolved in 100 µL of dimethylsulfoxide (DMSO). Absorbance was determined at an optical density (OD) of 570 nm using an Epoch 2 microplate reader (Biotek). Cells without treatments were used as negative controls. The absorbance values were normalized by considering the absorbance obtained from untreated cultures as 100%.

4.7.3. Crystal Violet Assay (CV)

The CV assay is based on the staining of the DNA and proteins of the cells available in the culture wells, and the color intensity is proportional to the number of viable cells [45]. VERO cells were seeded in 96-well microplates at a density of 4×10^4 cells/cm^2, allowing

their adhesion and proliferation for 24 h. After this time, the cells were incubated with RPMI 1640 medium containing ISO (at previously described concentrations) for 24 h. At the end of the treatments, the medium was removed, and the cells were washed with PBS, then fixed by depositing 100 µL of 4% paraformaldehyde solution in each well for 30 min at room temperature. Paraformaldehyde was discarded, and 100 µL of 0.5% CV solution in 6% methanol was added to each well for 30 min at room temperature. The CV was discarded, and each well was carefully rinsed with distilled water until the remaining dye was extracted. The plate was allowed to air dry for 24 h. To extract the CV bound to the DNA, 200 µL/well of methanol was used, and the plate was incubated for 20 min at room temperature on an orbital shaker with a frequency of 20 oscillations per minute. Finally, the absorbance was determined as indicated above. The results for both assays were expressed through dose–response curves using 16 ISO concentrations (9.76 to 2500 µg/mL). IC_{50} values (50% inhibitory concentration of the cell population) were calculated from the fit ($R^2 > 0.95$) of the Hill slope curve of the experimental data using nonlinear regression analysis in GraphPad Prism version 8.0 software.

4.8. Data Analysis

Results were analyzed using GraphPad Prism version 8.0 software. Normality was assessed using the Shapiro–Wilk test. One-way ANOVA was performed to assess the impact of ISO treatment on the inhibition of biofilm formation compared to the untreated control group; to compare the effects of ISO and AFB on the inhibition of biofilm formation, Tukey's test was used; to evaluate the effect of ISO on the integrity of the wall, the Tukey test was also used; and to evaluate the ΔΨm, Dunn's test was used.

5. Conclusions

In this investigation, we explore other antifungal action targets of ISO. Our results show that ISO has the ability to inhibit the formation of fungal biofilms, causes the loss of ΔΨm with the consequent mitochondrial dysfunction, and can affect the cell wall of these pathogens. Confirming that the monoterpene ISO has different targets of action against these yeasts. This intensifies the interest in continuing to investigate the mechanisms of action of this compound, which could be used as an adjuvant in the treatment and control of pathogenic yeasts resistant to antifungals.

Author Contributions: Conceptualization, O.I.C.M.; methodology, O.I.C.M., A.P.-T., R.B.S. and A.A.O.; formal analysis, O.I.C.M., A.P.-T., R.B.S. and A.A.O.; investigation, O.I.C.M., A.P.-T. and R.B.S.; resources, A.A.O. and G.S.P.; writing—original draft preparation, O.I.C.M., A.P.-T. and A.A.O.; writing—review and editing, O.I.C.M., A.A.O. and G.S.P.; visualization, O.I.C.M.; supervision, O.I.C.M., A.A.O. and G.S.P.; funding acquisition, A.A.O. and G.S.P. All authors have read and agreed to the published version of the manuscript.

Funding: This research was funded with resources from the FCB-02-19 project of the University of Córdoba, Montería, Colombia.

Institutional Review Board Statement: Not applicable.

Informed Consent Statement: Not applicable.

Data Availability Statement: The data presented in this study are available in the article.

Acknowledgments: To Homero San Juan, Specialized Diagnostic Center, Universidad del Norte, Barranquilla. María Fernanda Yasnot, GIMBIC Research Group, Universidad de Córdoba, Montería. Lida Espitia Pérez, Biomedical and Molecular Biology Research Group, Universidad del Sinú Elías Bechara Zainúm, Montería. O.C.M. thanks the scholarship program of the Ministry of Science, Technology and Innovation of Colombia for the granting of the doctoral scholarship.

Conflicts of Interest: The authors declare no conflict of interest.

References

1. El-kholy, M.A.; Helaly, G.F.; El Ghazzawi, E.F.; El-sawaf, G.; Shawky, S.M. Virulence factors and antifungal susceptibility profile of *C. tropicalis* isolated from various clinical specimens in Alexandria, Egypt. *J. Fungi* **2021**, *7*, 351. [CrossRef] [PubMed]
2. Zuza-Alves, D.L.; Sila-Rocha, W.P.; Chaves, G. An update on *Candida tropicalis* based on basic and clinical approaches. *Front. Microbiol.* **2017**, *8*, 1927. [CrossRef] [PubMed]
3. Munhoz-Alves, N.; Nishiyama Mimura, L.A.; Viero, R.M.; Bagagli, E.; Peron, J.P.S.; Sartori, A.; Fraga-Silva, T.F.d.C. *Candida tropicalis* systemic infection redirects leukocyte infiltration to the kidneys attenuating encephalomyelitis. *J. Fungi* **2021**, *7*, 757. [CrossRef]
4. Silva, S.; Negri, M.; Henriques, M.; Oliveira, R.; Williams, D.W.; Azeredo, J. *Candida glabrata*, *Candida parapsilosis* and *Candida tropicalis*: Biology, epidemiology, pathogenicity and antifungal resistance. *FEMS Microbiol. Rev.* **2012**, *36*, 288–305. [CrossRef]
5. Cortés, J.A.; Ruiz, J.F.; Melgarejo-Moreno, L.N.; Lemos, E.V. Candidemia in Colombia. *Biomedica* **2020**, *40*, 195–207. [CrossRef]
6. Avato, P. Editorial to the Special Issue—"Natural products and drug discovery". *Molecules* **2020**, *25*, 1128. [CrossRef]
7. Morales, I.; De La Fuente, J.; Sosa, V. Componentes de *Eupatorium saltense*. *An. Asoc. Quim. Argent.* **1991**, *79*, 141–144.
8. Hocquemiller, R.; Cortes, D.; Arango, G.J.; Myint, S.H.; Cave, A. Isolement et synthese de l'espintanol, nouveau monoterpene antiparasitaire. *J. Nat. Prod.* **1991**, *54*, 445–452. [CrossRef]
9. Rojano, B.; Pérez, E.; Figadère, B.; Martin, M.T.; Recio, M.C.; Giner, R.; Ríos, J.L.; Schinella, G.; Sáez, J. Constituents of *Oxandra* Cf. *xylopioides with anti-inflammatory activity. J. Nat. Prod.* **2007**, *70*, 835–838. [CrossRef]
10. Rojano, B.A.; Gaviria, C.A.; Gil, M.A.; Saéz, J.A.; Schinella, G.R.; Tournier, H. Antioxidant activity of the isoespintanol in diferent media. *Vitae* **2008**, *15*, 173–181.
11. Gavilánez Buñay, T.C.; Colareda, G.A.; Ragone, M.I.; Bonilla, M.; Rojano, B.A.; Schinella, G.R.; Consolini, A.E. Intestinal, urinary and uterine antispasmodic effects of isoespintanol, metabolite from *Oxandra xylopioides* leaves. *Phytomedicine* **2018**, *51*, 20–28. [CrossRef] [PubMed]
12. Rinaldi, G.J.; Rojano, B.; Schinella, G.; Mosca, S.M. Participation of NO in the vasodilatory action of isoespintanol. *Vitae* **2019**, *26*, 78–83. [CrossRef]
13. González Arbeláez, L.; Ciocci Pardo, A.; Fantinelli, J.C.; Rojano, B.; Schinella, G.; Mosca, S.M. Isoespintanol, a monoterpene isolated from *Oxandra* cf *xylopioides*, ameliorates the myocardial ischemia-reperfusion injury by AKT/PKCε/ENOS-dependent pathways. *Naunyn-Schmiedeberg's Arch. Pharmacol.* **2020**, *393*, 629–638. [CrossRef] [PubMed]
14. Usuga, A.; Tejera, I.; Gómez, J.; Restrepo, O.; Rojano, B.; Restrepo, G. Cryoprotective effects of ergothioneine and isoespintanol on canine semen. *Animals* **2021**, *11*, 2757. [CrossRef] [PubMed]
15. Rojano, B.A.; Montoya, S.; Yépez, F.; Saez, J. *Evaluación de Isoespintanol Aislado de Oxandra Cf. xylopioides (Annonaceae) Sobre Spodoptera Frugiperda J.E. Smith (Lepidoptera: Noctuidae)*; Universidad Nacional de Colombia: Medellín, Colombia, 2007; Volume 60.
16. Arango, N.; Vanegas, N.; Saez, J.; García, C.; Rojano, B. Actividad antifungica del isoespintanol sobre hongos del género *Colletotricum*. *Sci. Tech.* **2007**, *33*, 279–280. [CrossRef]
17. Contreras Martínez, O.I.; Angulo Ortíz, A.; Santafé Patiño, G. Antibacterial screening of isoespintanol, an aromatic monoterpene isolated from *Oxandra xylopioides* Diels. *Molecules* **2022**, *27*, 8004. [CrossRef]
18. Contreras Martínez, O.I.; Ortíz, A.A.; Patiño, G.S. Antifungal potential of isoespintanol extracted from *Oxandra xylopioides* Diels (Annonaceae) against intrahospital isolations of *Candida* spp. *Heliyon* **2022**, *8*, e11110. [CrossRef]
19. Contreras, O.; Angulo, A.; Santafé, G. Mechanism of antifungal action of monoterpene isoespintanol against clinical isolates of *Candida tropicalis*. *Molecules* **2022**, *27*, 5808. [CrossRef]
20. Kawai, A.; Yamagishi; Mikamo, H. Time-lapse tracking of *Candida tropicalis* biofilm formation and the antifungal efficacy of liposomal amphotericin B. *Jpn. J. Infect. Dis.* **2017**, *70*, 559–564. [CrossRef]
21. Guembe, M.; Cruces, R.; Peláez, T.; Mu, P.; Bouza, E. Assessment of biofilm production in *Candida* isolates according to species and origin of infection. *Enferm. Infecc. Microbiol. Clin.* **2017**, *35*, 37–40. [CrossRef]
22. Tascini, C.; Sozio, E.; Corte, L.; Sbrana, F. The role of biofilm forming on mortality in patients with candidemia: A study derived from real world data. *Infect. Dis.* **2017**, *50*, 214–219. [CrossRef]
23. Karpiński, T.M.; Ożarowski, M.; Seremak-Mrozikiewicz, A.; Wolski, H.; Adamczak, A. Plant preparations and compounds with activities against biofilms formed by *Candida* spp. *J. Fungi* **2021**, *7*, 360. [CrossRef] [PubMed]
24. Tariq, S.; Wani, S.; Rasool, W.; Shafi, K.; Bhat, M.A.; Prabhakar, A.; Shalla, A.H.; Rather, M.A. A Comprehensive review of the antibacterial, antifungal and antiviral potential of essential oils and their chemical constituents against drug-resistant microbial pathogens. *Microb. Pathog.* **2019**, *134*, 103580. [CrossRef] [PubMed]
25. Chang, C.K.; Kao, M.C.; Lan, C.Y. Antimicrobial activity of the peptide Lfcinb15 against *Candida albicans*. *J. Fungi* **2021**, *7*, 519. [CrossRef] [PubMed]
26. Hussain, S. Measurement of nanoparticle-induced mitochondrial membrane potential alterations. In *Nanotoxicity Methods and Protocols*, 1st ed.; Zhang, E., Ed.; Humana: New York, NY, USA, 2018; Volume 1894, pp. 123–131. [CrossRef]
27. Sakamuru, S.; Attene-Ramos, M.S.; Xia, M. Mitochondrial membrane potential assay. *Methods Mol Biol.* **2016**, *1473*, 17–22. [CrossRef]
28. Marika, G.J.; Saez, G.T.; O'Connor, J.-E. A fast kinetic method for assessing mitochondrial membrane potential in isolated hepatocytes with rhodamine 123 and flow cytometry. *Cytometry* **1994**, *15*, 335–342. [CrossRef]

29. Johnson, L.V.V.; Walsh, M.L.L.; Bockus, B.J.; Chen, L.B. Monitoring of relative mitochondrial membrane potential in living cells by fluorescence microscopy. *J. Cell Biol.* **1981**, *88*, 526–535. [CrossRef]
30. Baracca, A.; Sgarbi, G.; Solaini, G.; Lenaz, G. Rhodamine 123 as a probe of mitochondrial membrane potential: Evaluation of proton flux through F_0 during ATP synthesis. *Biochim. Biophys. Acta-Bioenerg.* **2003**, *1606*, 137–146. [CrossRef]
31. Zorova, L.D.; Popkov, V.A.; Plotnikov, E.Y.; Silachev, D.N.; Pevzner, I.B.; Jankauskas, S.S.; Babenko, V.A.; Zorov, S.D.; Balakireva, A.V.; Juhaszova, M.; et al. Mitochondrial membrane potential. *Anal. Biochem.* **2018**, *552*, 50–59. [CrossRef]
32. Holanda, M.A.; da Silva, C.R.; Neto, J.B.; do AV Sa, L.G.; do Nascimento, F.B.; Barrosos, D.; da Silva, L.; Cándido, T.M.; Leitao, A.D.; Barbosa, A.D.; et al. Evaluation of the antifungal activity in vitro of midazolam against fluconazole-resistant *Candida* spp. isolates. *Future Microbiol.* **2021**, *16*, 71–81. [CrossRef]
33. Lu, J.; Wu, L.; Wang, X.; Zhu, J.; Du, J.; Shen, B. Detection of mitochondria membrane potential to study CLIC4 knockdown-induced HN4 cell apoptosis in vitro. *J. Vis. Exp.* **2018**, *2018*, e56317. [CrossRef]
34. Hwang, I.; Lee, J.; Jin, H.-G.; Woo, E.-R.; Lee, D.G. Amentoflavone stimulates mitochondrial dysfunction and induces apoptotic cell death in *Candida albicans*. *Mycopathologia* **2012**, *173*, 207–218. [CrossRef] [PubMed]
35. Klis, F.M. Review: Cell wall assembly in yeast. *Yeast* **1994**, *10*, 851–869. [CrossRef] [PubMed]
36. Munro, C.A.; Gow, N.A.R. Chitin synthesis in human pathogenic fungi. *Med. Mycol. Suppl.* **2001**, *39*, 41–53. [CrossRef]
37. Ram, A.F.J.; Arentshorst, M.; Damveld, R.A.; vanKuyk, P.A.; Klis, F.M.; van den Hondel, C.A.M.J.J. The cell wall stress response in *Aspergillus niger* involves increased expression of the glutamine: Fructose-6-phosphate amidotransferase-encoding gene (GfaA) and increased deposition of chitin in the cell wall. *Microbiology* **2004**, *150*, 3315–3326. [CrossRef]
38. Hagen, S.; Marx, F.; Ram, A.F.; Meyer, V. The antifungal protein AFP from *Aspergillus giganteus* inhibits chitin synthesis in sensitive fungi. *Appl. Environ. Microbiol.* **2007**, *73*, 2128–2134. [CrossRef]
39. Costa de Oliveira, S.; Silva, A.; Miranda, I.; Salvador, A.; Azevedo, M.; Munro, C.; Rodríguez, A.; Pina-Vaz, C. Determination of chitin content in fungal cell wall: An alternative flow cytometric method. *Cytom. Part A* **2013**, *83A*, 324–328. [CrossRef]
40. Walker, L.A.; Munro, C.A.; De Bruijn, I.; Lenardon, M.D.; McKinnon, A.; Gow, N.A.R. Stimulation of chitin synthesis rescues *Candida albicans* from echinocandins. *PLoS Pathog.* **2008**, *4*, e1000040. [CrossRef]
41. Fotakis, G.; Timbrell, J.A. In vitro cytotoxicity assays: Comparison of LDH, neutral red, MTT and protein assay in hepatoma cell lines following exposure to cadmium chloride. *Toxicol. Lett.* **2006**, *160*, 171–177. [CrossRef]
42. Sliwka, L.; Wiktorska, K.; Suchocki, P.; Milczarek, M.; Mielczarek, S.; Lubelska, K.; Cierpial, T.; Lyzwa, P.; Kielbasinski, P.; Jaromin, A.; et al. The comparison of MTT and CVS assays for the assessment of anticancer agent interactions. *PLoS ONE* **2016**, *11*, e0155772. [CrossRef]
43. Petronek, M.; Stolwijk, J.; Murray, S.; Steinbach, E.; Zakharia, Y.; Buettner, G.; Spitz, D.; Allen, B. Utilization of redox modulating small molecules that selectively act as pro-oxidants in cancer cells to open a therapeutic window for improving cancer therapy. *Redox Biol.* **2021**, *42*, 101864. [CrossRef]
44. Boese, A.; Kang, S. Mitochondrial metabolism-mediated redox regulation in cancer progression. *Redox Biol.* **2021**, *42*, 101870. [CrossRef] [PubMed]
45. Feoktistova, M.; Geserick, P.; Leverkus, M. Crystal violet assay for determining viability of cultured cells. *Cold Spring Harb. Protoc.* **2016**, *2016*, 343–346. [CrossRef] [PubMed]
46. Weyermann, J.; Lochmann, D.; Zimmer, A. A practical note on the use of cytotoxicity assays. *Int. J. Pharm.* **2005**, *288*, 369–376. [CrossRef]
47. Marquez-Fernandez, M.; Munoz-Lasso, D.; Bautista Lopez, J.; Zapata, K.; Puertas Mejia, M.; Lopez-Alarcon, C.; Rojano, B.A. Effect of isoespintanol isolated from *Oxandra* Cf. xylopioides against DNA damage of human lymphocytes. *Pak. J. Pharm. Sci.* **2018**, *31*, 1777–1782.
48. Zapata, K.; Arias, J.; Cortés, F.; Alarcon, C.; Durango, D.; Rojano, B. Oxidative stabilization of palm olein with isoespintanol (2-isopropyl-3,6-dimethoxy-5-methylphenol) isolated from *Oxandra* Cf *xylopioides*. *J. Med. Plants Res.* **2017**, *11*, 218–225.
49. Cantón, E.; Martín, E.; Espinel-Ingroff, A. Métodos estandarizados por el CLSI para el estudio de la sensibilidad a los antifúngicos (Documentos M27-A3, M38-A y M44-A). *Rev. Iberoam. Micol.* **2007**, *15*, 1–17.
50. Rodriguez-tudela, J.L. Method for determination of minimal inhibitory concentration (MIC) by broth dilution of fermentative yeasts. *Clin. Microbiol. Infect.* **2003**, *9*, 467–474. [CrossRef]
51. Hoch, H.C.; Galvani, C.D.; Szarowski, D.H.; Turner, J.N. Two new fluorescent dyes applicable for visualization of fungal cell walls. *Mycologia* **2005**, *97*, 580–588. [CrossRef]
52. Monheit, J.G.; Brown, G.; Kott, M.M.; Schmidt, W.A.; Moore, D.G. Calcofluor white detection of fungi in cytopathology. *Am. J. Clin. Pathol.* **1986**, *85*, 222–225. [CrossRef]
53. Araldi, R.P.; dos Santos, M.O.; Barbon, F.F.; Manjerona, B.A.; Meirelles, B.R.; de Oliva Neto, P.; da Silva, P.I.; dos Santos, L.; Camargo, I.C.C.; de Souza, E.B. Analysis of antioxidant, cytotoxic and mutagenic potential of *Agave sisalana perrine* extracts using vero cells, human lymphocytes and mice polychromatic erythrocytes. *Biomed. Pharmacother.* **2018**, *98*, 873–885. [CrossRef] [PubMed]
54. Hussein, H.A.; Maulidiani, M.; Abdullah, M.A. Microalgal metabolites as anti-cancer/anti-oxidant agents reduce cytotoxicity of elevated silver nanoparticle levels against non-cancerous VERO cells. *Heliyon* **2020**, *6*, e05263. [CrossRef] [PubMed]
55. Motlhatlego, K.; Ali, M.; Leonard, C.; Eloff, J.; McGaw, L. Inhibitory effect of newtonia extracts and myricetin-3-O-rhamnoside (myricitrin) on bacterial biofilm formation. *BMC Complement. Med. Ther.* **2020**, *20*, 358. [CrossRef] [PubMed]

56. Negrette-Guzmán, M.; Huerta-Yepez, S.; Vega, M.I.; León-Contreras, J.C.; Hernández-Pando, R.; Medina-Campos, O.N.; Rodríguez, E.; Tapia, E.; Pedraza-Chaverri, J. Sulforaphane induces differential modulation of mitochondrial biogenesis and dynamics in normal cells and tumor cells. *Food Chem. Toxicol.* **2017**, *100*, 90–102. [CrossRef] [PubMed]
57. Mosmann, T. Rapid colorimetric assay for cellular growth and survival: Application to proliferation and cytotoxicity assays. *J. Immunol.* **1983**, *65*, 55–63. [CrossRef]

Anexo 3

"Antibacterial Screening of Isoespintanol, an Aromatic Monoterpene Isolated from *Oxandra xylopioides* Diels"

molecules

MDPI

Article

Antibacterial Screening of Isoespintanol, an Aromatic Monoterpene Isolated from *Oxandra xylopioides* Diels

Orfa Inés Contreras Martínez [1,*], Alberto Angulo Ortíz [2] and Gilmar Santafé Patiño [2]

[1] Biology Department, Faculty of Basic Sciences, University of Córdoba, Montería 230002, Colombia
[2] Chemistry Department, Faculty of Basic Sciences, University of Córdoba, Montería 230002, Colombia
* Correspondence: oicontreras@correo.unicordoba.edu.co

Abstract: The incidence of nosocomial infections, as well as the high mortality and drug resistance expressed by nosocomial pathogens, especially in immunocompromised patients, poses significant medical challenges. Currently, the efficacy of plant compounds with antimicrobial potential has been reported as a promising alternative therapy to traditional methods. Isoespintanol (ISO) is a monoterpene with high biological activity. Using the broth microdilution method, the antibacterial activity of ISO was examined in 90 clinical isolates, which included 14 different species: (*Escherichia coli* (38), *Pseudomonas aeruginosa* (12), *Klebsiella pneumoniae* (13), *Acinetobacter baumannii* (3), *Proteus mirabilis* (7), *Staphylococcus epidermidis* (3), *Staphylococcus aureus* (5), *Enterococcus faecium* (1), *Enterococcus faecalis* (1), *Stenotrophomonas maltophilia* (2), *Citrobacter koseri* (2), *Serratia marcescens* (1), *Aeromonas hydrophila* (1), and *Providencia rettgeri* (1). MIC_{90} minimum inhibitory concentration values ranged from 694.3 to 916.5 µg/mL and MIC_{50} values from 154.2 to 457.3 µg/mL. The eradication of mature biofilms in *P. aeruginosa* after 1 h of exposure to ISO was between 6.6 and 77.4%, being higher in all cases than the percentage of biofilm eradication in cells treated with ciprofloxacin, which was between 4.3 and 67.5%. ISO has antibacterial and antibiofilm potential against nosocomial bacteria and could serve as an adjuvant in the control of these pathogens.

Keywords: nosocomial infection; isoespintanol; *Oxandra xylopioides*; antibacterial activity; antibiofilms; *Pseudomonas aeruginosa*

Citation: Contreras Martínez, O.I.; Angulo Ortíz, A.; Santafé Patiño, G. Antibacterial Screening of Isoespintanol, an Aromatic Monoterpene Isolated from *Oxandra xylopioides* Diels. *Molecules* **2022**, *27*, 8004. https://doi.org/10.3390/molecules27228004

Academic Editor: Juraj Majtan

Received: 16 October 2022
Accepted: 16 November 2022
Published: 18 November 2022

1. Introduction

The incidence of health care-acquired infections, or nosocomial infections (NIs), is a challenging problem in medical practice. The high mortality rates and financial costs of these infections represent a serious problem for health services around the world [1–4]. Physicians currently face pathogens with resistance determinants that severely restrict therapeutic options; the genetic plasticity of microbes allows them to adapt to stressors through mutations, the acquisition or exchange of genetic material, and the modulation of gene expression, making them resistant to any antimicrobial used in clinical practice [5–8]. The evolution of hypervirulent strains [9–13], as well as the transmission of and increase in microorganisms with resistance genes, including New Delhi strains [1,14,15] and ESKAPE pathogens (*Enterococcus faecium*, *Staphylococcus aureus*, *Klebsiella pneumoniae*, *Acinetobacter baumannii*, *Pseudomonas aeruginosa* and *Enterobacter* spp.), increase the burden of disease and mortality rates due to treatment failure, representing a global threat to human health [16,17]. According to the World Health Organization (WHO), the global burden of NIs ranges between 7% and 12% [4]. In the United States, these infections are an important factor in patient morbidity, constituting the sixth leading cause of death, surpassing deaths from AIDS, cancer and traffic accidents [18]; Each year, it is estimated that more than 2 million infections are caused by antimicrobial-resistant pathogens, with 29,000 deaths [16]. The European Center for Disease Control and Prevention reported that more than 81,000 patients suffer from NIs daily, while these infections cause approximately

150,000 deaths per year [19]. In 2017, a study of the global burden of disease estimated there to be 48.9 million cases of sepsis worldwide, causing 11 million deaths that same year. The highest burden of sepsis was seen in low- and middle-income countries and accounted for 85% of all sepsis-related deaths worldwide; sepsis cases in India alone were estimated at 11.3 million, with 2.9 million deaths, which is equivalent to 297.7 per 100,000 population [20]. ESKAPE pathogens are responsible for the main cases of NIs worldwide; therefore, the WHO has placed them on the list of bacteria against which the development of new antibiotics is vital [21].

Gram-negative bacteria represent the main driver of NIs; some of these bacteria are naturally resistant to certain families of antibiotics, while others, when subjected to prolonged use, eventually develop resistance, worsening the prognosis of patients [22]. People who are immunocompromised or who are undergoing invasive medical treatment are more vulnerable to infections by this type of pathogen. This growing threat to human health stimulates our interest in the search for new compounds with antimicrobial potential, which are effective and safe for the host and can lead to innovative strategies and allow the development of new options and/or antimicrobial therapies for their control.

In this scenario, natural products and their structural analogs have historically made significant contribution to pharmacotherapy, especially in infectious diseases and cancer [23], moving around USD 20 billion in the global pharmaceutical market each year [24,25]. As a source of specialized metabolites with recognized medicinal properties, compounds of plant origin represent an excellent alternative [26]. They can be directly used as bioactive compounds, drug prototypes and/or as pharmacological tools for different targets [27]. The clinical relevance of monoterpenes has been extensively studied; its wide spectrum of biological and therapeutic activity [28–31], especially the antimicrobial potential of thymol, linalool, citral and carvacrol has been demonstrated [32–42]. Various studies have related the antimicrobial activity of monoterpenes with their chemical structure, indicating that their lipophilicity facilitates the penetration of pathogens into the cell membrane [38], and their broad spectrum of action has been attributed to the hydroxyl substituent present in their structure [43,44].

ISO (2-isopropyl-3,6-dimethoxy-5-methylphenol), a monoterpene first obtained from the aerial parts of *Eupatorium saltense* (Asteraceae) [45], whose synthesis has also been carried out [46], has also been extracted from leaves of *Oxandra xylopioides* (Annonaceae). This compound has been shown to have important biological activities that include: antioxidant [47], anti-inflammatory [48], and antispasmodic [49] effects; vasodilator properties [50]; cryoprotectant effects in canine semen [51]; insecticide activities [52]; and antifungal effects against phytopathogens [53] and human pathogenic yeasts [54,55]. However, despite its significant biological activity, antibacterial potential against human pathogens has not been reported. Therefore, we hypothesize that ISO could have activity against human pathogenic bacteria that cause NIs. This study aimed to evaluate the antibacterial activity of ISO extracted from the leaves of *O. xylopioides*, via a screening of 90 bacterial clinical isolates that included 14 different species, as well as estimating their ability to eradicate mature biofilms of *P. aeruginosa*. The results of this study contribute to the knowledge of the biological potential of this natural compound and further research of novel plant compounds that can be used as adjuvants in the control and treatment of these pathogens.

2. Results

2.1. Obtaining and Identification of Isoespintanol

ISO was obtained as a crystalline amorphous solid from the petroleum benzine extract of *O. xylopioides* leaves, and its structural identification was performed by GC-MS, ^{1}H-NMR, ^{13}C-NMR, DEPT, COSY ^{1}H-^{1}H, HMQC and HMBC. Information related to obtaining and identifying the ISO was reported in our previous study (Supplementary Materials) [54].

2.2. Antibacterial Susceptibility Testing

ISO showed antibacterial activity against the clinical isolates tested in this study. We observed an inhibition of the growth of bacteria treated with the ISO in comparison with the untreated isolates used as control. Table 1 shows the percentages of inhibition of bacterial growth in the presence of the different concentrations of ISO and commercial antibiotics (ATBs) used as positive controls. The inhibitory effect observed in the clinical isolates was shown to be dependent on ISO concentration; at a higher ISO concentration, we observed a higher percentage of growth inhibition in all clinical isolates. We emphasize that the effect of ISO was different for all isolates, even those belonging of the same species.

Table 1. Percentages of growth inhibition of clinical isolates at different ISO concentrations.

Isolates	ISO Concentrations (μg/mL)							
	19.5	**39.1**	**78.1**	**156.2**	**312.5**	**625**	**1000**	**ATBs**
E. coli								
A017 *	4.5 ± 1.3	14.6 ± 0.8	24.9 ± 3.0	49.5 ± 9.8	82.0 ± 8.6	90.2 ± 5.9	98.1 ± 0.9	96.0 ± 3.5
A018 *	1.4 ± 0.9	13.8 ± 1.6	17.0 ± 7.4	47.3 ± 5.1	60.1 ± 1.3	80.2 ± 5.5	98.3 ± 1.8	92.0 ± 2.6
A019 *	1.4 ± 2.0	13.8 ± 4.0	17.0 ± 4.0	47.3 ± 6.2	60.1 ± 8.4	80.2 ± 3.1	98.3 ± 0.9	92.0 ± 2.3
A020 *	6.4 ± 1.3	14.5 ± 1.2	25.5 ± 3.2	32.8 ± 4.5	48.0 ± 3.3	80.8 ± 4.2	97.5 ± 1.9	98.6 ± 3.0
A021 *	2.9 ± 1.6	7.2 ± 2.4	17.5 ± 2.5	36.3 ± 4.1	45.6 ± 5.2	75.8 ± 7.7	96.7 ± 2.3	98.7 ± 1.9
A022	6.4 ± 1.7	14.4 ± 7.1	21.6 ± 3.2	39.2 ± 2.0	66.3 ± 9.5	79.1 ± 2.3	95.5 ± 3.6	97.7 ± 1.9
A023	5.3 ± 2.3	19.7 ± 1.8	28.7 ± 3.9	33.4 ± 8.0	60.5 ± 3.5	73.7 ± 2.1	96.3 ± 3.3	95.9 ± 1.1
A031	6.4 ± 2.4	15.8 ± 4.3	37.5 ± 3.1	48.7 ± 4.1	74.8 ± 1.7	83.6 ± 3.7	95.2 ± 2.0	95.5 ± 0.5
A035	6.3 ± 2.8	16.6 ± 5.2	32.1 ± 4.5	47.7 ± 2.2	72.7 ± 3.9	87.3 ± 3.8	99.6 ± 0.3	98.9 ± 1.2
A036	2.7 ± 1.8	17.5 ± 4.8	27.7 ± 7.0	38.7 ± 6.0	56.7 ± 8.2	77.2 ± 6.5	99.7 ± 0.3	99.5 ± 0.6
A037 *	2.8 ± 0.2	18.5 ± 3.6	39.8 ± 3.1	48.9 ± 2.9	64.3 ± 1.2	79.7 ± 3.6	99.1 ± 4.5	96.4 ± 2.0
A038	2.5 ± 0.8	16.7 ± 4.1	35.2 ± 4.1	48.9 ± 3.8	67.0 ± 5.1	80.1 ± 1.8	96.7 ± 3.3	97.0 ± 1.1
A007	1.1 ± 1.3	10.7 ± 3.6	19.6 ± 6.6	32.3 ± 8.9	55.0 ± 5.1	84.6 ± 3.1	98.1 ± 0.5	97.8 ± 1.7
A006 *	2.7 ± 1.7	10.4 ± 2.1	15.9 ± 5.8	29.5 ± 3.7	44.8 ± 1.6	76.0 ± 4.3	91.9 ± 6.0	96.7 ± 2.0
A009	6.9 ± 1.2	16.3 ± 6.9	32.3 ± 8.7	46.2 ± 1.3	68.9 ± 4.8	82.7 ± 3.2	97.8 ± 1.5	94.8 ± 2.3
A016	3.5 ± 1.2	15.9 ± 2.4	35.2 ± 8.6	49.8 ± 4.8	63.5 ± 3.0	79.1 ± 4.6	99.1 ± 0.9	98.1 ± 1.0
A087	5.7 ± 3.4	15.1 ± 2.3	33.5 ± 4.3	49.9 ± 4.4	69.5 ± 3.4	82.9 ± 7.0	99.2 ± 0.5	98.8 ± 0.7
A091 *	7.0 ± 2.2	16.6 ± 6.5	30.6 ± 6.5	49.6 ± 2.8	69.9 ± 6.7	80.9 ± 2.9	97.5 ± 2.1	98.7 ± 1.6
A093	5.4 ± 2.7	16.1 ± 1.5	25.4 ± 1.7	43.2 ± 5.1	79.1 ± 5.7	86.9 ± 1.5	93.8 ± 3.3	94.1 ± 3.8
A094 *	3.8 ± 1.3	14.2 ± 0.7	24.5 ± 1.9	37.3 ± 6.2	77.6 ± 4.3	88.9 ± 8.3	96.2 ± 2.6	98.2 ± 2.1
A099	1.2 ± 0.5	22.2 ± 6.0	39.9 ± 4.8	46.0 ± 1.4	77.6 ± 1.0	85.2 ± 2.9	98.8 ± 1.8	98.3 ± 1.3
A0101	2.2 ± 0.1	15.9 ± 3.5	28.1 ± 1.7	49.9 ± 5.8	75.0 ± 3.8	89.8 ± 2.1	98.0 ± 2.2	98.8 ± 1.3
A0103 *	1.0 ± 0.5	16.1 ± 0.5	39.2 ± 1.9	47.4 ± 2.6	68.5 ± 1.8	85.9 ± 5.7	97.3 ± 2.5	98.9 ± 2.6
A0106 *	3.3 ± 1.4	14.8 ± 2.5	37.3 ± 3.4	49.0 ± 2.8	76.0 ± 2.1	86.7 ± 2.3	98.9 ± 2.5	98.9 ± 1.3
A024	3.6 ± 1.5	19.3 ± 4.5	28.9 ± 2.5	42.9 ± 3.9	63.7 ± 5.3	81.4 ± 3.7	97.3 ± 2.4	99.9 ± 1.7
A025 *	1.6 ± 1.1	13.4 ± 7.7	20.5 ± 4.2	30.3 ± 4.4	60.2 ± 4.5	88.2 ± 1.8	98.1 ± 1.1	98.1 ± 1.1
A026	5.3 ± 1.7	16.3 ± 2.5	29.6 ± 4.0	49.6 ± 5.0	68.9 ± 4.5	75.3 ± 1.1	97.1 ± 1.8	97.2 ± 1.5
A027 *	4.8 ± 1.0	19.2 ± 0.8	34.4 ± 1.9	48.8 ± 3.1	76.0 ± 3.9	83.5 ± 2.5	99.2 ± 0.7	99.8 ± 0.5
A028	4.7 ± 0.9	16.7 ± 1.7	33.7 ± 7.4	47.1 ± 3.2	68.0 ± 2.1	83.2 ± 3.8	97.7 ± 1.2	99.4 ± 0.4
A029 *	5.8 ± 1.4	11.6 ± 3.3	33.7 ± 4.5	47.7 ± 3.8	71.5 ± 2.8	84.1 ± 4.4	99.3 ± 0.2	99.2 ± 0.5
A030	0.6 ± 0.5	17.7 ± 1.5	28.5 ± 0.9	47.6 ± 1.9	69.8 ± 2.5	81.1 ± 4.0	98.7 ± 1.6	98.7 ± 1.0
A032 *	12.0 ± 2.4	24.1 ± 3.2	37.7 ± 2.6	49.5 ± 4.4	64.7 ± 4.5	84.6 ± 4.5	99.0 ± 1.2	99.1 ± 2.5
A033 *	4.6 ± 1.1	19.9 ± 5.5	30.9 ± 1.5	49.9 ± 5.5	60.0 ± 3.7	78.2 ± 2.2	96.7 ± 2.6	99.6 ± 3.3
A034	7.3 ± 1.1	15.4 ± 2.1	21.4 ± 5.7	37.3 ± 1.1	55.4 ± 3.4	80.1 ± 3.1	98.5 ± 1.7	97.8 ± 2.1
A005	6.1 ± 0.9	16.4 ± 0.8	25.5 ± 2.0	46.1 ± 0.9	59.7 ± 3.9	81.1 ± 1.7	95.7 ± 1.3	98.1 ± 2.1
A011	8.4 ± 1.5	16.2 ± 1.4	16.9 ± 2.0	28.3 ± 0.5	47.9 ± 0.9	82.9 ± 4.0	97.6 ± 1.1	98.5 ± 2.1
A013	17.2 ± 0.5	29.5 ± 2.2	38.9 ± 3.6	50.0 ± 6.9	68.7 ± 5.0	82.8 ± 4.7	97.9 ± 2.5	98.9 ± 1.3
A014	20.7 ± 4.3	30.1 ± 2.0	35.0 ± 6.8	49.7 ± 1.2	65.1 ± 2.7	79.6 ± 2.5	98.1 ± 3.8	98.7 ± 1.1

Table 1. *Cont.*

Isolates	ISO Concentrations (μg/mL)							
	19.5	**39.1**	**78.1**	**156.2**	**312.5**	**625**	**1000**	**ATBs**
P. aeruginosa								
A012	7.9 ± 2.5	11.5 ± 0.8	16.6 ± 4.7	27.2 ± 2.2	38.9 ± 5.2	70.0 ± 8.6	93.0 ± 6.3	99.4 ± 0.4
A015	16.9 ± 4.9	21.0 ± 6.7	37.9 ± 10.7	58.8 ± 4.7	69.2 ± 4.9	88.1 ± 4.2	96.3 ± 2.6	98.9 ± 0.7
A050	13.3 ± 4.5	26.4 ± 2.3	33.5 ± 8.6	47.8 ± 1.9	54.1 ± 1.6	78.1 ± 6.0	98.3 ± 2.0	97.7 ± 2.7
A051	27.4 ± 5.2	40.8 ± 5.4	50.8 ± 3.7	67.7 ± 4.9	79.8 ± 1.4	87.4 ± 1.6	98.1 ± 3.0	96.8 ± 1.1
A052	11.9 ± 5.5	25.3 ± 2.7	33.8 ± 3.3	46.3 ± 5.0	75.3 ± 7.1	83.6 ± 5.6	98.2 ± 2.0	99.3 ± 1.4
A053	8.9 ± 2.9	23.9 ± 5.7	35.7 ± 5.2	47.5 ± 5.7	74.7 ± 1.3	86.2 ± 6.9	99.4 ± 1.0	98.5 ± 3.2
A054	18.4 ± 3.3	24.2 ± 3.3	36.7 ± 0.8	50.3 ± 6.0	60.4 ± 3.2	81.0 ± 2.9	99.2 ± 0.3	100.2 ± 1.4
A055	14.3 ± 4.1	29.4 ± 1.2	37.1 ± 6.0	54.4 ± 1.0	75.7 ± 2.5	85.0 ± 2.6	99.3 ± 2.7	98.6 ± 3.2
A056	22.4 ± 1.4	33.7 ± 6.7	42.0 ± 8.3	56.2 ± 8.2	76.4 ± 3.5	86.9 ± 3.6	99.2 ± 5.1	99.9 ± 0.6
A057	9.3 ± 1.6	19.5 ± 1.0	27.4 ± 3.0	42.0 ± 1.3	64.6 ± 3.6	83.9 ± 4.2	99.6 ± 1.2	94.3 ± 0.7
A058	13.5 ± 2.8	30.7 ± 3.4	42.6 ± 5.9	53.1 ± 2.1	68.8 ± 2.9	85.7 ± 4.6	98.2 ± 1.5	96.2 ± 2.1
A097	7.9 ± 4.8	17.3 ± 3.1	28.8 ± 0.9	50.1 ± 0.7	69.7 ± 1.6	87.5 ± 1.7	96.9 ± 4.0	95.1 ± 0.9
P. mirabilis								
A059	23.7 ± 4.4	32.0 ± 1.1	42.8 ± 1.1	49.3 ± 7.7	75.9 ± 4.1	88.0 ± 5.0	99.6 ± 2.1	98.1 ± 2.7
A060	21.1 ± 2.5	30.1 ± 2.6	40.9 ± 5.7	50.4 ± 2.0	75.1 ± 3.6	85.0 ± 2.7	99.7 ± 1.3	99.3 ± 1.5
A061	20.0 ± 1.9	32.0 ± 3.4	38.3 ± 1.7	51.7 ± 1.2	82.8 ± 5.8	95.4 ± 1.6	98.7 ± 3.2	95.5 ± 3.7
A062	19.1 ± 4.2	29.7 ± 2.6	35.7 ± 3.8	41.5 ± 3.3	73.7 ± 2.5	82.9 ± 2.4	99.7 ± 0.3	94.8 ± 2.2
A063	18.3 ± 0.9	26.7 ± 2.1	36.2 ± 1.5	49.8 ± 1.7	65.1 ± 1.8	81.0 ± 4.9	99.0 ± 3.9	100.0 ± 2.9
A064	16.2 ± 2.8	30.1 ± 2.8	38.8 ± 2.6	49.3 ± 5.4	63.5 ± 4.5	79.3 ± 3.7	93.6 ± 10.0	99.4 ± 1.0
A090	18.7 ± 1.7	33.3 ± 3.9	44.6 ± 1.2	48.6 ± 2.6	61.5 ± 5.6	86.9 ± 7.5	99.7 ± 1.7	100.1 ± 1.7
S. epidermidis								
A065	18.5 ± 0.7	33.3 ± 2.5	43.1 ± 3.7	63.4 ± 3.3	85.4 ± 2.0	91.4 ± 4.2	99.9 ± 0.3	99.7 ± 1.4
A066	18.7 ± 1.2	30.4 ± 1.9	41.3 ± 1.7	46.2 ± 1.8	73.6 ± 2.2	89.6 ± 3.4	97.0 ± 0.5	98.4 ± 0.4
A067	16.0 ± 2.0	27.2 ± 5.3	38.4 ± 5.8	59.9 ± 1.4	71.8 ± 2.2	84.7 ± 6.7	95.0 ± 2.4	96.8 ± 1.6
A. baumannii								
A001	5.0 ± 2.0	14.0 ± 0.6	26.5 ± 1.7	38.6 ± 3.0	55.0 ± 1.9	75.2 ± 0.7	91.4 ± 0.6	98.5 ± 1.0
A070	13.2 ± 2.2	29.5 ± 3.6	35.4 ± 1.2	48.4 ± 1.8	65.5 ± 5.7	89.2 ± 4.2	95.7 ± 1.8	94.8 ± 1.2
A089	17.8 ± 1.5	27.9 ± 2.5	35.9 ± 0.8	46.6 ± 2.5	63.5 ± 2.1	81.1 ± 7.0	98.4 ± 2.5	96.8 ± 2.8
K. pneumoniae								
A008	25.7 ± 6.0	38.7 ± 2.1	43.1 ± 1.8	51.7 ± 1.2	67.3 ± 1.7	72.8 ± 3.0	96.9 ± 1.0	99.0 ± 1.6
A039	24.3 ± 2.6	31.4 ± 4.8	43.3 ± 4.5	55.3 ± 5.6	68.8 ± 2.7	79.7 ± 6.3	93.9 ± 3.6	99.9 ± 0.5
A040	17.2 ± 3.1	26.4 ± 1.9	34.1 ± 5.8	42.8 ± 7.1	73.4 ± 3.9	80.0 ± 0.8	90.3 ± 4.8	100.5 ± 1.5
A041	16.9 ± 2.4	24.1 ± 8.4	39.6 ± 5.5	48.8 ± 2.3	78.2 ± 1.6	89.2 ± 4.4	99.7 ± 2.5	97.8 ± 4.2
A042	18.7 ± 0.8	27.3 ± 5.7	33.3 ± 4.6	47.6 ± 6.5	80.5 ± 2.7	87.2 ± 3.4	91.0 ± 1.9	97.4 ± 3.2
A043+	10.8 ± 3.7	21.4 ± 2.8	36.3 ± 4.2	49.6 ± 7.9	79.8 ± 2.8	82.8 ± 4.5	98.9 ± 4.3	95.8 ± 0.7
A044	16.9 ± 1.6	27.6 ± 8.3	41.7 ± 2.7	48.9 ± 1.3	74.1 ± 2.6	85.8 ± 3.0	98.2 ± 3.2	97.6 ± 4.4
A045	16.2 ± 1.2	20.1 ± 2.6	34.0 ± 3.4	55.1 ± 7.7	69.4 ± 6.7	85.3 ± 6.7	99.4 ± 1.2	97.1 ± 0.6
A046	13.7 ± 2.3	16.7 ± 1.5	28.6 ± 5.8	45.3 ± 7.1	72.7 ± 5.8	89.6 ± 3.2	97.6 ± 7.5	99.9 ± 1.1
A047	24.1 ± 3.6	26.6 ± 4.4	38.2 ± 0.7	50.5 ± 0.9	67.8 ± 8.3	74.3 ± 3.9	90.7 ± 3.0	99.3 ± 2.2
A048	19.9 ± 4.8	30.1 ± 1.6	40.0 ± 1.3	47.7 ± 5.5	66.3 ± 10.8	79.7 ± 2.0	92.1 ± 1.8	99.2 ± 0.7
A049	17.5 ± 3.5	28.1 ± 4.8	35.3 ± 3.8	46.7 ± 3.3	74.5 ± 3.9	89.0 ± 5.4	91.6 ± 4.9	99.1 ± 0.8
A0104+	12.4 ± 3.1	26.5 ± 1.4	33.4 ± 6.0	49.8 ± 5.1	68.1 ± 4.4	81.4 ± 2.5	98.6 ± 2.9	100.3 ± 1.7
S. aureus								
A004	17.6 ± 4.9	25.8 ± 1.7	40.7 ± 0.8	48.8 ± 2.5	67.3 ± 6.9	77.9 ± 4.5	98.9 ± 2.0	99.3 ± 2.1
A010	21.2 ± 0.2	29.3 ± 3.1	41.4 ± 8.5	58.8 ± 3.5	69.4 ± 3.2	84.2 ± 1.9	98.6 ± 1.2	94.4 ± 7.0
A072	22.7 ± 1.2	32.7 ± 1.0	42.6 ± 3.2	49.2 ± 1.9	71.7 ± 2.4	88.6 ± 6.6	99.1 ± 1.4	99.5 ± 2.2
A073	13.8 ± 1.4	28.0 ± 0.1	35.8 ± 5.1	49.8 ± 2.6	68.1 ± 5.5	75.2 ± 4.5	93.2 ± 3.0	98.8 ± 1.1
A0100	20.5 ± 1.2	30.8 ± 3.1	40.1 ± 2.5	48.4 ± 2.7	77.7 ± 0.7	87.1 ± 2.6	99.6 ± 5.1	98.5 ± 1.3
E. faecium								
A0105	20.6 ± 6.3	32.2 ± 4.0	41.7 ± 5.7	56.8 ± 2.3	75.8 ± 1.1	85.9 ± 1.2	98.7 ± 2.5	99.4 ± 1.1

Table 1. *Cont.*

Isolates	ISO Concentrations (μg/mL)							
	19.5	**39.1**	**78.1**	**156.2**	**312.5**	**625**	**1000**	**ATBs**
E. faecalis								
A069	18.5 ± 1.7	31.8 ± 3.4	42.1 ± 3.5	50.2 ± 0.6	72.8 ± 2.4	84.0 ± 6.5	98.6 ± 2.3	99.2 ± 1.2
C. koseri								
A068	17.1 ± 1.3	29.6 ± 0.7	36.9 ± 3.6	47.2 ± 1.2	73.8 ± 3.0	89.8 ± 1.1	97.4 ± 1.8	99.4 ± 1.0
A079	17.2 ± 5.9	25.1 ± 2.0	36.2 ± 3.9	46.1 ± 0.8	54.9 ± 1.1	88.3 ± 4.8	99.4 ± 0.2	99.9 ± 0.7
S. marcescens								
A071	17.1 ± 0.6	27.1 ± 2.7	35.8 ± 1.7	47.1 ± 3.1	58.1 ± 2.3	71.5 ± 2.8	99.3 ± 0.5	95.6 ± 2.8
A. hydrophila								
A088	17.8 ± 0.8	31.1 ± 0.6	36.6 ± 0.5	49.6 ± 6.0	74.6 ± 1.7	84.9 ± 4.2	99.1 ± 1.4	98.5 ± 2.4
S. maltophilia								
A0102	17.1 ± 1.3	25.9 ± 2.5	40.9 ± 3.7	46.5 ± 2.3	67.0 ± 3.6	87.4 ± 4.7	98.7 ± 2.7	99.8 ± 0.5
A095	14.4 ± 1.0	29.2 ± 1.3	35.7 ± 1.5	52.5 ± 2.5	73.4 ± 1.7	86.7 ± 1.6	98.4 ± 3.6	98.4 ± 2.2
P. rettgeri								
A096	14.5 ± 1.9	24.1 ± 1.8	36.9 ± 3.4	52.1 ± 3.4	74.3 ± 2.6	84.0 ± 2.6	96.6 ± 1.9	99.3 ± 1.0

* BLEE (extended spectrum beta-lactamases); + multi-resistant; ATBs: (AMK 20 μg/mL: A006, A017, A018, A019, A020, A021, A025, A027, A029, A032, A033, A037, A091, A094, A0103, A0106), (GEN 8 μg/mL: A009, A016, A0104), (VAN 2 μg/mL: A065, A066, A067), (MEM 1 μg/mL: A043), (SAM 2 μg/mL: A089), (SXT 20 μg/mL: A095, A0102), (CIP 6 μg/mL was used for the rest of the isolates).

Table 2 shows the MIC_{90} and MIC_{50} values of ISO against the evaluated clinical isolates. The greatest effect was observed in isolate A065 of *S. epidermidis*, with MIC_{90} and MIC_{50} values of 694.3 and 154.2 μg/mL, respectively. The smallest effect was observed in *P. aeruginosa* isolate A012, with MIC_{90} and MIC_{50} values of 916.5 and 457.3 μg/mL, respectively.

Figure 1 shows the trend of the data and regression line with 95% confidence. A reduction in the percentage of growth inhibition of bacterial isolates exposed to ISO (MIC of each isolate) is observed, highlighting a strong positive correlation between the concentration of ISO and the percentage of growth inhibition, with Pearson correlation coefficients between 0.86 and 0.96 in most isolates. The hypothesis test on the correlation coefficient yields a *p*-value of <0.05, which indicates a significant linear relationship with 95% confidence. For the isolates of *P. aeruginosa* and *E. coli*, the Spearman test [Rho] (0.96 and 0.97, respectively) was used, which also shows a strong positive relationship between the ISO concentration and the growth reduction of these isolates.

Figure 2 shows the directly proportional relationship between the ISO concentration (μg/mL) and bacterial growth inhibition of each group of clinical isolates.

2.3. Biofilm Reduction

All *P. aeruginosa* isolates used in this study were moderate biofilm producers with OD_{590} between 1.52 and 2.79, unlike isolate A050, which was a strong biofilm producer with OD_{590} > 3.0, as shown in Figure 3A. Figure 3B shows the production of *P. aeruginosa* biofilms in the presence of ISO, CIP, and without treatment (INO), evidencing a lower biomass of biofilms when exposed to ISO and CIP compared to cells without treatment. Figure 3C shows the percentage of biofilm eradication of ISO and CIP, highlighting a significantly greater effect of ISO compared to CIP. In the biofilms treated with ISO, a biomass eradication of between 6.6 and 77.4% was obtained after 1 h of exposure. The biomass eradication of biofilms in cells treated with CIP was lower (between 4.3 and 67.5%). It should be noted that isolate A050, which presented a strong biofilm biomass production, was one of the isolates with the highest biofilm eradication (68.2%) by ISO.

Table 2. MIC_{90} and MIC_{50} values of ISO against bacterial clinical isolates.

Isolates	Isoespintanol μg/mL		Isolates	Isoespintanol μg/mL	
	MIC_{90}	MIC_{50}		MIC_{90}	MIC_{50}
E. coli			*P. aeruginosa*		
A017 *	731.6	296.8	A012	916.5	457.3
A018 *	798.8	367.4	A015	765.3	247.4
A019 *	783.2	358.3	A050	826.2	315.4
A020 *	828.7	387.9	A051	727.3	83.56
A021 *	849.4	422	A052	767.9	275.2
A022	816.2	362.4	A053	749.7	273.4
A023	846.8	372.9	A054	796.7	280.6
A031	782.5	297.3	A055	749.4	235.1
A035	747.5	298.5	A056	740.7	185.8
A036	811.9	365.6	A057	776.8	324
A037 *	788.9	312.9	A058	766.7	237.7
A038	798.2	322.9	A097	766.3	304.4
A007	798.3	389.2	*P. mirabilis*		
A006 *	884.9	442.8	A059	739.4	199.6
A009	781.2	316	A060	751.3	218.3
A016	791.5	324.4	A061	702.9	192.3
A087	768.6	308.6	A062	769.4	259.2
A091 *	786.6	314.6	A063	791.1	269.5
A093	775.8	318.3	A064	843.3	275.7
A094 *	760	329.6	A090	769.5	235.6
A099	750.6	283.4	*S. epidermidis*		
A0101	742.5	304	A065	694.3	154.2
A0103 *	770.4	309.3	A066	756.1	230.1
A0106 *	745.7	292.3	A067	783.9	233.7
A024	799.4	339.4	*A. baumannii*		
A025 *	781.1	373	A001	878.7	394.6
A026	811.6	331.6	A070	778.9	269
A027 *	756.6	291.7	A089	799.6	278.6
A028	780.3	316	*K. pneumoniae*		
A029 *	761.1	312.1	A008	852.2	212.5
A030	777.6	327.5	A039	831.4	215.1
A032 *	774.7	280.1	A040	849.1	289.6
A033 *	818.4	335.1	A041	730.3	235.9
A034	812.7	372.7	A042	795.2	248.5
A005	815.1	350.2	A043+	755.6	266.3
A011	824.3	397.2	A044	760.1	237.5
A013	784.6	251.3	A045	757.9	266.2
A014	805.9	263.2	A046	754.4	294.9
S. aureus			A047	891.1	268.8
A004	800.6	266.6	A048	852.3	263.7
A010	767	213.6	A049	794.5	254.8
A072	748.4	209.2	A0104+	784.6	281.9
A073	853.7	289.8	*E. faecium*		
A0100	740.7	216.8	A0105	748.1	196.5
C. koseri			*E. faecalis*		
A068	752.3	241.8	A069	767.1	225.1
A079	778	287.9	*S. maltophilia*		
S. marcescens			A0102	764.7	257.8
A071	843.9	306.7	A095	754.5	244.8
A. hydrophila			*P. rettgeri*		
A088	757.9	236.8	A096	774.6	258

* BLEE (extended spectrum beta-lactamases); + multi-resistant.

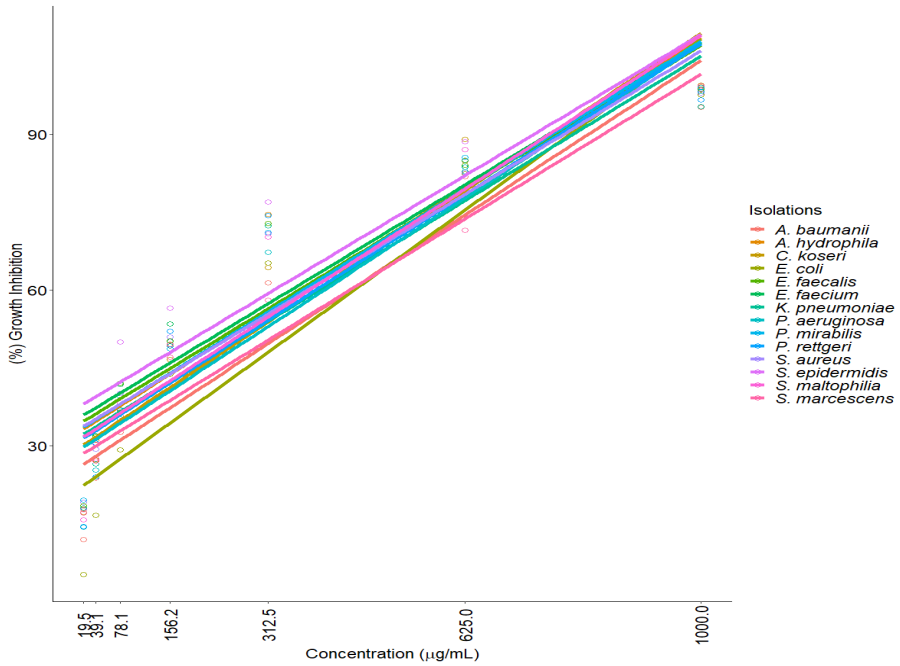

Figure 1. Strong positive correlation between the concentration of ISO and the percentage of growth inhibition of clinical isolates. We observed that the higher the ISO concentration, the higher the inhibition of microbial growth. The hypothesis test on the correlation coefficient with a p-value < 0.05, indicates that there is a significant linear relationship, with 95% confidence.

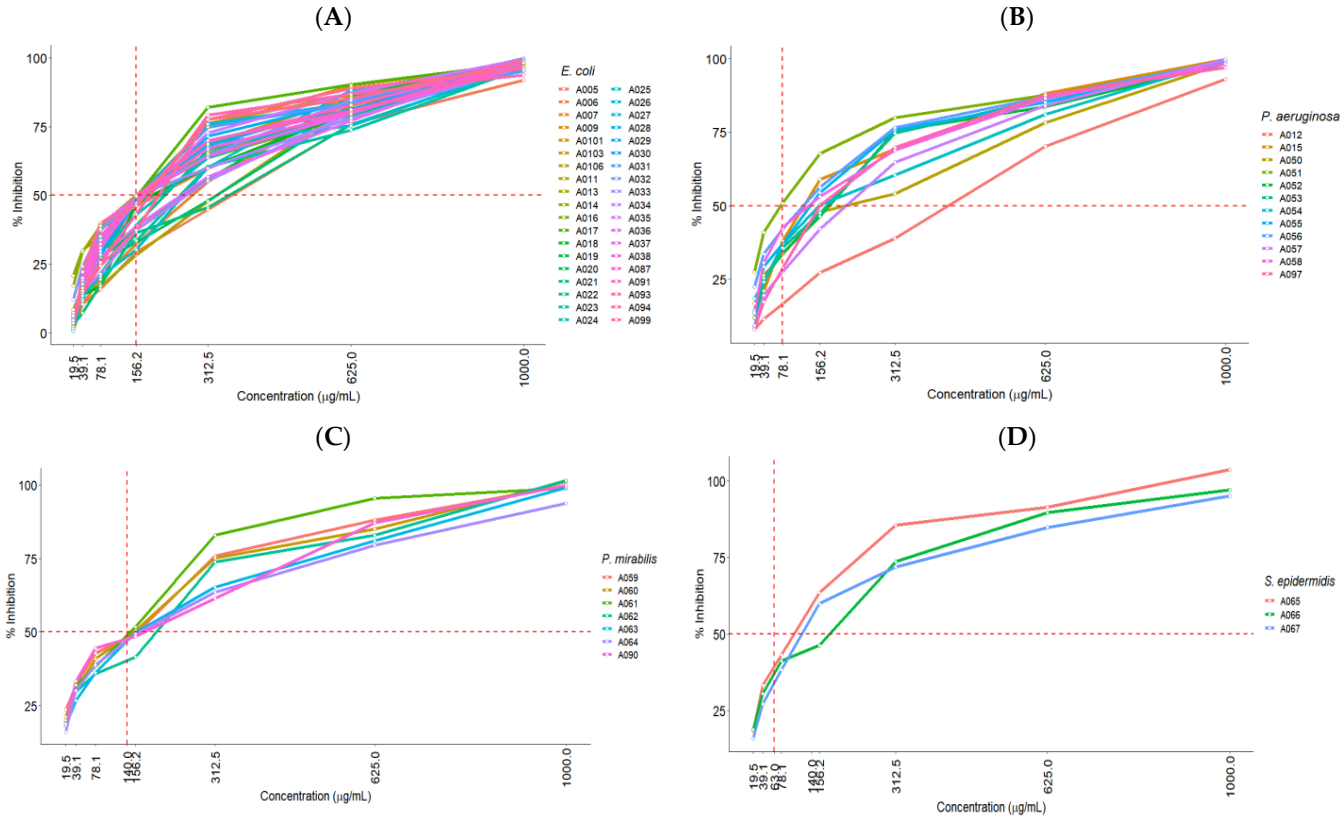

Figure 2. *Cont.*

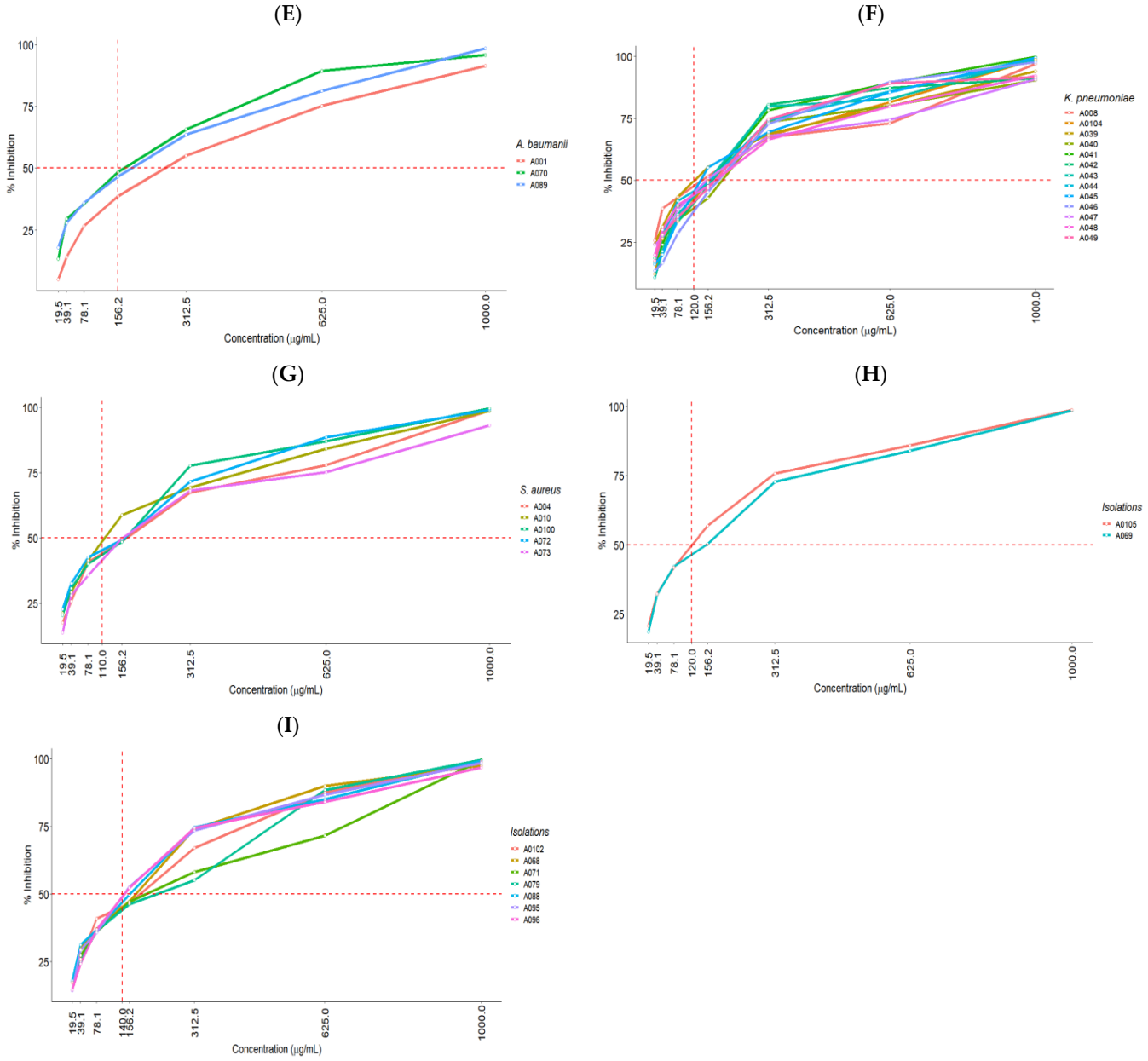

Figure 2. Percentages of growth inhibition showing the MIC_{50} of each group of species of clinical isolates at different ISO concentrations—(**A**): *E. coli*; (**B**): *P. aeruginosa*; (**C**): *P. mirabilis*; (**D**): *S. epidermidis*; (**E**): *A. baumannii*; (**F**): *K. pneumoniae*; (**G**): *S. aureus*; (**H**): *Enterococcus* (*E. faecium*, *E. faecalis*); (**I**): (*C. koseri*, *S. marcescens*, *A. hydrophila*, *S. maltophilia*, *P. rettgeri*).

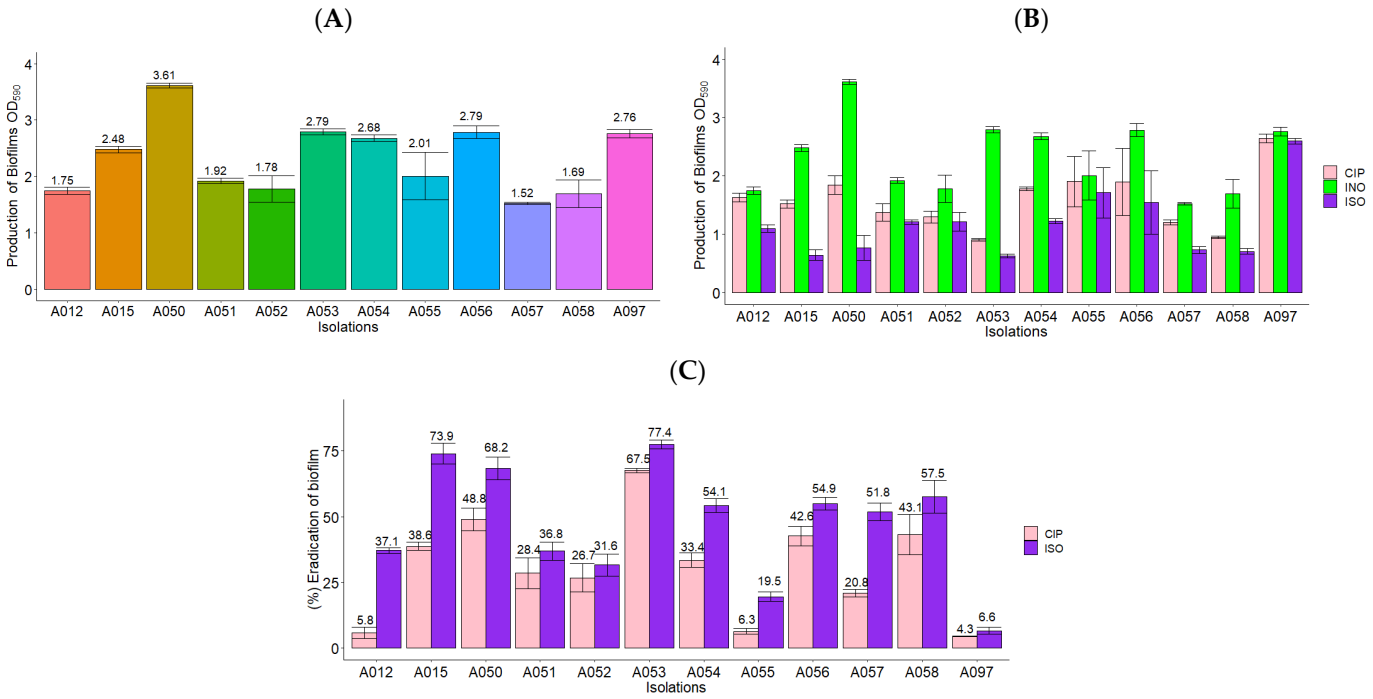

Figure 3. ISO and CIP action on *P. aeruginosa* biofilms. (**A**) Biofilm formation at 37 °C for 24 h.The OD_{590} between 1.1. and 3.0 indicates moderate biofilm production and OD_{590} > 3 indicates strong biomass production in biofilms. (**B**) Biofilm production in the presence of ISO, CIP and without treatment (INO). (**C**) Percentage of biofilm eradication after 1 h of treatment with the MIC of ISO and CIP for each isolate. The results of the ANOVA have a value of $p < 0.05$ and Tukey's test has a confidence level of 95%, indicating that there is a significant difference between the effect of ISO and the effect of CIP on the eradication of biofilms.

3. Discussion

The incidence of NIs represents a serious health problem, increasing rates of morbidity, mortality, and costs for health services around the world. An important factor in the increased mortality of NIs is the increasing prevalence of multiresistant microorganisms that render antibiotics ineffective in the treatment of many common infectious diseases [18]. In this context, Gram-positive [10,12], multiresistant Gram negative [11,12] and hypervirulent [9] bacteria are of great concern. For this reason, the search for alternative and novel compounds that have action against these pathogenic microorganisms is becoming increasingly urgent.

In this study, we evaluated the antibacterial activity of ISO against 90 nosocomial isolates, distributed in 14 species that include multiresistant clinical isolates. In this investigation, we report MIC_{90} values between 694.3 and 916.5 µg/mL and MIC_{50} values between 154.2 and 457.3 µg/mL. These results are in agreement with other studies that report the antimicrobial activity of terpenes against a wide variety of microorganisms [37,42,56,57]. However, our results are the first to reveal the antibacterial potential of the natural monoterpene ISO against human pathogenic bacteria. The hydrophobic character of the structure in the cell membranes of microorganisms makes them important targets for the action of monoterpenes; the correlation between the chemical structure of these metabolites and their antimicrobial activity has been described [38,44]. The antibacterial activity of monoterpenes with a chemical structure similar to ISO has been investigated. The treatment of Gram-negative and Gram-positive bacteria with phenolic terpenoids, such as carvacrol and thymol, indicates damage to the integrity of the cell membrane and leakage of intracellular material, highlighting the importance of hydrophobicity and the presence of a phenolic hydroxyl group, disrupting membrane integrity and establishment of its antibacterial activity [28,58]. Similarly, the antifungal activity of these terpenes against pathogenic yeasts has

been reported, indicating that their lipophilicity allows interaction with the fungal cell wall, facilitating their penetration into the cell membrane [38]. The monoterpene linalool has also been reported to have antimicrobial activity due to its action in membrane potential, suggesting membrane depolarization, the irregular activity of cell metabolism and damage to the respiratory chain, ultimately leading to cell death [37]. The antifungal action of ISO against pathogenic yeasts of the genus *Candida* was recently described, reporting damage to the cell membrane and the induction of intracellular reactive oxygen species, causing the death of the yeast [54,55]. On the other hand, it has also been reported that bacteria in the presence of compounds with structures similar to ISO, such as thymol, limonene, carvacrol, cinnamaldehyde and eugenol, can modulate the ratio of membrane fatty acids, from saturated to unsaturated; an increase in unsaturated membrane fatty acids and increased fluidity has been reported in the presence of these metabolites, which may affect transport or enzymatic processes at the membrane level; this could be related to the antibacterial action mechanisms of these compounds [59]. All of this indicates that the antibacterial action of ISO could also be associated with damage to the integrity of the bacterial cell membrane.

Quorum sensing (QS), is a cell density-based signaling system that aids bacteria-bacteria communication and regulates several virulence factors, including biofilm formation [60]. It is well known that the formation of biofilms is related to the resistance to antimicrobials expressed by pathogenic microorganisms, since they hinder or prevent the penetration of antimicrobials to the site of infection. *Pseudomonas aeruginosa* is known for its ability to form powerful biofilms, which increases its ability to cause a host infection and facilitates the establishment of chronic infections [61–63]. Respiratory infection by *P. aeruginosa* is the main cause of morbidity and mortality in patients with cystic fibrosis; biofilm formation in the respiratory tract is thought to increase persistence and resistance to antibiotics during infection [64]. Taking this into account, we also evaluated the ability of ISO to eradicate mature biofilms in this pathogen. All *P. aeruginosa* isolates in this study were biofilm producers. We highlight the role of ISO in the eradication of mature bacterial biofilms during 1 h of treatment, showing eradication percentages of between 6.6 and 77.4%. These results are consistent with previous studies that report the action of ISO against mature biofilms of pathogenic yeasts [54,55], most likely by the inhibition of important components of the biofilms formed by these bacteria, as described in [28]. Studies carried out with the essential oil (EO) of *Thymbra capitata*, a compound rich in thymol, showed an inhibition in the swarm motility, aggregation capacity and hydrophobic capacity of *P. aeruginosa*, further indicating a reduction in the production of three virulence factors regulated by the QS system, including pyocyanin, rhamnolipids, and LasA protease [65]. Monoterpenes, such as citral and carvacrol, are also reported to have antibiofilm activity against pathogenic bacteria [66]. On the other hand, the analysis of the structure-activity relationship, carried out with hordenine and its analogs against strains of *P. aeruginosa* and *S. marcescens*, indicates that the hydroxyl group in the benzene ring present in the structure of these compounds is related to its inhibitory activity of QS and the consequent formation of biofilms [67]. It should be noted that ISO also has this hydroxyl group on the benzene ring, which could be related to its ability to eradicate mature biofilms in these pathogens. Comparing the efficacy of ISO and CIP in the eradication of these biofilms, we found that ISO had a greater effect (between 6.6 and 77.4%), being greater than the effect of CIP in all cases (between 4.3 and 67.5%).

In addition to damage to cell membrane integrity, other mechanisms of the antibacterial action of monoterpenoids have been proposed, including the inhibition of efflux pumps, prevention of the formation and rupture of preformed biofilms, inhibition of bacterial motility, and inhibition of membrane ATPases. Furthermore, it was discovered that they can act synergistically with conventional antibiotics to overcome the problem of bacterial resistance [68]. For all the above, it is interesting to continue investigating the mechanisms of antibacterial action expressed by the natural monoterpene ISO.

Our results provide new and important knowledge on the antibacterial and antibiofilm potential of monoterpene ISO against bacteria causing NIs. In addition, these results serve as a basis for future research on the exploration of mechanisms of action of ISO against pathogenic bacteria.

4. Materials and Methods

4.1. Reagents

Mueller-Hinton broth (MHB) (Sigma, Mendota Heights, MN, USA) was used for the determination of MIC and cultures of bacterial isolates. Tryptic Soy Agar (TSA) and Tryptic Soy Broth (TSB) (Becton, Dickinson and Company, San Diego, CA, USA), Mueller-Hinton agar (MHA) (Sigma, Mendota Heights, MN, USA), and Brain Heart Infusion (BHI) broth (Sigma-Aldrich, St. Louis, MO, USA) were also used for bacterial cultures. Dimethyl sulfoxide (DMSO), phosphate-buffered saline (PBS), crystal violet (CV) and antibiotics (ATBs): ciprofloxacin (CIP), amikacin (AMK), ampicillin/sulbactam (SAM), gentamicin (GEN), meropenem (MEM), vancomycin (VAN), and trimethoprim/sulfamethoxazole (SXT) used in this study were obtained from Sigma-Aldrich, St. Louis, MO, USA; glacial acetic acid was obtained from Carlo Erba Reagents, Milano, Italy.

4.2. Microorganisms

In this study, 90 clinical isolates were evaluated, distributed in 14 species that included: *Escherichia coli* (38), *Pseudomonas aeruginosa* (12), *Klebsiella pneumoniae* (13), *Acinetobacter baumannii* (3), *Proteus mirabilis* (7), *Staphylococcus epidermidis* (3), *Staphylococcus aureus* (5), *Enterococcus faecium* (1), *Enterococcus faecalis* (1), *Stenotrophomonas maltophilia* (2), *Citrobacter koseri* (2), *Serratia marcescens* (1), *Aeromonas hydrophila* (1) and *Providencia rettgeri* (1). Isolates were cultured from tracheal aspirate samples, blood cultures, bronchoalveolar lavage, tissue secretions, surgical wound secretions, bronchial secretions, sputum, abscesses, and urine cultures from patients hospitalized at the Salud Social S.A.S. from the city of Sincelejo, Sucre, Colombia. All microorganisms were identified by standard systems: Vitek® 2 Compact. Biomerieux SA. (AST-P577, AST-N272, AST-GN93, AST-N271, AST-P612). To maintain the bacterial cultures, BHI broth, TSB, TSA, MHB, MHA and blood agar were used.

4.3. Antibacterial Susceptibility Testing

The minimal inhibitory concentration (MIC) of the ISO against clinical isolates was defined as the lowest concentration at which 90% (MIC_{90}) of bacterial growth was inhibited, compared to the control (untreated cells). The MIC_{50} was defined as the lowest concentration at which 50% of bacterial growth was inhibited. MIC was determined by performing broth microdilution assays, using 96-well microtiter plates (Nunclon Delta, Thermo Fisher Scientific, Waltham, MA, USA), as described in the *Clinical Laboratory Standards Institute* (CLSI) method M07-A9 [69], with minor modifications. Serial dilutions in MHB were made to accurately obtain final concentrations of 19.5, 39.1, 78.1, 156.2, 312.5, 625, and 1000 µg/mL of ISO in each reaction. A stock solution of ISO at 20,000 µg/mL in DMSO was prepared for carrying out the experiments; in addition, stock solutions of the ATBs used as controls were also prepared. The assays were developed at a final volume of 200 µL per well as follows: 100 µL of the bacterial inoculum at a concentration of 10^8 CFU/mL and 100 µL of the adjusted ISO system to reach the previously described concentrations in a final reaction. Wells with bacterial inoculum, either without ISO or with ATBs (CIP 6 µg/mL, AMK 20 µg/mL, SAM 2 µg/mL, GEN 8 µg/mL, MEM 1 µg/mL, VAN 2 µg/mL, SXT 20 µg/mL) were used as growth controls and positive controls, respectively. Wells with culture media without inoculum and without ISO were used as negative controls. For each experiment, the controls were made with different concentrations of ISO in culture medium without inoculum. The plates were incubated at 37 °C for 24 h. The experiments were performed in triplicate. The inhibition of bacterial growth by ISO was determined by changes in optical density using a SYNERGY LX microplate reader (Biotek), at

600 nm, from the start of incubation to the end of incubation (24 h). Finally, the percentage of inhibition of bacterial growth was calculated [70] using the following equation:

$$\%\text{Inhibition} = (1 - (OD_{t24} - OD_{t0}/OD_{gc24} - OD_{gc0})) \times 100$$

where OD_{t24}: optical density of the test well at 24 h post-inoculation; OD_{t0}: optical density of the test well at 0 h post-inoculation; OD_{gc24}: optical density of the growth control well at 24 h post-inoculation; OD_{gc0}: optical density of the growth control well at 0 h post-inoculation.

4.4. Quantitative Assessment of Biofilm Formation

Clinical isolates of *P. aeruginosa* were used as a model to quantify biofilm reduction caused by ISO following the reported methodology [71], with minor modifications. For the formation of biofilms, bacterial colonies of 24 h of incubation in TSA were used, standardizing the bacterial inoculum at 10^8 cell/mL. Then, in 96-well polystyrene microplates, 200 µL of the bacterial inoculum was discharged into each well and incubated at 37 °C for 24 h. Subsequently, the broth was removed from the microplates, and 200 µL of ISO was added to the MIC of each isolation in TSB broth and incubated at 37 °C for 1 h. Then, the floating cells were removed, and the biofilms at the bottom of the wells were washed three times with deionized water. Excess moisture was removed by tapping the microplates on sterile napkins, and the plates were dried for 5 min. Three assays were performed, and each isolate was tested in 6 replicates. Cultures without ISO were used as control, and CIP was used as positive control. Biofilm reductions were quantified by staining wells with 200 µL of 0.1% CV for 20 min. The samples were washed with deionized water until the excess dye was removed; the excess of water was carefully dried, and then the CV was solubilized in 250 µL of 30% glacial acetic acid. Absorbance values were measured at 590 nm (OD_{590}), using a SYNERGY LX microplate reader (Biotek). Biofilm production was grouped into the following categories: OD_{590} < 0.1: non-producers (NP), OD_{590} 0.1–1.0: weak producers (WP), OD_{590} 1.1–3.0: moderate producers (MP) and OD_{590} > 3.0: strong producers (SP). Biofilm reduction was calculated [72] using the following equation:

$$\%\ \text{Biofilm reduction: AbsCO} - \text{AbsISO/AbsCO} \times 100$$

where AbsCO: absorbance of the control sample and AbsISO: absorbance of the sample treated with ISO.

4.5. Statistical Analysis

The data were analyzed using the statistical software R version 4.1.1. (*R Development Core Team*, 2021, Copenhagen, Denmark) and the Excel program. In principle, the Shapiro–Wilk test was used to determine the distribution of data. Subsequently, the Pearson correlation coefficient (for most of the isolates) and Spearman's test (for *P. aeruginosa* and *E. coli*) were used to measure the degree of linear correlation between the ISO concentration and the reduction in bacterial growth. To compare the effects of ISO and CIP on the reduction in the biofilms, Tukey's test was used. All experiments were performed in triplicate.

5. Conclusions

In this study, we investigated the antibacterial effect of ISO against 90 clinical isolates, as well as its role in biofilm eradication in *P. aeruginosa*. Our results show an inhibition of the growth of the bacteria treated with ISO, in comparison with the untreated isolates used as controls. The inhibitory effect was dependent on ISO concentration and different for all isolates. We also highlight a significantly greater effect of ISO compared to CIP in eradicating mature *P. aeruginosa* biofilms. The antibacterial potential of ISO against these pathogens is demonstrated in this study.

Author Contributions: Conceptualization, O.I.C.M.; methodology, O.I.C.M. and A.A.O.; formal analysis, O.I.C.M. and A.A.O.; investigation, O.I.C.M.; resources, A.A.O. and G.S.P.; writing—original draft preparation, O.I.C.M. and A.A.O.; writing—review and editing, O.I.C.M., A.A.O. and G.S.P.; visualization, O.I.C.M.; supervision, O.I.C.M., A.A.O. and G.S.P.; funding acquisition, A.A.O. and G.S.P. All authors have read and agreed to the published version of the manuscript.

Funding: This research was funded with resources from the FCB-02-19 project of the University of Córdoba, Montería, Colombia.

Institutional Review Board Statement: Not applicable.

Informed Consent Statement: Not applicable.

Data Availability Statement: The data presented in this study are available in the article and the supporting information.

Acknowledgments: To the Social Health Clinic IPS S.A.S. Sincelejo, Colombia. Under the coordination of Eimi Brango Tarra and Yuly Paulin Ortíz for donating the clinical isolates used in this study. O.C.M. thanks the scholarship program of the Ministry of Science, Technology and Innovation of Colombia for the granting of the doctoral scholarship.

Conflicts of Interest: The authors declare no conflict of interest.

Sample Availability: The ISO is available from the authors.

References

1. Lemiech-Mirowska, E.; Kiersnowska, Z.; Michalkiewicz, M.; Depta, A.; Marczak, M. Nosocomial infections as one of the most important problems of the healthcare system. *Ann. Agric. Environ. Med.* **2021**, *28*, 361–366. [CrossRef] [PubMed]
2. Tan, X.Y.D.; Wiseman, T.; Betihavas, V. Risk factors for nosocomial infections and/or sepsis in adult burns patients: An integrative review. *Intensive Crit. Care Nurs.* **2022**, *73*, 103292. [CrossRef] [PubMed]
3. Suksatan, W.; Jasim, S.A.; Widjaja, G.; Jalil, A.T.; Chupradit, S.; Ansari, M.J.; Mustafa, Y.F.; Hammoodi, H.A.; Mohammadi, M.J. Assessment effects and risk of nosocomial infection and needle sticks injuries among patents and health care worker. *Toxicol. Rep.* **2022**, *9*, 284–292. [CrossRef] [PubMed]
4. Aman, S.; Mittal, D.; Shriwastav, S.; Tuli, H.S.; Chauhan, S.; Singh, P.; Sharma, S.; Saini, R.V.; Kaur, N.; Saini, A.K. Prevalence of multidrug-resistant strains in device associated nosocomial infection and their in vitro killing by nanocomposites. *Ann. Med. Surg.* **2022**, *78*, 103687. [CrossRef]
5. Khan, A.; Miller, W.R.; Arias, C.A. Mechanisms of antimicrobial resistance among hospital-associated pathogens. *Expert Rev. Anti. Infect. Ther.* **2018**, *16*, 269–287. [CrossRef]
6. Lupo, A.; Haenni, M.; Madec, J.-Y. Antimicrobial resistance in *Acinetobacter* spp. and *Pseudomonas* spp. *Microbiol. Spectr.* **2018**, *6*, S390–S400. [CrossRef]
7. Brooke, J.S. Advances in the microbiology of *Stenotrophomonas maltophilia*. *Clin. Microbiol. Rev.* **2021**, *34*, e0003019. [CrossRef]
8. Li, W.; Yang, Z.; Hu, J.; Wang, B.; Rong, H.; Li, Z.; Sun, Y.; Wang, Y.; Zhang, X.; Wang, M.; et al. Evaluation of culturable 'last-resort' antibiotic resistant pathogens in hospital wastewater and implications on the risks of nosocomial antimicrobial resistance prevalence. *J. Hazard. Mater.* **2022**, *438*, 129477. [CrossRef]
9. Russo, T.; Marr, C. Hypervirulent *Klebsiella pneumoniae*. *Clin. Microbiol. Rev.* **2019**, *32*, e00001-19. [CrossRef]
10. Gao, W.; Howden, B.P.; Stinear, T.P. Evolution of virulence in *Enterococcus faecium*, a hospital-adapted opportunistic pathogen. *Curr. Opin. Microbiol.* **2018**, *41*, 76–82. [CrossRef]
11. Harding, C.M.; Hennon, S.W.; Feldman, M.F. Uncovering the mechanisms of *Acinetobacter baumannii* virulence. *Nat. Rev. Microbiol.* **2017**, *16*, 91–102. [CrossRef] [PubMed]
12. Argemi, X.; Hansmann, Y.; Prola, K.; Prévost, G. Coagulase-negative staphylococci pathogenomics. *Int. J. Mol. Sci.* **2019**, *20*, 1215. [CrossRef] [PubMed]
13. Candan, E.D.; Aksöz, N. *Klebsiella pneumoniae*: Characteristics of carbapenem resistance and virulence factors. *Acta Biochim. Pol.* **2015**, *62*, 867–874. [CrossRef] [PubMed]
14. Contreras-Omaña, R.; Escorcia-Saucedo, A.E.; Velarde-Ruiz, J.A. Prevalencia e impacto de resistencias a antimicrobianos en infecciones gastrointestinales: Una revisión. *Rev. Gastroenterol. Mex.* **2021**, *86*, 265–275. [CrossRef]
15. Resurrección-Delgado, C.; Montenegro-Idrogo, J.; Chiappe-Gonzalez, A.; Vargas-Gonzalez, R.; Cucho-Espinoza, C.; Mamani-Condori, D.; Huaroto-Valdivia, L. *Klebsiella pneumoniae* Nueva Delhi metalo-betalactamasa en el Hospital Nacional Dos de Mayo. Lima, Perú. *Rev. Peru Med. Exp. Salud Publica* **2017**, *34*, 261–267. [CrossRef]
16. De Oliveira, D.; Forde, B.; Kidd, T.; Harris, P.; Schembri, M.; Beatson, S.; Paterson, D.; Walker, M. Antimicrobial resistance in ESKAPE pathogens. *Clin. Microbiol. Rev.* **2020**, *33*, e00181-19. [CrossRef]

17. Denissen, J.; Reyneke, B.; Waso-Reyneke, M.; Havenga, B.; Barnard, T.; Khan, S.; Khan, W. Prevalence of ESKAPE pathogens in the environment: Antibiotic resistance status, community-acquired infection and risk to human health. *Int. J. Hyg. Environ. Health* **2022**, *244*, 114006. [CrossRef]
18. Liu, J.Y.; Dickter, J.K. Nosocomial infections: A history of hospital-acquired infections. *Gastrointest. Endosc. Clin. N. Am.* **2020**, *30*, 637–652. [CrossRef]
19. Hazard, D.; von Cube, M.; Kaier, K.; Wolkewitz, M. Predicting potential prevention effects on hospital burden of nosocomial infections: A multistate modeling approach. *Value Health* **2021**, *24*, 830–838. [CrossRef]
20. Jeganathan, N. Burden of sepsis in India. *Chest* **2022**, *161*, 1438–1439. [CrossRef]
21. Bhatia, P.; Sharma, A.; George, A.J.; Anvitha, D.; Kumar, P.; Dwivedi, V.P.; Chandra, N.S. Antibacterial activity of medicinal plants against ESKAPE: An update. *Heliyon* **2021**, *7*, e06310. [CrossRef] [PubMed]
22. Ghodhbane, H.; Elaidi, S.; Sabatier, J.-M.; Achour, S.; Benhmida, J.; Regaya, I. Bacteriocins active against multi-resistant Gram negative bacteria implicated in nosocomial infections. *Infect. Disord. Drug Targets* **2015**, *15*, 2–12. [CrossRef] [PubMed]
23. Atanasov, A.; Zotchev, S.; Dirsch, V.; International Natural Product Sciences Taskforce; Supuran, C. Natural products in drug discovery: Advances and opportunities. *Nat. Rev. Drug Discov.* **2021**, *20*, 200–216. [CrossRef]
24. Araldi, R.P.; dos Santos, M.O.; Barbon, F.F.; Manjerona, B.A.; Meirelles, B.R.; Neto, P.D.O.; da Silva, P.I.; dos Santos, L.; Camargo, I.C.C.; de Souza, E.B. Analysis of antioxidant, cytotoxic and mutagenic potential of *Agave sisalana* Perrine extracts using Vero cells, human lymphocytes and mice polychromatic erythrocytes. *Biomed. Pharmacother.* **2018**, *98*, 873–885. [CrossRef] [PubMed]
25. Dutra, R.C.; Campos, M.M.; Santos, A.R.S.; Calixto, J.B. Medicinal plants in Brazil: Pharmacological studies, drug discovery, challenges and perspectives. *Pharmacol. Res.* **2016**, *112*, 4–29. [CrossRef]
26. Aylate, A.; Agize, M.; Ekero, D.; Kiros, A.; Ayledo, G.; Gendiche, K. In-Vitro and In-Vivo antibacterial activities of *Croton macrostachyus* methanol extract against *E. coli* and *S. aureus*. *Adv. Anim. Vet. Sci.* **2017**, *5*, 107–114. [CrossRef]
27. Avato, P. Editorial to the special issue—"Natural Products and Drug Discovery". *Molecules* **2020**, *25*, 1128. [CrossRef]
28. Kowalczyk, A.; Przychodna, M.; Sopata, S.; Bodalska, A.; Fecka, I. Thymol and thyme essential oil-new insights into selected therapeutic applications. *Molecules* **2020**, *25*, 4125. [CrossRef]
29. Salehi, B.; Upadhyay, S.; Orhan, I.E.; Jugran, A.K.; Jayaweera, S.L.D.; Dias, D.A.; Sharopov, F.; Taheri, Y.; Martins, N.; Baghalpour, N.; et al. Therapeutic potential of α-and β-pinene: A miracle gift of nature. *Biomolecules* **2019**, *9*, 738. [CrossRef]
30. Bergman, M.E.; Davis, B.; Phillips, M.A. Medically useful plant terpenoids: Biosynthesis, occurrence, and mechanism of action. *Molecules* **2019**, *24*, 3961. [CrossRef]
31. Anandakumar, P.; Kamaraj, S.; Vanitha, M.K. D-limonene: A multifunctional compound with potent therapeutic effects. *J. Food Biochem.* **2021**, *45*, e13566. [CrossRef] [PubMed]
32. Badawy, M.E.I.; Marei, G.I.K.; Rabea, E.I.; Taktak, N.E.M. Antimicrobial and antioxidant activities of hydrocarbon and oxygenated monoterpenes against some foodborne pathogens through in vitro and in silico studies. *Pestic. Biochem. Physiol.* **2019**, *158*, 185–200. [CrossRef] [PubMed]
33. Nabila, B.; Piras, A.; Fouzia, B.; Falconieri, D.; Kheira, G.; Fedoul, F.F.; Majda, S.R. Chemical composition and antibacterial activity of the essential oil of *Laurus nobilis* leaves. *Nat. Prod. Res.* **2020**, *36*, 989–993. [CrossRef] [PubMed]
34. Sokolik, C.G.; Ben-Shabat-Binyamini, R.; Gedanken, A.; Lellouche, J.P. Proteinaceous microspheres as a delivery system for carvacrol and thymol in antibacterial applications. *Ultrason. Sonochem.* **2017**, *41*, 288–296. [CrossRef] [PubMed]
35. Bouchekouk, C.; Kara, F.Z.; Tail, G.; Saidi, F.; Benabdelkader, T. Essential oil composition and antibacterial activity of *Pteridium aquilinum* (L.) Kuhn. *Biol. Futur.* **2019**, *70*, 56–61. [CrossRef]
36. Liu, Q.; Wang, Z.; Mukhamadiev, A.; Feng, J.; Gao, Y.; Zhuansun, X.; Han, R.; Chong, Y.; Jafari, S.M. Formulation optimization and characterization of carvacrol-loaded nanoemulsions: In Vitro antibacterial activity/mechanism and safety evaluation. *Ind. Crop. Prod.* **2022**, *181*, 114816. [CrossRef]
37. Liu, X.; Cai, J.; Chen, H.; Zhong, Q.; Hou, Y.; Chen, W.; Chen, W. Antibacterial activity and mechanism of linalool against *Pseudomonas aeruginosa*. *Microb. Pathog.* **2020**, *141*, 103980. [CrossRef]
38. Iraji, A.; Yazdanpanah, S.; Alizadeh, F.; Mirzamohammadi, S.; Ghasemi, Y.; Pakshir, K.; Yang, Y.; Zomorodian, K. Screening the antifungal activities of monoterpenes and their isomers against *Candida* species. *J. Appl. Microbiol.* **2020**, *129*, 1541–1551. [CrossRef]
39. Tao, N.; Ouyang, Q.; Jia, L. Citral inhibits mycelial growth of *Penicillium italicum* by a membrane damage mechanism. *Food Control* **2014**, *41*, 116–121. [CrossRef]
40. De Oliveira, F.; Moura, J.; De Oliveira, E. Investigation on mechanism of antifungal activity of eugenol against *Trichophyton rubrum*. *Med. Mycol.* **2013**, *51*, 507–513. [CrossRef]
41. De Oliveira, M.; Araújo, A.; Souza, K.; Cardoso, G.; de Oliveira, E.; de Oliveira, F. Investigation of the antifungal potential of linalool against clinical isolates of fluconazole resistant *Trichophyton rubrum*. *J. Mycol. Med.* **2017**, *27*, 195–202. [CrossRef] [PubMed]
42. Marchese, A.; Orhan, I.E.; Daglia, M.; Barbieri, R.; Di Lorenzo, A.; Nabavi, S.F.; Gortzi, O.; Izadi, M.; Nabavi, S.M. Antibacterial and antifungal activities of thymol: A brief review of the literature. *Food Chem.* **2016**, *210*, 402–414. [CrossRef] [PubMed]
43. Boye, A.; Addo, J.K.; Acheampong, D.O.; Thomford, A.K.; Asante, E.; Amoaning, R.E.; Kuma, D.N. The hydroxyl moiety on carbon one (C1) in the monoterpene nucleus of thymol is indispensable for anti-bacterial effect of thymol. *Heliyon* **2020**, *6*, e03492. [CrossRef] [PubMed]

44. Wang, K.; Jiang, S.; Pu, T.; Fan, L.; Su, F.; Ye, M. Antifungal activity of phenolic monoterpenes and structure-related compounds against plant pathogenic fungi. *Nat. Prod. Res.* **2019**, *33*, 1423–1430. [CrossRef] [PubMed]
45. Morales, I.; De La Fuente, J.; Sosa, V. Componentes de *Eupatorium saltense*. *Asoc. Quim. Argent.* **1991**, *79*, 141–144.
46. Hocquemiller, R.; Cortes, D.; Arango, G.J.; Myint, S.H.; Cave, A. Isolement et synthese de l'espintanol, nouveau monoterpene antiparasitaire. *J. Nat. Prod.* **1991**, *54*, 445–452. [CrossRef]
47. Rojano, B.; Saez, J.; Schinella, G.; Quijano, J.; Vélez, E.; Gil, A.; Notario, R. Experimental and theoretical determination of the antioxidant properties of isoespintanol (2-isopropyl-3,6-dimethoxy-5-methylphenol). *J. Mol. Struct.* **2008**, *877*, 1–6. [CrossRef]
48. Rojano, B.; Pérez, E.; Figadère, B.; Martin, M.T.; Recio, M.C.; Giner, R.; Ríos, J.L.; Schinella, G.; Sáez, J. Constituents of *Oxandra* Cf. *xylopioides* with anti-inflammatory activity. *J. Nat. Prod.* **2007**, *70*, 835–838. [CrossRef]
49. Gavilánez, T.C.; Colareda, G.A.; Ragone, M.I.; Bonilla, M.; Rojano, B.A.; Schinella, G.R.; Consolini, A.E. Intestinal, urinary and uterine antispasmodic effects of isoespintanol, metabolite from *Oxandra xylopioides* leaves. *Phytomedicine* **2018**, *51*, 20–28. [CrossRef]
50. Rinaldi, G.J.; Rojano, B.; Schinella, G.; Mosca, S.M. Participation of NO in the vasodilatory action of isoespintanol. *Vitae* **2019**, *26*, 78–83. [CrossRef]
51. Usuga, A.; Tejera, I.; Gómez, J.; Restrepo, O.; Rojano, B.; Restrepo, G. Cryoprotective effects of ergothioneine and isoespintanol on canine semen. *Animals* **2021**, *11*, 2757. [CrossRef] [PubMed]
52. Rojano, B.A.; Montoya, S.; Yépez, F.; Saez, J. Evaluación de isoespintanol aislado de *Oxandra* Cf. *xylopioides (Annonaceae)* sobre *Spodoptera frugiperda* J.E. Smith (Lepidoptera: Noctuidae). *Rev. Fac. Nac. Agron. Medellín* **2007**, *60*, 3691–3702.
53. Arango, N.; Vanegas, N.; Saez, J.; García, C.; Rojano, B. Actividad antifungica del isoespintanol sobre hongos del género *Colletotricum*. *Sci. Tech.* **2007**, *33*, 279–280. [CrossRef]
54. Contreras, O.; Angulo, A.; Santafé, G. Mechanism of antifungal action of monoterpene isoespintanol against clinical isolates of *Candida tropicalis*. *Molecules* **2022**, *27*, 5808. [CrossRef]
55. Contreras, O.I.; Angulo, A.; Santafé, G. Antifungal potential of isoespintanol extracted from *Oxandra xylopioides* diels (Annonaceae) against intrahospital isolations of *Candida* spp. *Heliyon* **2022**, *8*, e11110. [CrossRef]
56. Kamatou, G.P.; Vermaak, I.; Viljoen, A.M.; Lawrence, B.M. Menthol: A simple monoterpene with remarkable biological properties. *Phytochemistry* **2013**, *96*, 15–25. [CrossRef]
57. Cowan, M. Plant products as antimicrobial agents. *Clin. Microbiol. Rev.* **1999**, *12*, 564–582. [CrossRef]
58. Ergüden, B. Phenol group of terpenoids is crucial for antibacterial activity upon ion leakage. *Lett. Appl. Microbiol.* **2021**, *73*, 438–445. [CrossRef]
59. Siroli, L.; Patrignani, F.; Gardini, F.; Lanciotti, R. Effects of sub-lethal concentrations of thyme and oregano essential oils, carvacrol, thymol, citral and trans-2-hexenal on membrane fatty acid composition and volatile molecule profile of *Listeria monocytogenes*, *Escherichia coli* and *Salmonella enteritidis*. *Food Chem.* **2015**, *182*, 185–192. [CrossRef]
60. Alam, K.; Al Farraj, D.A.; Mah-E-Fatima, S.; Yameen, M.A.; Elshikh, M.S.; Alkufeidy, R.M.; Mustafa, A.; Bhasme, P.; Alshammari, M.K.; Alkubaisi, N.A.; et al. Anti-biofilm activity of plant derived extracts against infectious pathogen-*Pseudomonas aeruginosa* PAO1. *J. Infect. Public Health* **2020**, *13*, 1734–1741. [CrossRef]
61. Yousefpour, Z.; Davarzani, F.; Owlia, P. Evaluating of the effects of sub-MIC concentrations of gentamicin on biofilm formation in clinical isolates of *Pseudomonas aeruginosa*. *Iran. J. Pathol.* **2021**, *16*, 403–410. [CrossRef] [PubMed]
62. Brindhadevi, K.; LewisOscar, F.; Mylonakis, E.; Shanmugam, S.; Verma, T.N.; Pugazhendhi, A. Biofilm and quorum sensing mediated pathogenicity in *Pseudomonas aeruginosa*. *Process Biochem.* **2020**, *96*, 49–57. [CrossRef]
63. Jurado-Martín, I.; Sainz-Mejías, M.; McClean, S. *Pseudomonas aeruginosa*: An audacious pathogen with an adaptable arsenal of virulence factors. *Int. J. Mol. Sci.* **2021**, *22*, 3128. [CrossRef] [PubMed]
64. Yu, S.; Ma, L. Iron uptake and biofilm formation in *Pseudomonas aeruginosa*. *Chin. J. Biotechnol.* **2017**, *33*, 1489–1512. [CrossRef]
65. Qaralleh, H. Thymol rich *Thymbra capitata* essential oil inhibits quorum sensing, virulence and biofilm formation of beta lactamase producing *Pseudomonas aeruginosa*. *Nat. Prod. Sci.* **2019**, *25*, 172–180. [CrossRef]
66. Espina, L.; Berdejo, D.; Alfonso, P.; García-Gonzalo, D.; Pagán, R. Potential use of carvacrol and citral to inactivate biofilm cells and eliminate biofouling. *Food Control* **2017**, *82*, 256–265. [CrossRef]
67. Liu, Y.; Li, J.J.; Li, H.Y.; Deng, S.M.; Jia, A.Q. Quorum sensing inhibition of hordenine analogs on *Pseudomonas aeruginosa* and *Serratia marcescens*. *Synth. Syst. Biotechnol.* **2021**, *6*, 360–368. [CrossRef]
68. Kachur, K.; Suntres, Z. The antibacterial properties of phenolic isomers, carvacrol and thymol. *Crit. Rev. Food Sci. Nutr.* **2020**, *60*, 3042–3053. [CrossRef]
69. Clinical and Laboratory Standards Institute. *Methods for Dilution Antimicrobial Susceptibility Tests for Bacteria That Grow Aerobically*, 9th ed.; Clinical and Laboratory Standards Institute: Wayne, AR, USA, 2012; Volume 32.
70. Quave, C.L.; Plano, L.R.; Pantuso, T.; Bennett, B.C. Effects of extracts from italian medicinal llants on planktonic growth, biofilm formation and adherence of methicillin-resistant *Staphylococcus aureus*. *J. Ethnopharmacol.* **2008**, *118*, 418–428. [CrossRef]

71. Rossi, C.; Serio, A.; Chaves, C.; Anniballi, F.; Auricchio, B.; Goffredo, E.; Cenci-Goga, B.; Lista, F.; Fillo, S.; Paparella, A. Biofilm formation, pigment production and motility in *Pseudomonas* spp. isolated from the dairy industry. *Food Control* **2018**, *86*, 241–248. [CrossRef]
72. Donadu, M.G.; Peralta, Y.; Usai, D.; Maggio, F.; Molina, J.; Rizzo, D.; Bussu, F.; Rubino, S.; Zanetti, S.; Paparella, A.; et al. Colombian essential oil of *Ruta graveolens* against nosocomial antifungal resistant *Candida* strains. *J. Fungi* **2021**, *7*, 383. [CrossRef] [PubMed]

Anexo 4

"Antifungal potential of isoespintanol extracted from *Oxandra xylopioides* diels (Annonaceae) against intrahospital isolations of *Candida* SPP"

Heliyon 8 (2022) e11110

Contents lists available at ScienceDirect

Heliyon

journal homepage: www.cell.com/heliyon

Research article

Antifungal potential of isoespintanol extracted from *Oxandra xylopioides* diels (Annonaceae) against intrahospital isolations of *Candida* SPP

Orfa Inés Contreras Martínez *, Alberto Angulo Ortíz, Gilmar Santafé Patiño

Universidad de Córdoba, Facultad de Ciencias Básicas, Montería, Córdoba, Colombia

ARTICLE INFO

Keywords:
Isoespintanol
Oxandra xylopioides
Candida spp.
Antifungal

ABSTRACT

The aim of this study was to evaluate the antifungal activity of isoespintanol (ISO) extracted from *Oxandra xylopioides* Diels (Annonaceae) against clinical isolates of *Candida* spp. Isoespintanol was obtained from the petroleum benzine extract of the leaves and was identified by nuclear magnetic resonance (NMR) and mass spectrometry (MS). For antifungal activity experiments, the broth microdilution method was used. The results show an inhibitory effect against *Candida* spp., with minimum inhibitory concentration (MIC) values between 450.4–503.3 μg/mL. Furthermore, the inhibitory effect of ISO against fungal biofilms is highlighted, even in some cases, greater than the effect shown by amphotericin B (AFB) and in others, where AFB showed no effect. Assays with fluorescent staining with acridine orange (AO) and ethidium bromide (EB), transmission electron microscopy (TEM), Evans blue, measurement of extracellular pH and leakage of intracellular material, evidenced damage at the level of fungal membranes and general cell damage, when cells were exposed to ISO, compared to untreated cells. The results of this research, serve as the basis for future studies in the establishment of the mechanisms of antifungal action of ISO, which could serve as an adjunct in the treatment of infections by these yeasts.

1. Introduction

Fungi are a major cause of opportunistic infections. They infect countless numbers of people each year, raising morbidity and mortality rates, especially in immunocompromised people; in recent years, these infections have garnered significant attention in medical and pharmaceutical science, due to the rapid increase in its incidence. Currently, more than one billion people are affected by fungal infections (Kakar et al., 2021) and more than 1.5 million deaths are produced per year (Bongomin et al., 2017). Recent studies estimate that infections caused by fungi, which especially include *Candida* spp., are difficult to treat and the associated mortality remains very high, even when antifungal treatments are available (Janbon et al., 2019). More than 90% of people infected with HIV develop debilitating diseases caused by species of the genus *Candida*, these being the most common pathogens isolated from patients in intensive care. Candidemia is one of the most frequent opportunistic mycoses in the world, *C. albicans* is considered the most prevalent and clinically important pathogenic yeast (Kakar et al., 2021). However, an important epidemiological change has been observed in recent decades, species such as *C. glabrata*, *C. tropicalis*, *C. krusei*. *C. parapsilosis*, *C. auris*, have begun to be isolated with frequencies in severe candidemia around the world (Donadu et al., 2021). The increasing number of patients at risk of invasive mycosis has a complex management, since drug interactions, intolerance of currently available antifungals and innate or acquired resistance pose a problem for their treatment, which is restricted to five established classes of antifungal medications; The Centers for Disease Control and Prevention (CDC) further predicts that these infections pose a threat that will worsen and may become urgent (Scorneaux et al., 2017). In this context, the search and development of new compounds with antifungal potential, which are more effective and safe, as well as the development of new treatment strategies with better host tolerance has become a priority objective today (Gintjee et al., 2020).

Natural products play a valuable role in the discovery and development of many drugs used today; especially plants play a main role as a source of specialized metabolites with recognized medicinal properties (Aylate et al., 2017). Due to their wide chemical diversity, these metabolites can be used directly as bioactive compounds, as drug prototypes and/or be used as pharmacological tools for different targets (Avato, 2020). About 80% of the world's population use herbal treatments for health care (Mekonnen Bayisa and Aga Bullo, 2021); These have been used in traditional medicine and in the pharmaceutical industry for a

* Corresponding author.
E-mail address: oicontreras@correo.unicordoba.edu.co (O.I. Contreras Martínez).

https://doi.org/10.1016/j.heliyon.2022.e11110
Received 12 December 2021; Received in revised form 24 April 2022; Accepted 11 October 2022

long time due to their invaluable therapeutic potential (Naman et al., 2016). ISO (2,5-dimethoxy-3-hydroxy-*p*-cymene), is a monoterpene known for its anti-inflammatory activity ((Rojano B. et al., 2007), vasodilator (Rinaldi et al., 2019), antispasmodic (Gavilánez et al., 2018), with a high antioxidant potential (Rojano et al., 2008). Its insecticidal activity against *Spodoptera frugiperda* (Rojano B.A. et al., 2007) and antifungal against *Colletrotichum* (Arango et al., 2007) have also been tested. However, its potential against clinical isolates has not been reported. The purpose of this study was to investigate the antifungal effect of ISO against clinical isolates of *Candida* species and its effect on the inhibition of fungal biofilms. The results highlight the antifungal activity of ISO against clinical isolates of *Candida* spp., probably due, at least in part, to damage to the integrity of fungal cell membranes, resulting in the alteration of its permeability and the consequent loss of intracellular material; furthermore, we highlight the role of ISO in the inhibition of fungal biofilms.

2. Materials and methods

2.1. Reagents

Fluconazole (FLC) was obtained from Pfizer. Amphotericin B, acridine orange, ethidium bromide, Evans blue, sabouraud dextrose broth (SDB) and sabouraud dextrose agar (SDA) used in this study were obtained from Sigma-Aldrich. Glacial acetic acid from Carlo Erba Reagents, Italy.

2.2. Vegetal material

The ISO was isolated from leaves of *O. xylopioides*, which were collected from a specimen located in the Municipality of Montería, Department of Córdoba, with coordinates 08° 48′17″ north latitude and 75°42′07″ west longitude. A specimen of herbarium is deposited in the Joaquín Antonio Uribe Botanical Garden, with the collection number JAUM 037849.

2.3. Isolation and identification of isoespintanol

The ISO was obtained by hydrodistillation and crystallization, from 15 g of petroleum benzyne extract of the leaves of *O. xylopioides*, following the methodology described in a previous work (Ramírez et al., 2015), with some modifications that included successive crystallizations with n-hexane that led to obtaining 3.92 g of the pure compound. The chromatographic monitoring was done with aluminum thin layer chromatography TLC plate, silica gel coated with fluorescent indicator F254 (Merck®). The purity was verified using a gas chromatograph coupled to a Thermo Scientific model Trace 1310 mass spectrometer, with an AB-5MS column, (30 m × 0.25 mm i.d. × 0.25 μm). The temperature gradient system started at 80 °C for 10 min (min) up to 200 °C at 10 °C/min. The temperature was increased to 240 °C at 4 °C/min and finally it was brought up to 290 °C for 10 min at 10 °C/min. The injection was splitless type, with an injection volume of 1 μL. The mass spectrum was obtained in electron impact ionization mode at 70 eV. The structure of the ISO was determined using ^{1}H-NMR, ^{13}C-NMR, DEPT, COSY ^{1}H–^{1}H, HMQC and HMBC spectra, performed on a 400MHz Bruker Advance DRX spectrometer, in deuterated chloroform ($CDCl_3$). The ISO was purified as a creamy white amorphous solid. The EI-MS: $[M]^+$ m/z 210 (49%) and fragments m/z 195 (100%), 180, 165, 150, 135 and 91. ^{1}H-NMR ($CDCl_3$): δ 6.22 s, 1H (H6), δ 5.85 s, 1H (HO-3), δ 3.77 s, 3H (H12), δ 3.76 s, 3H (H11), δ 3.52 hep, J = 7.1 Hz, 1H (H8), δ 2.29 s, 3H (H7), δ 1.33 d, J = 7.1 Hz, 6H (H9–H10). ^{13}C-NMR ($CDCl_3$): δ 154.3 (C5), δ 147.4 (C3), δ 139.7 (C2), δ 126.8 (C1), δ 120.4 (C4), δ 104.4 (C6), δ 24.6 (C8), δ 60.8 (C11), δ 55.7 (C12), δ 20.6 (C9, C10), δ 15.8 (C7).

2.4. Tested microorganisms

Fifteen clinical isolates belonging to *Candida* spp., including: *C. albicans*, *C. glabrata C. tropicalis*, *C. auris*, were used in this study. The isolates were cultured from tracheal aspirate samples, blood cultures and urine cultures from hospitalized patients at the Salud Social S.A.S. from the city of Sincelejo, Sucre, Colombia. All microorganisms were identified by standard methods: Vitek 2 Compact. Biomerieux SA., YST vitek 2 Card and AST-YS08 Vitek 2 Card (Ref 420739). The medium SDA, was used to maintain the cultures until the tests were carried out.

2.5. Antifungal susceptibility assay

Minimum inhibitory concentration (MIC) of the ISO against the clinical isolates of *Candida* spp., was defined as the lowest concentration at which 90% (IC_{90}) of the fungal growth was inhibited, compared to the control. IC_{50} was defined as the lowest concentration at which 50% of fungal growth was inhibited. The MIC was determined by performing the microdilution assay in broth, using 96-well microtitration plates (Nunclon Delta, Thermo Fisher Scientific, Waltham, MA, USA), as described in the method M27-A3 of the Clinical Laboratory Standards Institute (CLSI) (Cantón et al., 2007) and EUCAST (European Committee for Antimicrobial Susceptibility Testing) (Rodriguez-Tudela, 2003), with minor modifications. Serial dilutions were made in SDB to obtain final concentrations of 15.62–500 μg/mL of the ISO in each reaction well. The assays were developed at a final volume of 200 μL per well as follows: 100 μL of the fungal inoculum at a concentration of 1×10^5 CFU/mL read at 530nm on a Spectroquant® Prove 300 spectrophotometer and 100 μL of the ISO adjusted to achieve in a final reaction system the concentrations described above. Yeast isolates without ISO and with FLC were used as controls. The plates were incubated at 37 °C for 24 h. The experiments were carried out in triplicate. The inhibition of fungal growth by ISO was determined by change in optical density (OD) using a SYNERGY LX microplate reader (Biotek), at 590 nm, from the beginning of the incubation to the final moment (24 h) and the reduction percentage growth was calculated (Quave et al., 2008). The OD_{590} value of the untreated cells was assigned 100% growth. Subsequently, the minimum fungicidal concentration (MFC) was determined by taking 10 μL from each well and inoculating it on SDA. The plates were sealed and incubated at 37 °C for 24/48 h, checking for microbial growth. MFC was considered the lowest concentration capable of inhibiting 99% of yeasts (Donadu et al., 2021). The experiments were carried out in triplicate.

2.6. Live/Dead assay

The LIVE/DEAD assay were developed following the methodology proposed by (Zhang et al., 2020) with some modifications. The yeast suspension was previously standardized (1–5 × 10^6 CFU/mL), then sterile coverslips were placed in six-well plates and 2 mL of the fungal solution was added to each well. After incubation for 24 h, the cells were washed three times with phosphate-buffered saline (PBS). The ISO and FLC at MIC concentration for each yeast were added to the experimental groups and the fungal inoculum in SDB was used as a control. The prepared six-well dishes were incubated at 35 °C for 24 h. Then the coverslips were washed three times with PBS. Acridine orange (AO) (5 μL, 100 mg/L) and ethidium bromide (EB) (5 μL, 100 mg/L) were mixed under dark conditions, then the AO/EB mixture was added to the coverslips in dark conditions for 30 s. An Olympus BX43 fluorescence microscope with DP72 camera was used to observe and photograph.

2.7. Transmission electron microscopy (TEM)

The morphology of *C. albicans* after ISO treatment was analyzed through TEM. The *C. albicans* concentration was adjusted to 1×10^6 CFU/mL; the suspension was mixed with ISO (200 μg/mL) and incubated at 37 °C for 24 h. Subsequently, the cells were collected and fixed in 2.5% glutaraldehyde at 4 °C; they were centrifuged at 13000 rpm for 3 min and the button at the bottom of the vial was post-fixed in 1% osmium tetroxide in water, for 2 h at 4 °C. Then pre-imbibition with 3% uranyl acetate was performed for 1 h at room temperature, then the cells were

dehydrated in an ethanol gradient (50% for 10 min, 70% for 10 min, 90% for 10 min, 100% for 10 min), acetone-ethanol (1:1) for 15 min and embedded in SPURR epoxy resin. The samples were cut on a Leica EM UC7 ultramicrotome, at 130 nm thick and contrasted with 6% uranyl acetate and lead citrate, finally they were observed in a JEOL 1400 plus transmission electron microscope. The photographs were obtained with a Gatan Orius CCD camera.

2.8. Quantitative evaluation of biofilm formation

The standardized samples of *C. albicans*, *C. glabrata*, *C. tropicalis*, *C. auris* were evaluated to quantify the reduction of biofilms in the presence of ISO in plates of 96 wells following the methodology reported by (Donadu et al., 2021) with some modifications. For biofilm formation, 200 μL of the samples were cultured in each well in SDB and incubated at 37 °C for 48 h. Then the broth was removed from the microplate and 200 μL of the ISO MIC for each isolate were added and incubated at 37 °C for 1 h. Then the floating bacteria were removed and the biofilm at the bottom of the wells was washed with deionized water three times. Six replicas of each sample were made. The cultures without ISO were taken as a control and AFB was used as a positive control, a drug with known efficacy against biofilms in *Candida* spp. (Mukherjee et al., 2009). Biofilm reduction was quantified by staining the wells with 0.1% crystal violet (Sigma-Aldrich) for 20 min. The samples were washed with deionized water until the excess of dye was removed. Finally, the samples were soaked in 250 μL of 30% glacial acetic acid (Carlo Erba Reagents).

Absorbance values at 590 nm (OD_{590}) were measured for each strain using a SYNERGY LX microplate reader (Biotek). Biofilm production was grouped into the following categories: $OD_{590} < 0.1$: non-producers (NP), OD_{590} 0.1–1.0: weak producers (WP), OD_{590} 1.1–3.0: moderate producers (MP) and $OD_{590} > 3.0$: strong producers (SP). Biofilm reduction was calculated using the following equation:

$$\% \text{ reduction of biofilms} : \ Abs_{CO} - Abs_{ISO}/Abs_{CO} \times 100$$

where, Abs_{CO}: absorbance of the control sample and Abs_{ISO}: absorbance of the sample treated with ISO.

2.9. Release of cellular material through the fungal membrane

The release of cellular constituents in the supernatants was measured according to the methodology proposed by (Tao et al., 2014) with some modifications; 20 mL of fungal culture in SDB was centrifuged at 4000 g for 20 min, washed 3 times and resuspended in 20 mL of PBS (pH 7.0). The suspension was then treated with ISO (MIC) and incubated at 37 °C for 0, 30, 60 and 120 min of treatment. Subsequently, 2 mL of the sample were collected and centrifuged at 4000 g for 20 min. To determine the concentration of the released constituents, 2 ml of supernatant was used to measure the absorbance at 260 nm with the Spectroquant® Prove 300 UV/Vis spectrophotometer. Samples without ISO and samples with FLC were used as controls.

2.10. Extracellular pH measurement

The extracellular pH of the *Candida* spp. treated with the ISO (MIC) was determined according to the methodology proposed by (Tao et al., 2014) with some modifications. 100 μL of the fungal suspension (1×10^5 CFU/mL) was added to 20 mL of SDB and incubated at 37 °C for 48 h. Subsequently, the samples were centrifuged at 4000 g for 20 min; the pellet was collected, resuspended, and washed three times with double distilled water and resuspended again in 20 mL of sterile double distilled water. After the addition of ISO (MIC), the extracellular pH of *Candida* spp., was determined at 0, 30, 60 and 120 min, using a Schott® Instruments Handylab pH 11 m. Untreated samples and samples with FLC were analyzed as control.

2.11. Effect of ISO on membrane integrity

Damage to yeast cell membranes produced by ISO was also evidenced using Evans blue staining (Sigma-Aldrich) according to the methodology proposed by (Chaves-Lopez et al., 2018) with some modifications. Before assay, Evans blue was prepared 1% in PBS. 100 μL of the fungal suspension in SDB were incubated on coverslips (22 mm × 22 mm) in triplicate at 37 °C for 24 h. Subsequently, the samples were treated with ISO (MIC) for 1 h, and then, 1 mL of Evans blue was added to the samples for 5 min. Cells not treated with ISO were used as a control. The samples were observed under the microscope, Olympus CX31.

2.12. Statistical analysis

The results were analyzed using the statistical software R version 4.1.1. Pearson's correlation coefficient was used to measure the degree of linear relationship between the ISO concentration and the percentage reduction in microbial growth. To compare the effects of ISO and AFB on the reduction of the percentage of biofilms, the Mann-Whitney U Test was used. The Student's T test was applied to compare the effects of ISO and FLC on the exit of intracellular material through the membrane (reading OD_{260} nm). The one-factor analysis of variance was used to compare the effects of the treatments on the extracellular pH and the honest Tukey test was used to evaluate the significant differences produced by the analysis of variance.

3. Result and discussion

3.1. Obtaining isoespintanol

ISO (3.92 g) were obtained from 15 g of petroleum benzyne extract of the leaves of *O. xylopioides*, with a purity greater than 99%, verified by GC-MS. Its structural identification by ^{1}H-NMR, ^{13}C-NMR, DEPT, COSY ^{1}H–^{1}H, HMQC and HMBC, led unequivocally to propose the structure of 2,5-dimethoxy-3-hydroxy-*p*-cymene, isoespintanol, Figure 1.

3.2. Antifungal susceptibility assay

Our results show that ISO extracted from *O. xylopioides* has antifungal activity against clinical isolates of *Candida* spp. When *C. albicans*, *C. tropicalis*, *C. glabrata* and *C. auris* are exposed to ISO, a reduction in cell growth is observed compared to the untreated strains used as controls. In Figure 2(a), the strong and positive linear relationship between the ISO concentration and the growth reduction percentage is evidenced, as can be seen, as the ISO concentration increases, the percentage of microbial growth reduction also increases, which coincides with Pearson's correlation coefficient (0.998). Furthermore, the hypothesis test on the

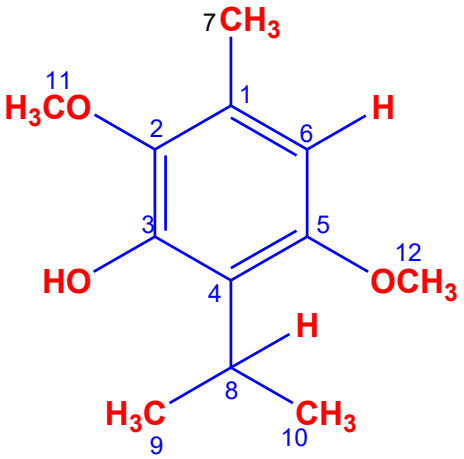

Figure 1. Structure of isoespintanol

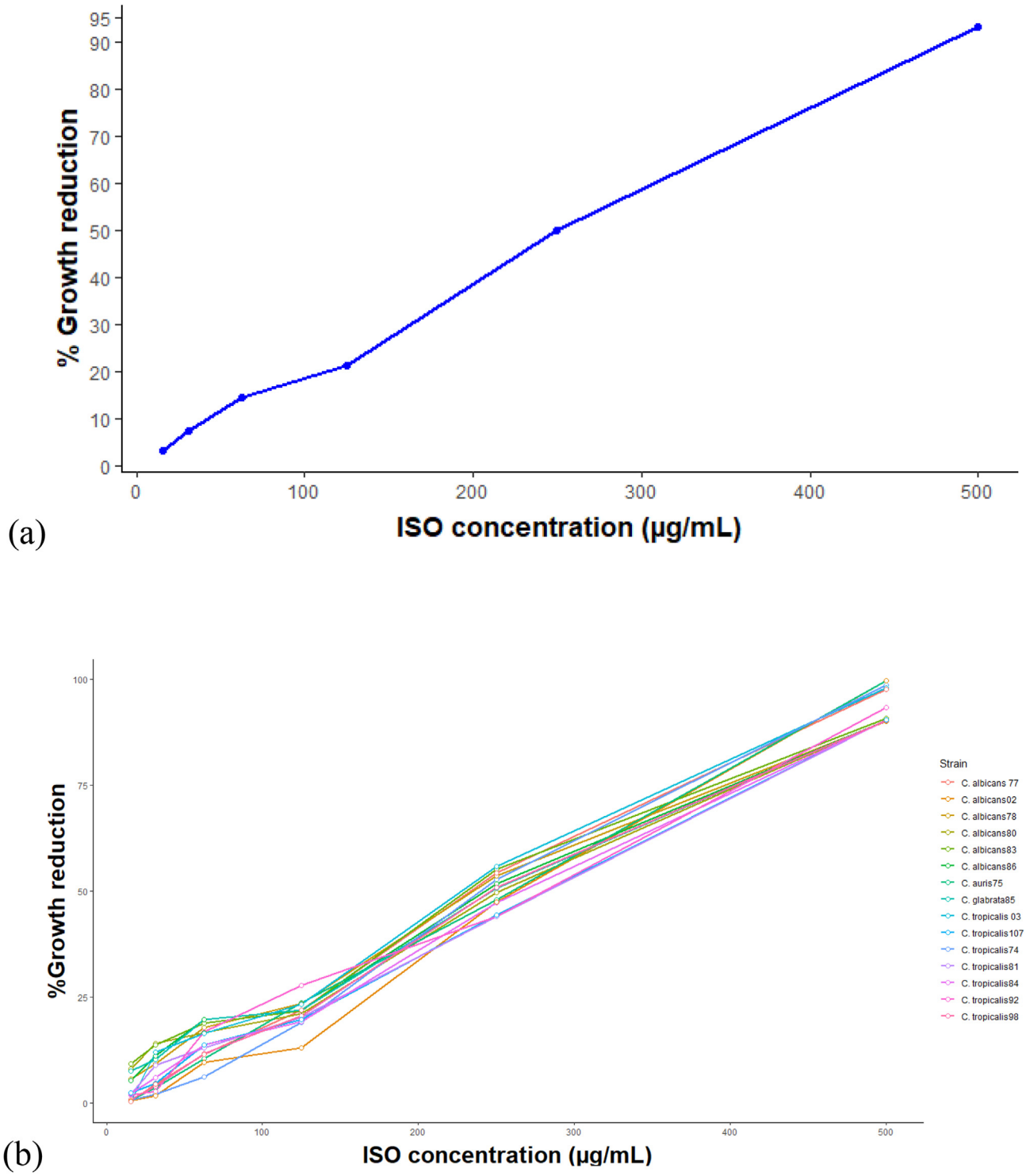

Figure 2. Percentages of reduction of the fungal growth of *Candida* spp., in the presence of different concentrations of the ISO. In (a) positive linear relationship between ISO concentration and growth reduction percentage. In (b), a similar trend between each of the isolates as the percentage of growth reduction increases as the ISO concentration increases.

correlation coefficient yields a p-value < 0.05, which indicates that with 95% confidence, there is a significant linear relationship. In Figure 2(b), the similar tendency between each of the isolates is shown to increase the percentage of growth reduction as the ISO concentration increases. It should be noted that all clinical isolates of *Candida* spp., in this study were resistant to FLC. Table 1 shows the ISO IC_{90}, IC_{50} and MFC values against *Candida* spp. Our research highlights the antifungal effect of ISO against *C. auris* (IC_{50}: 257.4–IC_{90}: 453.5 µg/mL) an emerging pathogen with a high percentage of mortality associated with therapeutic failure (Carvajal et al., 2021); *C. glabrata* (IC_{50}: 261.7–IC_{90}: 496.0 µg/mL) considered the second most isolated *Candida* species, associated with invasive candidiasis after *C. albicans* and resistant to antifungal drugs, particularly FLC and other azole derivatives (Hassan and Chew, 2021) and *C. tropicalis* (with IC_{90} values between: 450,4 and 500.7 µg/mL) one of the most important non-albicans species with resistance to azoles (Chen et al., 2021), showing MIC values with an increasing trend towards

Table 1. Minimum inhibitory concentration (IC_{90} μg/mL), IC_{50} and minimum fungicidal concentration of the ISO against *Candida* spp., After 24 h of treatment.

Fungi	Isoespintanol (μg/mL) 24 h		
	IC_{50}	IC_{90}	MFC
C. albicans 02	266,9 ± 0,01	459,2 ± 0,01	459,2
C. albicans 77	254,8 ± 0,02	452,4 ± 0,02	452,4
C. albicans 78	259,7 ± 0,01	488,4 ± 0,01	488,4
C. albicans 80	263,2 ± 0,30	499,8 ± 0,30	499,8
C. albicans 83	252,9 ± 0,02	487,9 ± 0,02	487,9
C. albicans 86	261,1 ± 0,03	493 ± 0,03	493
C. tropicalis 03	245 ± 0,01	450,4 ± 0,01	450,4
C. tropicalis 74	260,7 ± 0,3	452,1 ± 0,3	452,1
C. tropicalis 81	278,2 ± 0,02	503,3 ± 0,02	503,3
C. tropicalis 84	276,1 ± 0,02	497,0 ± 0,02	497,0
C. tropicalis 92	266,6 ± 0,02	483,3 ± 0,02	483,3
C. tropicalis 98	273,5 ± 0,02	487,9 ± 0,02	487,9
C. tropicalis 107	279,5 ± 0,04	500,7 ± 0,04	500,7
C. glabrata 85	261,7 ± 0,03	496,0 ± 0,03	496,0
C. auris 75	257,4 ± 0,29	453,5 ± 0,29	453,5

The MIC (IC_{90}) was defined as the lowest ISO concentration that reduced fungal growth (≥90%) compared to untreated cells used as controls.

high MICs, which is consistent with studies reported by (El-Kholy et al., 2021). The MIC and MFC of the ISO was between 450.4–503.3 μg/mL (Table 1), these values varied between species and within the same *Candida* species. The MFC values for all isolates were the same for MIC; being the concentration of the ISO determining in the degree of sensitivity of the species of *Candida*. Our results are consistent with studies reported with other monoterpenes with a chemical structure similar to ISO, such as thymol (Dias de Castro et al., 2015), and carvacrol (Oliveira Lima et al., 2013), to which, antifungal activity against *Candida* spp., has been reported, apparently by binding to ergosterol in the fungal membrane, altering the permeability of the membrane and causing cell death. Citral has also been reported with antifungal activity against *Penicillium italicum*, due to damage to the integrity of the membrane and increased permeability as reported by (Tao et al., 2014). Studies with eugenol (De Oliveira et al., 2013) and linalool (De Oliveira Lima et al., 2017) have also shown antifungal activity, showing action on the *Trichophyton rubrum* membrane through a mechanism that seems to involve the inhibition of biosynthesis ergosterol, with MIC values similar to those found in our results; in general, numerous terpenes are known to be active against a wide variety of microorganisms (Murphy Cowan, 1999), however, unlike our research, the activity of ISO against fungal clinical isolates has not been reported.

3.3. Live/Dead assay

After double fluorescent staining with AO and EB, the morphology of the cells was observed under fluorescence microscopy. In living cells, AO diffuses through intact cytoplasmic membranes (Byvaltsev et al., 2019), intercalates with DNA, and emits a bright green fluorescence (Zhang et al., 2020). However, EB penetrates only dead cells with compromised cell wall and membrane systems (Wu et al., 2015), intercalates with DNA, and emits a red-orange fluorescence. In our results (Figure 3), untreated cells grew well after 24 h (A), while dead cells were observed massively in the group treated with ISO (B) and to a lesser extent in the group treated with FLC (C); These results are probably due to damage to the integrity of the membranes of cells treated with ISO.

3.4. Transmission electron microscopy (TEM)

The images (Figure 4) show the irregular morphology of some *C. albicans* cells 24 h after ISO treatment. In some cells, the cell membrane looks discontinuous, partially dissolved and irregular regions unlike cells not treated with ISO. However, some cells with apparently intact membranes show a cellular disorganization at the cytoplasm level with intense vacuolization and nuclear fragmentation, this could indicate that ISO can cross the membrane, penetrating inside the cells and interacting with specific intracellular sites. which could also be responsible for its antimicrobial activity, taking into account that studies reported by (Trombetta et al., 2005) suggest a real transfer of monoterpenes through lipid bilayers; the discrepancy with what was observed with cells treated with fluconazole could indicate that there are other molecules or other target sites, in addition to the membrane, that determine the sensitivity of *Candida* species to ISO, so it could be speculated that the mechanism of action of the ISO could also be associated with other fungal cell target sites as indicated (Cheng et al., 2021). The cells treated with FLC, some remained normal with intact cell walls, the damage at the membrane level and at the level of the cytoplasm was less than that observed in cells treated with ISO.

3.5. Quantitative evaluation of biofilm formation

The formation of fungal biofilms increases the persistence and dissemination ability of yeasts, especially in hospital environments (Hassan and Chew, 2021). Biofilm-forming *Candida* strains are associated with high mortality, probably due to the low permeability of the matrix to antifungal drugs (Tascini et al., 2017). In our study, all isolates were biofilm producers (Figure 5(a)), classified as follows: $OD_{590} < 0.1$: no production, OD_{590} 0.1–1.0: weak production, OD_{590} 1.0–3.0: moderate production and $OD_{590} > 3$: strong production; highlighting the *C. tropicalis* isolates for presenting higher biofilm biomass, compared to the other species. This is consistent with the findings of (Marcos--Zambrano et al., 2014) who reports a strong production of biofilms in 80% of isolates of *C. tropicalis*; studies by (Guembe et al., 2017) report similar results indicating that biofilm production varies according to the *Candida* species and the physiology of the infection site; the species of *C. tropicalis* in our study were isolated from the urinary and respiratory tracts, which agrees with what was reported by (El-Kholy et al., 2021) where the isolates of *C. tropicalis* from blood, urinary and respiratory tracts produced a strong biofilm biomass. In our study *C. glabrata* had less biofilm production similar to that reported by (El-Kholy et al., 2021).

Our results report antibiofilm activity of ISO (IC_{50}) against isolates of *C. tropicalis* 84, showing biofilm reduction percentages of 23.25% after 1 h of treatment, exhibiting a greater effect than AFB for some isolates. Likewise, the ISO (IC_{50}) showed a 20% reduction of biofilms in *C. glabrata*, for which AFB had no effect (Figure 5(b)). shows the percentage of biofilm reduction after 1 h of treatment with ISO (MIC μg/mL) and AFB (1.0 μg/mL). The Mann-Whitney U test with a p-value > 0.05 and a confidence level of 95% tells us that there are no statistically significant differences between the effects of ISO and AFB on biofilm reduction. For *C. tropicalis* 81 and 107 an insignificant reduction of biofilms was observed (2.6 and 3% respectively) while for *C. auris* 75 and *C. albicans* (80, 83, 86) there was no reduction of biofilms, during the first hour of treatment. The ISO biofilm reduction percentages varied between species and between members of the same species, which is consistent with what was reported by (Prażyńska et al., 2018), which indicates that the inhibition of fungal biofilms may depend on the species and the degree of maturation of the biofilms. It should be noted that this is the first report of the effect of ISO on fungal biofilms in *Candida* spp. Regarding the treatment with AFB, detachment of biofilms was observed after 1 h of exposure in *C. auris* 75 (13.31%), *C. tropicalis* 84 (12%), *C. albicans* 86 (12.6%) and *C. tropicalis* 107 (5.11%), while for the rest of isolates it did not show reduction in the percentage of biofilms, during the first hour of treatment. Statistical analysis shows that there are no statistically significant differences between the effect of ISO and AFB against the reduction of fungal biofilms, however, our results show (Figure 5(b)) the effect of ISO on the biofilms of *C. tropicalis* (81 and 92), *C. albicans* (78 and 02) and *C. glabrata*, where AFB showed no effect.

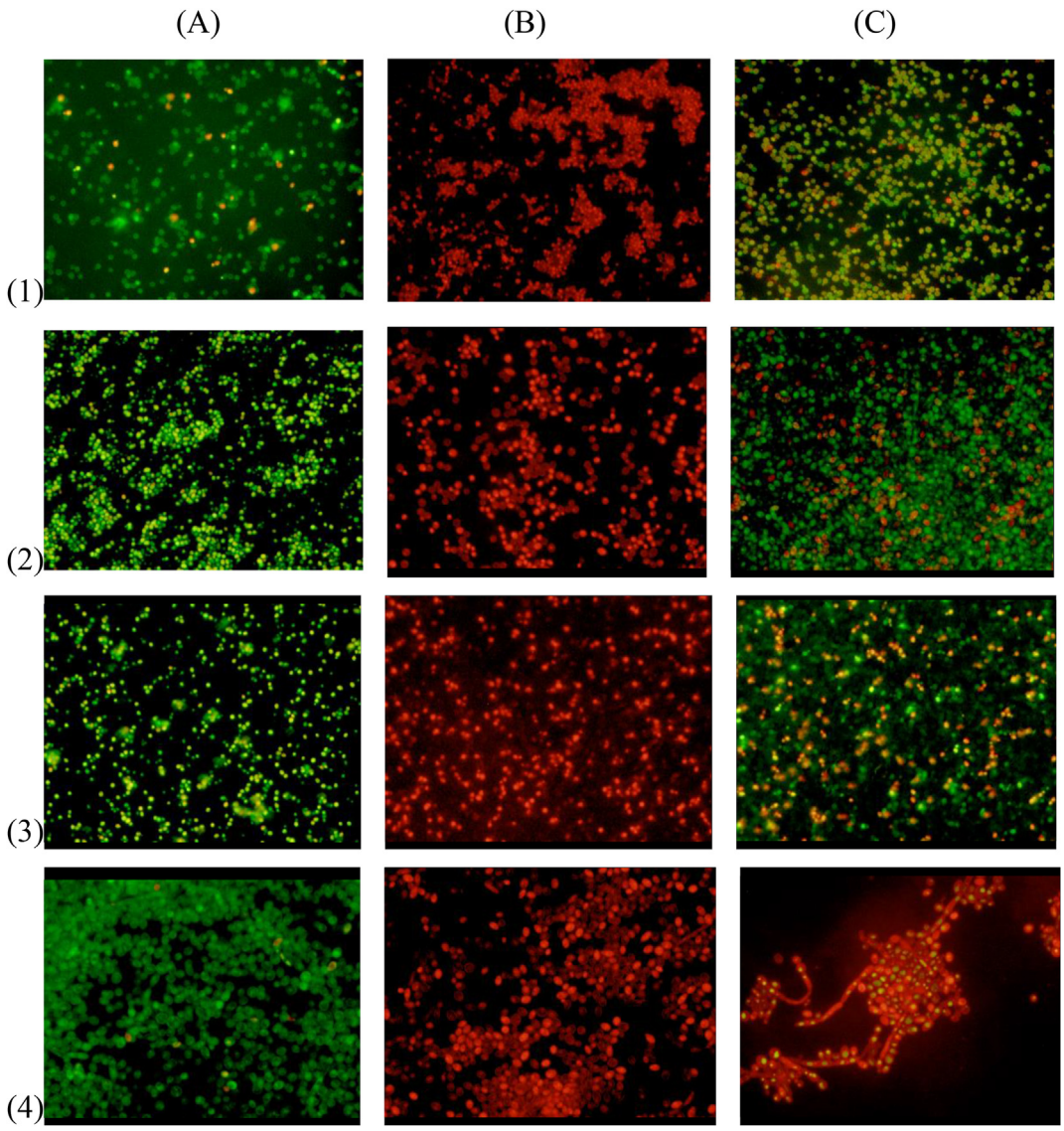

Figure 3. Fluorescence microscopy of *Candida* spp., Treated with ISO (MIC μg/mL) and FLC after 24 h. Cells were stained with OA/EB. *C. auris* (1) *C. albicans* (2), *C. glabrata* (3) and *C. tropicalis* (4). In column (A) untreated cells, (B) ISO treated cells and (C) FLC treated cells. Live cells appear green and dead cells red with double fluorescent staining.

3.6. Release of cellular material through the fungal membrane

The effect of ISO on the integrity of the *Candida* spp. membrane, and the release of cellular material at 0, 30, 60 and 120 min after ISO treatment was determined (Figure 6). The results are expressed as the absorbance of the sample (treated with ISO) minus the absorbance of the control (samples without ISO). The Student's T test with 95% confidence shows statistically significant differences between the effects of ISO and FLC against all *Candida* spp., in this study. Our results show a significant and marked, early release of cell content 1 h after ISO treatment compared to FLC-treated cells and untreated cells in all isolates evaluated in this study, probably as a result of damage to the cytoplasmic membrane, altering the permeability and causing leakage of intracellular material; the effect on the function and structure of the membrane has been generally used to explain the antimicrobial action of terpenes; as a result of their lipophilic character, they can interact with the membrane resulting in expansion, increased fluidity and permeability of the membrane, alteration of proteins embedded in the membrane, inhibition of respiration and alteration of the ion transport process as reported by (Trombetta et al., 2005).

3.7. Extracellular pH

The extracellular pH of the fungal cells treated with ISO, FLC and cells not treated is shown in Figure 7. The extracellular pH in *C. auris* decreased in the first 60 min and then increased unlike untreated cells and the cells with FLC; while the extracellular pH in *C. albicans* and *C. glabrata* decreased in the first 30 min, to then significantly increase in the cells treated with ISO unlike the cells treated with FLC and the cells without treatment. In contrast, the extracellular pH of *C. tropicalis* showed a considerable increase in the first 30 min and was constantly increasing. In the species of *C. albicans*, *C. glabrata* and *C. tropicalis*, the analysis of variance shows statistically significant differences between the averages of extracellular pH of the different groups, the honest Tukey test with 95% confidence shows significant differences between the extracellular pH means of the ISO-treated groups and the other groups (FLC-treated and untreated). With *C. auris*, although differences are observed, according to the analysis of variance with 95% confidence, these differences are not statistically significant, with a p-value > 0.05. In all cases, the extracellular pH of the cells treated with ISO is superior to the values obtained with the cells treated with fluconazole and those not

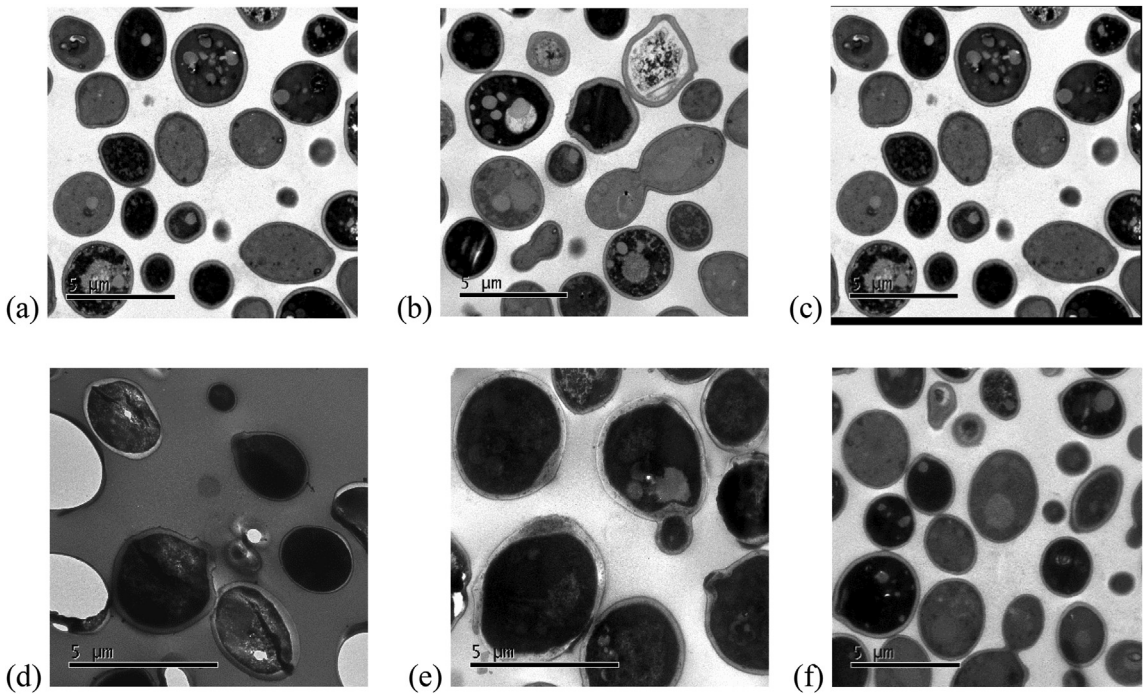

Figure 4. TEM analysis of *C. albicans*. (a, b, c) *C. albicans* treated with ISO. (d) *C. albicans* without treatment. (e and f) *C. albicans* treated with FLC.

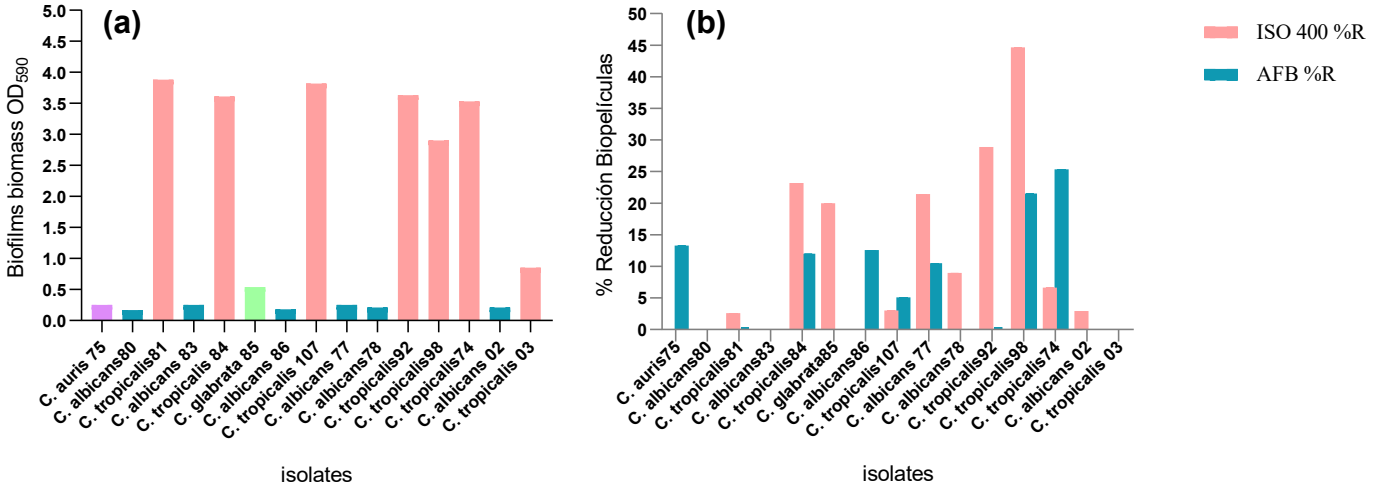

Figure 5. Effect of ISO on *C. auris*, *C. albicans*, *C. glabrata* and *C. tropicalis*. (a) shows the formation of biofilms at 37 °C for 48 h. (b) shows the percentage of biofilm reduction after 1 h of treatment with ISO (MIC µg/mL) and AFB (1.0 µg/mL).

treated. As we can observe, our results evidenced the early intracellular loss of protons, which is reflected with an increase in extracellular pH, more than that presented by the cells treated with fluconazole and the cells without treatment. Hyperpolarization has been reported as an important type of damage to the membrane and occurs mainly due to changes in pH or increase in ion movement affecting cellular homeostasis as reported by (Shi et al., 2016), it is our intention to suggest that the ISO powder alters the integrity of the membrane exchanging homeostasis, allowing the loss of ions and release of the cellular content, which could also be responsible for antifungal activity.

3.8. Integrity of the cellular membrane

The Evans blue staining also showed damage to the integrity of the membrane similar to the studies reported by (Donadu et al., 2021) with essential oil of *Ruta graveolens* against nosocomial cephalopods; studies of (Trombetta et al., 2005) suggest that this effect seems to depend on the composition of lipids and the net surface charge of the microbial membranes.

As indicated in Figure 8, the results show that when the cells were treated with ISO and observed under the light microscope, most of the cells stained blue, suggesting that the cell membranes were compromised after 1 h of treatment with ISO, therefore the ISO could act on the membrane affecting its integrity and consequently resulting in an increase in intracellular leakage of macromolecules, so we could suggest that the plasma membrane is a target of the ISO mode of action against *Candida* spp.

Our study revealed the antifungal effect of ISO against clinical isolates of Candida and highlights its possible potential usefulness as a component of new antifungals or as an adjunct in the treatment of infections caused by these yeasts. In addition, our results serve as the basis for future studies with a view to expanding our knowledge, establishing the mechanisms of antifungal action of the ISO.

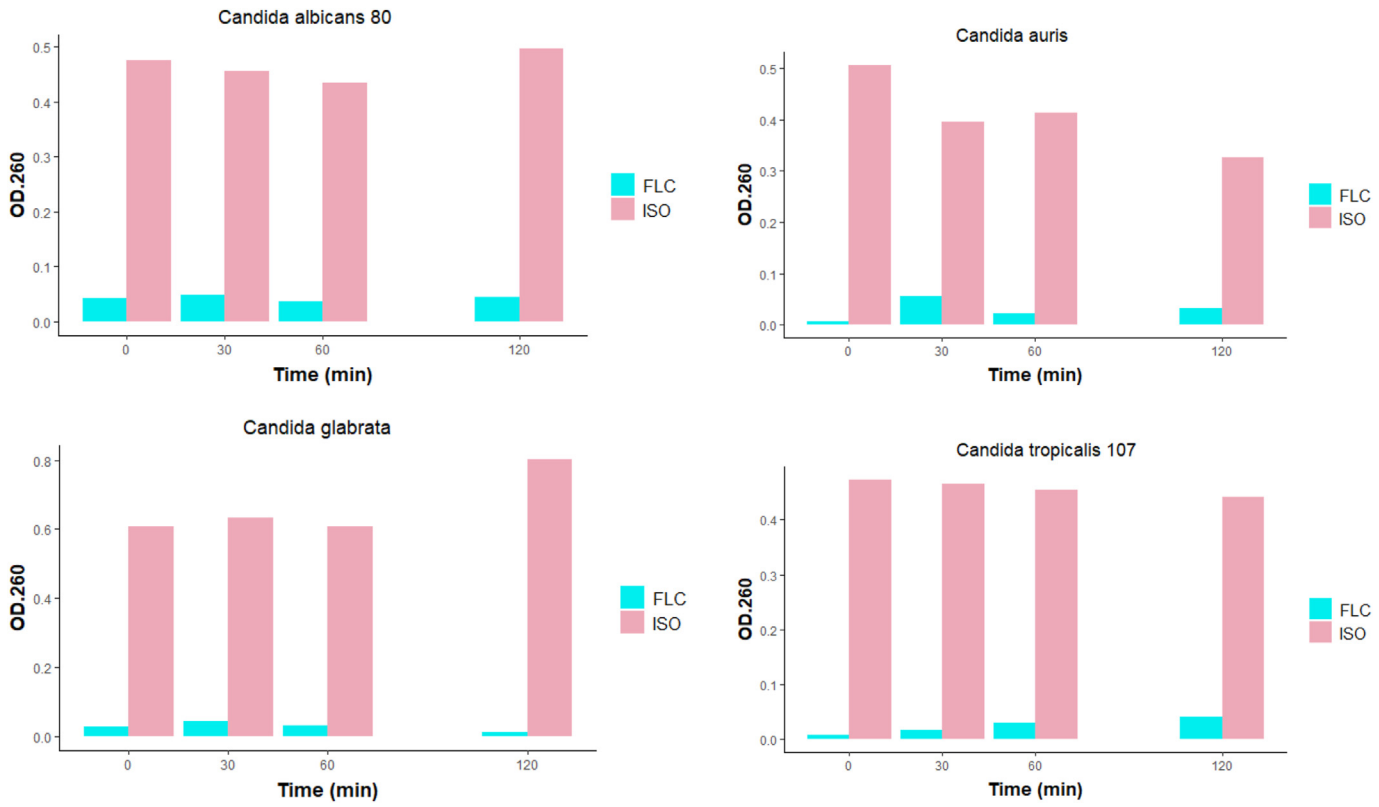

Figure 6. Effect of ISO and FLC on the release of intracellular components at 260 nm versus time. Significant differences are observed between the release of intracellular material from cells treated with ISO and cells treated with FLC.

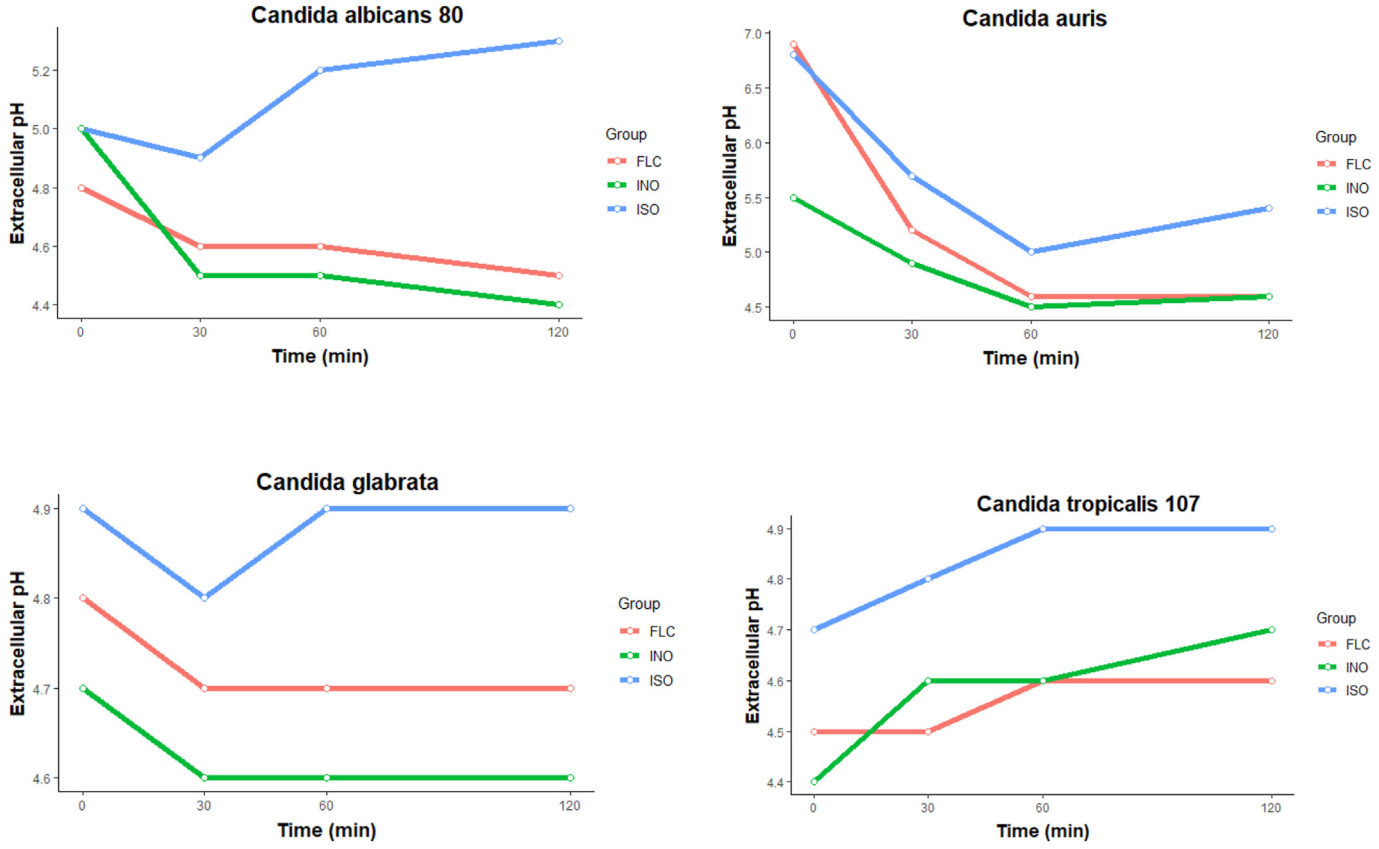

Figure 7. Extracellular pH of *Candida* spp., treated with ISO, FLC and untreated cells (INO). Important significant differences are observed between the increase in pH of the ISO-treated cells compared to the FLC-treated cells and the untreated cells.

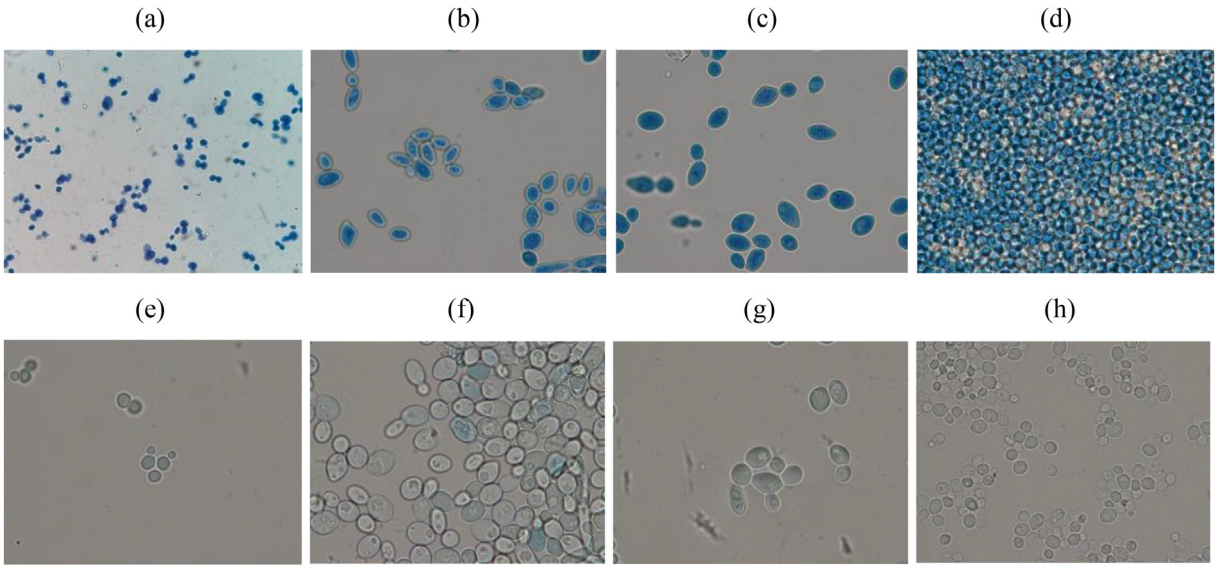

Figure 8. Microscopic observation (100x) of *C. albicans* (a), *C. tropicalis* (b), *C. glabrata* (c) and *C. auris* (d) before and after treatment with ISO: (a, b, c, d) cells treated with ISO (MIC) and control samples, not treated (e, f, g, h).

4. Conclusions

In conclusion, the results found allow us to propose that the antifungal activity of ISO is due, at least partially, to the fact that this molecule is capable of disturbing the integrity of fungal plasma membranes, resulting in the alteration of the permeability of the membrane and the consequent loss of intracellular material. Therefore, ISO is a natural chemical compound with antifungal properties.

Declarations

Author contribution statement

Orfa Inés Contreras Martínez; Alberto Angulo Ortíz; Gilmar Santafé Patiño: Conceived and designed the experiments; Performed the experiments; Analyzed and interpreted the data; Contributed reagents, materials, analysis tools or data; Wrote the paper.

Funding statement

Orfa Inés Contreras Martínez was supported by Universidad de Córdoba (FCB-02-19 project).

Data availability statement

Data will be made available on request.

Declaration of interest's statement

The authors declare no conflict of interest.

Additional information

No additional information is available for this paper.

Acknowledgements

The authors acknowledge: To the Social Health Clinic IPS S.A.S. Sincelejo, Sucre, Colombia. Under the coordination of Dr. Eimi Brango Tarra and Yuly Paulin Ortíz for donating the clinical isolates used in this study.

Orfa Contreras Martínez thanks the scholarship program of the Ministry of Science, Technology and Innovation of Colombia for the granting of the doctoral scholarship.

References

Arango, N., Vanegas, N., Sáez, J., García, C., Rojano, B., 2007. Actividad antifúngica del isoespintanol sobre hongos del género Colletotricum. Sci. Tech. 33, 279–280.

Avato, P., 2020. Editorial to the special Issue –" natural products and drug discovery. Molecules 25, 1128.

Aylate, A., Agize, M., Ekero, D., Kiros, A., Ayledo, G., Gendiche, K., 2017. In-Vitro and In-Vivo Antibacterial Activities of Croton Macrostachyus Methanol Extract against E. coli and S. aureus. Adv. Anim. Vet. Sci. 5, 107–114.

Bongomin, F., Gago, S., Oladele, R., Denning, D., 2017. Global and multi-national prevalence of fungal diseases-estimate precision. J. Fungi 3, 1–29.

Byvaltsev, V.A., Bardonova, L.A., Onaka, N.R., Polkin, R.A., 2019. Acridine orange : a Review of Novel Applications for surgical cancer imaging and therapy. Front. Oncol. 9 (September), 1–8.

Cantón, E., Martín, E., Espinel-Ingroff, A., 2007. Métodos estandarizados por el CLSI para el estudio de la sensibilidad a los antifúngicos (documentos M27-A3, M38-A y M44-A). Revista Iberoamericana de Micología.

Carvajal, S.K., Alvarado, M., Rodriguez, Y.M., Parra-Giraldo, C.M., Varón, C., Morales, S.E., Rodriguez, J., Gómez, B.L., Escandón, P., 2021. Pathogenicity assessment of Colombian strains of *Candida auris* in the *Galleria mellonella* invertebrate model. J. Fungi 7, 1–10.

Chaves-Lopez, C., Nguyen, H.N., Oliveira, R.C., Nadres, E.T., Paparella, A., Rodrigues, D.F., 2018. A morphological, enzymatic and metabolic approach to elucidate apoptotic-like cell death in fungi exposed to h- and α-molybdenum trioxide nanoparticles. Nanoscale 10, 20702–20716.

Chen, P., Chuang, Y., Wu, U., Sun, H., Wang, J., Sheng, W., Chen, Y., Chang, S., 2021. Mechanisms of azole resistance and trailing in *Candida tropicalis* Bloodstream isolates. J. Fungi 7 (8).

Cheng, R., Xu, Q., Hu, F., Li, H., Yang, B., Duan, Z., Zhang, K., Wu, J., Li, W., Luo, Z., 2021. Antifungal activity of MAF-1A peptide against *Candida albicans*. Int. Microbiol. 24, 233–242.

De Oliveira Lima, M.I., Araújo de Medeiros, A.C., Souza Silva, K.V., Cardoso, G.N., de Oliveira Lima, E., de Oliveira Pereira, F., 2017. Investigation of the antifungal potential of linalool against clinical isolates of fluconazole resistant *Trichophyton rubrum*. J. Mycol. Med. 27 (2), 195–202.

De Oliveira Pereira, F., Moura Mendes, J., De Oliveira Lima, E., 2013. Investigation on mechanism of antifungal activity of eugenol against *Trichophyton rubrum*. Med. Mycol. 51 (July), 507–513.

Dias de Castro, R., Souza, P. A. de, Dornelas Bezerra, L., Silva Ferreira, G., Melo de Brito Costa, E., Leite Cavalcanti, A., 2015. Antifungal activity and mode of action of thymol and its synergism with nystatin against Candida species involved with infections in the oral cavity: an *in vitro* study. BMC Compl. Alternative Med. 15 (1).

Donadu, M.G., Peralta-Ruiz, Y., Usai, D., Maggio, F., Molina-Hernandez, J.B., Rizzo, D., Bussu, F., Rubino, S., Zanetti, S., Paparella, A., Chaves-Lopez, C., 2021. Colombian essential oil of *Ruta graveolens* against nosocomial antifungal resistant Candida strains. Journal of Fungi 7, 383.

El-Kholy, M.A., Helaly, G.F., El Ghazzawi, E.F., El-Sawaf, G., Shawky, S.M., 2021. Virulence factors and antifungal susceptibility profile of *C . Tropicalis* isolated from various clinical specimens in. J. Fungi 7 (5).

Gavilánez, T.C., Colareda, G.A., Ragone, M.I., Bonilla, M., Rojano, B.A., Schinella, G.R., Consolini, A.E., 2018. Intestinal, urinary and uterine antispasmodic effects of isoespintanol, metabolite from *Oxandra xylopioides* leaves. Phytomedicine 51, 20–28.

Gintjee, T.J., Donnelley, M.A., Thompson III, G.R., 2020. Aspiring antifungals : Review of current antifungal pipeline developments. J. Fungi 6 (28).

Guembe, M., Cruces, R., Peláez, T., Mu, P., Bouza, E., 2017. Assessment of biofilm production in Candida isolates according to species and origin of infection. Enferm. Infecc. Microbiol. Clín. 35 (1), 37–40.

Hassan, Y., Chew, S.Y., 2021. Candida glabrata : pathogenicity and resistance mechanisms for adaptation and survival. Journal of Fungi 7.

Janbon, G., Quintin, J., Lanternier, F., Enfert, D., 2019. Studying Fungal Pathogens of Humans and Fungal Infections : Fungal Diversity and Diversity of Approaches. Gene Immun.

Kakar, A., Holzknecht, J., Dubrac, S., Gelmi, M.L., Romanelli, A., 2021. New perspectives in the antimicrobial activity of the Amphibian Temporin B : peptide Analogs are effective Inhibitors of *Candida albicans* growth. J. Fungi 7 (6).

Marcos-zambrano, L.J., Escribano, P., Bouza, E., Guninea, J., 2014. Production of biofilm by Candida and non- Candida spp. isolates causing fungemia : Comparison of biomass production and metabolic activity and development of cut-off points. Int. J. Med. Microbiol. 304 (8), 1192–1198.

Mekonnen Bayisa, Y., Aga Bullo, T., 2021. Optimization and characterization of oil extracted from *Croton macrostachyus* seed for antimicrobial activity using experimental analysis of variance. Heliyon 7.

Mukherjee, P.K., Long, L., Kim, H.G., Ghannoum, M.A., 2009. International Journal of Antimicrobial Agents Amphotericin B lipid complex is efficacious in the treatment of *Candida albicans* biofilms using a model of catheter-associated Candida biofilms. Int. J. Antimicrob. Agents 33 (2), 149–153.

Murphy Cowan, M., 1999. Plant products as antimicrobial Agents. Clin. Microbiol. Rev. 12 (4), 564–582.

Naman, C.B., Benatrehina, P.A., Kinghorn, A.D., 2016. Pharmaceuticals, plant drugs. In: Encyclopedia of Applied Plant Sciences, , second ed.2. Elsevier.

Oliveira Lima, I., de Oliveira Pereira, F., Araújo de Oliveira, W., de Oliveira Lima, E., Albuquerque Menezes, E., 2013. Antifungal activity and mode of action of carvacrol against *Candida albicans* strains. J. Essent. Oil Res. 25 (2), 37–41.

Prażyńska, M., Bogiel, T., Gospodarek-Komkowska, E., 2018. *In vitro* activity of micafungin against biofilms of *Candida albicans* , *Candida glabrata* , and *Candida parapsilosis* at different stages of maturation. Folia Microbiol. 63 (2), 209–216.

Quave, C.L., Plano, L.R.W., Pantuso, T., Bennett, B.C., 2008. Effects of extracts from Italian medicinal plants on planktonic growth, biofilm formation and adherence of methicillin-resistant *Staphylococcus aureus*. J. Ethnopharmacol. 118 (3), 418–428.

Ramírez, R.D., Páez, M.S., Angulo, A.A., 2015. Obtención de isoespintanol por hidrodestilación y cristalización a partir del extracto bencínico de *Oxandra xylopioides*. Inf. Tecnol. 26 (6), 13–18.

Rinaldi, G.J., Rojano, B., Schinella, G., Mosca, S.M., 2019. Participation of NO in the vasodilatory action of isoespintanol. Vitae 26, 78–83.

Rodriguez-Tudela, J.L., 2003. Method for Determination of Minimal Inhibitory Concentration (MIC) by Broth Dilution of Fermentative Yeasts EUCAST Discussion Document E . Dis 7 . 1 JUNE 2002. In: Method for the determination of minimum inhibitory concentration (MIC) by broth dilution of. Clin. Microbiol. Infect., August.

Rojano, B.A., Gaviria, C.A., Gil, M.A., Sáez, J.A., Schinella, G.R., Tournier, H., 2008. Antioxidant activity of the isoespintanol in diferent media. Vitae 15 (1), 173–181.

Rojano, B.A., Montoya, S., Yépez, F., Saez, J., 2007. Evaluación de isoespintanol aislado de *Oxandra cf. xylopioides* (Annonaceae) sobre *Spodoptera frugiperda* J.E. SMITH (Lepidoptera: noctuidae). Rev. Fac. Nac. Agron. Medellin 60, 3691–3702.

Rojano, B., Pérez, E., Figadère, B., Martin, M.T., Recio, M.C., Giner, R., Ríos, J.L., Schinella, G., Sáez, J., 2007. Constituents of *Oxandra cf. xylopioides* with anti-inflammatory activity. J. Nat. Prod. 70 (5), 835–838.

Scorneaux, B., Angulo, D., Borroto-Esoda, K., Ghannoum, M., Peel, M., Wring, S., 2017. SCY-078 is fungicidal against Candida species in time-kill studies. Antimicrob. Agents Chemother. 61 (3), 1–10.

Shi, C., Sun, Y., Zheng, Z., Zhang, X., Song, K., Jia, Z., Chen, Y., Yang, M., Liu, X., Dong, R., Xia, X., 2016. Antimicrobial activity of syringic acid against *Cronobacter sakazakii* and its effect on cell membrane. Food Chem. 197, 100–106.

Tao, N., Ouyang, Q., Jia, L., 2014. Citral inhibits mycelial growth of *Penicillium italicum* by a membrane damage mechanism. Food Control 41, 116–121.

Tascini, C., Sozio, E., Corte, L., Sbrana, F., 2017. The role of biofilm forming on mortality in patients with candidemia : a study derived from real world data. Infect. Dis. 50 (3), 1–6.

Trombetta, D., Castelli, F., Sarpietro, M.G., Venuti, V., Cristani, M., Daniele, C., Saija, A., Mazzanti, G., Bisignano, G., 2005. Mechanisms of antibacterial action of three monoterpenes. Antimicrob. Agents Chemother. 49 (6), 2474–2478.

Wu, G.P., Chen, S.H., Levin, R.E., 2015. Application of ethidium bromide Monoazide for quantification of viable and dead cells of *Salmonella enterica* by real-time loop-mediated isothermal amplification. J. Microbiol. Methods 117, 41–48.

Zhang, X., Zhang, T., Guo, S., Zhang, Y., Sheng, R., Sun, R., Chen, L., Lv, R., Qi, Y., 2020. *In vitro* antifungal activity and mechanism of Ag3PW12O40 composites against Candida species. Molecules 25, 6012.

Anexo 5

"Transcriptional Reprogramming of *Candida tropicalis* in Response to Isoespintanol Treatment"

Journal of Fungi

IMPACT FACTOR 4.7

Indexed in: PubMed

CITESCORE 4.9

Article

Transcriptional Reprogramming of *Candida tropicalis* in Response to Isoespintanol Treatment

Orfa Inés Contreras-Martínez, Alberto Angulo-Ortíz, Gilmar Santafé-Patiño, Katia Aviña-Padilla, María Camila Velasco-Pareja and María Fernanda Yasnot

Special Issue

Pathogenesis in Human Fungal Pathogens

Edited by

Prof. Dr. Tongbao Liu and Prof. Dr. Chen Ding

MDPI

https://doi.org/10.3390/jof9121199

Journal of *Fungi*

MDPI

Article

Transcriptional Reprogramming of *Candida tropicalis* in Response to Isoespintanol Treatment

Orfa Inés Contreras-Martínez [1,*], Alberto Angulo-Ortíz [2], Gilmar Santafé-Patiño [2], Katia Aviña-Padilla [3], María Camila Velasco-Pareja [4] and María Fernanda Yasnot [4]

1 Biology Department, Faculty of Basic Sciences, University of Córdoba, Montería 230002, Colombia
2 Chemistry Department, Faculty of Basic Sciences, University of Córdoba, Montería 230002, Colombia; aaangulo@correo.unicordoba.edu.co (A.A.-O.); gsantafe@correo.unicordoba.edu.co (G.S.-P.)
3 Center for Research and Advanced Studies of the I.P.N. Unit Irapuato, Irapuato 36821, Mexico; ib.katia@gmail.com
4 Bacteriology Department, Faculty of Health Sciences, University of Córdoba, Montería 230002, Colombia; mariavelascop@correo.unicordoba.edu.co (M.C.V.-P.); myasnot@correo.unicordoba.edu.co (M.F.Y.)
* Correspondence: oicontreras@correo.unicordoba.edu.co

Abstract: *Candida tropicalis*, an opportunistic pathogen, ranks among the primary culprits of invasive candidiasis, a condition notorious for its resistance to conventional antifungal drugs. The urgency to combat these drug-resistant infections has spurred the quest for novel therapeutic compounds, with a particular focus on those of natural origin. In this study, we set out to evaluate the impact of isoespintanol (ISO), a monoterpene derived from *Oxandra xylopioides*, on the transcriptome of *C. tropicalis*. Leveraging transcriptomics, our research aimed to unravel the intricate transcriptional changes induced by ISO within this pathogen. Our differential gene expression analysis unveiled 186 differentially expressed genes (DEGs) in response to ISO, with a striking 85% of these genes experiencing upregulation. These findings shed light on the multifaceted nature of ISO's influence on *C. tropicalis*, spanning a spectrum of physiological, structural, and metabolic adaptations. The upregulated DEGs predominantly pertained to crucial processes, including ergosterol biosynthesis, protein folding, response to DNA damage, cell wall integrity, mitochondrial activity modulation, and cellular responses to organic compounds. Simultaneously, 27 genes were observed to be repressed, affecting functions such as cytoplasmic translation, DNA damage checkpoints, membrane proteins, and metabolic pathways like trans-methylation, trans-sulfuration, and trans-propylamine. These results underscore the complexity of ISO's antifungal mechanism, suggesting that it targets multiple vital pathways within *C. tropicalis*. Such complexity potentially reduces the likelihood of the pathogen developing rapid resistance to ISO, making it an attractive candidate for further exploration as a therapeutic agent. In conclusion, our study provides a comprehensive overview of the transcriptional responses of *C. tropicalis* to ISO exposure. The identified molecular targets and pathways offer promising avenues for future research and the development of innovative antifungal therapies to combat infections caused by this pathogenic yeast.

Keywords: transcriptomics; *Candida tropicalis*; isoespintanol; genetic dysregulation; mitochondria; cell wall

Citation: Contreras-Martínez, O.I.; Angulo-Ortíz, A.; Santafé-Patiño, G.; Aviña-Padilla, K.; Velasco-Pareja, M.C.; Yasnot, M.F. Transcriptional Reprogramming of *Candida tropicalis* in Response to Isoespintanol Treatment. *J. Fungi* **2023**, *9*, 1199. https://doi.org/10.3390/jof9121199

Academic Editors: Tongbao Liu and Chen Ding

Received: 10 November 2023
Revised: 12 December 2023
Accepted: 13 December 2023
Published: 15 December 2023

1. Introduction

Candidemias represent a significant healthcare challenge, ranking among the foremost causes of morbidity and mortality, particularly in patients with healthcare-associated infections (HAI) [1–5]. Invasive candidiasis (IC) accounts for over 95% of these infections, with *Candida albicans*, *Candida glabrata*, *Candida tropicalis*, *Candida parapsilosis*, *Candida krusei*, and, in certain regions, *Candida auris* being the primary culprits. The Latin American region witnesses a significant burden of IC, with incidence rates ranging from 0.74 to 6.0 per 1000 hospital admissions and alarmingly high mortality rates ranging from 30%

to 76% [6–9]. Notably, admission to intensive care units (ICUs) significantly escalates the risk, with at least half of ICU patients succumbing to this diagnosis [10]. The surge in infections by these Candida species is attributed to multiple factors, encompassing sustained exposure to antifungal agents, the utilization of catheters in hospitalized patients, underlying malignancies, advancing age, and geographic distribution [11]. Furthermore, the development of antifungal resistance and the capacity to elude host immunity add to the intricate challenge of managing candidiasis in clinical practice [12,13].

Candida tropicalis has emerged as one of the most important non-albicans Candida spp., due to its high incidence in systemic candidiasis and greater resistance to commonly used antifungals [14,15]. This pathogen not only possesses the capability to infiltrate vital organs [16] but is also linked to elevated mortality rates when compared to *C. albicans* and other non-albicans Candida species. *Candida tropicalis* exhibits a propensity for dissemination, particularly among neutropenic individuals and those grappling with malignancies, notably in cases demanding prolonged catheterization, extensive use of broad-spectrum antibiotics, or underlying cancer [17]. Recent increases in antifungal resistance have been associated with mutations in the *ERG11* gene, encoding ergosterol-synthase, and the overexpression of the transcriptional regulator *UPC2* [18,19]. Considering these developments, *Candida tropicalis* has emerged as a prominent etiological agent in IC, notably in Latin America and certain Asian countries, further accentuating its clinical significance [20,21].

Regrettably, the three principal antifungal drug classes (polyenes, echinocandins, and azoles) have been unable to stem the surge in life-threatening fungal infections observed over the past few decades [22]. In response to this pressing clinical challenge, compounds derived from botanical sources have gained traction as a promising alternative [23–25]. In our previous investigations, we established that isoespintanol (ISO), a monoterpene derived from *Oxandra xylopioides*, exhibits potent antifungal properties against *Candida tropicalis* [26,27]. Our findings elucidated ISO's ability to induce intracellular reactive oxygen species, disrupt cell membranes, and eradicate mature biofilms as part of its multifaceted antifungal action.

However, the precise mechanism by which ISO orchestrates genetic dysregulation in *Candida tropicalis* remains an enigma. Herein, we propose that ISO plays a pivotal role in reshaping the transcriptional landscape of *Candida tropicalis*. Our primary objective is to decipher the differential gene expression patterns underlying processes such as membrane biogenesis and biofilm formation, among other critical biological pathways impacted by ISO. By delving into the potential targets of this antifungal biomolecule and their distinctive gene expression profiles, our research offers essential insights. These insights are poised to unlock novel therapeutic avenues for the treatment of candidiasis, presenting a holistic understanding of the genetic perturbations provoked by ISO.

Our study endeavors to provide a perspective on potential therapeutic targets in the battle against candidiasis. Our transcriptomics-based approach offers a comprehensive view of the biological behavior of these pathogenic yeasts and their genetic adaptations when exposed to ISO. These findings hold the promise of paving the way for innovative therapies to combat these resilient pathogens within the realm of medical practice.

2. Materials and Methods

2.1. Isolation and Identification of Isoespintanol

Isoespintanol (ISO) was isolated from "*yaya prieta*" leaves (*Oxandra xylopioides*) collected in October 2019. The specimen was located at coordinates 08°48′17″ north latitude and 75°42′07″ west longitude in the Municipality of Montería, Department of Córdoba, Colombia. A herbarium specimen (collection number JAUM 037849) was deposited in the Joaquín Antonio Uribe Botanical Garden in Medellín, Colombia. To isolate ISO, 5 g of petroleum benzine extract was subjected to hydrodistillation and successive crystallizations with *n*-hexane, following a modified version of the methodology described in [28]. This process yielded 1.2 g of purified ISO. The purity of ISO was confirmed using gas chromatography coupled to a Thermo Scientific model Trace 1310 mass spectrometer equipped

with an AB-5MS column (30 m × 0.25 mm id × 0.25 µm). The temperature gradient system initiated at 80 °C for 10 min and increased to 200 °C at a rate of 10 °C/min. Subsequently, the temperature was raised to 240 °C at 4 °C/min and finally to 290 °C for 10 min at 10 °C/min. The injection was split less, with a volume of 1 µL. Mass spectrometry was conducted in electron impact ionization mode at 70 eV, and ion detection was performed in positive full-scan mode. The structure of ISO was elucidated through a combination of spectroscopic techniques, including ^{1}H-NMR, ^{13}C-NMR, DEPT, ^{1}H-^{1}H COSY, HMQC, and HMBC spectra. These analyses were performed on a 400 MHz Bruker Advance DRX spectrometer using deuterated chloroform ($CDCl_3$) as the solvent.

2.2. Yeast Strain and Culture Conditions

The yeast strain utilized in this study, identified as *Candida tropicalis* (CLI007), was originally isolated from a blood culture sample obtained from a hospitalized patient at Salud Social S.A.S. in Sincelejo, Colombia. Standard methods for yeast identification, including Vitek 2 Compact, Biomerieux SA, Y.S.T. Vitek 2 Card, and AST-YS08 Vitek 2 Card (Ref 420739), were employed to initially identify the yeast strain. Further confirmation of its identification was established through a comprehensive genome-wide taxonomic study, as detailed in Contreras [26]. To maintain the yeast cultures, Sabouraud Dextrose Agar (SDA) and BBL CHROMagar Candida media were employed. Prior to conducting the experiments, a yeast suspension was meticulously adjusted to a concentration of 10^7 colony-forming units per milliliter (CFU/mL) in phosphate-buffered saline (PBS) with a pH of 7.4. This standardized yeast suspension served as the inoculum for the subsequent assays.

2.3. RNA-Sequencing and Read Count Data Acquisition

Total RNA was extracted from yeast samples following a 4 h exposure to ISO at its minimum inhibitory concentration (MIC: 391.6 µg/mL) [26]. Additionally, control yeast samples without ISO treatment were processed in parallel. RNA extraction was carried out using the Trizol reagent, following the manufacturer's standard protocol (Trizol TM Reagent, Invitrogen (Vilnius, Lithuania); Total RNA extraction protocol). The quantification of the total RNA was performed using the ribogreen colorimetric method (Invitrogen, Vilnius, Lithuania). Furthermore, the integrity of the RNA was assessed by measuring the RNA Integrity Number (RIN) through capillary electrophoresis on an Agilent 2100 bioanalyzer (Agilent Technologies, Santa Clara, CA, USA). A RIN score exceeding 7.0 was established as the threshold for acceptable RNA quality. Subsequently, the extracted RNA was employed to construct RNA-Seq libraries for sequencing, utilizing the Illumina Novaseq platform with 150 bp paired-end sequencing (Illumina-Transcriptome, TruSeq mRNA/Illumina). For the generation of RNA counts, *Bowtie 2* was utilized, aligning the sequencing data to the Ensemble GTF files corresponding to the reference genome *Candida tropicalis* (REF GCA000006335v3).

2.4. Bioinformatics Analyses

2.4.1. Differential Gene Expression Analysis

To identify differentially expressed genes (DEGs), we utilized the read counts generated from the RNA-sequencing data. The differential gene expression analysis was conducted using the *EdgeR* package within the RStudio environment. The dataset was submitted to the analysis pipeline to assess the directionality of gene expression changes between two stages: Stage A, which comprised control/untreated *Candida tropicalis* samples, and Stage B, which included ISO-treated *Candida tropicalis* samples. We considered genes with a log2-fold change (Log2FC) greater than 1 and a false discovery rate (FDR) less than 0.05 as significant DEGs. DEGs with positive Log2-fold change and significant *p*-values were categorized as exhibiting increased expression (UP), while DEGs with negative Log2-fold change represented decreased expression (DN). Genes with *p*-values exceeding

0.05 were categorized as showing no significant change in expression between the two stages (NC).

2.4.2. Functional Enrichment Analysis for DEGs

Functional enrichment analysis was conducted on the set of 186 differentially expressed genes (DEGs) identified in the *Candida tropicalis* dataset. This analysis was performed using gene set enrichment analysis (GSEA), encompassing all Gene Ontology (GO) terms. To ensure robustness, GO terms with values exceeding 0.05 were filtered out from the analysis. Subsequently, the resulting *p*-values underwent adjustment for multiple hypothesis testing using the Benjamini and Hochberg approach [29]. For the assessment of functional enrichment, two distinct gene sets were examined: the upregulated genes (UP) and the downregulated genes (DN). The background universe for these analyses was defined as the total number of DEGs. To facilitate data analysis and visualization, we employed ShinyGO 0.77 [30], based on the *Candida tropicalis* genome derived from STRING-db. This resource provided comprehensive insights into the functional enrichment of GO terms (http://bioinformatics.sdstate.edu/go, accessed on 10 May 2023).

2.5. Computational Prediction of DEGs and Primer Design

To enhance the functional annotation of the transcriptome, we obtained an orthologous gene pair list between *Candida tropicalis* and *Candida albicans* from the Ensembl database. This was achieved through the utilization of the BioMart package, facilitated by R scripts. From the pool of 186 differentially expressed genes (DEGs), we refined our selection to focus on genes enriched in key biological functions, namely mitochondria, cell wall, lipid metabolism, and general metabolism. For data visualization, we employed the RStudio environment to create plots featuring the selected genes. Subsequently, we designed primers for specific genes of interest, namely ERG6 (upregulated, associated with steroid metabolism), KRE1 (upregulated, linked to cell wall processes), and CTRG_03786 (downregulated, implicated in cell wall functions). These primers were designed using PrimerQuest (IDT, Integrated DNA Technologies, MI, USA, https://www.idtdna.com/pages/tools/primerquest?returnurl=/PrimerQuest/Home/Index accessed on 16 June 2023). For primer details, please refer to Table S1 in Supplementary Materials.

2.6. Gene Expression Assessment by Quantitative RT-PCR

For experimental validation, RNA isolation was carried out using the TRIzol® reagent, following the manufacturer's instructions precisely (Trizol TM Reagent, Invitrogen, Vilnius, Lithuania; Total RNA extraction protocol), as previously detailed in Section 2.3. For gene expression analysis, cDNA synthesis was conducted using SuperScript III (Invitrogen Cat No. 12574026) following the manufacturer's recommended protocols. Quantitative RT-PCR was performed using the StepOnePlus system (Applied Biosystems, Vilnius, Lithuania) with Power Up SYBR Master Mix (Applied Biosystems). This approach allowed us to determine the relative expression levels of mRNA transcripts for three target genes: ERG6, KRE1, and CTRG_03786. The housekeeping gene ACTIN-1 served as the reference for normalization. Each reaction mixture consisted of 100 ng of cDNA, 2X master mix, and 500 picomolar of each primer, resulting in a final volume of 10 µL. PCR cycling conditions encompassed an initial denaturation step at 95 °C for 2 min, followed by 40 cycles of 15 s at 95 °C, 15 s at 62 °C, and 60 s at 72 °C. The primer sequences for ERG6, KRE1, CTRG_03786, and ACTIN-1 [31] are detailed in Supplementary Table S1. Gene expression analysis was carried out employing the $2^{(-\Delta\Delta CT)}$ method of relative quantification [32].

2.7. Determination of Total Ergosterol Content

The quantification of the total ergosterol content in *C. tropicalis* isolates treated with ISO was conducted in accordance with the protocol outlined in [33], with some modifications. Initially, the cells were exposed to ISO at their respective minimum inhibitory concentrations (MICs) and incubated at 35 °C for a duration of 3 h. Subsequently, the

treated cells were subjected to centrifugation and washed with phosphate-buffered saline (PBS). To initiate ergosterol extraction, a wet weight of 0.5 g of cells was mixed with PBS. Saponification was achieved by adding 4 mL of a freshly prepared 30% (*w*/*v*) methanolic KOH solution and 8 mL of absolute ethanol. This mixture was maintained at 80 °C for a period of 1 h. The ensuing mixture was extracted using petroleum ether and then washed with a saturated NaCl solution. Following the extraction, the samples were concentrated under vacuum conditions at 60 °C. The resulting residue was dissolved in 0.5 mL of methanol and subsequently filtered through a 0.45 µm micromembrane. The quantification of ergosterol content was determined by comparing the peak areas of the samples against a standard curve generated from ergosterol (95% Sigma-Aldrich, St. Louis, MO, USA). The concentrations used in the standard curve spanned 1, 10, 50, 100, 250, 500, 750, and 1000 mg/L of ergosterol. Ergosterol content analysis was performed using a UHPLC Ultimate 3000 system (Thermo Scientific, Waltham, MA, USA) equipped with a diode array detector (DAD). A C18 Hypersil Gold column (150 mm × 4.6 mm, 5 µm) was maintained at 30 °C. Each injection had a volume of 30 µL, and the mobile phase consisted of methanol/water (97/3, 100% HPLC grade) at a flow rate of 0.6 mL/min. All measurements were conducted in triplicate, and ergosterol was detected at a wavelength of 205 nm.

The ergosterol inhibition ratio was calculated as follows:

Ergosterol Inhibition Ratio = (1 − Ergosterol Content of Treated Cells/Ergosterol Content of Untreated Cells) × 100%.

3. Results

3.1. Isolation and Purification of Isoespintanol Molecules

Isoespintanol (ISO) in the amount of 1.2 g was isolated and purified to a crystalline amorphous solid with a purity exceeding 99%. The high purity was verified using gas chromatography-mass spectrometry (GC-MS). Structural identification of ISO was accomplished through various spectroscopic techniques, including ^{1}H-NMR, ^{13}C-NMR, DEPT, ^{1}H-^{1}H COSY, HMQC, and HMBC. This rigorous analysis led to the unequivocal proposal of the structure of 2,5-dimethoxy-3-hydroxy-*p*-cymene isoespintanol, as illustrated in Figure 1. Furthermore, electron impact mass spectrometry (EI-MS) provided essential data, with the observed molecular ion at *m*/*z* 210 (49%) and prominent fragment ions at *m*/*z* 195 (100%), 180, 165, 150, 135, and 91. Detailed nuclear magnetic resonance (NMR) spectra were recorded. In the ^{1}H-NMR spectrum (400 MHz, $CDCl_3$), the chemical shifts were observed at δ 6.22 (singlet, 1H, H6), δ 5.85 (singlet, 1H, HO-3), δ 3.77 (singlet, 3H, H12), δ 3.76 (singlet, 3H, H11), δ 3.52 (heptet, J = 7.1 Hz, 1H, H8), δ 2.29 (singlet, 3H, H7), and δ 1.33 (doublet, J = 7.1 Hz, 6H, H9-H10). In the ^{13}C-NMR spectrum (100 MHz, $CDCl_3$), the carbon chemical shifts were observed at δ 154.3 (C5), δ 147.4 (C3), δ 139.7 (C2), δ 126.8 (C1), δ 120.4 (C4), δ 104.4 (C6), δ 24.6 (C8), δ 60.8 (C11), δ 55.7 (C12), δ 20.6 (C9, C10), and δ 15.8 (C7).

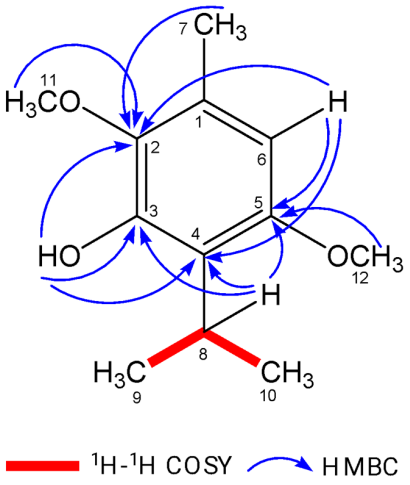

Figure 1. Key ^{1}H–^{1}H COSY and HMBC correlations of ISO.

3.2. RNA Preparation, Library Construction, and Sequence Analysis

The results of RNA extraction from *Candida tropicalis*, both with ISO treatment and without treatment (control), are summarized in Table S2. Specifically, we obtained a total RNA yield of 0.797 µg for ISO-treated samples and 0.785 µg for untreated control cells. For a detailed overview of the sequencing statistics and transcriptome data, including the mapping of reads to the *Candida tropicalis* reference genome (REF GCA000006335v3), please refer to Tables S3 and S4, in Supplementary Materials.

Transcriptomes obtained by RNA-seq were mapped on the reference genome *Candida_tropicalis* REF GCA000006335v3.

3.3. Analysis of the Transcriptional Profile of Differentially Expressed Genes

Our findings reveal distinct patterns of gene expression between yeast exposed to ISO and untreated yeast. A comprehensive analysis identified a total of 186 differentially expressed genes. Among these, 159 genes displayed induction in their expression levels, while 27 genes exhibited repression (Figure 2).

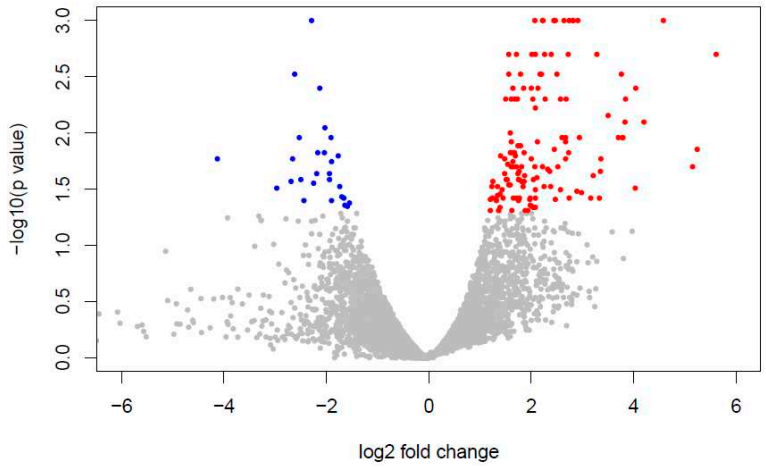

Figure 2. Differential gene expression analysis. Volcano plot of DEG; red (up) and blue (down) colored dots indicate the DEGs, while the gray dots represent genes without expression changes (NC) among *Candida tropicalis* and control samples.

Figure 3 presents the key DEGs that are upregulated and downregulated in response to ISO treatment in the *C. tropicalis* dataset. Noteworthy among the upregulated genes is the SET domain methyltransferase protein superfamily, encompassing proteins known for their histone methylation activity at lysine residues. Histone methylation is a pivotal process involved in chromatin regulation and gene expression [34]. Additionally, the upregulated genes encompass components of transmembrane transport systems, particularly those associated with the allenoate transport system [35]. Furthermore, genes related to the 3β-HSD enzyme system, crucial for the biosynthesis of various classes of steroid hormones, are observed [36,37]. The dataset also includes hydrolase enzyme genes involved in sphingolipid metabolism reactions [38,39], as well as genes contributing to the structural integrity of the ribosome.

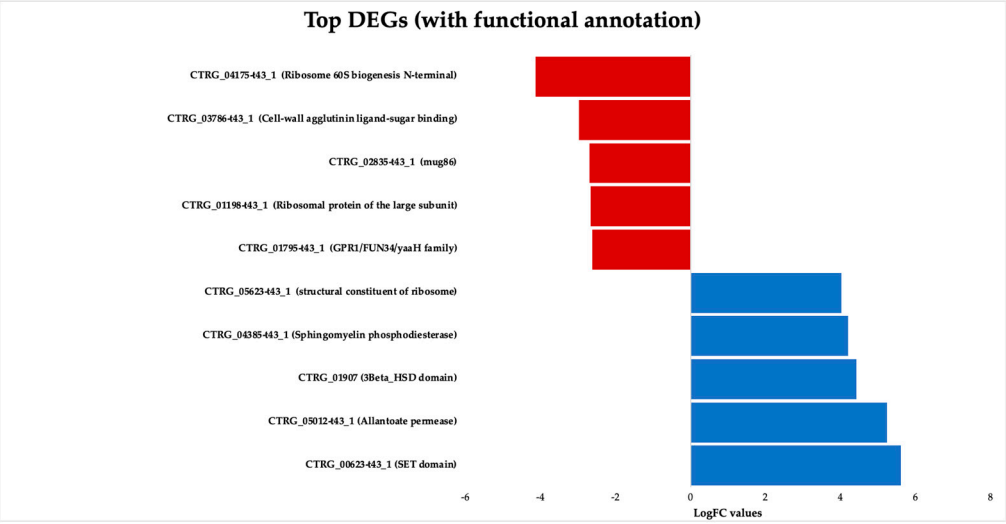

Figure 3. Top upregulated and downregulated genes with functional annotations in *Candida tropicalis* dataset. Bars show the top upregulated (red) and downregulated (blue) genes, according to their Log2FC values.

3.3.1. Stress Response, Metabolism, and Mitochondrial Functional Processes Are Enriched in Upregulated Genes in *C. tropicalis* Treated with ISO

In response to ISO treatment, upregulated genes in *C. tropicalis* were found to be associated with critical biological processes. Notably, these upregulated genes included ATP-dependent proteases of the Clpa/b family and the DnaJ domain (DnaJ/Hsp40: heat shock protein 40), which serve as essential chaperones involved in translation, protein folding, and protein translocation [40,41]. This suggests that ISO may impact protein synthesis in this yeast. Furthermore, the expression of the STI1 domain, known for its presence in the DNA damage response protein Rad23 [42], was notable. This domain has a role in recognizing DNA damage, indicating that ISO's antifungal action might involve DNA damage to these pathogens. The upregulated genes also included those from the Aldo-Keto Reductase (AKR) superfamily, catalyzing redox transformations essential for biosynthesis, intermediary metabolism, and detoxification [43]. Additionally, overexpression of zinc-binding dehydrogenase family proteins, involved in oxidoreductase and catalytic activities, was observed, suggesting their role in responding to oxidative stress. Moreover, proteins related to the cellular response to organic substances, such as dioxygenases catalyzing critical reactions in aerobic microbial degradation of aromatic compounds [44], were upregulated. Figure 4 illustrates the overexpression of genes associated with ergosterol biosynthesis, mitochondrial function, signaling pathways, and carbohydrate metabolism.

3.3.2. Upregulation of Specific Steroid and Cell Metabolism Genes Is an Effect of *C. tropicalis* Treated with ISO

Treatment of *Candida tropicalis* with ISO at its minimum inhibitory concentration (MIC) led to the notable upregulation of specific genes involved in ergosterol biosynthesis, including ERG1, ERG6, ERG2, and ERG26 (Figure 5). Ergosterol is a fundamental component of the plasma membrane, and the increased expression of these genes suggests that ISO might impact its synthesis. Additionally, our results indicate the induction of genes associated with metabolism and the upregulation of Vip1, an inositol polyphosphate kinase known for its role as a signaling molecule. Vip1 regulates various essential biophysical processes, including autophagy and pathogenicity in *C. albicans* [45].

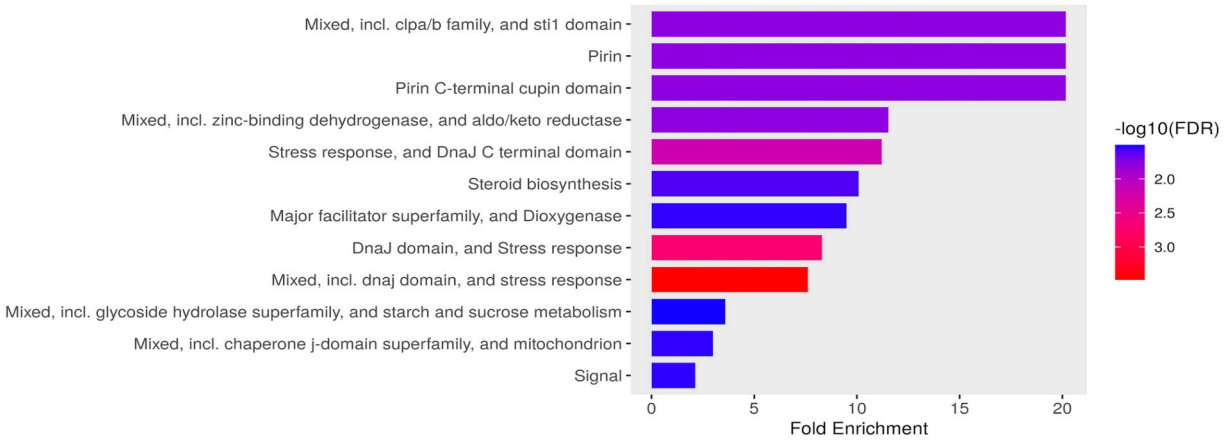

Figure 4. Functional enrichment of DEG in *Candida tropicalis* treatment. FDR is calculated based on a nominal *p*-value from the hypergeometric test. Fold Enrichment is defined as the percentage of differentially expressed genes belonging to a pathway, divided by the corresponding percentage in the background. FDR reports how likely the enrichment is by chance; higher values are colored on a scale of red to blue. In the x-axis, Fold Enrichment indicates how drastically genes of a certain pathway are overrepresented.

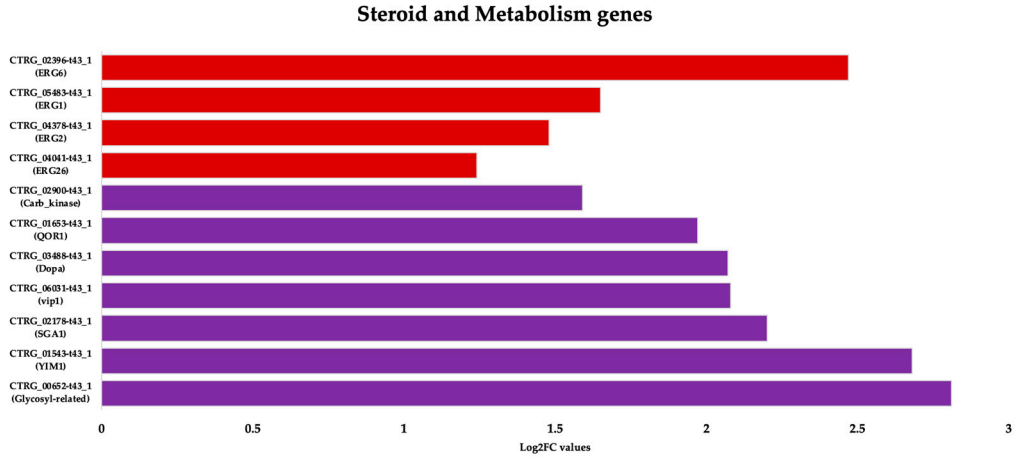

Figure 5. Functional annotation of upregulated DEGs in *Candida tropicalis* following ISO treatment, with focus on genes associated with steroid biosynthesis (ERG6, ERG26, ERG2, ERG1) represented by the red bars, showcasing their upregulation based on Log2FC values. Additionally, the purple bars highlight the upregulated genes involved in cell metabolism functions, reflecting their corresponding Log2FC values.

3.3.3. ISO-Induced Dysregulation of Mitochondrial and Cell Wall Genes in *C. tropicalis*

We also deepen insight into the genes that undergo dysregulation in response to ISO treatment, particularly those associated with mitochondrial function and cell wall pathways (Figure 6). Noteworthy among these genes is KRE1, which is involved in the synthesis of β-glucan in the cell wall of *C. albicans* [46]. Additionally, the upregulation of the btgC gene, encoding a glucan endo-1,3-β-glucosidase, suggests potential involvement in β-glucan degradation. Furthermore, the overexpression of Mid2, cell surface sensors in cell wall integrity signaling [47], and calcium-activated chloride channels (CaCC), essential for cell physiology [48], was observed in *C. tropicalis*. ISO treatment also induced the overexpression of HSP82 heat shock proteins, an essential gene family in yeast cells [49]. Additionally, enzymes such as formate dehydrogenase (FDH), crucial metalloenzymes catalyzing the reversible conversion of formate into carbon dioxide [50], were upregulated.

These enzymes can utilize various electron donors, including ferredoxin, NAD, NADP, quinones, or F420 [51], playing a vital role in mitochondrial metabolism.

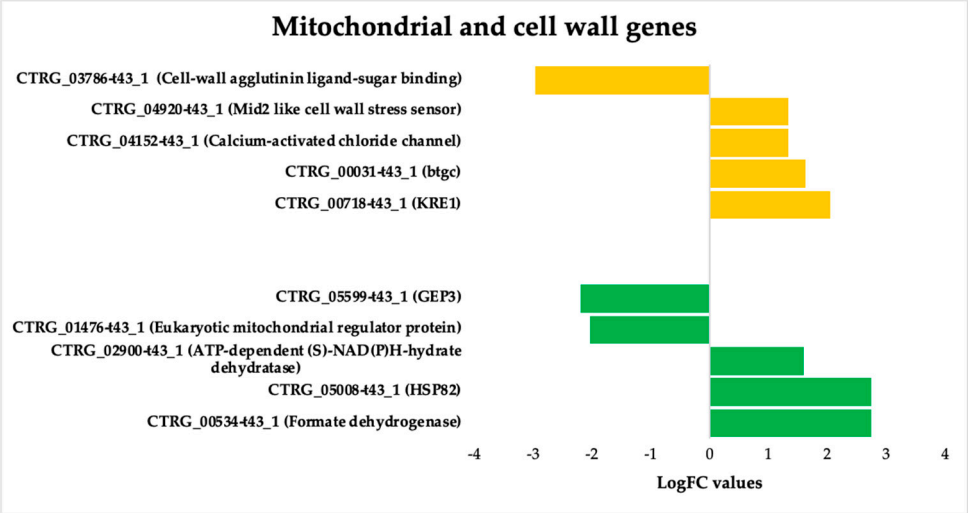

Figure 6. Deregulated genes in *Candida tropicalis* treatment enriched in mitochondria and cell wall processes. Green bars depict the deregulated transcripts involved in mitochondrial processes according to their Log2FC values, while cell-wall-related transcripts are depicted by yellow bars according to their corresponding Log2FC values.

Furthermore, the upregulation of ATP-dependent-(S)-NAD(P)H-hydrate dehydratase, catalyzing the dehydration of the S-form of NAD(P)HX at the expense of ATP, converting it to ADP, was also observed.

3.3.4. Gene Expression Validation Using qPCR

Experimental validation was conducted using quantitative PCR (qPCR) to confirm the differential expression of specific genes in *C. tropicalis* treated with ISO, as depicted in Figure 7. Notably, the CTRG_03786 and ERG6 genes exhibited 1.14- and 1.8-fold higher expression, respectively, compared to the housekeeping gene in the case group. In contrast, the KRE1 gene demonstrated an eightfold higher expression in yeasts treated with isoespintanol compared to ACTIN-1. These qPCR results align with the findings obtained from the biostatistical analysis of RNA-seq.

3.3.5. Methylation-Related Genes Are Downregulated in *C. tropicalis* after ISO Treatment

The downregulation of genes associated with methylation in response to ISO treatment, as illustrated in Figure 8, highlights an interesting facet of the antifungal activity of ISO against *C. tropicalis*. One of the downregulated genes, TRM7, encodes the tRNA methyltransferase TRM7, which is responsible for introducing modifications to transfer RNA (tRNA) [52,53]. These modifications are crucial for tRNA functionality in processes such as translation. The downregulation of TRM7 implies that ISO treatment may interfere with tRNA modifications, potentially affecting protein synthesis and cellular metabolism in *C. tropicalis.* Similarly, the downregulation of the TRM2 gene, which encodes tRNA(m5U54) methyltransferase, indicates ISO's impact on the formation of modified nucleosides within tRNA [54]. These modifications are essential for tRNA stability and functionality in protein synthesis. The disruption of this process could further contribute to the inhibition of protein synthesis in the yeast cells.

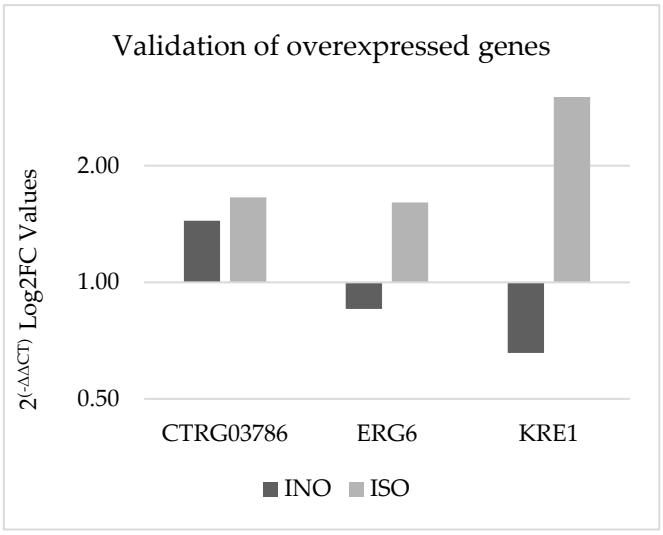

Figure 7. Validation of gene overexpression by qPCR using the $2^{(-\Delta\Delta CT)}$ method. The dark bars represent the genetic expression of *C. tropicalis* without treatment (control group), and the light bars represent *C. tropicalis* treated with ISO. The data are presented by calculating the logarithm to base 2 (Log2FC).

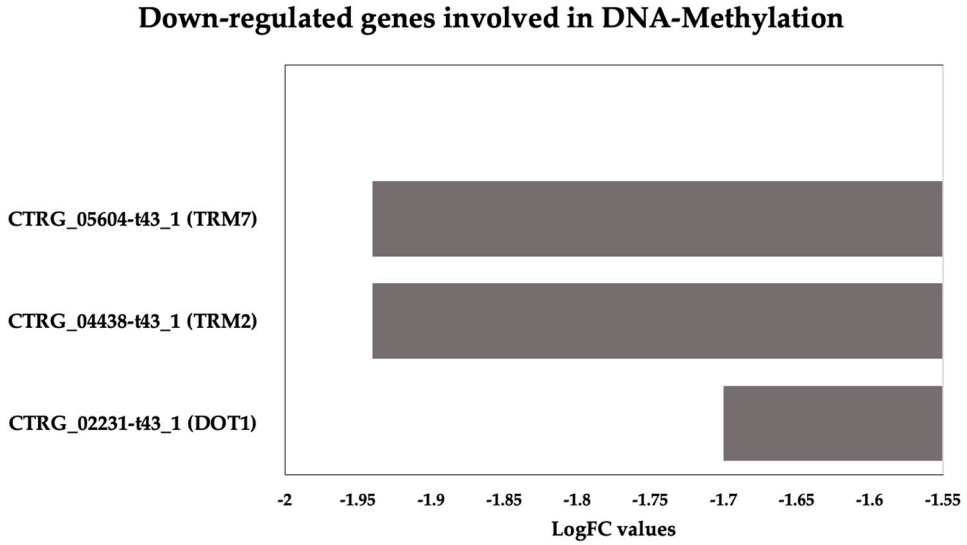

Figure 8. DNA methylation Down-DEGs in *Candida tropicalis* subsequent to ISO treatment. Gray bars represent the downregulated genes (TRM7, TRM2, DOT1) in accordance with their respective Log2FC values.

One of the most intriguing findings is the deregulation of the DOT1 gene, which encodes a histone methyltransferase targeting nucleosomal H3-Lys79. Histone modifications play a crucial role in chromatin remodeling and gene expression regulation [55–58]. The involvement of DOT1 in critical cellular processes, such as the DNA damage checkpoint, nucleotide excision repair, recombination, and chromatin silencing at telomeres, underscores the multifaceted impact of ISO on *C. tropicalis*. The fact that DOT1 is primarily located in the nucleus suggests that ISO treatment may disrupt chromatin structure and gene regulation in the yeast [55–58]. This could have downstream effects on DNA repair mechanisms and overall cellular integrity.

In summary, the downregulation of methylation-related genes in response to ISO treatment provides insight into the complex molecular mechanisms through which ISO exerts its antifungal activity. It highlights the potential disruption of essential cellular

processes, including translation, nucleotide metabolism, and chromatin regulation, ultimately contributing to the inhibition of *C. tropicalis* growth and survival. Further research is needed to elucidate the precise molecular interactions underlying these effects and their implications for antifungal therapy.

3.3.6. Downregulated Genes Are Enriched in Cell Membrane Roles and S-Adenosyl-L-Methionine (SAM) Pathways in Response to ISO Treatment

We analyzed the functional enrichment pathways of the downregulated genes. In this analysis, in addition to the previously mentioned downregulated genes in *C. tropicalis* exposed to ISO treatment, several genes exhibited downregulation, shedding light on the multifaceted impact of ISO on the yeast's transcriptome. These downregulated genes encompass membrane proteins and SAM-related processes, each with unique implications for the cellular functions and metabolism of the yeast. Among the downregulated genes, members of the membrane protein family, including mug84GPR1/FUN34/YaaH and mug86GPR1/FUN34/Satp, drew attention. These genes encode membrane proteins that are involved in acetate permease activity [59], a process responsible for transporting acetate across the fungal cell membrane. The downregulation of these genes implies that ISO treatment may disrupt acetate transport in *C. tropicalis*, potentially affecting various metabolic pathways. Furthermore, these membrane proteins are known to play a role in the regulation of morphogenesis and hyphal formation in *C. albicans* [60,61]. Consequently, their downregulation by ISO treatment may contribute to the inhibition of hyphal growth and morphological changes observed in *C. tropicalis*. Moreover, the downregulation of S-adenosyl-L-methionine (SAM) was observed. SAM is a critical nucleoside that serves as a central molecule in various cellular processes. It acts as a methyl donor for transmethylation reactions, playing essential roles in epigenetic modifications, gene regulation, and protein methylation [62,63]. Additionally, SAM is involved in trans-sulfuration and trans-propylamine reactions, contributing to the synthesis of crucial molecules such as cysteine and polyamines. The downregulation of SAM in response to ISO treatment suggests that this monoterpene disrupts these essential metabolic pathways. Consequently, this disruption may affect gene regulation, protein function, and the overall cellular physiology of *C. tropicalis.*

In summary, the downregulation of specific membrane protein genes and SAM-related processes highlights the diverse and profound effects of ISO on the yeast's cellular processes. ISO's impact extends beyond the previously discussed deregulated genes and encompasses disruptions in acetate transport, morphogenesis regulation, and critical metabolic pathways like trans-methylation and trans-sulfuration. These findings underscore the intricate and multifaceted nature of ISO's antifungal mechanism, providing valuable targets for further exploration into the molecular mechanisms underlying ISO's antifungal activity and its potential as a therapeutic agent against *C. tropicalis* infections (Figure 9).

3.3.7. Overexpression of Zinc-Regulated Transcription Factors (TFs) in *Candida tropicalis* Induced by ISO Treatment

In this study, we observed a notable overexpression of genes encoding transcription factors (TFs) in *C. tropicalis* in response to ISO treatment, shedding light on the intricate transcriptional changes elicited by this monoterpene. The upregulation of these TFs indicates their pivotal role in orchestrating various cellular responses and adaptations to ISO exposure. The observed overexpression of zinc-regulated TFs in *C. tropicalis* subjected to ISO treatment sheds light on the intricate transcriptional landscape influenced by this monoterpene. The upregulation of GAL4-like Zn, a DNA-binding TF, suggests its involvement in regulating the transcription of specific genes. GAL4-like Zn is known for its role in recognizing the palindromic DNA sequence of galactose metabolizing enzyme genes [64]. The overexpression of this TF may signify a shift in metabolic processes in response to ISO treatment, potentially influencing galactose metabolism or related pathways. Another induced TF is RRN11, a DNA-binding TF for RNA polymerase I, it plays a crucial role in the transcription of large nuclear rRNA transcripts [65]. Its overexpression suggests potential

alterations in rRNA transcription in *C. tropicalis* following ISO exposure, which may impact ribosomal biogenesis and protein synthesis. The upregulated GAL4-like Zn TF hints at potential alterations in metabolic pathways, possibly affecting galactose metabolism or related processes [64]. Concurrently, the upregulation of RRN11 TF points toward changes in rRNA transcription, impacting ribosomal biogenesis and protein synthesis [65]. Moreover, the overexpression of RPN4 TF suggests ISO-induced stress responses, potentially affecting protein turnover and DNA repair mechanisms [66,67]. The upregulated USV1 TF implies shifts in respiratory pathways, impacting energy metabolism and cellular respiration [68,69]. Additionally, the upregulation of ZPR1 suggests potential disruptions in the cell cycle progression [70]. ELA1 overexpression indicates ISO-induced DNA damage responses [71]. Furthermore, the overexpression of UPC2 TF implies ISO's impact on ergosterol biosynthesis pathways, influencing membrane composition and integrity [72,73]. Lastly, the overexpression of genes related to environmental stress responses, such as STP4, suggests that ISO triggers stress-related adaptations in *C. tropicalis* [74] (Figure 10).

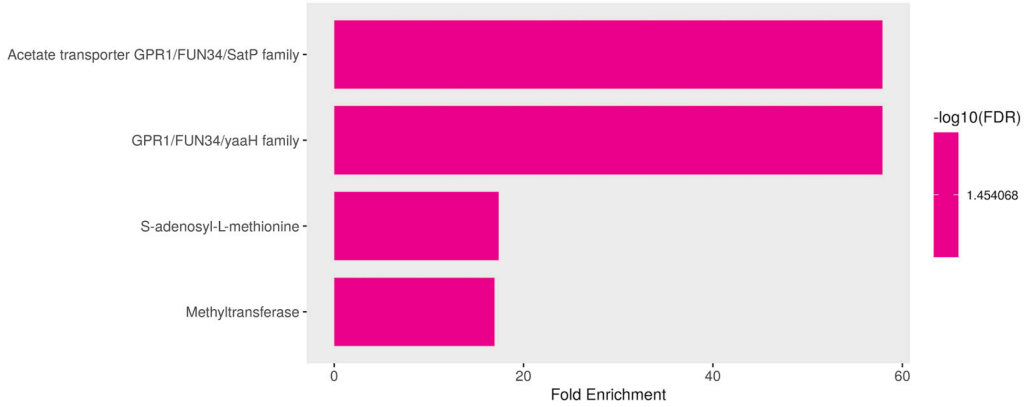

Figure 9. Functional enrichment of downregulated genes in *Candida tropicalis* treated with ISO. FDR is calculated based on a nominal *p*-value from the hypergeometric test. Fold Enrichment is defined as the percentage of differentially expressed genes belonging to a pathway divided by the corresponding percentage in the background. FDR reports how likely the enrichment is by chance. In the x-axis, Fold Enrichment indicates how drastically genes of a certain pathway are overrepresented.

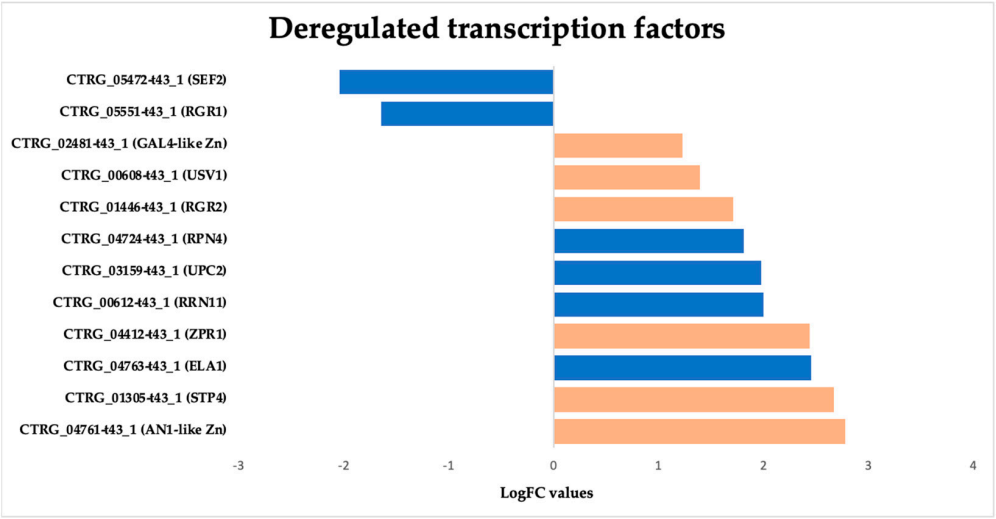

Figure 10. Deregulated transcription factors in *Candida tropicalis* treatment. The orange bars represent the dysregulated zinc domain transcripts, while the blue bars represent other differentially expressed transcription factors (DEG TFs) based on their Log2FC values.

Overall, the overexpression of these zinc-regulated TFs underscores the complex and multifaceted transcriptional responses of *C. tropicalis* to ISO treatment. These TFs play pivotal roles in regulating various cellular processes, including metabolism, stress responses, DNA damage repair, and cell cycle progression. Understanding the regulatory networks governed by these TFs is crucial for unraveling the mechanisms underlying ISO's antifungal activity and its potential as a therapeutic agent.

3.4. Disruption of Fungal Membrane Integrity: Ergosterol Content Analysis Reveals ISO's Antifungal Mechanism

The analysis of ergosterol content was conducted using UHPLC-DAD, revealing pertinent insights into the impact of ISO treatment on *C. tropicalis*. The retention time for ergosterol, as determined by UHPLC-DAD analysis, was consistently observed at approximately 10.8 min (Figure 11). The ergosterol content was quantified in both control (T1) and ISO-treated (T2) samples following a 3 h incubation period. Notably, the ergosterol content in the control samples (T1) was measured at 28.40 ± 1.48 mg/L, while ISO-treated samples (T2) exhibited a notably reduced ergosterol content of 15.58 ± 0.37 mg/L ($p < 0.05$). Furthermore, the standard curve employed in the analysis demonstrated excellent linearity, as evidenced by an R^2 value of 0.9965. These findings unequivocally indicate that ISO treatment resulted in a substantial reduction in ergosterol content in the membrane of *C. tropicalis*, underscoring the pronounced effect of ISO on the fungal membrane composition. The significant reduction in ergosterol content in ISO-treated samples compared to control samples is a compelling finding. Ergosterol is essential for maintaining the integrity and fluidity of the fungal cell membrane. Therefore, a decrease in ergosterol levels can lead to membrane dysfunction, compromising the ability of *C. tropicalis* to adapt and survive in different environments. This reduction in ergosterol content is consistent with the observed upregulation of genes associated with ergosterol biosynthesis in the transcriptomic analysis, suggesting that ISO may disrupt the synthesis of this critical membrane component.

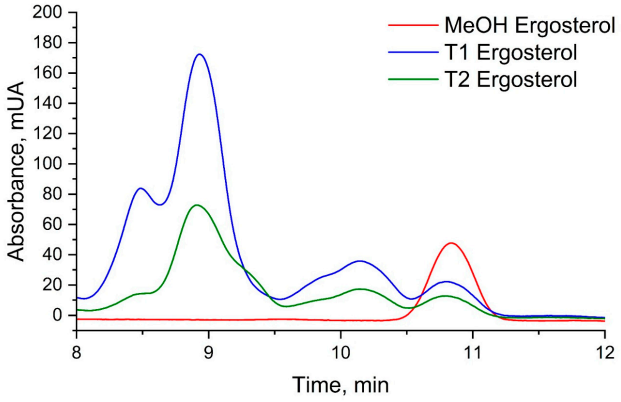

Figure 11. UHPLC chromatograms of ergosterol in *Candida tropicalis* with and without ISO treatment. Ergosterol extractions from the negative control and the ISO-treated group were dissolved in methanol for analysis. Each graph represents the results of three repeated experiments.

The linearity of the standard curve, as indicated by an R^2 value of 0.9965, further validates the accuracy of the ergosterol quantification method, strengthening the credibility of the results. These findings collectively emphasize the pronounced effect of ISO on the fungal membrane composition, which is crucial for the pathogenicity and survival of *C. tropicalis*. Understanding the impact of ISO on ergosterol content provides valuable information for future research and the development of antifungal therapies targeting membrane integrity and function.

4. Discussion

Candida tropicalis has gained prominence within the Candida genus due to its rising incidence, drug resistance, and heightened mortality rates, particularly among immunocompromised individuals [14,16,18,75,76]. Despite the effectiveness of existing antifungal drugs, the emergence of drug-resistant Candida spp. presents a significant therapeutic challenge [77]. Furthermore, the limited treatment options and potential toxicity associated with current therapies necessitate the exploration of novel antifungal compounds, with natural plant-based compounds emerging as promising alternatives [78–83]. In prior studies, we established the efficacy of isoespintanol (ISO) against clinical Candida spp. isolates, including *C. tropicalis*, and elucidated its molecular targets [26,27,84]. In this study, we employ a transcriptomic approach to delineate gene expression profiles, providing insights into the intricate mechanisms underlying ISO's antifungal activity.

Ergosterol, an essential component of fungal cell membranes, governs membrane fluidity, permeability, and the activity of membrane-associated proteins [85]. It is distributed across various cellular components, including the cell membrane, intracellular endomembranes, and mitochondrial membranes [86]. Because ergosterol is absent in mammals, it serves as an attractive target for antifungal agents. These lipids house numerous biologically essential proteins involved in signaling, stress responses, nutrient transport, and other vital processes [77]. Ergosterol biosynthesis is a complex process regulated by numerous ERG genes [87]. Our findings reveal the upregulation of ERG1, ERG6, ERG2, and ERG26 genes, all involved in ergosterol biosynthesis. The precise mechanism responsible for the global upregulation of ERG genes in response to azoles remains unclear. However, it has been postulated that disruptions in ergosterol or other sterol pathway components lead to widespread ERG gene expression increases [88]. Alternatively, the accumulation of early substrates or toxic sterol byproducts may trigger ERG expression [33,89]. This study demonstrated a reduction in *C. tropicalis* ergosterol content in response to ISO treatment, leading to an increase in ERG gene expression. Inhibition of the ergosterol synthesis pathway results in an accumulation of toxic sterols, which, coupled with the reduction in ergosterol, damages the cell membrane's integrity, inhibiting fungal cell growth [90]. These results align with previous findings where *C. albicans* treated with azoles exhibited similar responses [91,92]. Notably, the ERG6 gene and its protein products may serve as valuable antifungal targets for a new generation of ergosterol biosynthesis inhibitors, such as ISO. This gene is particularly interesting because it encodes sterol C-24 methyltransferase, which is not involved in cholesterol biosynthesis in human cells. Furthermore, it has been reported that ERG6 deletion leads to hypersensitivity to several metabolic inhibitors and an inability to import tryptophan or utilize respiratory energy sources. Hence, the use of inhibitors that target the ERG6 gene product could render pathogenic yeast hypersensitive to currently known antifungal agents, as well as novel compounds [93,94]. Furthermore, the regulation of ergosterol synthesis involves overlapping mechanisms, including transcriptional expression, feedback inhibition of enzymes, and changes in subcellular localization [85]. Considering the pivotal physiological role of ergosterol in these pathogenic yeasts [95] and ISO's impact on ergosterol biosynthesis and associated transcription factors, ISO emerges as a promising compound in the battle against these pathogens.

It is well known that fungal cell walls are critical for viability, morphogenesis, and pathogenesis [96]. *Candida albicans*' cell wall comprises an inner skeletal layer rich in β-(1,3)- and β-(1,6)-glucan and chitin, along with an outer fibrillar layer primarily composed of highly mannosylated cell wall proteins [97,98]. Given that the cell wall plays a crucial role in maintaining cellular osmotic integrity, any damage to it triggers various responses [99], previous studies have shown that inhibiting β-(1,3)-glucan synthesis leads to compensatory chitin synthesis and alterations in wall macromolecule arrangements in *C. albicans.* Similarly, *C. tropicalis* has been shown to activate a chitin compensatory response upon exposure to D-limonene [98] and ISO [84].

Of particular interest is the upregulation of the KRE1 gene, which is involved in β-glucan synthesis and assembly in yeast cell walls like *Saccharomyces cerevisiae* and *C.*

albicans. Mutations in this gene are associated with abnormal (1,6)-β-glucan production in yeast cell walls [46,100,101]. This suggests that ISO may indeed alter the cell wall structure in *C. tropicalis*. As cell wall β-glucans are common in fungi and absent in mammals, enzymes involved in β-glucan biosynthesis are potential targets for specific antifungal agents [96,102].

Monoterpenes have been reported to interact with various intracellular targets, including DNA and RNA, leading to disruptions in protein synthesis, metabolic processes, biosynthetic pathways, mitochondrial membrane potential, and more [103,104]. Our results indicate that ISO can penetrate *C. tropicalis* cells, interacting with intracellular structures, thereby disrupting the pathogens' normal metabolic processes, enzymatic activity, mitochondrial function, and signaling pathways. Notably, we observe the upregulation of genes related to protein translation and folding, suggesting that protein synthesis may be a critical target in ISO's antifungal activity. Furthermore, the upregulation of the STI1 domain, known for its role in various cellular processes, including the transfer of hydrophobic substrates and the DNA damage response, suggests that ISO's antifungal action also involves DNA damage in *C. tropicalis*. Our results are in accordance with previous studies in *C. tropicalis* and *C. parapsilosis*, where terpenes like D-limonene have exhibited multiple action targets [24,25,103].

Additionally, we note the downregulation of methylation-related genes in *C. tropicalis* following ISO treatment. Genes such as TRM7, TRM2, and DOT1, known for their roles in tRNA modification and histone methylation, were downregulated [52–58]. This phenomenon suggests that ISO may alter key methylation processes within yeast cells, ultimately affecting various vital cellular functions. Moreover, genes involved in acetate permease activity and the expression of S-adenosyl-L-methionine (SAM), a crucial nucleoside serving as a methyl donor in various processes, including choline, carnitine, creatine, DNA, and protein methylation, were found to be downregulated [105]. These findings suggest that ISO's antifungal action involves complex regulation processes, potentially including post-transcriptional events.

Interestingly, our results reveal the upregulation of genes encoding transcription factors (TFs) in response to ISO treatment. These include GAL4-like Zn, RRN11, RPN4, USV1, ZPR1, ELA1, and UPC2. These TFs play various roles, from binding to specific DNA sequences to regulating DNA repair and stress responses. This deregulation underscores the complexity of ISO's antifungal mechanism, suggesting that it may involve multiple regulatory processes. These findings highlight the multifaceted nature of ISO's action against *C. tropicalis*.

In summary, ISO's antifungal activity against *C. tropicalis* employs a multi-molecular target approach, encompassing disruptions in ergosterol and protein biosynthesis, alterations in cell wall and membrane structure, perturbation of multiple cellular processes, and potentially the induction of DNA damage. Compounds with multiple molecular targets have been shown to enhance activity against multidrug-resistant strains and inhibit resistance development [106]. Consequently, ISO, by targeting various aspects of the biology of these pathogens, could serve as a versatile tool for different objectives or as a starting point for the development of new drugs, drug precursors, or adjuvants in the treatment and control of these pathogens. This approach holds promise in countering drug resistance and improving treatment outcomes against *C. tropicalis.* Furthermore, considering that some ISO targets are not present in human cells, this monoterpene could be a compelling candidate for designing, synthesizing, and developing new molecular prototypes with antifungal potential. The intricate nature of ISO's antifungal mechanism underscores its potential as a promising antifungal agent against drug-resistant Candida species.

5. Conclusions

In this study, we conducted a comprehensive transcriptomic analysis of *C. tropicalis* exposed to ISO, a natural monoterpene isolated from *O. xylopioides.* Our findings not only reaffirm the antifungal properties of ISO, as previously reported, but also shed light

on the intricate mechanisms underlying its antifungal activity. The complexity of ISO's action, as revealed by our results, underscores its potential as a promising antifungal agent against *C. tropicalis*, a clinically significant pathogenic yeast known for its increasing drug resistance and mortality rates among immunocompromised individuals. These results provide valuable insights into potential clinical molecular targets within *C. tropicalis* that may be explored in the future for the development of novel treatments against this pathogenic yeast. This research contributes to our understanding of the molecular basis of ISO's antifungal activity and opens new avenues for the development of effective therapies for combating drug-resistant Candida species in clinical settings.

Supplementary Materials: The following supporting information can be downloaded at https://www.mdpi.com/article/10.3390/jof9121199/s1, Table S1: List of real-time qPCR primers. Table S2: RNA extraction of *C. tropicalis*. Quality control total RNA extracted from Zoea-type larvae of *Callinectus sapidus*. Table S3: NGS sequencing by RNA-seq of *C. tropicalis*. Table S4: Mapping of transcriptomes obtained by RNA-seq.

Author Contributions: Conceptualization, O.I.C.-M., K.A.-P. and A.A.-O.; methodology, O.I.C.-M., M.C.V.-P., K.A.-P. and A.A.-O.; software, O.I.C.-M. and K.A.-P.; validation, O.I.C.-M., M.C.V.-P., M.F.Y. and K.A.-P.; formal analysis, O.I.C.-M., K.A.-P., M.C.V.-P. and A.A.-O.; investigation, O.I.C.-M., M.C.V.-P. and K.A.-P.; resources, A.A.-O., M.F.Y. and G.S.-P.; writing—original draft preparation, O.I.C.-M., K.A.-P., M.C.V.-P. and A.A.-O.; writing—review and editing, O.I.C.-M., A.A.-O., K.A.-P. and G.S.-P.; visualization, O.I.C.-M. and K.A.-P.; supervision, O.I.C.-M., A.A.-O. and G.S.-P.; funding acquisition, A.A.-O., M.F.Y. and G.S.-P. All authors have read and agreed to the published version of the manuscript.

Funding: O.I.C.-M. thanks the scholarship program of the Ministry of Science, Technology and Innovation of Colombia for the granting of the doctoral scholarship. This research was funded with resources from the FCB-02-19 project of the University of Córdoba, Montería, Colombia. K.A.-P. (CVU:227919) received financial support from CONACyT and a fellowship from the Fulbright García-Robles Foundation.

Institutional Review Board Statement: Not applicable.

Informed Consent Statement: Not applicable.

Data Availability Statement: The datasets used are available from https://github.com/kap8416/transcriptomicsofcandidatropicalis_isoespintanol accessed on 16 June 2023. Code and Supplementary Materials have been deposited in https://github.com/kap8416/transcriptomicsofcandidatropicalis_isoespintanol accessed on 16 June 2023.

Acknowledgments: The authors thank Loranda Calderón Zamora for her technical assistance in data visualization.

Conflicts of Interest: The authors declare no conflict of interest.

References

1. Schils, R.; Rampat, R.; Rakic, J.-M.; Crahay, F.-X. Candida Chorioretinitis in Renal Transplant Recipient with Candidemia Related to Contaminated Organ Preservation Fluid: A Role for Dilated Fundus Examination in Its Management. *IDCases* **2023**, *32*, e01793. [CrossRef]
2. Ohashi, Y.; Matono, T.; Suzuki, S.; Yoshino, S.; Alshahni, M.M.; Komori, A.; Makimura, K. The First Case of Clade I *Candida auris* Candidemia in a Patient with COVID-19 in Japan. *J. Infect. Chemother.* **2023**, *29*, 713–717. [CrossRef]
3. Papadimitriou-Olivgeris, M.; Kolonitsiou, F.; Kefala, S.; Spiliopoulou, A.; Aretha, D.; Bartzavali, C.; Siapika, A.; Marangos, M.; Fligou, F. Increased Incidence of Candidemia in Critically Ill Patients during the Coronavirus Disease 2019 (COVID-19) Pandemic. *Braz. J. Infect. Dis.* **2022**, *26*, 102353. [CrossRef]
4. Kimura, S.; Kameda, K.; Harada, K.; Saburi, M.; Okinaka, K.; Shinohara, A.; Uchida, N.; Nishijima, A.; Ozawa, Y.; Tanaka, M.; et al. Risk and Predictive Factors for Candidemia After Allogeneic Hematopoietic Cell Transplantation: JSTCT Transplant Complications Working Group. *Transplant. Cell. Ther.* **2022**, *28*, 209.e1–209.e9. [CrossRef]
5. Lin, J.; Zhou, M.; Chen, J.; Zhang, L.; Lu, M.; Liu, Z. De-Escalation from Echinocandins to Azole Treatment in Critically Ill Patients with Candidemia. *Int. J. Infect. Dis.* **2022**, *121*, 69–74. [CrossRef]
6. Saiprom, N.; Wongsuk, T.; Oonanant, W.; Sukphopetch, P.; Chantratita, N.; Boonsilp, S. Characterization of Virulence Factors in Candida Species Causing Candidemia in a Tertiary Care Hospital in Bangkok, Thailand. *J. Fungi* **2023**, *9*, 353. [CrossRef]

7. Vargas-Espíndola, L.A.; Cuervo-Maldonado, S.I.; Enciso-Olivera, J.; Gómez-Rincón, J.; Jiménez-Cetina, L.; Sánchez-Pedraza, R.; García-Guzmán, K.; López-Mora, M.J.; Álvarez-Moreno, C.; Cortés, J.A.; et al. Fungemia in Hospitalized Adult Patients with Hematological Malignancies: Epidemiology and Risk Factors. *J. Fungi* **2023**, *9*, 400. [CrossRef]
8. Alvarez-Moreno, C.A.; Morales-López, S.; Rodriguez, G.J.; Rodriguez, J.Y.; Robert, E.; Picot, C.; Ceballos-Garzon, A.; Parra-Giraldo, C.M.; Le Pape, P. The Mortality Attributable to Candidemia in *C. auris* Is Higher than That in Other Candida Species: Myth or Reality? *J. Fungi* **2023**, *9*, 430. [CrossRef]
9. Pappas, P.; Lionakis, M.; Cavling, M.; Ostrosky-Zeichner, L.; Kullberg, B. Invasive Candidiasis. *Dis. Prim.* **2018**, *4*, 18026. [CrossRef]
10. McCarty, T.P.; White, C.M.; Pappas, P.G. Candidemia and Invasive Candidiasis. *Infect. Dis. Clin. N. Am.* **2021**, *35*, 389–413. [CrossRef]
11. Gómez-Gaviria, M.; Ramírez-Sotelo, U.; Mora-Montes, H.M. Non-Albicans Candida Species: Immune Response, Evasion Mechanisms, and New Plant-Derived Alternative Therapies. *J. Fungi* **2023**, *9*, 11. [CrossRef]
12. Ceballos-Garzon, A.; Peñuela, A.; Valderrama-Beltrán, S.; Vargas-Casanova, Y.; Ariza, B.; Parra-Giraldo, C.M. Emergence and Circulation of Azole-Resistant *C. albicans*, *C. auris* and *C. parapsilosis* Bloodstream Isolates Carrying Y132F, K143R or T220L Erg11p Substitutions in Colombia. *Front. Cell. Infect. Microbiol.* **2023**, *13*, 1136217. [CrossRef]
13. Osset-Trénor, P.; Pascual-Ahuir, A.; Proft, M. Fungal Drug Response and Antimicrobial Resistance. *J. Fungi* **2023**, *9*, 565. [CrossRef]
14. El-kholy, M.A.; Helaly, G.F.; El Ghazzawi, E.F.; El-sawaf, G.; Shawky, S.M. Virulence Factors and Antifungal Susceptibility Profile of *C. tropicalis* Isolated from Various Clinical Specimens in Alexandria, Egypt. *J. Fungi* **2021**, *7*, 351. [CrossRef]
15. De Oliveira, J.S.; Pereira, V.S.; Castelo-Branco, D.d.S.C.M.; Cordeiro, R.d.A.; Sidrim, J.J.C.; Brilhante, R.S.N.; Rocha, M.F.G. The Yeast, the Antifungal, and the Wardrobe: A Journey into Antifungal Resistance Mechanisms of *Candida tropicalis*. *Can. J. Microbiol.* **2020**, *66*, 377–388. [CrossRef]
16. Munhoz-Alves, N.; Nishiyama Mimura, L.A.; Viero, R.M.; Bagagli, E.; Schatzmann, J.; Sartori, A.; Fraga-Silva, T.F.d.C. *Candida tropicalis* Systemic Infection Redirects Leukocyte Infiltration to the Kidneys Attenuating Encephalomyelitis. *J. Fungi* **2021**, *7*, 757. [CrossRef]
17. Silva, S.; Negri, M.; Henriques, M.; Oliveira, R.; Williams, D.W.; Azeredo, J. *Candida glabrata*, *Candida parapsilosis* and *Candida tropicalis*: Biology, Epidemiology, Pathogenicity and Antifungal Resistance. *FEMS Microbiol. Rev.* **2012**, *36*, 288–305. [CrossRef]
18. Wang, D.; An, N.; Yang, Y.; Yang, X.; Fan, Y.; Feng, J. *Candida tropicalis* Distribution and Drug Resistance Is Correlated with ERG11 and UPC2 Expression. *Antimicrob. Resist. Infect. Control* **2021**, *10*, 54. [CrossRef]
19. Fan, X.; Xiao, M.; Liao, K.; Kudinha, T.; Wang, H.; Zhang, L.; Hou, X.; Kong, F.; Xu, Y.C. Notable Increasing Trend in Azole Non-Susceptible *Candida tropicalis* Causing Invasive Candidiasis in China (August 2009 to July 2014): Molecular Epidemiology and Clinical Azole Consumption. *Front. Microbiol.* **2017**, *8*, 464. [CrossRef]
20. Spruijtenburg, B.; Baqueiro, C.C.S.Z.; Colombo, A.L.; Meijer, E.F.J.; de Almeida, J.; Berrio, I.; Fernández, N.B.; Chaves, G.M.; Meis, J.; de Groot, T. Short Tandem Repeat Genotyping and Antifungal Susceptibility Testing of Latin American *Candida tropicalis* Isolates. *J. Fungi* **2023**, *9*, 207. [CrossRef]
21. Zuza-Alves, D.L.; Sila-Rocha, W.P.; Chaves, G. An Update on *Candida tropicalis* Based on Basic and Clinical Approaches. *Front. Microbiol.* **2017**, *8*, 1927. [CrossRef] [PubMed]
22. Argüelles, A.; Sánchez-Fresneda, R.; Guirao-Abad, J.P.; Lozano, J.A.; Solano, F.; Argüelles, J.C. Insight into the Antifungal Effects of Propolis and Carnosic Acid—Extension to the Pathogenic Yeast *Candida glabrata*: New Propolis Fractionation and Potential Synergistic Applications. *J. Fungi* **2023**, *9*, 442. [CrossRef] [PubMed]
23. Iraji, A.; Yazdanpanah, S.; Alizadeh, F.; Mirzamohammadi, S.; Ghasemi, Y.; Pakshir, K.; Yang, Y.; Zomorodian, K. Screening the Antifungal Activities of Monoterpenes and Their Isomers against Candida Species. *J. Appl. Microbiol.* **2020**, *129*, 1541–1551. [CrossRef] [PubMed]
24. Leite-Andrade, M.C.; de Araújo Neto, L.N.; Buonafina-Paz, M.D.S.; de Assis Graciano dos Santos, F.; da Silva Alves, A.I.; de Castro, M.C.A.B.; Mori, E.; de Lacerda, B.C.G.V.; Araújo, I.M.; Coutinho, H.D.M.; et al. Antifungal Effect and Inhibition of the Virulence Mechanism of D-Limonene against *Candida parapsilosis*. *Molecules* **2022**, *27*, 8884. [CrossRef] [PubMed]
25. Yu, H.; Lin, Z.; Xiang, W.; Huang, M.; Tang, J.; Lu, Y.; Zhao, Q.; Zhang, Q.; Rao, Y.; Liu, L. Antifungal Activity and Mechanism of D -Limonene against Foodborne Opportunistic Pathogen *Candida tropicalis*. *LWT-Food Sci. Technol.* **2022**, *159*, 113144. [CrossRef]
26. Contreras Martínez, O.I.; Angulo Ortíz, A.A.; Santafé Patiño, G. Mechanism of Antifungal Action of Monoterpene Isoespintanol against Clinical Isolates of *Candida tropicalis*. *Molecules* **2022**, *27*, 5808. [CrossRef] [PubMed]
27. Contreras Martínez, O.I.; Angulo Ortíz, A.A.; Santafé Patiño, G. Antifungal Potential of Isoespintanol Extracted from *Oxandra xylopioides* Diels (Annonaceae) against Intrahospital Isolations of *Candida* spp. *Heliyon* **2022**, *8*, e11110. [CrossRef] [PubMed]
28. Ramírez, R.D.; Páez, M.S.; Angulo, A.A. Obtención de Isoespintanol Por Hidrodestilación y Cristalización a Partir Del Extracto Bencínico de *Oxandra xylopioides*. *Inf. Tecnol.* **2015**, *26*, 13–18. [CrossRef]
29. Benjamini, Y.; Hochberg, Y. Controlling the False Discovery Rate: A Practical and Powerful Approach to Multiple Testing. *J. R. Stat. Soc. Ser. B* **1995**, *57*, 289–300. [CrossRef]
30. Ge, S.X.; Jung, D.; Yao, R. ShinyGO: A Graphical Gene-Set Enrichment Tool for Animals and Plants. *Bioinformatics* **2020**, *36*, 2628–2629. [CrossRef]

31. Silva, M.; Cardozo, D.; Fernando, P.; Freitas, F.; Fuzo, C.; Santos, C.; Rodrigues, M.; Santana, J. Modulation of ERG Genes Expression in Clinical Isolates of *Candida tropicalis* Susceptible and Resistant to Fluconazole and Itraconazole. *Mycopathologia* **2020**, *6*, 675–684. [CrossRef] [PubMed]
32. Livak, K.J.; Schmittgen, T.D. Analysis of Relative Gene Expression Data Using Real-Time Quantitative PCR and the 2-ΔΔCT Method. *Methods* **2001**, *25*, 402–408. [CrossRef] [PubMed]
33. Zhang, X.; Zhang, T.; Guo, S.; Zhang, Y.; Sheng, R.; Sun, R.; Chen, L.; Lv, R.; Qi, Y. In Vitro Antifungal Activity and Mechanism of Ag3PW12O40 Composites against Candida Species. *Molecules* **2020**, *25*, 6012. [CrossRef] [PubMed]
34. Dillon, S.C.; Zhang, X.; Trievel, R.C.; Cheng, X. The SET-Domain Protein Superfamily: Protein Lysine Methyltransferases. *Genome Biol.* **2005**, *6*, 227. [CrossRef] [PubMed]
35. Rai, R.; Genbauffe, F.; Cooper, T. Structure and Transcription of the Allantoate Permease Gene (DAL5) from *Saccharomyces cerevisiae*. *J. Bacteriol.* **1988**, *170*, 266–271. [CrossRef] [PubMed]
36. Simard, J.; Ricketts, M.; Gingras, S.; Soucy, P.; Feltus, A.; Melner, M. Molecular Biology of the 3β-Hydroxysteroid Dehydrogenase/Δ^5-Δ^4 Isomerase Gene Family. *Endocr. Rev.* **2005**, *26*, 525–582. [CrossRef] [PubMed]
37. Wang, L.; Salavaggione, E.; Pelleymounter, L.; Eckloff, B.; Wieben, E.; Weinshilboum, R. Human 3β-Hydroxysteroid Dehydrogenase Types 1 and 2: Gene Sequence Variation and Functional Genomics. *J. Steroid Biochem. Mol. Biol.* **2007**, *107*, 88–99. [CrossRef]
38. Han, L.; Ding, G.; Liu, Y.; Huang, J.; Wu, J. Characterization of Sphingomyelin Phosphodiesterase Expression in Bumblebee (*Bombus lantschouensis*). *J. Insect Sci.* **2018**, *18*, 20. [CrossRef]
39. Ueda, S.; Manabe, Y.; Kubo, N.; Morino, N.; Yuasa, H.; Shiotsu, M.; Tsuji, T.; Sugawara, T.; Kambe, T. Early Secretory Pathway-Resident Zn Transporter Proteins Contribute to Cellular Sphingolipid Metabolism through Activation of Sphingomyelin Phosphodiesterase 1. *Am. J. Physiol. Cell Physiol.* **2022**, *322*, C948–C959. [CrossRef]
40. Sherman, M.Y.S.; Goldberg, A.L. Involvement of Molecular Chaperones in Intracellular Protein Breakdown. *Stress-Inducible Cell. Responses* **1996**, *77*, 57–78.
41. Qiu, X.B.; Shao, Y.M.; Miao, S.; Wang, L. The Diversity of the DnaJ/Hsp40 Family, the Crucial Partners for Hsp70 Chaperones. *Cell. Mol. Life Sci.* **2006**, *63*, 2560–2570. [CrossRef] [PubMed]
42. Fry, M.Y.; Saladi, S.M.; Clemons, W.M. The STI1-Domain Is a Flexible Alpha-Helical Fold with a Hydrophobic Groove. *Protein Sci.* **2021**, *30*, 882–898. [CrossRef] [PubMed]
43. Barski, O.A.; Tipparaju, S.M.; Bhatnagar, A. The Aldo-Keto Reductase Superfamily and Its Role in Drug Metabolism and Detoxification. *Drug Metab. Rev.* **2008**, *40*, 553–624. [CrossRef] [PubMed]
44. Fetzner, S. Ring-Cleaving Dioxygenases with a Cupin Fold. *Appl. Environ. Microbiol.* **2012**, *78*, 2505–2514. [CrossRef] [PubMed]
45. Ma, T.; Yu, Q.; Ma, C.; Mao, X.; Liu, Y.; Peng, X.; Li, M. Role of the Inositol Polyphosphate Kinase Vip1 in Autophagy and Pathogenesis in *Candida albicans*. *Future Microbiol.* **2020**, *15*, 1363–1377. [CrossRef] [PubMed]
46. Boone, C.; Sdicu, A.M.; Laroche, M.; Bussey, H. Isolation from *Candida albicans* of a Functional Homolog of the *Saccharomyces cerevisiae* KRE1 Gene, Which Is Involved in Cell Wall β-Glucan Synthesis. *J. Bacteriol.* **1991**, *173*, 6859–6864. [CrossRef]
47. Philip, B.; Levin, D.E. Wsc1 and Mid2 Are Cell Surface Sensors for Cell Wall Integrity Signaling That Act through Rom2, a Guanine Nucleotide Exchange Factor for Rho1. *Mol. Cell. Biol.* **2001**, *21*, 271–280. [CrossRef]
48. Hartzell, C.; Putzier, I.; Arreola, J. Calcium-Activated Chloride Channels. *Annu. Rev. Physiol.* **2005**, *67*, 719–758. [CrossRef]
49. Borkovich, K.A.; Farrelly, F.W.; Finkelstein, D.B.; Taulien, J.; Lindquist, S. Hsp82 Is an Essential Protein That Is Required in Higher Concentrations for Growth of Cells at Higher Temperatures. *Mol. Cell. Biol.* **1989**, *9*, 3919–3930. [CrossRef]
50. Dong, G.; Ryde, U. Reaction Mechanism of Formate Dehydrogenase Studied by Computational Methods. *J. Biol. Inorg. Chem.* **2018**, *23*, 1243–1254. [CrossRef]
51. Ljungdahl, L.G. *Formate Dehydrogenases: Role of Molybdenum, Tungsten and Selenium*; Pergamon Press Ltd.: Oxford, UK, 1980; pp. 463–486. [CrossRef]
52. Hirata, A.; Okada, K.; Yoshii, K.; Shiraishi, H.; Saijo, S.; Yonezawa, K.; Shimizu, N.; Hori, H. Structure of TRNA Methyltransferase Complex of Trm7 and Trm734 Reveals a Novel Binding Interface for TRNA Recognition. *Nucleic Acids Res.* **2019**, *47*, 10942–10955. [CrossRef] [PubMed]
53. Pintard, L.; Lecointe, F.; Bujnicki, J.M.; Bonnerot, C.; Grosjean, H.; Lapeyre, B. Trm7p Catalyses the Formation of Two 2¢-O-Methylriboses in Yeast TRNA Anticodon Loop Lionel. *EMBO J. Vol.* **2002**, *21*, 1811–1820. [CrossRef] [PubMed]
54. Nordlund, M.E.; Johansson, J.O.M.; Von Pawel-Rammingen, U.; Byström, A.S. Identification of the TRM2 Gene Encoding the TRNA(M5U54) Methyltransferase of *Saccharomyces cerevisiae*. *RNA* **2000**, *6*, 844–860. [CrossRef] [PubMed]
55. Van Leeuwen, F.; Gafken, P.R.; Gottschling, D.E. Dot1p Modulates Silencing in Yeast by Methylation of the Nucleosome Core. *Cell* **2002**, *109*, 745–756. [CrossRef]
56. San-segundo, P.A.; Roeder, G.S. Role for the Silencing Protein Dot1 in Meiotic Checkpoint Control. *Mol. Biol. Cell* **2000**, *11*, 3601–3615. [CrossRef]
57. Wysocki, R.; Javaheri, A.; Sha, F.; Co, J. Role of Dot1-Dependent Histone H3 Methylation in G 1 and S Phase DNA Damage Checkpoint Functions of Rad9. *Mol. Cell. Biol.* **2005**, *25*, 8430–8443. [CrossRef]
58. Frederiks, F.; Heynen, G.J.J.E.; Van Deventer, S.J.; Janssen, H.; Van Leeuwen, F. Two Dot1 Isoforms in *Saccharomyces cerevisiae* as a Result of Leaky Scanning by the Ribosome. *Nucleic Acids Res.* **2009**, *37*, 7047–7058. [CrossRef]

59. Robellet, X.; Flipphi, M.; Pégot, S.; MacCabe, A.; Vélot, C. AcpA, a Member of the GPR1/FUN34/YaaH Membrane Protein Family, Is Essential for Acetate Permease Activity in the Hyphal Fungus *Aspergillus nidulans*. *Biochem. J.* **2008**, *493*, 485–493. [CrossRef]
60. Miwa, T.; Takagi, Y.; Shinozaki, M.; Yun, C.W.; Schell, W.A.; Perfect, J.R.; Kumagai, H.; Tamaki, H. Gpr1, a Putative G-Protein-Coupled Receptor, Regulates Morphogenesis and Hypha Formation in the Pathogenic Fungus *Candida albicans*. *Eukaryot. Cell* **2004**, *3*, 919–931. [CrossRef]
61. Maidan, M.M.; De Rop, L.; Serneels, J.; Exler, S.; Rupp, S.; Tournu, H.; Thevelein, J.; Van Dijck, P. The G Protein-Coupled Receptor Gpr1 and the Gα Protein Gpa2 Act through the $_C$AMP-Protein Kinase A Pathway to Induce Morphogenesis in *Candida albicans*. *Mol. Biol. Cell* **2005**, *16*, 1971–1986. [CrossRef]
62. Fontecave, M.; Atta, M.; Mulliez, E. S-Adenosylmethionine: Nothing Goes to Waste. *Trends Biochem. Sci.* **2004**, *29*, 243–249. [CrossRef] [PubMed]
63. Chen, H.; Wang, Z.; Cai, H.; Zhou, C. Progress in the Microbial Production of S-Adenosyl-l-Methionine. *World J. Microbiol. Biotechnol.* **2016**, *32*, 153. [CrossRef] [PubMed]
64. Pan, T.; Coleman, J.E. GAL4 Transcription Factor Is Not a "Zinc Finger" but Forms a Zn(II)2Cys6 Binuclear Cluster. *Proc. Natl. Acad. Sci. USA* **1990**, *87*, 2077–2081. [CrossRef] [PubMed]
65. Lalo, D.; Steffan, J.S.; Dodd, J.A.; Nomura, M. RRN11 Encodes the Third Subunit of the Complex Containing Rrn6p and Rrn7p That Is Essential for the Initiation of RDNA Transcription by Yeast RNA Polymerase I. *J. Biol. Chem.* **1996**, *271*, 21062–21067. [CrossRef] [PubMed]
66. Xie, Y.; Varshavsky, A. RPN4 Is a Ligand, Substrate, and Transcriptional Regulator of the 26S Proteasome: A Negative Feedback Circuit. *Proc. Natl. Acad. Sci. USA* **2001**, *98*, 3056–3061. [CrossRef] [PubMed]
67. Mannhaupt, G.; Schnall, R.; Karpov, V.; Vetter, I.; Feldmann, H. Rpn4p Acts as a Transcription Factor by Binding to PACE, a Nonamer Box Found Upstream of 26S Proteasomal and Other Genes in Yeast. *FEBS Lett.* **1999**, *450*, 27–34. [CrossRef]
68. Böhm, S.; Frishman, D.; Werner Mewes, H. Variations of the C2H2 Zinc Finger Motif in the Yeast Genome and Classification of Yeast Zinc Finger Proteins. *Nucleic Acids Res.* **1997**, *25*, 2464–2469. [CrossRef]
69. Hlynialuk, C.; Schierholtz, R.; Vernooy, A.; van der Merwe, G. Nsf1/Ypl230w Participates in Transcriptional Activation during Non-Fermentative Growth and in Response to Salt Stress in *Saccharomyces cerevisiae*. *Microbiology* **2008**, *154*, 2482–2491. [CrossRef]
70. Gangwani, L.; Mikrut, M.; Galcheva-Gargova, Z.; Davis, R.J. Interaction of ZPR1 with Translation Elongation Factor-1α in Proliferating Cells. *J. Cell Biol.* **1998**, *143*, 1471–1484. [CrossRef]
71. Ribar, B.; Prakash, L.; Prakash, S. ELA1 and CUL3 Are Required Along with ELC1 for RNA Polymerase II Polyubiquitylation and Degradation in DNA-Damaged Yeast Cells. *Mol. Cell. Biol.* **2007**, *27*, 3211–3216. [CrossRef]
72. Marie, C.; Leyde, S.; White, T.C. Cytoplasmic Localization of Sterol Transcription Factors Upc2p and Ecm22p in *S. cerevisiae*. *Fungal Genet. Biol.* **2008**, *45*, 1430–1438. [CrossRef] [PubMed]
73. Vik, A.; Rine, J. Upc2p and Ecm22p, Dual Regulators of Sterol Biosynthesis in *Saccharomyces cerevisiae*. *Mol. Cell. Biol.* **2001**, *21*, 6395–6405. [CrossRef] [PubMed]
74. Truernit, E.; Schmid, J.; Epple, P.; Illig, J.; Sauer, N. The Sink-Specific and Stress-Regulated Arabidopsis SPP4 Gene: Enhanced Expression of a Gene Encoding a Monosaccharide Transporter by Wounding, Elicitors, and Pathogen Challenge. *Plant Cell* **1996**, *8*, 2169–2182. [PubMed]
75. Chen, P.; Chuang, Y.; Wu, U.; Sun, H.; Wang, J.; Sheng, W.; Chen, Y.; Chang, S. Mechanisms of Azole Resistance and Trailing in *Candida tropicalis* Bloodstream Isolates. *J. Fungi* **2021**, *7*, 612. [CrossRef] [PubMed]
76. Maikan, H.K.; Jabbar, S.; Al-Haishawi, H. Isolation and Identification of *Candida tropicalis* as a Cause of Cutaneous Candidiasis in Kalar District, Iraq. *Arch. Razi Inst.* **2022**, *77*, 1377–1382. [CrossRef] [PubMed]
77. Bhattacharya, S.; Sae-Tia, S.; Fries, B.C. Candidiasis and Mechanisms of Antifungal Resistance. *Antibiotics* **2020**, *9*, 312. [CrossRef] [PubMed]
78. Beattie, S.R.; Krysan, D.J. Antifungal Drug Screening: Thinking Outside the Box to Identify Novel Antifungal Scaffolds. *Curr. Opin. Microbiol.* **2020**, *57*, 1–6. [CrossRef]
79. Houšť, J.; Spížek, J.; Havlíček, V. Antifungal Drugs. *Metabolites* **2020**, *10*, 106. [CrossRef]
80. Scorneaux, B.; Angulo, D.; Borroto-Esoda, K.; Ghannoum, M.; Peel, M.; Wring, S. SCY-078 Is Fungicidal against Candida Species in Time-Kill Studies. *Antimicrob. Agents Chemother.* **2017**, *61*, 10–1128. [CrossRef]
81. Avato, P. Editorial to the Special Issue—"Natural Products and Drug Discovery". *Molecules* **2020**, *25*, 1128. [CrossRef]
82. Atanasov, A.; Zotchev, S.; Dirsch, V.; Taskforce, T.I.N.P.S.; Supuran, C. Natural Products in Drug Discovery: Advances and Opportunities. *Nat. Rev.* **2021**, *20*, 200–216. [CrossRef] [PubMed]
83. Aylate, A.; Agize, M.; Ekero, D.; Kiros, A.; Ayledo, G.; Gendiche, K. *In-Vitro* and *In-Vivo* Antibacterial Activities of *Croton macrostachyus* Methanol Extract against *E. coli* and *S. aureus*. *Adv. Anim. Vet. Sci.* **2017**, *5*, 107–114. [CrossRef]
84. Contreras Martínez, O.I.; Angulo Ortíz, A.; Santafé Patiño, G.; Peñata-Taborda, A.; Berrio Soto, R. Isoespintanol Antifungal Activity Involves Mitochondrial Dysfunction, Inhibition of Biofilm Formation, and Damage to Cell Wall Integrity in *Candida tropicalis*. *Int. J. Mol. Sci.* **2023**, *24*, 10187. [CrossRef] [PubMed]
85. Jordá, T.; Puig, S. Regulation of Ergosterol Biosynthesis in *Saccharomyces cerevisiae*. *Genes* **2020**, *11*, 795. [CrossRef]
86. Sun, L.; Liao, K. The Effect of Honokiol on Ergosterol Biosynthesis and Vacuole Function in *Candida albicans*. *J. Microbiol. Biotechnol.* **2020**, *30*, 1835–1842. [CrossRef]

87. Liu, J.F.; Xia, J.J.; Nie, K.L.; Wang, F.; Deng, L. Outline of the Biosynthesis and Regulation of Ergosterol in Yeast. *World J. Microbiol. Biotechnol.* **2019**, *35*, 98. [CrossRef]
88. Cheng, R.; Xu, Q.; Hu, F.; Li, H.; Yang, B.; Duan, Z.; Zhang, K.; Wu, J.; Li, W.; Luo, Z. Antifungal Activity of MAF-1A Peptide against *Candida albicans*. *Int. Microbiol.* **2021**, *24*, 233–242. [CrossRef]
89. Bhattacharya, S.; Esquivel, B.D.; White, T.C. Overexpression or Deletion of Ergosterol Biosynthesis Genes Alters Doubling Time, Response to Stress Agents, and Drug Susceptibility in *Saccharomyces cerevisiae*. *MBio* **2018**, *9*, 10–1128. [CrossRef]
90. Quiles-Melero, I.; García-Rodríguez, J. Antifúngicos de Uso Sistémico. *Rev. Iberoam. Micol.* **2021**, *38*, 42–46. [CrossRef]
91. De Backer, M.D.; Ilyina, T.; Ma, X.J.; Vandoninck, S.; Luyten, W.H.M.L.; Bossche, H. Vanden. Genomic Profiling of the Response of *Candida albicans* to Itraconazole Treatment Using a DNA Microarray. *Antimicrob. Agents Chemother.* **2001**, *45*, 1660–1670. [CrossRef]
92. Florio, A.R.; Ferrari, S.; De Carolis, E.; Torelli, R.; Fadda, G.; Sanguinetti, M.; Sanglard, D.; Posteraro, B. Genome-Wide Expression Profiling of the Response to Short-Term Exposure to Fluconazole in *Cryptococcus neoformans* Serotype A. *BMC Microbiol.* **2011**, *11*, 97. [CrossRef] [PubMed]
93. Kodedová, M.; Sychrová, H. Changes in the Sterol Composition of the Plasma Membrane Affect Membrane Potential, Salt Tolerance and the Activity of Multidrug Resistance Pumps in *Saccharomyces cerevisiae*. *PLoS ONE* **2015**, *10*, e0139306. [CrossRef] [PubMed]
94. Jensen-Pergakes, K.L.; Kennedy, M.A.; Lees, N.D.; Barbuch, R.; Koegel, C.; Bard, M. Sequencing, Disruption, and Characterization of the Candida Albicans Sterol Methyltransferase (ERG6) Gene: Drug Susceptibility Studies in Erg6 Mutants. *Antimicrob. Agents Chemother.* **1998**, *42*, 1160–1167. [CrossRef] [PubMed]
95. Parks, L.W.; Smith, S.J.; Crowley, J.H. Biochemical and Physiological Effects of Sterol Alterations in Yeast-A Review. *Lipids* **1995**, *30*, 227–230. [CrossRef] [PubMed]
96. Ahmadipour, S.; Field, R.A.; Miller, G.J. Prospects for Anti-Candida Therapy through Targeting the Cell Wall: A Mini-Review. *Cell Surf.* **2021**, *7*, 100063. [CrossRef] [PubMed]
97. Lenardon, M.D.; Sood, P.; Dorfmueller, H.C.; Brown, A.J.P.; Gow, N.A.R. Scalar Nanostructure of the *Candida albicans* Cell Wall; a Molecular, Cellular and Ultrastructural Analysis and Interpretation. *Cell Surf.* **2020**, *6*, 100047. [CrossRef] [PubMed]
98. Ibe, C.; Munro, C.A. Fungal Cell Wall Proteins and Signaling Pathways Form a Cytoprotective Network to Combat Stresses. *J. Fungi* **2021**, *7*, 739. [CrossRef]
99. Popolo, L.; Gualtieri, T.; Ragni, E. The Yeast Cell-Wall Salvage Pathway. *Med. Mycol. Suppl.* **2001**, *39*, 111–121. [CrossRef]
100. Boone, C.; Sommer, S.S.; Hensel, A.; Bussey, H. Yeast KRE Genes Provide Evidence for a Pathway of Cell Wall β-Glucan Assembly. *J. Cell Biol.* **1990**, *110*, 1833–1843. [CrossRef]
101. Nagahash, S.; Lussier, M.; Bussey, H. Isolation of *Candida glabrata* Homologs of the *Saccharomyces cerevisiae* KRE9 and KNH1 Genes and Their Involvement in Cell Wall β-1,6-Glucan Synthesis. *J. Bacteriol.* **1998**, *180*, 5020–5029. [CrossRef]
102. García, R.; Botet, J.; Rodríguez-Peña, J.M.; Bermejo, C.; Ribas, J.C.; Revuelta, J.L.; Nombela, C.; Arroyo, J. Genomic Profiling of Fungal Cell Wall-Interfering Compounds: Identification of a Common Gene Signature. *BMC Genom.* **2015**, *16*, 683. [CrossRef] [PubMed]
103. Xiong, H.; Zhou, X.; Xiang, W.; Huang, M.; Lin, Z.; Tang, J.; Cai, T.; Zhang, Q. Integrated Transcriptome Reveals That D -Limonene Inhibits *Candida tropicalis* by Disrupting Metabolism. *LWT-Food Sci. Technol.* **2023**, *176*, 114535. [CrossRef]
104. Sun, F.-J.; Li, M.; Gu, L.; Wang, M.; Yang, M. Recent Progress on Anti-Candida Natural Products. *Chin. J. Nat. Med.* **2021**, *19*, 561–579. [CrossRef] [PubMed]
105. Hymbaugh Bergman, S.J.; Comstock, L.R. N-Mustard Analogs of S-Adenosyl-l-Methionine as Biochemical Probes of Protein Arginine Methylation. *Bioorganic Med. Chem.* **2015**, *23*, 5050–5055. [CrossRef]
106. Sun, B.; Dong, Y.; Lei, K.; Wang, J.; Zhao, L.; Liu, M. Design, Synthesis and Biological Evaluation of Amide-Pyridine Derivatives as Novel Dual-Target (SE, CYP51)Antifungal Inhibitors. *Bioorganic Med. Chem.* **2019**, *27*, 2427–2437. [CrossRef]